DOCUMENT RELEASE AND CHANGE FORM

Prepared For the U.S. Department of Energy, Assistant Secretary for Environmental Management
By Washington River Protection Solutions, LLC., PO Box 850, Richland, WA 99352
Contractor For U.S. Department of Energy, Office of River Protection, under Contract DE-AC27-08RV14800

TRADEMARK DISCLAIMER: Reference herein to any specific commercial product, process, or service by trade name, trademark, manufacturer, or otherwise, does not necessarily constitute or imply its endorsement, recommendation, or favoring by the United States government or any agency thereof or its contractors or subcontractors. Printed in the United States of America.

Release Stamp

DATE: Feb 22,2021

HANFORD RELEASE

1. **Doc No:** RPP-RPT-58949 **Rev.** 00A

2. **Title:**
Flow and Contaminant Transport Numerical Model for the WMA C Performance Assessment and RCRA Closure Analysis

3. **Project Number:** T2R26 ☐N/A

4. **Design Verification Required:** ☐Yes ☒No

5. **USQ Number:** ☒ N/A RPP-27195

6. **PrHA Number** **Rev.** ☒ N/A

Clearance Review Restriction Type: public

7. **Approvals**

Title	Name	Signature	Date
Clearance Review	Harrison, Sarah E	*Harrison, Sarah E*	02/22/2021
Document Control Approval	Alvarez, Efren	*Alvarez, Efren*	02/18/2021
Originator	Bergeron, Marcel P	*Bergeron, Marcel P*	02/10/2021
Responsible Manager	Rutland, Paul L	*Rutland, Paul L*	02/11/2021

8. **Description of Change and Justification**

This update removes Tables 3-1 and 3-2 and adds text to cite specific appendices from RPP-RPT-42323, Rev. 3 as the source of radiological and hazardous chemical residual waste inventories used in STOMP model simulations. A footnote is added to p. 3-8 that provides some clarification of alternative conceptualizations of pipeline releases at different depths used in STOMP model input files.

9. **TBDs or Holds** ☒N/A

10. **Related Structures, Systems, and Components**

a. **Related Building/Facilities** ☒N/A	b. **Related Systems** ☒N/A	c. **Related Equipment ID Nos. (EIN)** ☒N/A

11. **Impacted Documents – Engineering** ☒N/A

Document Number	Rev.	Title

12. **Impacted Documents (Outside SPF):**

N/A

13. **Related Documents** ☒N/A

Document Number	Rev.	Title

14. **Distribution**

Name	Organization
Bergeron, Marcel P	CLOSURE & INTERIM MEASURES
Field, Jim G	PROCESS ENGINEERING
Hasan, Nazmul	
Lee, Kearn (Pat)	CLOSURE & INTERIM MEASURES
Parker, Dan	CLOSURE & INTERIM MEASURES
Rutland, Paul L	CLOSURE & INTERIM MEASURES
Singleton, Kristin M	CLOSURE & INTERIM MEASURES
Watson, David (Dj) J	CLOSURE & INTERIM MEASURES

INFORMATION CLEARANCE REVIEW AND RELEASE APPROVAL

Part I: Background Information

Title: Model Package Report Flow and Contaminant Transport Numerical Model used in WMA C Performance Assessment and RCRA Closure Analysis	Information Category: ☐ Abstract ☐ Journal Article ☐ Summary ☐ Internet ☐ Visual Aid ☐ Software ☐ Full Paper ☐ Report ☑ Other Model Package Report
Publish to OSTI? ☐ Yes ☑ No	

	Yes	NA
Trademark/Copyright "Right to Use" Information or Permission Documentation	☐	☑

Document Number: RPP-RPT-58949 Revision 0A	Date: November 2020
Author: Bergeron, Marcel P	

Part II: External/Public Presentation Information

Conference Name:		
Sponsoring Organization(s): WRPS		
Date of Conference:	Conference Location:	
Will Material be Handed Out? ☐ Yes ☑ No	Will Information be Published? ☐ Yes ☑ No	*(If Yes, attach copy of Conference format instructions/guidance.)*

Part III: WRPS Document Originator Checklist

Description	*Yes*	*N/A*	*Print/Sign/Date*
Information Product meets requirements in TFC-BSM-AD-C-01?	☐	☑	
Document Release Criteria in TFC-ENG-DESIGN-C-25 completed? (Attach checklist)	☐	☑	
If product contains pictures, safety review completed?	☑	☐	Roberts, Sheryl K Approved - IDMS data file att.

Part IV: WRPS Internal Review

Function	*Organization*	*Date*	*Print Name/Signature/Date*
Subject Matter Expert	WRPS	02/01/2021	Bergeron, Marcel P Approved - IDMS data file att.
Responsible Manager	WRPS	11/03/2020	Rutland, Paul L Approved - IDMS data file att.
Other:			

Part V: IRM Clearance Services Review

Description	*Yes*	*No*	*Print Name/Signature*
Document Contains Classified Information?	☐	☒	If Answer is "Yes," ADC Approval Required Print Name/Signature/Date
Document Contains Information Restricted by DOE Operational Security Guidelines?	☐	☒	Reviewer Signature: Print Name/Signature/Date
Document is Subject to Release Restrictions? *If the answer is "Yes," please mark category at right and describe limitation or responsible organization below:*	☐	☒	Document contains: ☐ Applied Technology ☐ Protected CRADA ☐ Personal/Private ☐ Export Controlled ☐ Proprietary ☐ Procurement – Sensitive ☐ Patentable Info. ☐ OUO ☐ Predecisional Info. ☐ UCNI ☐ Restricted by Operational Security Guidelines ☐ Other (Specify)
Additional Comments from Information Clearance Specialist Review?	☐	☒	Information Clearance Specialist Approval APPROVED By Sarah Harrison at 12:12 pm, Feb 10, 2021 Print Name/Signature/Date

When IRM Clearance Review is Complete – Return to WRPS Originator for Final Signature Routing (Part VI)

INFORMATION CLEARANCE REVIEW AND RELEASE APPROVAL

Part VI: Final Review and Approvals

Description	*Approved for Release*		*Print Name/Signature*	
	Yes	*N/A*		
WRPS External Affairs	☒	☐	Mc Cune, Hal C	Approved - IDMS data file att.
WRPS Office of Chief Counsel	☒	☐	Roden, Mari L	Approved - IDMS data file att.
DOE – ORP Public Affairs/Communications	☒	☐	Tyree, Geoffrey T	Approved - IDMS data file att.
Other: ORP OCC	☒	☐	King, Grace J	Approved - IDMS data file att.
Other: ORP SME	☒	☐	Lobos, Rodrigo A	Approved - IDMS data file att.

Comments Required for WRPS-Indicate Purpose of Document:

This model package report documents the development of the integrated vadose and saturated zone flow and transport model for the Waste Management Area C performance assessment. This update removes Tables 3-1 and 3-2 and adds text to cite specific appendices from RPP-RPT-42323, Rev. 3 as the source of radiological and hazardous chemical residual waste inventories used in STOMP model simulations. A footnote is added to p. 3-8 that provides some clarification of alternative conceptualizations of pipeline releases at different depths used in STOMP model input files.

APPROVED
By Sarah Harrison at 12:12 pm, Feb 10, 2021

Approved for Public Release; Further Dissemination Unlimited

Information Release Station

Was/Is Information Product Approved for Release? ☒ Yes ☐ No

If Yes, what is the Level of Releaser? ☑ Public/Unrestricted ☐ Other (Specify) _____

Date Information Product Stamped/Marked for Release: 02/10/2021

Was/Is Information Product Transferred to OSTI? ☐ Yes ☒ No

Forward Copies of Completed Form to WRPS Originator

```
- <workflow name="(SEH) Normal - RPP-RPT-58949 Rev0A" id="279254550">
  - <task name="Clearance Process" id="0" date-initiated="20201103T1324"
      performer="SARAH E HARRISON" performer-id="252341659"
      username="h5635746">
      <comments>Due Tuesday November 17th 2020 - COB Please approve the
        Model Package Report Flow and Contaminant Transport Numerical Model
        used in WMA C Performance Assessment and RCRA Closure Analysis,
        Revision 0A, submitted by the Marcel Bergeron for public release. Thank
        you, Sarah Harrison Information Clearance</comments>
    </task>
    <task name="Add XML" id="1" date-done="20201103T1324" />
    <task name="Manager Approval" id="41" date-due="20201106T1324" date-
      done="20201103T1407" performer="PAUL L RUTLAND" performer-
      id="140633218" username="h4494439" disposition="Approve"
      authentication="true" />
    <task name="Document Reviewer1" id="54" date-due="20201106T1407" date-
      done="20201105T1044" performer="SHERYL K ROBERTS" performer-
      id="171787680" username="h0081997" disposition="Public Release"
      authentication="true" />
    <task name="Document Reviewer2" id="53" date-due="20201106T1407" date-
      done="20201105T1137" performer="HAL C MC CUNE" performer-
      id="226350486" username="h7687509" disposition="Public Release"
      authentication="true" />
    <task name="Document Reviewer4" id="51" date-due="20201106T1407" date-
      done="20201215T1258" performer="RODRIGO A LOBOS" performer-
      id="232334741" username="h2488419" disposition="Public Release"
      authentication="true" />
    <task name="Document Reviewer3" id="52" date-due="20201106T1407" date-
      done="20210131T1523" performer="MARI L RODEN" performer-id="262637370"
      username="h0048955" disposition="Public Release" authentication="true" />
    <task name="Doc Owner Clearance Review" id="13" date-due="20210202T1523"
      date-done="20210201T0619" performer="MARCEL P BERGERON" performer-
      id="172635544" username="h0006384" disposition="Send On"
      authentication="true" />
    <task name="Milestone 1" id="24" date-done="20210201T0619" />
    <task name="ORP Document Reviewer3" id="59" date-due="20210203T0619"
      date-done="20210208T1708" performer="GRACE J KING" performer-
      id="211901436" username="h9807759" disposition="Public Release"
      authentication="true" />
    <task name="ORP Document Reviewer1" id="57" date-due="20210203T0619"
      date-done="20210209T1541" performer="GEOFFREY T TYREE" performer-
      id="6158846" username="h0068565" disposition="Public Release"
      authentication="true" />
    <task name="Doc Owner Reviews ORP Comments" id="61" date-
      due="20210210T1541" date-done="20210209T1557" performer="MARCEL P
      BERGERON" performer-id="172635544" username="h0006384"
      disposition="Send On" authentication="true" />
    <task name="Milestone 2" id="62" date-done="20210209T1557" />
    <task name="Verify Doc Consistency" id="4" date-due="20210210T1557" date-
      done="20210210T1103" performer="SARAH E HARRISON" performer-
      id="252341659" username="h5635746" disposition="Cleared"
      authentication="true" />
  </workflow>
```

RPP-RPT-58949
Revision 0A

Model Package Report Flow and Contaminant Transport Numerical Model used in WMA C Performance Assessment and RCRA Closure Analysis

Prepared by:
W. J. McMahon
CH2M HILL Plateau Remediation Company

Prepared for:
Washington River Protection Solutions, LLC

Date:
Version 1.0
February 2021

Prepared for the U.S. Department of Energy
Office of River Protection
Contract No. DE-AC27-08RV14800

Approved for public release; distribution unlimited

Version History

Version	Date	Author	Change Description
Draft A	30-Nov-2015	W. J. McMahon	Initial draft for DOE-ORP review
Draft B	28-Jan-2016	W. J. McMahon	Updates to address comments from DOE-ORP review
Rev. 0	08-01-2016	W. J. McMahon	Updates to address comments related to aquifer dispersivity in the Low-Level Federal Review Group (LFRG) review of Draft B of RPP-ENV-58782, "Performance Assessment of Waste Management Area C, Hanford Site, Washington". Also includes signature cover sheet to meet new QA requirements for Model Package Reports.
Rev. 0A	10-Feb-2021	W. J. McMahon	Updates that remove Tables 3-1 and 3-2 with added text to cite specific appendices from RPP-RPT-42323, Rev. 3 as the source of radiological and hazardous chemical residual waste inventories used in STOMP model simulations. A footnote is added to p. 3-8 that provides some clarification of alternative conceptualizations of pipeline releases at different depths used in STOMP model input files. Due to the type of changes made, no additional checking is included in this version of the model package report.

ENVIRONMENTAL MODEL PACKAGE REPORT COVER PAGE

Section 1 - Completed by Responsible Manager

Project: Waste Management Area C Performance Assessment

Date: 07/20/2016

Environmental Model Name and Version: WMA C PA Tank Residual Flow and Transport Model

RELEASE/ISSUE

Section 2 - Completed by Preparer

Document Number: RPP-RPT-58949 Revision No.: 0

Revision History

Revision No.	Description	Date	Affected Pages
0	INITIAL ISSUE	07/27/2016	ALL

Section 3 - Completed by Responsible Manager

Document Control	Yes	No
1. Is document intended to be controlled within the Document Management Control System (DMCS)?	●	○
2. Does document contain scientific and technical information intended for public use?	●	○
3. Does document contain controlled-use information?	○	●

Section 4 - Training and Software Installation Approval (Completed Prior to Model Implementation)

Modeler-Required Training Completed:

Print	Position	Signature	Date
William E. Nichols (Training Coordinator)	Scientist (CH-PRC)		28 JUL 2016

Implementation Software Installation and Checkout Certified:

Print	Position	Signature	Date
William E. Nichols (Training Coordinator)	Scientist (CH-PRC)		28 JUL 2016

Section 5 - Document Review & Approval

Print	Position	Signature	Date
William McMahon (Model Developer)	Engineer (CH-PRC)		07/27/2016
Nazmul Hasan (Model Checker)	Scientist (INTERA, Inc.)		07/27/2016
Raziuddin Khaleel (Model Senior Reviewer)	Sr. Sci. (INTERA, Inc.)		07/27/16

Page 1 of 1 A-6006-960 (REV 0)

EXECUTIVE SUMMARY

This model package report documents the development of the integrated vadose and saturated zone flow and transport model for the Waste Management Area (WMA) C performance assessment. This modeling capability is intended for use in addressing the requirements outlined in Appendix I of the *Hanford Federal Facility Agreement and Consent Order* (Ecology et al. 1989) for assessment of the radiological impacts of waste residuals in a closed WMA C under U.S. Department of Energy Order 435.1, *Radioactive Waste Management* and evaluation of the hazardous chemical impacts for the same wastes under *Resource Conservation and Recovery Act of 1976*. The overall objective of the modeling effort is to provide a basis for making informed closure decisions pertinent to WMA C. The results of the flow and transport model are intended to assist in evaluating the potential long-term impact on groundwater of post-retrieval single-shell tank waste residuals and residual waste left in ancillary equipment, which includes the 244-CR Vaults, the 241-C-301 catch tank, and the associated pipelines. Impacts related to past unplanned releases are outside the scope of this modeling effort.

This report discusses the development and translation of the conceptual model for flow and contaminant transport into the WMA C three-dimensional (3-D) numerical flow and transport model evaluated using the Subsurface Transport Over Multiple Phases©[1] simulator. The development of representative geologic stratigraphy is described along with the implementation of waste release models used to represent contaminant release from waste residuals remaining in tanks and ancillary equipment. The report provides the technical basis for specific model parameters and boundary conditions, along with description of modeling assumptions.

The modeling results are used to estimate the possible future concentration in groundwater of various radionuclides and non-radiological contaminants. The methodology used to calculate time-series concentration values (breakthrough curves) and estimate the peak concentrations is described in detail. The modeling includes a screening process used to identify and shorten the list of contaminants of potential concern that require specific evaluation in the 3-D numerical flow and transport model.

The model package report documents the 3-D numerical flow and transport base case model and its applicability, along with certain calculations that are necessary to demonstrate the soundness of the model. The use of the model to perform base case and sensitivity and uncertainty calculations, including inputs and results, is documented separately in environmental calculation files as indicated by the documentation requirements associated with the preparation and issue of environmental calculations. Control of all software used to implement the model is directed by the requirements of procedure PRC-PRO-IRM-309, “Controlled Software Management.”

[1] Subsurface Transport Over Multiple Phases (STOMP)© is copyrighted by Battelle Memorial Institute, 1996.

CONTENTS

1 PURPOSE 1-1

1.1 PURPOSE AND NECESSITY FOR MODELING TO SUPPORT THE WASTE MANAGEMENT AREA C APPENDIX I PERFORMANCE ASSESSMENT 1-2

1.2 BACKGROUND 1-3

1.2.1 Waste Management Area C Facility Details 1-4

1.2.2 Waste Management Area C Performance Assessment Data Sources 1-5

1.3 DOCUMENT ORGANIZATION 1-7

2 MODEL OBJECTIVES 2-1

3 MODEL CONCEPTUALIZATION 3-1

3.1 FEATURES, EVENTS, AND PROCESSES 3-1

3.1.1 Model Domain and Boundary Conditions 3-2

3.1.2 Geologic Setting 3-3

3.1.3 Source Term 3-7

3.1.4 Vadose Zone Hydrogeology and Contaminant Transport 3-8

3.1.5 Infiltration and Recharge 3-13

3.1.6 Geochemistry and Sorption 3-15

3.1.7 Groundwater Domain 3-17

3.1.8 Point of Calculation, Protectiveness Metric, and Timeframe Considerations 3-19

3.2 NATURE AND EXTENT OF CONTAMINATION 3-26

4 MODEL IMPLEMENTATION 4-1

4.1 DISCRETIZATION 4-1

4.2 PARAMETERIZATION 4-8

4.3 MODELING STAGES 4-8

4.4 CALIBRATION 4-9

4.5 SCREENING 4-11

4.6 BASE CASE ANALYSIS 4-16

4.7 SENSITIVITY AND UNCERTAINTY ANALYSIS 4-16

5 MODEL APPLICATION 5-1

5.1 WASTE MANAGEMENT AREA C PERFORMANCE ASSESSMENT MODEL LIMITATIONS 5-1

5.2 WASTE MANAGEMENT AREA C PERFORMANCE ASSESSMENT MODEL RECOMMENDATIONS 5-1

6 SUBSURFACE TRANSPORT OVER MULTIPLE PHASES SOFTWARE 6-1

6.1 SUBSURFACE TRANSPORT OVER MULTIPLE PHASES SOFTWARE QUALITY ASSURANCE 6-2

6.2 SUBSURFACE TRANSPORT OVER MULTIPLE PHASES CONTROLLED CALCULATION SOFTWARE 6-2

6.3 SOFTWARE INSTALLATION AND CHECKOUT 6-3

6.4 STATEMENT OF VALID SOFTWARE APPLICATION 6-3

7 MODEL CONFIGURATION MANAGEMENT 7-1

8 REFERENCES 8-1

APPENDICES

APPENDIX A – KEY ASSUMPTIONS IN THE PERFORMANCE ASSESSMENT ..... A-i

APPENDIX B – BASIS FOR DEVELOPMENT OF VADOSE ZONE HYDRAULIC PROPERTIES AT WASTE MANAGEMENT AREA C ..... B-i

APPENDIX C – TECHNICAL BASIS FOR WASTE MANAGEMENT AREA C UNCONFINED AQUIFER CONCEPTUAL MODEL: FIELD DATA AND RELATED INVESTIGATIONS ..... C-i

FIGURES

Figure 1-1. Waste Management Area C Tanks and Associated Infrastructure and Unplanned Releases. 1-5

Figure 3-1. Plan View of Waste Management Area C Performance Assessment Model Domain Showing the Horizontal Distribution and Surface Type of the Irregularly-Spaced Calculation Nodes. The resolution increases in the area of Waste Management Area C. 3-5

Figure 3-2. Fence Diagram of Alternative Geologic Models Used in the Performance Assessment for Waste Management Area C. 3-6

Figure 3-3. Elevation of Pipeline Source in Waste Management Area C Three-Dimensional Model Domain. 3-9

Figure 3-4. Central Plateau Groundwater Model Calibration Results in the Vicinity of Waste Management Area C. 3-20

Figure 3-5. Hindcast Estimate of the Water Table Elevation in 1944 Prior to the Start of Significant Hanford Site Operations. 3-21

Figure 3-6. Points of Calculation 100 Meters Downgradient of Waste Management Area C. 3-24

Figure 4-1. Horizontal Alignment of Three-Dimensional Model Computational Nodes with Waste Management Area C Single-Shell Tanks, 241-C-301 Catch Tank, 244-CR Vault, and Other Waste Management Area C Ancillary Equipment. 4-2

Figure 4-2. Horizontal and Vertical Alignment and Distribution of Waste Management Area C Performance Assessment Three-Dimensional Model Computational Nodes. 4-4

Figure 4-3. Relative Change in Moisture Content (Volume %) from the Pre-Hanford Steady-State Condition at the Four Vertical Boundaries of the Model at Three Times of Interest: Year 2020, Year 2520, and Year 3020. 4-5

Figure 4-4. Comparison at the Nine Points of Calculation Located 100 meters Downgradient for the Technetium-99 Concentration between the Base Case Dispersivity Values and the Numerical Dispersion Test Case Dispersivity Values. 4-7

Figure 4-5. Groundwater Pathway Screening Analysis Indicating the Arrival Time of Radionuclides and Non-Radiological Contaminants at the Water Table. 4-14

TABLES

Table 1-1. Exposure Scenarios, Performance Objectives and Measures, and Points of Assessment for the Waste Management Area C Performance Assessment. 1-1

Table 3-1. Composite van Genuchten-Mualem Parameters for Various Hydrostratigraphic Units at the Waste Management Area C Site Used in the Base Case Evaluations of Alternative Geologic Models I and II (Appendix B). 3-10

Table 3-2. Macrodispersivity Estimates for Various Hydrostratigraphic Units at Waste Management Area C Used in the Base Case Evaluations of Alternative Geologic Models I and II (Appendix B). 3-12

Table 3-3. Effective Bulk Density Estimates for Various Hydrostratigraphic Units at Waste Management Area C Used in the Base Case Evaluations of Alternative Geologic Models I and II (Appendix B). 3-12

Table 3-4. Base Case Recharge Rate (Net Infiltration) Estimates for Surface Conditions during the Pre-Construction, Operational, and Post-Closure Periods. 3-14

Table 3-5. Summary of the Waste Management Area C Performance Assessment Base Case K_d (mL/g) Values. 3-16

Table 3-6. Relationship Between Saturated Longitudinal Macrodispersivity (α_L) and Scale of Measurement (L_s). 3-22

Table 3-7. Waste Management Area C Performance Assessment Unconfined Aquifer Flow and Transport Properties (Appendix C). 3-23

Table 3-8. Dimension of Widths for Point of Calculation Segments 100 meters Downgradient of Waste Management Area C. 3-25

Table 4-1. Horizontal and Vertical Spacing of the Finite Difference Cells in the Three-Dimensional Waste Management Area C Flow and Transport Model Domain. 4-3

Table 4-2. Comparison Using Vadose Zone Dispersivity Values and Numerical Dispersion Test Case Dispersivity Values. 4-8

Table 4-3. Waste Management Area C Performance Assessment Vadose Zone Courant Criteria and Numerical Dispersion Evaluation. 4-9

Table 4-4. Summary of Key Elements and Base Case Parameters Associated with Site-Specific Model Components for Waste Management Area C. 4-10

Table 4-5. Maximum Net Infiltration (Recharge) Estimates Used in the Screening Analysis for Pre-Construction Period, Operational Period, and Post-Closure of Waste Management Area C. 4-12

Table 4-6. van Genuchten-Mualem Parameters Associated with the Maximum Pore Water Velocity at Specific Tension Ranges Based on Cumulative Distribution Functions. 4-13

Table 4-7. First-Arrival Time (in Calendar Year) of Radionuclides for Various K_d Values Based on Screening Analysis Using Subsurface Transport Over Multiple Phases. 4-13

Table 4-8. Radionuclides that Arrive at the Water Table within the 1,000-Year Compliance and 10,000-Year Sensitivity and Uncertainty Timeframe Based on the Screening Analysis Conducted Using Subsurface Transport Over Multiple Phases. 4-15

TERMS

2-D	two-dimensional
3-D	three-dimensional
CERCLA	*Comprehensive Environmental Response, Compensation, and Liability Act of 1982*
CHPRC	CH2M HILL Plateau Remediation Company
Ci	curie(s)
cm	centimeter(s)
cm/s	centimeters per second
cm^3/g	cubic centimeters per gram
CPGWM	Central Plateau Groundwater Model
Cr	chromium
DOE	U.S. Department of Energy
DWS	drinking water standards
Ecology	State of Washington Department of Ecology
EHM	equivalent homogeneous medium
EMMA	Environmental Model Management Archive
EPA	U.S. Environmental Protection Agency
FEPs	Features, Events, and Processes
ft	feet
g	gram(s)
h	hour(s)
HFFACO	*Hanford Federal Facility Agreement and Consent Order*
HSU	hydrostratigraphic unit

in.	inch
K_d	distribution coefficient
kg	kilogram(s)
km	kilometer(s)
km^2	square kilometer(s)
m	meter(s)
MCL	maximum contaminant level
m/s	meters per second
µg/L	micrograms per liter
mg/kg	milligrams per kilogram
mg/L	milligrams per liter
mL/g	milliliters per gram
mm/yr	millimeters per year
MPR	model package report
NAVD88	*North American Vertical Datum of 1988*
NRC	U.S. Nuclear Regulatory Commission
pCi/g	picocuries per gram
pCi/L	picocuries per liter
PA	performance assessment
PNNL	Pacific Northwest National Laboratory
PUREX	Plutonium Uranium Extraction (Plant)
RCRA	*Resource Conservation and Recovery Act of 1976*
RETC	RETention Curve (software)

SSL	Soil Screening Level
SST	Single-Shell Tank
STOMP	Subsurface Transport Over Multiple Phases
TFC	tank farm contractor
UPR	unplanned release
VSZ	vadose and saturated zone
WAC	*Washington Administrative Code*
WMA	Waste Management Area
WRPS	Washington River Protection Solutions
yr	year

1 PURPOSE

The integrated three-dimensional (3-D) vadose and saturated zone (VSZ) flow and transport model for the Waste Management Area (WMA) C performance assessment (PA) provides estimates of future radiological and non-radiological contaminant concentrations in groundwater from a closed WMA C. The purpose of this evaluation is to determine the extent of protection to human health and the environment the planned WMA C retrieval and closure activities provide. U.S. Department of Energy (DOE) O 435.1, *Radioactive Waste Management* dictates that DOE radioactive waste management activities shall protect the public from exposure to radiation from radioactive materials, protect the environment, and comply with applicable Federal, State, and local laws and regulations and any applicable Executive Orders and other DOE directives. DOE M 435.1-1, *Radioactive Waste Management Manual* identifies specific performance objectives and other performance-related factors that need to be considered in the PA.

Of particular relevance to the 3-D VSZ flow and transport model evaluations are the "All Pathways" calculation of the highest projected dose or concentration (in groundwater) beyond a 100-meter buffer zone surrounding the disposed waste and the requirement to evaluate the impacts to water resources. An extended discussion of the regulatory requirements and other elements of the assessment context is presented in report RPP-RPT-41918, *Assessment Context for Performance Assessment for Waste in C Tank Farm Facilities after Closure*. The performance objectives comprise a combination of DOE O 435.1, *Resource Conservation and Recovery Act of 1976* (RCRA) closure requirements and State of Washington Department of Ecology (Ecology) requirements. Those performance objectives addressed by the 3-D VSZ flow and transport model and are shown in Table 1-1.

Table 1-1. Exposure Scenarios, Performance Objectives and Measures, and Points of Assessment for the Waste Management Area C Performance Assessment.

Exposure Scenario	Performance Objective and Measures	Point of Assessment	
		Operational and Active Institutional Control Periods[a]	Post-Institutional Control Period
All pathways	25 mrem/yr [b]	Facility Boundary	100 m [c]
Water Resources Protection	Ecology requirements on concentration	At the Source and 100 m [c]	100 m [c]
Chemical Toxicity/Risk	Ecology and RCRA Closure requirements related to risk	At the Source and 100 m [c]	100 m [c]

[a] The active institutional control period includes final closure.

[b] Excluding radon in air.

[c] The point of highest projected dose or concentration beyond a 100- meter buffer zone surrounding the disposed waste. Additionally, concentrations found in tank residuals will be compared against the standard Model Toxics Control Act (*Revised Code of Washington* 70.105D, "Hazardous Waste Cleanup—Model Toxics Control Act") three-phase model.

Ecology = State of Washington Department of Ecology RCRA = *Resource Conservation and Recovery Act of 1976*

This model package report (MPR) documents the 3-D numerical flow and transport model and its applicability, the base case analysis, and certain calculations that are necessary to demonstrate the soundness of the model. The use of the model to perform sensitivity and uncertainty calculations, including inputs and results, is to be documented in environmental calculation files as required by the documentation requirements associated with the preparation and issue of environmental calculations. Control of all software used to implement the model is directed by the requirements of PRC-PRO-IRM-309, "Controlled Software Management."

1.1 PURPOSE AND NECESSITY FOR MODELING TO SUPPORT THE WASTE MANAGEMENT AREA C APPENDIX I PERFORMANCE ASSESSMENT

Appendix I Section 2.5 "Performance Assessment" of the *Hanford Federal Facility Agreement and Consent Order* (HFFACO) (Ecology et al. 1989) stipulates that WMA PAs must evaluate the risk associated with the individual components of the WMA after retrieval and include the ability to account for the risk of each component relative to the risk associated with the WMA as a whole. In addition, the PA must include the flexibility to account for new or evolving information as it becomes available. The need for the WMA C PA flow and transport modeling derives from the requirements of DOE O 435.1 and the additional requirements imposed by Appendix I. According to Appendix I of the HFFACO, the analysis needs to include time history results of the transport of radionuclides and non-radiological contaminants individually and collectively and be suitable for estimating the maximum concentration in the environment. These requirements derive from the specific performance objectives identified in DOE M 435.1-1 Chapter 4 Section P "Disposal," as well as other performance measures related to intruder scenarios required by DOE M 435.1-1. In summary, these requirements, as implemented in the WMA C PA flow and transport model, implement the DOE M 435.1-1 requirement that the WMA C PA include calculations of potential doses to representative future members of the public and environmental impacts from potential releases from the tank residuals for a 1,000-year period after closure.

Previous modeling of WMA C includes the Single-Shell Tank (SST) PA (DOE/ORP-2005-01, *Initial Single-Shell Tank System Performance Assessment for the Hanford Site*) and DOE/EIS-0391, *Final Tank Closure and Waste Management Environmental Impact Statement for the Hanford Site, Richland, Washington*. The SST PA includes a two-dimensional (2-D) numerical model representation of WMA C that involves certain simplifications of the detailed conceptual model. The 2-D numerical model for WMA C assumes that the groundwater flows beneath the WMA parallel to tank row 241-C-103, 241-C-106, 241-C-109, and 241-C-112, consistent with the estimated post-Hanford unconfined aquifer hydraulic gradient. To account for 3-D aspects, the tank centerline mass flux and concentration are transformed to average values across the tank farm fenceline according to a linear scalar. The SST PA evaluation does not include interaction between radionuclides and non-radiological contaminants from sources located in different parallel rows, or calculation of concentration 100 meters downgradient of the WMA C fenceline.

The DOE/EIS-0391 approach to the groundwater impact analysis includes the development of a single, large-scale saturated-zone model followed by the development of multiple small-scale

vadose zone-only models, including one representing WMA C. The DOE/EIS-0391 vadose zone model includes three dimensions in an attempt to incorporate the spatial heterogeneity of geologic and recharge conditions, and to incorporate lateral spreading and preferential flow. The alternatives analysis evaluates impacts from the tank farms as entities, not individual tanks; thus the tank residual wastes, ancillary equipment wastes, past release wastes, and hypothesized unplanned releases (UPRs) are composited into single source terms for entire tank farms. DOE/EIS-0391 presents groundwater results for polygonal lines of analysis, referred to as "barriers." For example, Barrier A encompasses both WMA C and WMA A-AX. However, the Barrier A results presented in Appendix O of DOE/EIS-0391 do not distinguish between the groundwater concentration resulting from contaminant sources within WMA C and the concentration resulting from sources within WMA A-AX, or indicate where along Barrier A relative to WMA C the concentration occurs.

1.2 BACKGROUND

The purpose of the WMA C PA flow and transport modeling is to evaluate the impacts to groundwater associated with waste remaining in tank residuals after closure of WMA C. The modeling is conducted in accordance with the DOE G 435.1-1, *Implementation Guide for Use with DOE M 435.1-1, Radioactive Waste Management Manual* performance assessment guidelines. For the WMA C PA evaluation, the modeling provides a detailed evaluation of the groundwater concentrations and radionuclide arrival times during the 1,000-year compliance and 10,000-year sensitivity-uncertainty periods per DOE O 435.1.

The flow and transport model incorporates three dimensions to account for the lateral movement of water and radionuclides and to maintain comparability with other vadose zone transport analyses conducted at the Hanford Site. The model accounts for the impacts to groundwater from the WMA C sources both individually and collectively. In addition, the model includes the flexibility to account for new or evolving information.

This analysis does not consider contaminant release during WMA C operations, only the post-closure impacts to the environment of the radionuclides and non-radiological contaminants remaining in the residual waste. The estimated inventory of tank and ancillary equipment residuals will continue to evolve until retrieval is completed. RPP-RPT-42323, *Hanford C-Farm Tank and Ancillary Equipment Residual Waste Inventory Estimates* provides estimates of residual inventory as of September 1, 2014, and provides the basis for the WMA C PA analysis.

The flow and transport modeling includes a screening phase with the intent to expedite the analysis by limiting the modeling to those radionuclides sufficiently mobile to impact groundwater within the compliance and sensitivity-uncertainty periods. The outcome of the screening phase is to determine the maximum distribution coefficient (K_d) value of contaminants in the WMA C tank residuals that can possibly reach the water table in 1,000 and 10,000 years. Contaminants with K_d values greater than the threshold values determined from screening may be excluded from the compliance and sensitivity/uncertainty analyses. To insure that the screening analysis only excludes those contaminants that would only produce zero groundwater concentration values, screening involves applying the maximum recharge rates associated with

each type of surface and assigning the vadose zone hydraulic properties that produce the fastest pore water velocity for each hydrostratigraphic unit (HSU) in the 3-D VSZ flow and transport model. This approach to screening follows Federal soil screening guidance and DOE performance assessment guidelines (EPA/540/F-95/041, *Soil Screening Guidance: Fact Sheet*; DOE G 435.1-1, Chapter 4) that approve of the use of site-specific models for risk assessment screening purposes.

1.2.1 Waste Management Area C Facility Details

WMA C was placed in service in 1946, and used to store and transfer waste until mid-1980. Because of its long operational history, 241-C Tank Farm (C Farm) received waste generated by essentially all of the Hanford Site major chemical processing operations including bismuth phosphate fuel processing, uranium recovery, Plutonium Uranium Extraction Plant (PUREX) fuel processing, Hot Semi-Works Facility pilot plant operations, fission product recovery, and tank farm interim stabilization and isolation activities. By 2003, all except two of the 100- and 200-series tanks were declared stabilized on an interim basis, indicating that the tank contains less than 50,000 gal of drainable interstitial liquid and less than 5,000 gal of supernate (RPP-ENV-33418, *Hanford C-Farm Leak Inventory Assessments Report*). Since 2003, there has been a concerted and ongoing effort to retrieve the waste from the SSTs within WMA C. The fate and transport modeling addresses the waste remaining in the tanks, ancillary equipment, and pipelines after retrieval concludes.

WMA C contains 12 100-series SSTs and 4 200-series SSTs that were constructed in 1943 to 1944 along with associated ancillary equipment (i.e., diversion boxes, pipes). Additional ancillary equipment (244-CR Process Tank Vault [244-CR vault] and CR diversion boxes) were added in the early 1950s. In general, the WMA C boundary is represented by the fenceline surrounding C Farm (Figure 1-1). To support the transfer and storage of waste within WMA C SSTs, there is a complex waste transfer system of pipelines (transfer lines), diversion boxes, vaults, valve pits, and other miscellaneous structures. Collectively, these are referred to as ancillary equipment. Multiple levels of piping were installed over time in WMA C. A time line of piping installations is described in RPP-7494, *Historical Vadose Zone Contamination from A, AX, and C Tank Farm Operations*. It is estimated that there are approximately 7 miles of waste transfer piping in C Farm that are estimated to contain 1,575 gal of residuals after closure (RPP-PLAN-47559, *Single-Shell Tank Waste Management Area C Pipeline Feasibility Evaluation*).

The 244-CR vault is located south of the tanks. This vault and associated diversion boxes 241-CR-151, 241-CR-152, and 241-CR-153 were constructed in 1951 and ceased operating in 1988. The vault is a two-level, multi-cell, reinforced-concrete structure constructed below grade (DOE/RL-92-04, *PUREX Source Aggregate Area Management Study Report*), which contains four underground tanks along with overhead piping and equipment. Two tanks (TK-CR-001 and TK-CR-011) have a capacity of 170,343 L (45,000 gal) each. The other two tanks (TK-CR-002 and TK-CR-003) have capacities of 55,494 L (14,700 gal) each. The diversions boxes and 244-CR vault with its tanks are currently assumed to contain approximately 200 L (60 gal) and 4,200 L (1,100 gal) at closure, respectively (RPP-RPT-42323).

Figure 1-1. Waste Management Area C Tanks and Associated Infrastructure and Unplanned Releases.

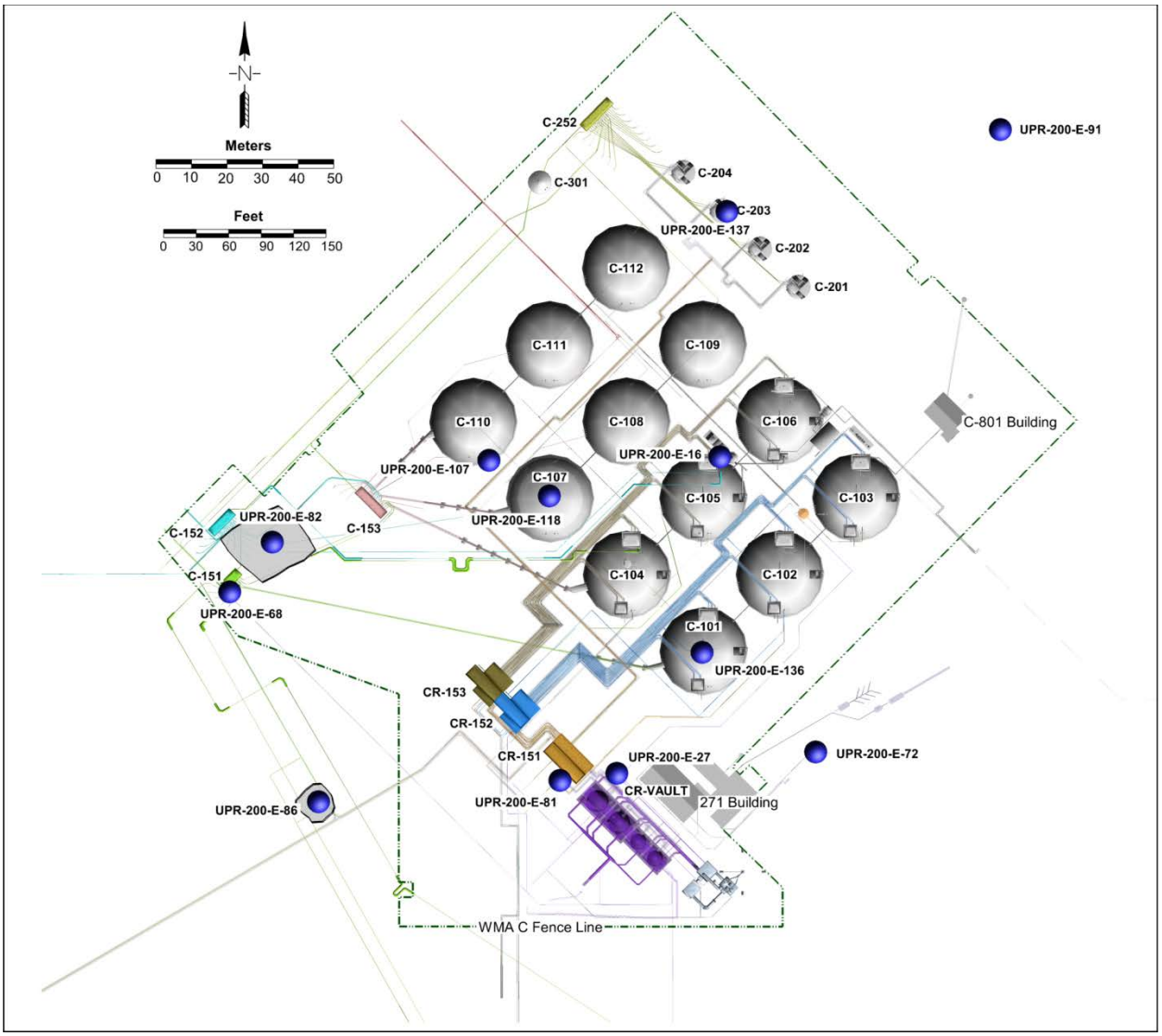

WMA = Waste Management Area

1.2.2 Waste Management Area C Performance Assessment Data Sources

Details of the site are provided in documents that describe to-date conditions, geologic and hydrologic interpretations, subsurface contamination approximations, and source term estimates. The list of these documents is provided below. The majority of these documents were produced to support the WMA C PA working sessions that took place from February 2009 to May 2011. In addition to the data packages, several other documents have been produced since the working sessions that provide updated information on WMA C facility characteristics.

- RPP-RPT-49425, *Ecological Risk Assessment Approach for Hanford Waste Management Area C*, Revision 1. Released September 2011; provides information on the ecological

resources of WMA C and surrounding area. Working Session Number 10 was held in May 2011.

- RPP-RPT-46879, *Corrosion and Structural Degradation within Engineered System in Waste Management Area C*, Revision 2. Released February 2011; presents information related to tank and ancillary equipment corrosion and degradation and how it relates to contaminant releases from waste contained within the engineered system in WMA C. Working Session Number 7 was held in July 2010.

- RPP-RPT-46088, *Flow and Transport in the Natural System at Waste Management Area C*, Revision 1. Released September 2010; provides data and information related to the flow and transport in the vadose zone and groundwater systems at WMA C. Working Session Number 6 was held in May 2010.

- RPP-RPT-44042, *Recharge and Waste Release within Engineered System in Waste Management Area C*, Revision 0. Released May 2010; provides data and information related to the most current long-term estimates of recharge and contaminant releases from waste contained within the engineered system in WMA C. Working Session Number 4 was held in January 2010.

- RPP-RPT-42294, *Hanford Waste Management Area C Soil Contamination Inventory Estimates*, Revision 1. Released May 2010; provides estimated contaminated soil inventories after waste is retrieved from tanks in WMA C at the Hanford Site. These estimates are expected to be updated based on the latest leak volume estimates provided in RPP-ENV-33418, *Hanford C-Farm Leak Assessments Report*, Revision 2A. Working Session Number 3 was held in October 2009.

- RPP-RPT-42323, *Hanford C-Farm Tank and Ancillary Equipment Residual Waste Inventory Estimates*, Revision 1. Released May 2010; provides the basis for chemical and radiological inventory estimates for residual waste remaining in C Farm SSTs and associated transfer equipment after tank waste is retrieved. This document is in the process of being updated based on the current retrieval process at WMA C. Working Session Number 3 was held in October 2009.

- HNF-EP-0182, *Waste Tank Summary Report for Month Ending June 30, 2014*, Revision 318. Released August 2014; provides the current state of retrieval operations for WMA C.

- RPP-RPT-56356, *Development of Alternative Digital Geologic Models of Waste Management Area C*, Revision 0. Released July 2014; provides alternative geologic models for WMA C. The first alternative model is based on the interpretations of WRPS staff, while the second alternative model is based on interpretations from Dr. Stan Sobczyk of the Nez Perce.

- RPP-PLAN-47559, *Single-Shell Tank Waste Management Area C Pipeline Feasibility Evaluation*, Revision 1. Released July 2012; provides a summary of available

information on the history, physical attributes, and inventory associated with WMA C pipelines.

- RPP-ENV-33418, *Hanford C-Farm Leak Assessments Report*, Revision 2A. Released January 2012; provides reassessment of UPR sites and tank inventory estimates in C Farm.

Ecology placed DOE under RCRA Corrective Action because wastes from the SSTs and associated facilities had leaked and appeared to have impacted groundwater during SST farm operations. To comply with this action, DOE gathered all data that would be useful in estimating past releases and their contaminant nature and extent to allow Ecology and U.S. Environmental Protection Agency (EPA) to evaluate the potential human health and environmental impacts and to identify appropriate interim corrective measures. Among the many documents created for this activity, two documents in particular provided baseline information important for the WMA C PA:

- RPP-14430, *Subsurface Conditions Description of the C and A-AX Waste Management Area*

- RPP-35484, *Field Investigation Report for Waste Management Areas C and A-AX*.

1.3 DOCUMENT ORGANIZATION

The model report package addresses three basic topics: (1) basis for development of the model, including the identification of objectives; (2) software qualifications; and (3) model implementation and parameterization. These topics are organized into seven sections within the report. Section 1 provides introductory and background information. Section 2 presents the modeling objectives. Section 3 presents the geology of WMA C and the relevant Features, Events, and Processes (FEPs) that affect flow and transport in the 200 East Area, along with the modeling assumptions and the source characteristics of the residual contamination. Section 4 describes the modeling implementation details, initial conditions, boundary conditions, and parameter values. Section 5 discusses the Subsurface Transport Over Multiple Phases (STOMP)©[2] software used to conduct the analysis. Section 6 identifies the limitations of the model, and the applicability of the results. Section 7 provides the details related to configuration management of the model inputs and outputs including the software used.

Appendix A provides a list of all the key assumptions associated with the WMA C PA including the assumptions relevant to the 3-D VSZ modeling. Appendixes B and C provide a description of the basis for the selection of hydraulic properties for HSUs identified at WMA C, and the technical basis for aquifer parameter selection and use in the WMA C PA modeling, respectively. During its operational history, a number of confirmed or suspected waste release events have occurred at WMA C. These included suspected tank leaks and known UPRs from waste transfer lines and systems. Although these suspected tank leaks and UPRs are believed to

[2] Subsurface Transport Over Multiple Phases (STOMP)© is copyrighted by Battelle Memorial Institute, 1996.

have impacted groundwater, the evaluation of their impacts to groundwater is outside the scope of this modeling.

2 MODEL OBJECTIVES

The objectives of the WMA C PA vadose zone fate and transport model include the capability to provide results that support the water resource impact evaluation and the estimation of dose at the point of assessment for the "all-pathways" exposure scenario described in DOE M 435.1-1 Chapter IV Section P. While there are no Federal requirements for protection of water resources for a radioactive waste disposal facility, the impacts from the WMA C tank residuals must comply with any applicable State or local law, regulation, or other legally applicable requirement for water resource protection [DOE G 435.1-1 Chapter IV Section P.(2)]. For water resources protection, impacts are assessed on the basis of comparison to Washington State [*Washington Administrative Code* (WAC) 246-290, "Group A Public Water Supplies," WAC 246-290-310, "Maximum contaminant levels (MCLs) and maximum residual disinfectant levels (MRDLs)"] or Federal Drinking Water Standards (EPA drinking water standards [DWSs] such as maximum contaminant levels [MCLs]), whichever are more restrictive. The point of compliance for evaluating comparisons to MCLs should be at the point of highest calculated concentration or dose beyond a 100 m buffer zone surrounding WMA C, although a larger or smaller buffer zone may be used with justification, and some volume averaging based on projected groundwater use may be appropriate (DOE M 435.1-1 Chapter IV Section P, DOE G 435.1-1 Chapter IV Section P). For the purpose of evaluating compliance with DOE O 435.1, the analysis period is to cover 1,000 years following closure of WMA C. Inherent in the modeling objectives is the expectation that the groundwater impacts or receptor doses do not exceed the performance objectives identified in DOE M 435.1-1 Chapter IV Section P.

Also included in the modeling objectives is the intent to increase confidence in the outcome(s) of the modeling. The sensitivity/uncertainty analysis extends beyond 1,000 years to calculate the maximum dose at a time period after closure. The basis and applicability for parametric values used in the base case modeling are identified, explained, and justified, as are model initial conditions, boundary conditions, and changes in properties with time. Increasing confidence also requires identifying, explaining, and if possible, evaluating the significance of the assumptions used in the development of the transport modeling and their relevance to the controlling pathways or scenarios analyzed (NCRP Report No. 152, *Performance Assessment of Near-Surface Facilities for Disposal of Low-Level Radioactive Waste*). Assumptions necessary to develop inputs to the transport models, address uncertainties or data gaps, or address linkages to other models used in the analysis are identified, justified, and shown to be consistent with the conceptual model. Overall, a thorough understanding of the implications of the uncertainty associated with the assumptions is clearly presented.

This page intentionally left blank.

3 MODEL CONCEPTUALIZATION

This section describes the modeling methodology and approach for the determination of the WMA C residual waste impacts to groundwater. A synopsis of the 3-D VSZ conceptual model and conceptual model components and the technical basis and rationale for the selection of parameters is provided here, along with supporting information and rationale. This section includes a description of the WMA C vadose zone geology and the pertinent vadose zone physical and chemical characteristics. A summary of the rationale and basis for selection of the Point of Calculation, a protectiveness metric, and the timeframe for compliance is also presented.

3.1 FEATURES, EVENTS, AND PROCESSES

The development of conceptual models and exposure scenarios for the WMA C PA builds upon work that began in 1999 at Hanford. The intent of that work was to promote consistency and completeness in the development of conceptual models to support ongoing long-term PAs (RPP-RPT-41918). The international community devised the FEPs Analysis Methodology to develop conceptual models to support nuclear waste disposal system PAs, and the FEPs methodology, with some modifications that account for Hanford's history of operations, has been successfully implemented at the Hanford Site (RPP-RPT-41918). DOE/RL-2011-50, *Regulatory Basis and Implementation of a Graded Approach to Evaluation of Groundwater Protection* identifies and describes the FEPs applicable to most vadose zone modeling applications in the 200 Areas and concludes with the development of a "basic" Hanford Site specific vadose zone conceptual model. This conceptual model provides a basis for identifying the model attributes and criteria that lead to the selection of the appropriate model type (at least two dimensions) and computer code (STOMP©) applicable to the particular needs of the WMA C PA.

The following list of key conceptual model components derives from the basic Hanford Site vadose zone conceptual model identified in DOE/RL-2011-50:

- Model domain and boundary conditions
- Geologic setting
- Source term
- Vadose zone hydrogeology and contaminant transport
- Infiltration and recharge
- Geochemistry and sorption
- Groundwater domain.

These conceptual model components are consistent with those identified in EPA guidelines for the evaluation of the protection of groundwater pathway [EPA 402-R-94-012, *A Technical Guide to Ground-Water Model Selection At Sites Contaminated with Radioactive Substances*; OSWER No. 9200.4-18, "Establishment of Cleanup Levels for CERCLA Sites with Radioactive Contamination"; and HNF-5294, *Computer Code Selection Criteria for Flow and Transport Code(s) To Be Used in Vadose Zone Calculations for Environmental Analyses in the Hanford*

Site's Central Plateau]. The principal FEPs associated with these conceptual model components include the following:

- Relatively thick vadose zone composed of sedimentary deposits (geologic setting conceptual model component)
- Semi-arid region (infiltration/recharge conceptual model component)
- Underlying unconfined aquifer (groundwater domain conceptual model component)
- Relatively limited number of contaminants of concern (COCs) in the vadose zone soils (source term) that have potential impacts to groundwater.

For the WMA C PA, the conceptual model components must account for the source release of radionuclides and non-radiological contaminants from the grouted tanks, contaminant transport through engineered barriers, and contaminant transport through the natural environment, while accounting for decay and in-growth of daughter isotopes (RPP-RPT-48490, *Technical Approach and Scope for Flow and Contaminant Transport Analysis in the Initial Performance Assessment of Waste Management Area C*). Transport through engineered barriers must take into account the degradation of the tank structures, flow of water through the waste in the tanks and contaminant releases into the vadose zone (RPP-RPT-41918). These processes include details of physical and chemical mechanisms on a refined local scale.

The key conceptual model components listed above and their associated FEPs are discussed in the following subsections. The discussion includes the rationale and basis for each of the conceptual model components, the function each conceptual model component and corresponding FEPs serve in the model, the assumptions associated with model components, and a qualitative assessment of the impact the component has on the model results.

3.1.1 Model Domain and Boundary Conditions

The model domain and boundary conditions establish both a framework and limiting conditions for the numerical model. The model domain for flow and transport in the vadose zone is represented numerically in 3-D space with one of the horizontal axes aligned in the general direction of groundwater flow. Aligning an axis with the general direction of groundwater flow allows concentrations to be calculated more easily down-gradient of the waste sites. The numerical model adapts the physical elements of the conceptual model to a Cartesian grid and also assigns numerical values to the parameters used in algorithms to represent the physical and geochemical systems and processes.

The WMA C model domain is 737.9 m (2,421 ft) northwest to southeast by 795.3 m (2,609 ft) southwest to northeast by 116 m (381 ft), vertically, extending about 12 m (49 ft) below the water table. The southwestern and northwestern boundaries of the model are 574656.09 m, 136454.41 m, and 575218.45 m, 137016.78 m, respectively (Lambert Coordinate system easting, NOAA Manual NOS NGS 5, *State Plane Coordinate System of 1983*). The southeastern and northeastern boundaries are 575177.86 m, 135932.64 m, and 575740.22 m, 136495.00 m,

respectively. The vertical base elevation of the model is nominally 95 m (NAVD88, *North American Vertical Datum of 1988*), although the bottom and top of the model domain vary spatially according to the top of basalt elevation and surface relief, respectively (RPP-RPT-56356).

A specified-flux boundary condition is applied at the surface and net infiltration rates representing recharge vary spatially and temporally along the upper boundary. The rates depend on site and surface conditions simulated, the location and physical dimensions of WMA C (recharge parameterization is discussed in Section 3.1.5), and the time of WMA C operations (RPP-RPT-44042) (Figure 3-1). The bottom boundary of the unsaturated (vadose) zone is the water table and the bottom of the model (aquifer) is defined as a vertical no flow boundary condition. Boundary conditions at the sides of the model domain are assumed to be no flow in the vadose zone and prescribed flux and prescribed head in the aquifer on the up-gradient and down-gradient boundaries, respectively.

The boundary condition in the aquifer on the upgradient boundary applies a prescribed flux calculated on the basis of the aquifer hydraulic conductivity and gradient, independent of recharge. The prescribed flux boundary condition value includes a factor to account for the fact that the thickness of the unconfined aquifer varies because of the uneven surface of the underlying basalt. To account for the non-uniform aquifer thickness from the underlying basalt boundary, the nominal flux rate calculated as the product of the hydraulic conductivity and gradient (base case values of 11,000 m/day and 2.0×10^{-5} m/m, respectively; see Section 3.1.7) is proportioned according to the ratio of the average aquifer area throughout the model domain (9,440 m^2) and the aquifer area along the northwest boundary (6,151 m^2) where the prescribed flux is applied. The aquifer area refers to the area perpendicular to the direction of groundwater flow.

3.1.2 Geologic Setting

The geological setting information presented here is a summary and synopsis of the information presented in RPP-RPT-46088 and RPP-RPT-56356. Waste Management Area C is located near the eastern edge of the 200 East Area on the Hanford Site on what is known colloquially as the Central Plateau. The vadose zone is ~80 to 100 m (262.4 to 328.1 ft) thick, and there are ~68 m between the base of the WMA C 100-series tanks and the present-day water table. Waste Management Area C lies within the gravel-dominated Hanford formation unit H1 (H1) in the vadose zone. The stratigraphic units recognized in the WMA C area include the following.

- Recent (Holocene) backfill material (~10 m thick).
- Hanford formation unit H1 – Gravel-dominated sequence (~10 m to 30 m thick).
- Hanford formation unit H2 (H2) – Sand-dominated sequence (~45 m to 70 m thick). Alternative Geologic Model II includes two subunits of H2 (based on interpretations from Dr. Stan Sobczyk of the Nez Perce, RPP-RPT-56356):
    - Hanford H2 Coarse subunit (gravel/coarse-grained facies that underlies the H2 sands)

  - Hanford H2 Silty sand subunit (silty sand lower permeability laminations/lenses).

- Hanford formation unit H3 (H3) – gravel-dominated sequence (~0 m to 20 m thick).

- Columbia River Basalt Group.

As part of the RCRA facility investigations (DOE/ORP-2008-01, *RCRA Facility Investigation Report for Hanford Single-Shell Tank Waste Management Areas* and RPP-PLAN-39114, *Phase 2 RCRA Facility Investigation/Corrective Measures Study Work Plan for Waste Management Area C*), the geologic strata underlying WMA C has been characterized in conjunction with soil sampling and borehole logging for radionuclides and hazardous waste constituents. The geophysical and geologic logging from the boreholes has been used to identify the elevations of tops of the geologic units in the vicinity of WMA C. Specifically, potassium, uranium, thorium (K-U-T) data from geophysical logs were used to map the tops of the different geologic units at WMA C (RPP-RPT-56356).

In discussions associated with the 2009 to 2011 working sessions and additional discussions with regulators in 2013 and 2014, two alternative geological models were proposed and developed on the basis of the data discussed in the preceding paragraph. Both of these models have been incorporated into the WMA C PA as a means to explore the performance implications of the alternative conceptualizations. This section provides a brief summary of important differences between these alternative models. Details on the basis for their development are provided in RPP-RPT-56356 and only briefly summarized here.

The primary difference between the two alternative models concerns whether or not a sandy gravel facies followed by a silty sand layer exist at the bottom of the H2 subunit in the vicinity of WMA C. The K-U-T data (i.e., a lower gross gamma and potassium count) indicates that there is a coarsening of the sand at the bottom of the H2 that turns into more of a sandy gravel. Underlying this sandy gravel facies is a silty sand unit that presents a strong potassium peak and an occasional but strong natural uranium peak. The difficulty in making the determination between the two alternative models is that there are few direct pushes or dry wells that go deep enough in which there are both good geophysical logs and geologic logs (with drill cuttings). For the most part, only the nearby groundwater wells extend to a sufficient depth. The drill cuttings from nearby ground wells indicate that there is a definite fining of the sands along with some silty sands found at the vertical location as indicated by the K-U-T data in the geophysical logs, but a competent silt layer was not observed. Alternative Model I does not distinguish the sandy gravel and underlying silty sand unit distinctly from Hanford H2, while Alternative Model II does distinguish them. The significance of distinguishing these layers is that their differing characteristics, as expressed by different soil hydraulic property values, could potentially cause increased lateral movement in the vadose zone. A series of fence diagrams showing the differences between the two models within WMA C is given in RPP-RPT-56356. The fence diagram for both these models running southwest to northeast through the center of WMA C is given in Figure 3-2.

Figure 3-1. Plan View of Waste Management Area C Performance Assessment Model Domain Showing the Horizontal Distribution and Surface Type of the Irregularly-Spaced Calculation Nodes. The resolution increases in the area of Waste Management Area C.

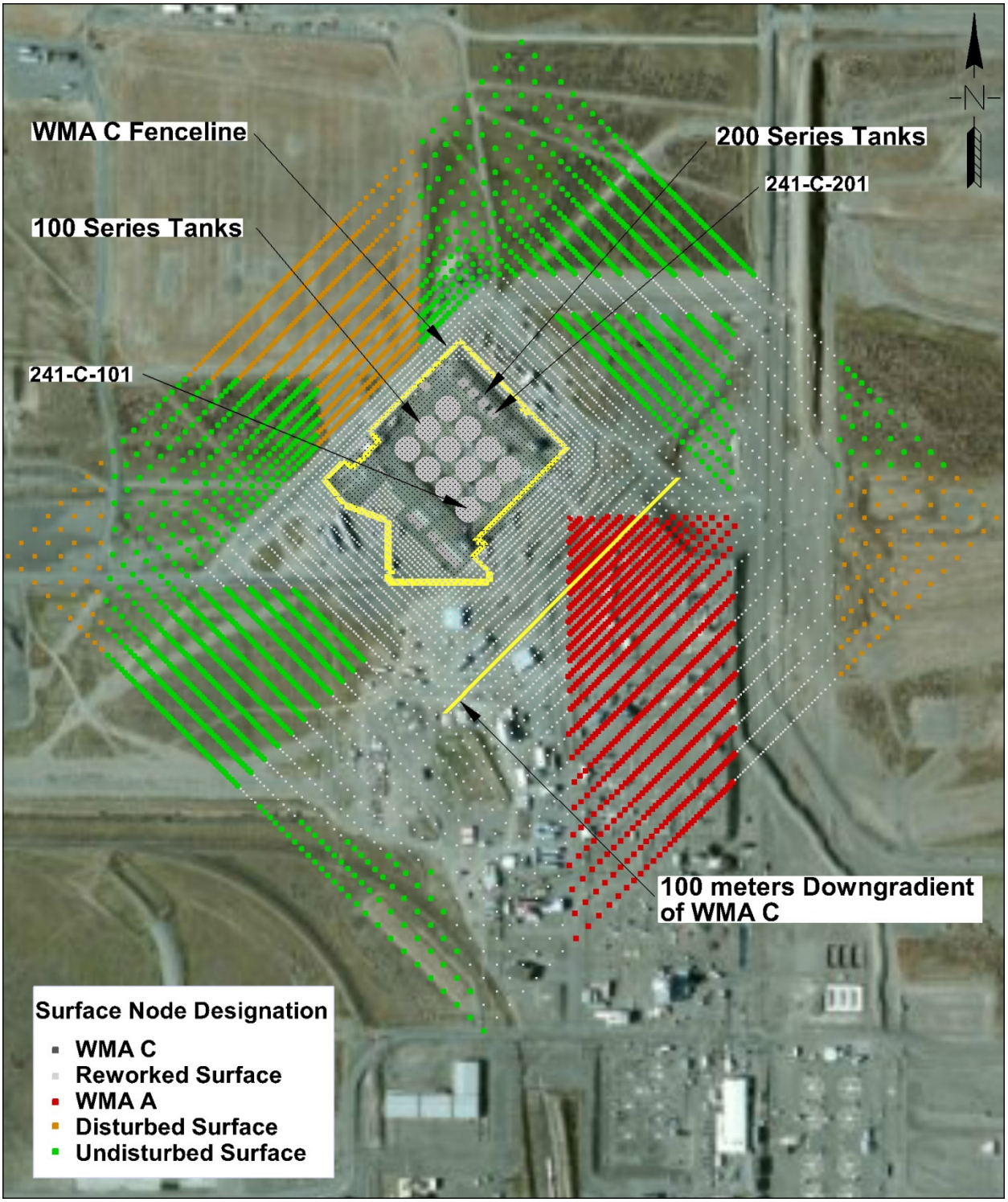

WMA = Waste Management Area

Figure 3-2. Fence Diagram of Alternative Geologic Models Used in the Performance Assessment for Waste Management Area C.

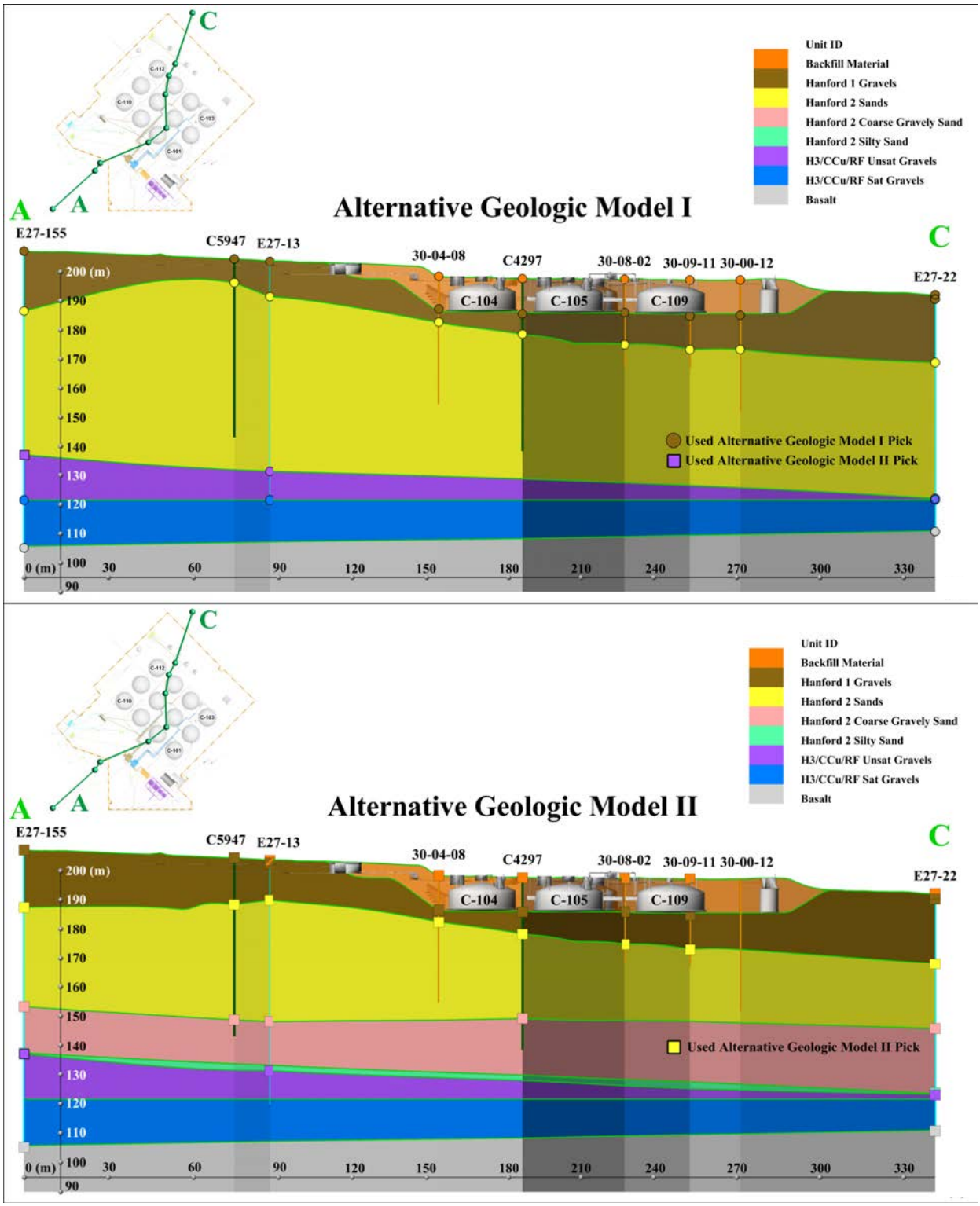

H3/CCu/RF = undifferentiated H3, Cold Creek unit and Ringold Formation

Reference: RPP-RPT-56356, *Development of Alternative Digital Geologic Models of Waste Management Area C.*

Although the intent of this MPR is to address the base case model development and parameters, this MPR includes the description and parameters applicable to Alternative Model II because it represents an alternative conceptualization of the entire geologic model and not just a single parameter variation.

3.1.3 Source Term

The source term conceptual model component defines the characteristics of the inventory and the release of residual waste from the tanks, ancillary equipment, and pipelines. RPP-RPT-42323 presents the basis for chemical and radiological inventory estimates for residual waste remaining in C Farm SSTs and associated transfer equipment after tank waste is retrieved and the radionuclides are decayed to January 1, 2020. As discussed in RPP-RPT-42323, a conservative or upper bounding bias is built into the inventory estimating process and thus the inventory estimates. Within RPP-RPT-42323, residual inventories in retrieved tanks are provided in Appendix B.2, estimated residual inventories in unretrieved tanks are provided in Appendix C.2, and estimated residual inventories in ancillary equipment are provided in Appendix C.3.

RPP-RPT-58948, *Model Package Report System Model for the WMA C Performance Assessment and RCRA Closure Analysis Version 1.0* presents a detailed discussion about the theoretical and empirical development and applicability of the equations and the parameters incorporated into the release functions developed for the individual radionuclides and non-radiological contaminants. That discussion and those equations, and the resulting release functions, are not repeated in this report. The discussion presented here only provides context and rationale for how the STOMP© fate and transport model imports the release functions and distributes them beneath the individual tanks, the vault, and the pipelines.

Radionuclide and non-radiological contaminant releases from the grout inside the tanks and 244-CR vault are controlled by diffusion processes while the grout is assumed to remain intact. Prior to diffusing out of the tanks or vault, analytes must release from the grout matrix into the grout pore space. Both mineral phase solubility-limited and matrix degradation rate-limited processes have been incorporated in the tank and 244-CR vault source term analysis for the key radionuclides and non-radiological contaminants ^{99}Tc, chromium, and uranium. In particular, the following matrix release models are used, which are based on empirical evidence:

- Matrix-degradation-rate-based release of ^{99}Tc that considers an initial 6% fraction of the ^{99}Tc inventory to be instantaneously available for release while the remaining 94% fraction undergoes relatively slower release at the fractional rate of 6×10^{-4} day^{-1}

- Solubility-controlled releases of uranium that impose a solubility limit of 1×10^{-4} M for 1,000 years followed by solubility limit of 1×10^{-6} M thereafter

- Dissolved concentration limited release for chromium that imposes a dissolved concentration upper limit of 2,000 µg/L.

For the other analytes evaluated in the WMA C PA, conservative source-term calculations are performed whereby all the analytes are assumed to be instantly and completely available in

solution for immediate diffusive release within the tank and 244-CR vault residual waste volume. While the tank (and ancillary equipment) in-fill material remains intact, it is assumed that releases occur by a diffusion process through thin water films within the pore spaces of the 8-in. combined thickness of the grout and concrete layer at the base of the tank (the presence of the steel plate is ignored). The effective diffusion coefficient for all radionuclides and non-radiological contaminants diffusing through the concrete is estimated to be 3×10^{-8} cm^2/s. Release mechanisms from the pipelines and degraded tank and vault grout include both advection and diffusion, up to the imposed solubility limit of uranium and the imposed dissolved concentration limit for chromium.

In the STOMP© flow and transport model the grouted residual releases are assumed to occur uniformly through the entire base of the tank or vault. The nodes representing the tanks and vault structures are inactive within the flow and transport model domain so the releases are located in the nodes immediately below the structures. The base of each 100-series tank consists of 32 nodes; the base of each 200- and 300-series tank consists of 2 nodes, and the base of the 244-CR vault consists of 8 nodes. Thus the quantity that the release functions indicate is released from the 100-series, 200- and 300-series, and 244-CR vault is divided by 32, 2, and 8, respectively. The pipeline residual releases are assumed to occur uniformly throughout the entire area of WMA C. The pipelines are assumed to be at the depth where the 100-series tanks begin to dome upward (Figure 3-3). This places the pipeline releases approximately 8.4 m (27.5 ft) above the tank releases. The pipeline area excludes the nodes occupied by the tank domes because those nodes are inactive. This area represents approximately 22,720 m^2 and occupies 1,413 nodes in the model[3].

3.1.4 Vadose Zone Hydrogeology and Contaminant Transport

The flow and transport pathway process used for the WMA C PA vadose zone modeling is porous media continuum flow. Porous media continuum transport in unsaturated media is regarded as the fundamental process for modeling contaminant fate and transport behavior in the vadose zone at the Hanford Site (DOE/RL-2011-50). The porous media continuum assumption and the soil relative permeability/saturation/capillary pressure relations provide the basis for vadose zone flow and transport equations contained in STOMP© (PNNL-11216, *STOMP Subsurface Transport Over Multiple Phases Application Guide*; PNNL-12030, *STOMP Subsurface Transport Over Multiple Phases Version 2.0 Theory Guide*).

The vadose zone at the Hanford Site is composed of sediments ranging in particle size associated with gravels to silts or clays, and different flow and transport parameter values (hydraulic conductivity, bulk density, and dispersivity) characterize each geologic unit. Because the intent of the model is to evaluate overall and eventual radionuclide impacts to groundwater, the model estimates bulk (or mean) flow and radionuclide transport behavior in the vadose zone. The flow and transport model incorporates parameter upscaling, variable (moisture-dependent) anisotropy,

[3] Alternative conceptualizations of the pipeline releases include the assumption that the releases occur from a depth about midway between the base of the tank domes and the bottom of the tanks, or that releases occur immediately below the tanks, which is the same assumption about the starting depth of the past releases from the tanks. These alternate assumptions about the starting depth of the pipeline releases can provide some insight into the impact the release depth has on the results.

and the equivalent homogeneous medium (EHM) approach to approximate the flow and transport parameters and account for the substantial heterogeneity present within the various geologic units.

Figure 3-3. Elevation of Pipeline Source in Waste Management Area C Three-Dimensional Model Domain.

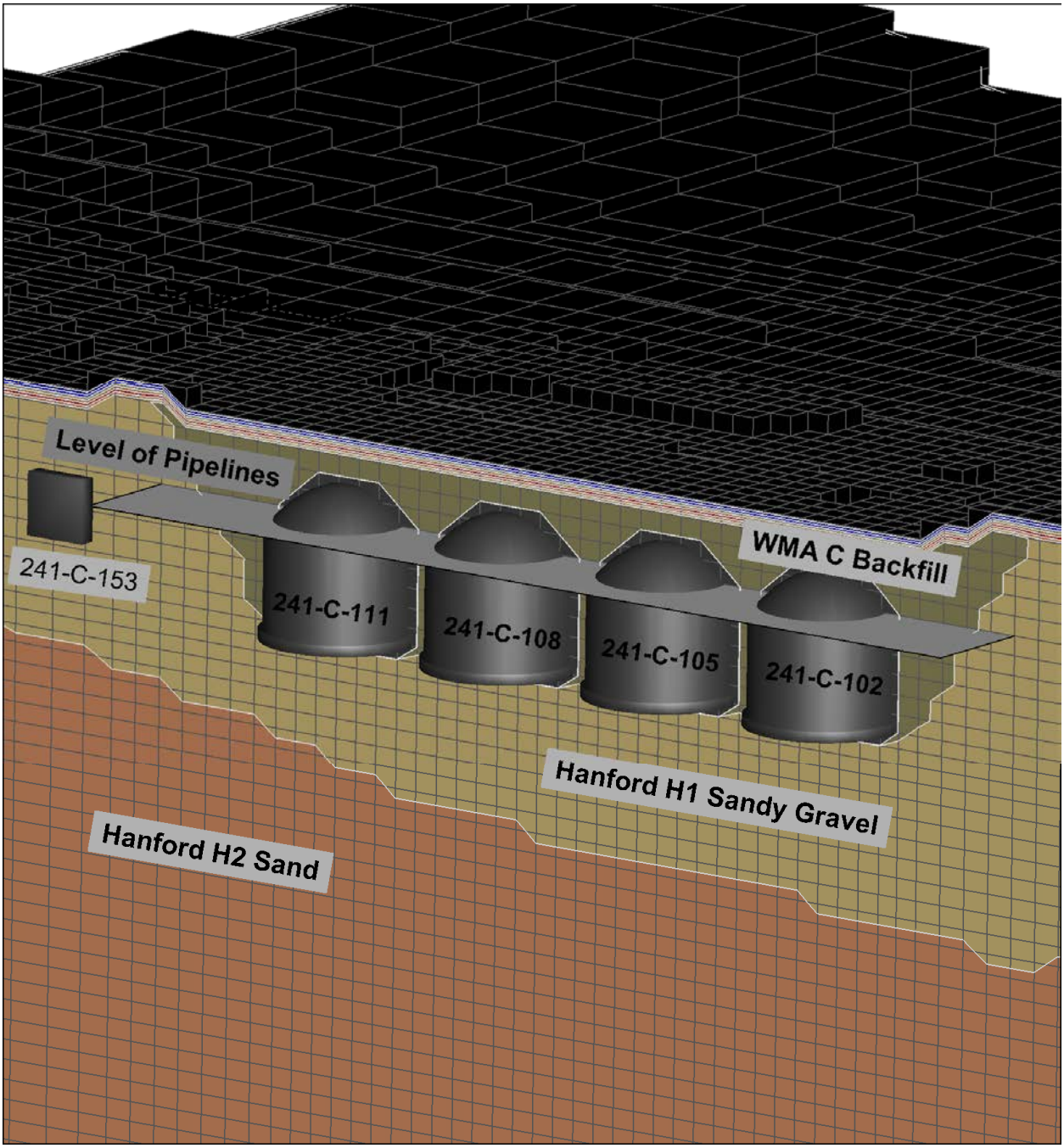

WMA = Waste Management Area

The vadose zone hydrogeology and transport information presented here is a summary and synopsis of the information presented in Appendix B. The process used to develop estimates of hydraulic properties needed for the WMA C PA included an iterative step. After estimating hydraulic properties representative of the major HSUs identified at WMA C from sample data collected at different sites with similar sediments within the 200 Area, simulation results of the WMA C vadose zone flow field were cross-checked against measured field moisture contents for the different WMA C HSUs. This step allowed an updating of the properties presented in RPP-RPT-46088 by incorporating data sets developed from data collected at other nearby sites within the 200 Areas that are consistent with WMA C field data.

Table 3-1 lists the upscaled composite-fitted van Genuchten-Mualem parameters for the various strata at the WMA C site ("A Closed-form Equation for Predicting the Hydraulic Conductivity of Unsaturated Soils" [van Genuchten 1980]; "A New Model for Predicting the Hydraulic Conductivity of Unsaturated Porous Media" [Mualem 1976]; EPA/600/2-91/065, *The RETC Code for Quantifying the Hydraulic Functions of Unsaturated Soils*). A simultaneous fit of both laboratory-measured moisture retention and unsaturated conductivity data was used in this work, and all five unknown parameters θ_r, θ_s, α, n, and K_s, with m=1-1/n (van Genuchten 1980) were fitted to the data via a code named RETention Curve (RETC) (EPA/600/2-91/065). K_s is treated as a fitted parameter during the curve fitting process in order to obtain a better agreement with experimental data for the region of interest (i.e., relatively dry moisture regime). Estimated unsaturated conductivities, based on saturated conductivity (K_s) and the van Genuchten retention model parameters, have been shown to differ by up to several orders of magnitude with measured conductivities at the dry end (e.g., "Evaluation of van Genuchten-Mualem Relationships to Estimate Unsaturated Hydraulic Conductivity at Low Water Contents" [Khaleel et al. 1995]). The pore size distribution factor, ℓ (Mualem 1976) was kept fixed at 0.5 during the simultaneous fitting.

Table 3-1. Composite van Genuchten-Mualem Parameters for Various Hydrostratigraphic Units at the Waste Management Area C Site Used in the Base Case Evaluations of Alternative Geologic Models I and II (Appendix B).

Hydrostratigraphic Unit	Number of Samples	θ_s	θ_r	α (1/cm)	n	ℓ	Fitted K_s (cm/s)
Backfill (Gravelly)	10	0.138	0.010	0.021	1.374	0.5	5.60E-04
Hanford H1/H3 (Gravel-dominated)	15	0.171	0.011	0.036	1.491	0.5	7.70E-04
Hanford H2 (Sand-dominated)	44	0.315	0.039	0.063	2.047	0.5	4.15E-03
Hydrostratigraphic Units only applicable to Alternative Geologic Model II							
Hanford H2 – Gravel/coarse sand subunit*	not applicable (95th Percentile)	0.265	0.002	0.108	1.724	0.5	1.68E-02
Hanford H2 – Silty-sand subunit*	not applicable (5th Percentile)	0.354	0.0289	0.040	1.633	0.5	1.79E-03

* Hydraulic properties of these units are only used in numerical model simulation of Alternative Geologic Model II. As an initial estimate of these properties, the hydraulic properties associated with the 5th and 95th percentile realizations of unsaturated hydraulic conductivity curves developed in the Uncertainty and Sensitivity Analysis for the Hanford H2 sand unit were considered to be representative of the Hanford H2 gravel/coarse sand and the Hanford H2 silty sand subunits.

A stochastic model of variable moisture or tension-dependent anisotropy provides the framework for upscaling small-scale measurements to the effective (upscaled) properties for the large-scale vadose zone (Application of Stochastic Methods to Transient Flow and Transport in Heterogeneous Unsaturated Soils [Polmann 1990]). The upscaling processes factor the inherent spatial variability that occurs on different scales in heterogeneous media into the field scale parameter estimates ("Stochastic analysis of moisture plume dynamics of a field injection experiment" [Ye et al. 2005]; "Estimation of effective unsaturated hydraulic conductivity tensor using spatial moments of observed moisture plume" [Yeh et al. 2005]). Specific upscaled flow parameters include moisture retention, saturated, and unsaturated hydraulic conductivity. Upscaled transport parameters include bulk density, diffusivity, sorption coefficients, and macrodispersivity. Detailed discussion of the Polmann (1990) model and the derivation of the upscaled parameters are presented in Appendix B.

For the Alternative Geologic Model II evaluation, the Hanford H2 gravel/coarse sand subunit was assumed to be more transmissive and the Hanford H2 silty sand less transmissive than the Hanford H2 sand. Therefore, as an initial estimate of these properties, the hydraulic properties associated with the 5th and 95th percentile realizations of unsaturated hydraulic conductivity curves developed for the Hanford H2 sand unit were considered representative of the Hanford H2 gravel/coarse sand and the Hanford H2 silty sand subunits, respectively.

The effective transport parameters include dispersivity estimates applicable to the field scale, (referred to as macrodispersivity), bulk density, and diffusivity. The transport parameters are all spatially variable. Field-scale heterogeneities induce variations in bulk density, hydraulic conductivity and matric potential (or soil moisture content), which influence dispersivity and diffusivity. According to "Solute transport in heterogeneous porous formations" (Dagan 1984) macrodispersivity reaches a constant, asymptotic value after the solute travels a few tens of correlation scales (~50 cm) of the hydraulic conductivity field, therefore the use of a constant (asymptotic) macrodispersivity value is considered appropriate in the WMA C PA simulations. As detailed in Appendix B, on the basis of results of numerical simulation, stochastic theory, and 200 Areas experimental data, the recommendation is to use a longitudinal macrodispersivity value of 25 cm for the H2 sand unit in the WMA C PA base case. For H1/H3/Backfill sediments, the recommendation is to use a longitudinal macrodispersivity value of 20 cm (Appendix B). The transverse macrodispersivity is typically much lower; in saturated media, it may range from 1 to 10% of the longitudinal macrodispersivity ("Three-dimensional stochastic analysis of macrodispersion in aquifers" [Gelhar and Axness 1983]). In the absence of unsaturated media experimental data, the recommendation is to use a transverse macrodispersivity 1/10th of the longitudinal macrodispersivity. The estimated values of macrodispersivity applicable to the scale of the WMA C PA model for the base case are shown in Table 3-2.

Table 3-2. Macrodispersivity Estimates for Various Hydrostratigraphic Units at Waste Management Area C Used in the Base Case Evaluations of Alternative Geologic Models I and II (Appendix B).

Hydrostratigraphic Unit	A_L (cm)	A_T (cm)
Backfill (Gravelly)	~20	2
Hanford H1/H3 (Gravel-dominated)	~20	2
Hanford H2 (Sand-dominated)	~25	2.5
Hydrostratigraphic Units only applicable to Alternative Geologic Model II		
Hanford H2 – Gravel/coarse sand subunit	~25	2.5
Hanford H2 – Silty-sand subunit	~25	2.5

The effective, large-scale estimates for bulk density are the averages of small-scale laboratory measurements (Table 3-3 and Appendix B). It is assumed that the effective, large-scale diffusion coefficients for all strata in the vadose zone at the WMA C site are a function of volumetric moisture content, θ, and can be expressed using the Millington-Quirk ("Permeability of Porous Solids" [Millington and Quirk 1961]) empirical relation:

$$D_e(\theta) = D_0 \frac{\theta^{10/3}}{\theta_s^2} \tag{4-1}$$

Where:

$D_e(\theta)$ = the effective diffusion coefficient of an ionic species
D_0 = the effective diffusion coefficient for the same species in free water
θ = the localized volumetric moisture content.

Table 3-3. Effective Bulk Density Estimates for Various Hydrostratigraphic Units at Waste Management Area C Used in the Base Case Evaluations of Alternative Geologic Models I and II (Appendix B).

Hydrostratigraphic Unit	ρ_b, (g/cm^3)
Backfill (Gravelly)	2.13
Hanford H1/H3 (Gravel-dominated)	2.05
Hanford H2 (Sand-dominated)	1.71
Hydrostratigraphic Units only applicable to Alternative Geologic Model II	
Hanford H2 – Gravel/coarse sand subunit	1.83
Hanford H2 – Silty-sand subunit	1.61

The tortuosity formulation in the Millington-Quirk model is based on theoretical considerations absent from other empirical models and accounts for the ranges of moisture contents present in

the vadose zone around WMA C. The molecular diffusion coefficient for all species in pore water is assumed to be 2.5×10^{-5} cm^2/sec (WHC-SD-WM-EE-004, *Performance Assessment of Grouted Double-Shell Tank Waste Disposal at Hanford*), which is consistent with and representative of values used in other Hanford PAs.

3.1.5 Infiltration and Recharge

RPP-RPT-44042 supported the WMA C PA working sessions by providing and summarizing data and information related to the long-term estimates of recharge applicable to the WMA C PA. The data and information contained in RPP-RPT-44042 serve as the basis for the base case recharge estimates. The magnitude of the recharge estimates for soils at the Hanford Site varies as a function of the soil type, condition of the vegetation cover, and soil integrity (e.g., disturbed versus undisturbed). The range of recharge values reported in RPP-RPT-44042 represents distinct populations of data based on lysimetry, isotopic measurements, and interpretation and extrapolation (in some instances) by Hanford Site subject matter experts. The natural background recharge rates represent a population for natural vegetated conditions. The range of values for operational conditions represents a population of recharge rates for vegetation-free disturbed soil. Table 3-4 presents a summary of the base case recharge rates applied to the different surface types.

The design for the WMA C surface barrier at closure has not been finalized but it is expected to function comparably to a Modified RCRA Subtitle C Barrier, which PNNL-16688, *Recharge Data Package for Hanford Single-Shell Tank Waste Management Areas* indicates should function similarly to the Prototype Hanford Barrier. Summary of data collected over 13 years at the Prototype Hanford Barrier (PNNL-17176, *200-BP-1 Prototype Hanford Barrier Annual Monitoring Report for Fiscal Years 2005 Through 2007*; DOE/RL-93-33, *Focused Feasibility Study of Engineered Barriers for Waste Management Units in the 200 Areas*) indicates that infiltration through the prototype is much less than 0.1 mm/yr, and evaluations of the design using lysimeter data indicate that the barrier is capable of limiting recharge to this amount even with a complete lack of vegetation ("Multiple-Year Water Balance of Soil Covers in a Semiarid Setting" [Fayer and Gee 2006]). However, for PA simulations involving WMA C with a functioning surface barrier, a base case recharge rate of 0.5 mm/yr is assumed, which is consistent with the drainage design specification in DOE/RL-93-33.

At the end of 500 years, the surface barrier performance is assumed to degrade to permit an infiltration rate of 3.5 mm/yr and maintain that infiltration rate for the remainder of the sensitivity and uncertainty analysis time frame. No quantifying data are available for specifying the performance of the barrier top after its design life. According to PNNL-13033, *Recharge Data Package for the Immobilized Low-Activity Waste 2001 Performance Assessment*, the erosion of the silt loam layer and deposition of dune sand on the barrier is not likely to alter the barrier performance significantly. The value of 3.5 mm/yr (0.14 in./yr) corresponds to the recharge in an undisturbed area, which indicates that native vegetation is assumed to reclaim the land.

Although the side slopes and berm are likely to function and perform differently than the surface of the barrier, they are included as part of the barrier surface. The impact of the side slopes on

the overall recharge rate is expected to be relatively minor. The sandy gravel/gravelly sand barrier side slope and berm are assumed eventually to resemble a Burbank loamy sand, and if that assumption is valid, then PNNL-16688 indicates that the long-term recharge rate for that soil type is 1.9 mm/yr, which is less than the value of 3.5 mm/yr used in the analysis for the degraded barrier surface.

Table 3-4. Base Case Recharge Rate (Net Infiltration) Estimates for Surface Conditions during the Pre-Construction, Operational, and Post-Closure Periods.

Period	Waste Management Area (WMA) C Region and Surface Condition	Base Case Value of Recharge Rate (mm/yr)
Pre-construction (before 1944)	Undisturbed region (Rupert sand with vegetation)	3.5
Operational period (1945 to 2020)	Undisturbed region (Rupert sand with vegetation)	3.5
	WMA C Surface region (Gravel without vegetation)	100
	WMA A Surface region (Gravel without vegetation)	100
	Disturbed revegetated region (Rupert sand with vegetation)	22[a]
	Disturbed unrevegetated region (Rupert sand with no vegetation)	63[b]
Early post-closure (2020 to 2520)	Undisturbed region (Rupert sand with vegetation)	3.5
	WMA C Surface region (Surface barrier with vegetation)	0.5
	WMA A Surface region (Surface barrier with vegetation beginning in 2050)	0.5
	Disturbed revegetated region (Rupert sand with vegetation beginning in 2050 with vegetation recovery completed in 2080)	3.5
	Disturbed unrevegetated region (Rupert sand with no vegetation until vegetation recovery begins in 2050 and completes in 2080)	3.5
Late post-closure (2520 to 3020 and beyond)	Undisturbed region (Rupert sand with vegetation)	3.5
	WMA C Surface region (Surface barrier with vegetation)	3.5
	WMA A Surface region (Degraded surface barrier with vegetation begins in 2550)	3.5
	Disturbed revegetated region (Rupert sand with vegetation recovery completed in 2080)	3.5
	Disturbed unrevegetated region (Rupert sand with vegetation recovery completed in 2080)	3.5

[a]PNNL-14702, *Vadose Zone Hydrogeology Data Package for Hanford Assessments* and DOE/RL-2007-27, *Feasibility Study for the Plutonium/Organic-Rich Process Condensate/Process Waste Group Operable Unit: Includes the 200-PW-1, 200-PW-3, and 200-PW-6 Operable Units.*

[b]PNNL-16688, *Recharge Data Package for Hanford Single-Shell Tank Waste Management Areas*, and DOE/RL-2007-27.

General source: RPP-RPT-44042, *Recharge and Waste Release within Engineered System in Waste Management Area C.*

RPP-RPT-44042 does not include information about recharge occurring in areas outside of WMA C apart from those assumed to remain undisturbed. As indicated in Figure 3-1, much of the area outside of WMA C but within the model domain has been impacted by Hanford operations. These areas include disturbed areas that allow vegetation, such as the surface of burial grounds, and disturbed areas immediately outside of WMA C that are reworked such that vegetation does not grow. Very few recharge data are available for these types of conditions. PNNL-14702, *Vadose Zone Hydrogeology Data Package for Hanford Assessments* estimates that plant cover consisting of grasses will limit recharge rates to between 22 and 26 mm/yr in the eastern portion of 200 East Area, and DOE/RL-2007-27, *Feasibility Study for the Plutonium/Organic-Rich Process Condensate/Process Waste Group Operable Unit: Includes the 200-PW-1, 200-PW-3, and 200-PW-6 Operable Units* applies the estimate of 22 mm/yr to represent ground where only shallow rooted vegetation is assumed to revegetate the surface. Therefore, the WMA C PA base case applies a recharge estimate of 22 mm/yr to areas outside of WMA C disturbed in this manner.

Construction and operations outside the WMA C removed the surface soil, broke up any near-surface layering, and exposed Hanford formation sands. These sediments tend to be coarser than the original soil, and as indicated in photographs of the area around WMA C, plants have difficulty growing on them. PNNL-14702 recommends a recharge rate of 63 mm/yr for this type of surface. This value is supported by drainage data collected from the 300 North Lysimeter, which contains coarse Hanford formation material screened to less than 1% gravel (material > 2 mm); the long-term recharge rate averaged 62 mm/yr from 1981 to 2005 (PNNL-16688). DOE/RL-2007-27 applies the recharge estimate of 63 mm/yr to represent ground conditions during the operational period of the cribs where Hanford Sand remains disturbed with no vegetation. Therefore, the WMA C PA base case applies a recharge estimate of 63 mm/yr to areas outside of WMA C disturbed similarly.

3.1.6 Geochemistry and Sorption

The geochemistry conceptual model component involves the partitioning behavior or sorption characteristics regarding release, retardation, and attenuation mechanisms and any simplifying assumptions for specific radionuclides and non-radiological contaminants. The key aspects of this geochemistry conceptual model, and its applicability to the Hanford Site 200 Areas, include the following, which are discussed in detail in DOE/RL-2011-50:

- The rationale for the simplifying assumption that the use of a linear K_d isotherm is a reasonable conservative description for the release and attenuation of radionuclides in the context of providing an upper-bounding condition
- The rationale and source(s) of the data used in the selection of radionuclide K_d values
- The rationale for the use of a single K_d in the vadose zone units.

The geochemistry conceptual models for the Hanford Site are based on extensive laboratory studies, testing, and measurements of adsorption and desorption coefficients under saturated and unsaturated conditions involving Hanford Site-specific sediments, contaminants, and conditions

(DOE/RL-2011-50; RPP-RPT-46088; PNNL-13895, *Hanford Contaminant Distribution Coefficient Database and Users Guide*; PNNL-16663, *Geochemical Processes Data Package for the Vadose Zone in the Single-Shell Tank Waste Management Areas at the Hanford Site*; and PNNL-17154, *Geochemical Characterization Data Package for the Vadose Zone in the Single-Shell Tank Waste Management Areas at the Hanford Site*). The basis for the K_d values used to approximate the transport of the radionuclides and non-radiological contaminants and the gravel corrected base case values are presented in Table 3-5. The differing values for the different geologic units represent the adjustment of values resulting from the approximate gravel content of each unit.

Table 3-5. Summary of the Waste Management Area C Performance Assessment Base Case K_d (mL/g) Values.

Radionuclide or Non-radiological Contaminant	Gravel Corrected K_d (mL/g)				
	Backfill	Hf1	Hf2	H3	Reference Basis
Carbon-14 (C-14)	0.46	0.58	0.8	0.58	PNNL-17154
Cobalt/Cobalt-60 (Co/Co-60)	0	0	0	0	PNNL-17154
Chromium (Cr)	0	0	0	0	PNNL-17154
Fluoride (F)	0	0	0	0	PNNL-17154
Tritium (H-3)	0	0	0	0	PNNL-17154
Iodine-129 (I-129)	0.09	0.12	0.16	0.12	PNNL-17154
Niobium-93m (Nb-93m)	0	0	0	0	PNNL-16663
Nitrite (NO2)	0	0	0	0	PNNL-17154
Nitrate (NO3)	0	0	0	0	PNNL-17154
Radon-222 (Rn-222)	0	0	0	0	None
Selenium/Selenium-79 (Se/Se-79)	0.05	0.06	0.08	0.06	PNNL-17154
Tin/Tin-126 (Sn/Sn-126)	0.23	0.29	0.4	0.29	PNNL-17154
Technetium-99 (Tc-99)	0	0	0	0	PNNL-16663
Total Uranium/Uranium-238 (U Total/U-238*)	0.28	0.35	0.48	0.35	RPP-RPT-46088
Tributyl Phosphate (TBP)	1.89	0.87	1.1	1.5	RPP-RPT-46088

*The base case analysis also includes Uranium-232, Uranium-233, Uranium-234, Uranium-235, Uranium-236, and the Uranium-238 daughter products, but these isotopes were not evaluated directly using the Subsurface Transport Over Multiple Phases (STOMP)© model.

Subsurface Transport Over Multiple Phases (STOMP)© is copyrighted by Battelle Memorial Institute, 1996.

References:

PNNL-16663, *Geochemical Processes Data Package for the Vadose Zone in the Single-Shell Tank Waste Management Areas at the Hanford Site*.
PNNL-17154, *Geochemical Characterization Data Package for the Vadose Zone in the Single-Shell Tank Waste Management Areas at the Hanford Site*.
RPP-RPT-46088, *Flow and Transport in the Natural System at Waste Management Area C*.

The radionuclides listed in Table 3-5 are limited to those with K_d values less than 3 mL/g (prior to any adjustments because of gravel content) because the results of the screening analysis indicated that radionuclides with K_d values greater than 3 mL/g did not impact groundwater within the 10,000-year sensitivity-uncertainty timeframe (see Section 4.5, Screening).

3.1.7 Groundwater Domain

The integrated, saturated-unsaturated, 3-D WMA C model calculates groundwater concentrations of contaminants approximately 100 m downgradient of the WMA C fenceline that are estimated to occur several hundred to several thousand years into the future. The unconfined aquifer flow and transport parameters play a critical role in WMA C PA modeling because of the dilution that occurs as recharge containing contaminants enters the aquifer. Additional dilution and concentration attenuating dispersion occurs as the contaminants travel through the aquifer. The dilution and dispersion are strongly dependent on the groundwater flux, which is a rate measure defined as the flow through a defined area. Groundwater flow beneath WMA C has been difficult to measure historically because the hydraulic gradient is very small and the hydraulic conductivity is very large in this region of the Hanford Site.

The groundwater in the aquifer system in the vicinity of WMA C has been studied extensively as part of the site characterization as discussed in RPP-RPT-46088 and Appendix C (Figure C-5). The groundwater conceptual model for WMA C includes the uppermost unconfined aquifer system that exists within a channel eroded by the cataclysmic floods of the Pleistocene. The base of the aquifer is the underlying basalt surface. The undifferentiated lower sands and gravels associated with the Hanford formation, Cold Creek unit, and the Ringold Formation (Unit A) that comprise the aquifer sediments are simply categorized as saturated Hanford H3 sediments in the model. The thickness of the uppermost aquifer beneath WMA C is approximately 12 m (39 ft). The model results provided represent concentrations in the upper 5 m (16.4 ft) of the aquifer. The 5-meter vertical interval corresponds to the well screen length of a conceptual groundwater monitoring well. The basis for that delimiter to the groundwater concentrations calculation is presented in section 3.1.8, Point of Calculation, Protectiveness Metric, and Timeframe Considerations. The aquifer, identified as Hanford H3 – aquifer, is separated from that portion of the Hanford H3 above the water table, reflecting the distinctly different saturation conditions.

For the WMA C PA modeling, the unconfined aquifer is treated as an EHM that requires parameterization for the appropriate scale. Effective parameterization for WMA C saturated media hydraulic conductivity appears to be best achieved via a field-scale calibrated regional groundwater model which accounts for appropriate local-scale boundary conditions, flow configuration, and history matching of well head data (Appendix C). The Central Plateau Groundwater Model (CPGWM, CP-47631, *Model Package Report: Central Plateau Groundwater Model Version 6.3.3*) provides calibrated hydraulic conductivity estimates for the model layers and HSUs present within the aquifer in the vicinity of WMA C. The thicknesses of the different aquifer HSUs are mapped from the CPGWM onto the WMA C PA STOMP© model flow domain. An averaging scheme weighted according to HSU thickness provides estimates of the EHM effective saturated hydraulic conductivity and the hydraulic gradient.

The weighted average of hydraulic conductivity of the CPGWM HSUs mapped onto the WMA C flow domain indicates that the effective STOMP© EHM saturated hydraulic conductivity is approximately 11,000 m/day. As discussed previously, field-scale calibrated groundwater models provide an effective parameterization for WMA C saturated media hydraulic conductivity for the overall dimensions of the WMA C PA model domain. The hydraulic gradient is calculated from a planar rectangular window (300 m × 200 m) in the CPGWM having an unconfined aquifer depth that encompasses most of WMA C flow domain (Figure 3-4) by taking into account the net volumetric flux through the domain. Volumetric flux through the window is divided by the vertical cross-sectional area of the aquifer and the STOMP© EHM hydraulic conductivity to calculate the hydraulic gradient.

In the future, the gradient is generally expected to be from northwest to southeast. The water table in the unconfined aquifer is expected to continue declining because the large discharges of operational liquid to the ground at 216-B-3 Pond system and other large discharge sites in 200 East Area have ceased. The hydraulic heads around WMA C are expected to continue declining slowly until they stabilize around year 2030 at 119.5 m (392 ft) (Figure 3-4, adapted from CP-47631, 2015). For Year 2100 (approximating post-closure steady state conditions), the CPGWM-calculated flow through the window volume is 730 m^3/day, which divided by the cross-sectional area of 3,300 m^2 associated with the CPGWM window translates to a Darcy flux of 0.22 m/day with a hydraulic gradient of 2×10^{-5}, which is close to the one observed prior to start of Hanford operations, as estimated from Figure 3-5 (adapted from Figure II.3-14 in ERDA-1538, *Final Environmental Impact Statement, Waste Management Operations, Hanford Reservation, Richland, Washington*). Changes in hydraulic gradient are only expected to occur within the first 10 to 50 years of the post-closure simulation period, which, according to the screening analysis (see Section 4.5, Screening), is before the mobile radionuclides reach the water table. Thus, the hydraulic gradient is assumed to be stable for this analysis.

According to RPP-14430, porosity is generally estimated to be about 30% for unconsolidated coarse-grained sediments, but a value closer to 20% may be more appropriate where boulders and cobbles are present and mixed with sand and gravels, such as at WMA C. The STOMP© EHM porosity value of 0.20 is consistent with the vadose zone value of 0.17 for the Hanford H1 and H3 sediments, and the aquifer test results from well 699-55-50 presented in HW-60601, *Aquifer Characteristics and Ground-Water Movement at Hanford*. The STOMP© EHM includes the CPGWM estimate of 0.1 (CP-47631) for the anisotropy, which is defined here as the ratio of vertical to horizontal hydraulic conductivity. The longitudinal and transverse macrodispersivity estimates in the saturated zone are based on a review of three general relationships ("Universal Scaling of Hydraulic Conductivities and Dispersivities in Geologic Media" [Neuman 1990]; "Longitudinal Dispersivity Data and Implications for Scaling Behavior" [Schulze-Makuch 2005]; and "Use of Weighted Least-Squares Method in Evaluation of the Relationship Between Dispersivity and Field Scale" [Xu and Eckstein 1995]) that quantify the dependence of this parameter on measurement scale (L_s). For 100 m, which is the approximate distance of travel to the compliance well located in the saturated zone, the calculated values fall within the range of 1 to 20 m (Table 3-6). Thus a value of 10.5 m is chosen for the base calculation. The ratio of longitudinal to transverse macrodispersivity is chosen to be 10 based on RPP-17209, *Modeling Data Package for an Initial Assessment of Closure of the S and SX Tank Farms*, and "Field Study of a Long and Very Narrow Contaminant Plume" (van der Kamp et al. 1994). Table 3-7

presents a summary of the aquifer hydraulic parameters for the Hanford H3 – aquifer used for the base case.

The aquifer transverse dispersivity value used in the model appears to be consistent with the distribution of the ^{99}Tc in the aquifer around WMA C. Data show that the elevated ^{99}Tc concentrations around WMA C extend throughout the depth of the aquifer indicating that the plume is vertically well mixed. The peak ^{99}Tc activity (20,800 pCi/L) was measured at a depth of ~9 m below the water table in well 299-E27-23 during depth discrete sampling, and the activity was relatively constant at every depth measured in the well (19,900 pCi/L and 20,500 pCi/L at depths of 3 m and 6 m, respectively) (DOE/RL-2011-01, *Hanford Site Groundwater Monitoring Report for 2010*). Depth discrete samples collected at wells 299-E27-4, 299-E27-7, and 299-E27-21 further indicate that ^{99}Tc activity increases with depth and that the ^{99}Tc is not contained in the upper part of the aquifer. For example, well 299-E27-4 had activity measurements of 727 and 761 pCi/L in the first two intervals but 7,260 pCi/L in the lowest sample interval (DOE/RL-2011-01). These data show that relatively large values of transverse dispersivity are appropriate when modeling transport in groundwater at WMA C, consistent with the selection of values used in the PA.

3.1.8 Point of Calculation, Protectiveness Metric, and Timeframe Considerations

In accordance with risk and performance assessment guidelines, the determination of soil contamination impacts to groundwater also requires the definition and rationale for (1) the point of calculation, i.e., the place and points in the groundwater domain where modeled groundwater concentrations are to be assessed for potential impacts and protectiveness, (2) the protectiveness metric, i.e., the groundwater metric(s) to be used in the assessment of protectiveness at the point of calculation, and (3) the timeframe considered applicable for the calculation of impacts to groundwater. The point of calculation is intended to effectively serve as the point where exposure point groundwater concentrations are evaluated in the model for the purpose of evaluating the achievement of the groundwater protection performance objectives. The point of calculation for the protection of groundwater is related to “Point of Compliance” in DOE PA requirements (DOE M 435.1-1, Chapter IV Section P) and described as follows:

> “The point of compliance shall correspond to the point of highest projected dose or concentration beyond a 100 meter buffer zone surrounding the disposed waste. A larger or smaller buffer zone may be used if adequate justification is provided.”

Thus, the point of calculation for the groundwater impact analysis is 100 m down gradient from the WMA C fenceline. While the DOE manual and guide state that point of compliance is the point of highest calculated dose (groundwater concentration), neither indicates how that groundwater concentration should be calculated, i.e., within what volume is the concentration calculated, apart from indicating that the aquifer mixing must be consistent with State or local laws, regulations, or agreements.

Figure 3-4. Central Plateau Groundwater Model Calibration Results in the Vicinity of Waste Management Area C.

a)

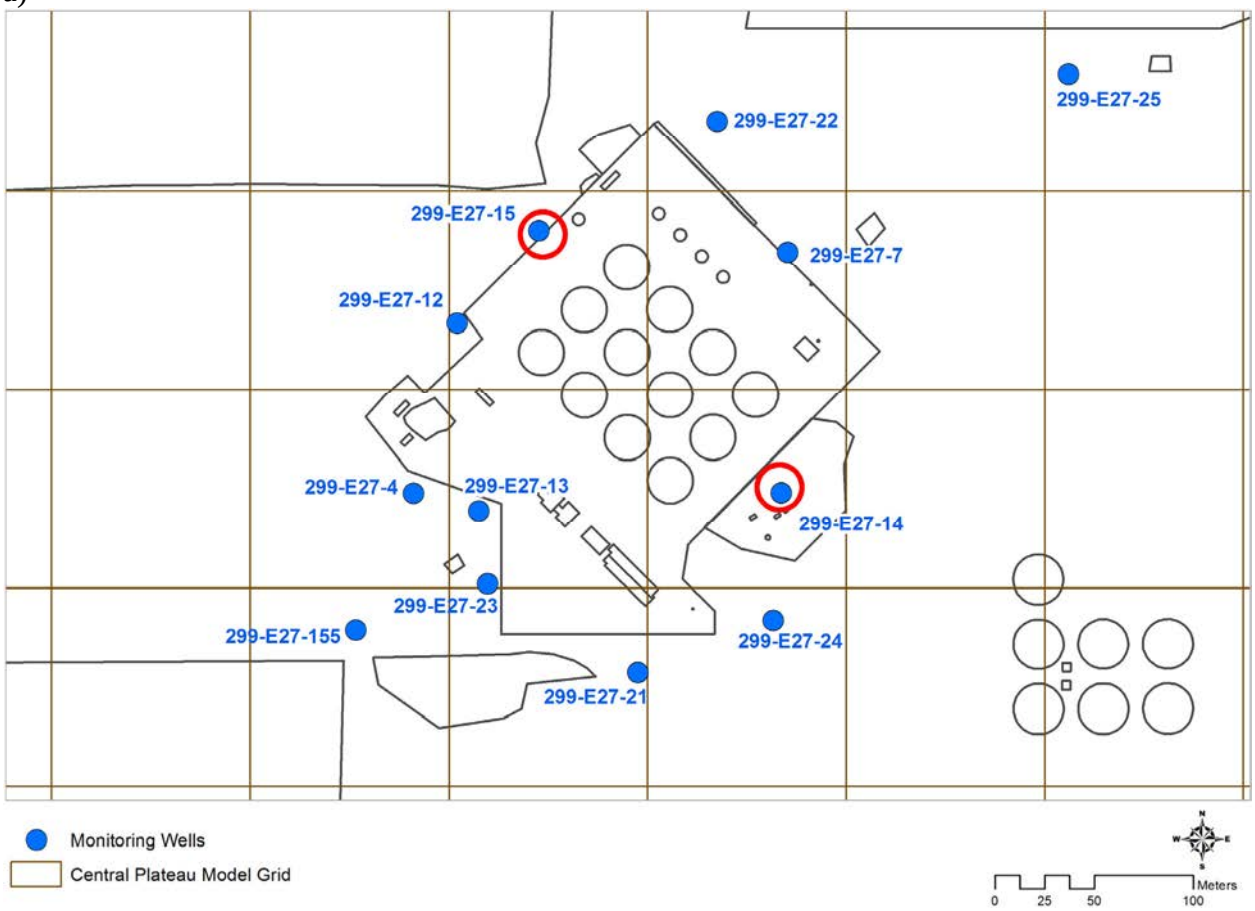

b)

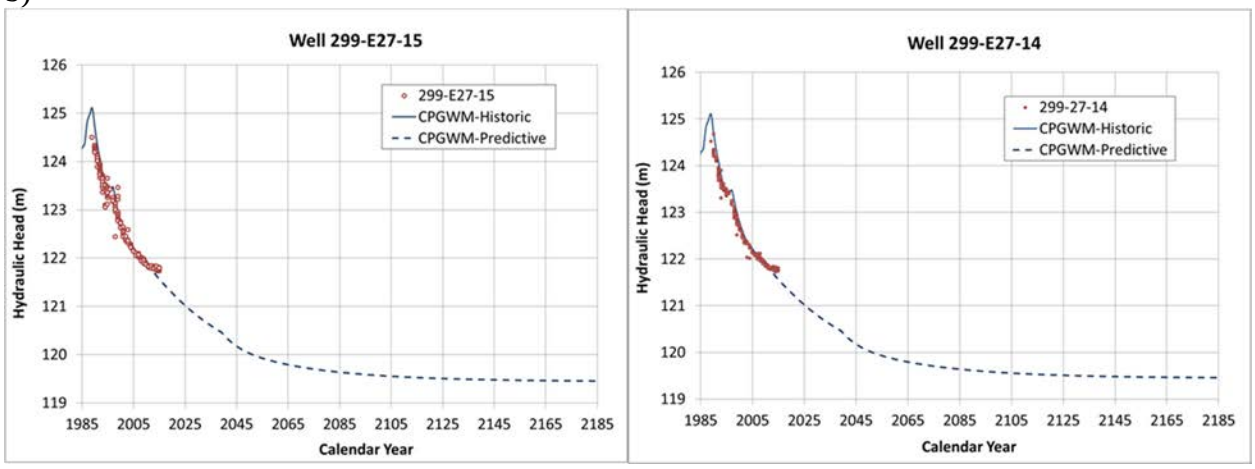

Sources:
Appendix C – Technical Basis for Waste Management Area C Unconfined Aquifer Conceptual Model: Field Data and Related Investigations.
CP-47631, *Model Package Report: Central Plateau Groundwater Model Version 6.3.3.*

Figure 3-5. Hindcast Estimate of the Water Table Elevation in 1944 Prior to the Start of Significant Hanford Site Operations.

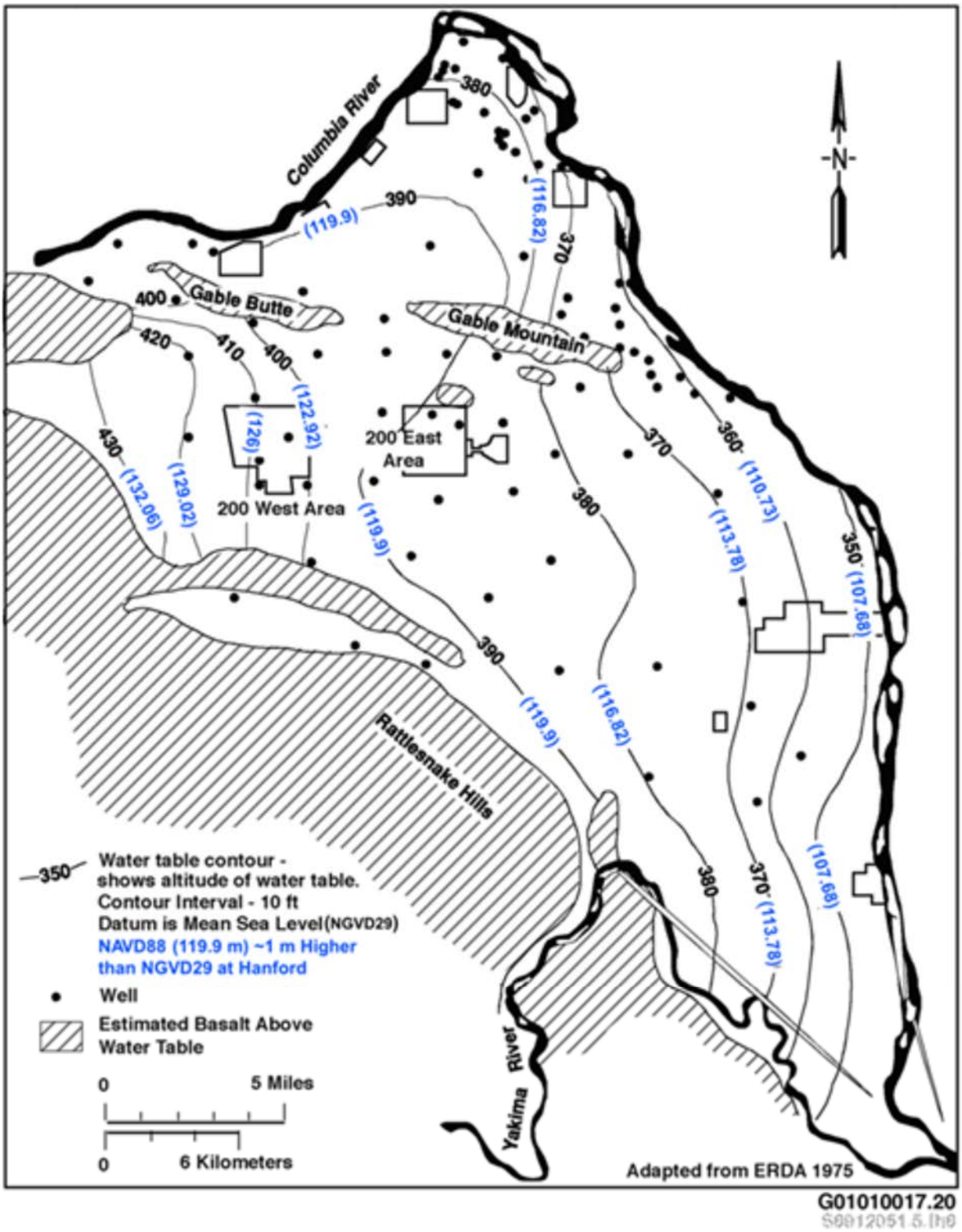

Note: ERDA 1975 refers to ERDA-1538, *Final Environmental Impact Statement, Waste Management Operations, Hanford Reservation, Richland, Washington*.

Table 3-6. Relationship Between Saturated Longitudinal Macrodispersivity (α_L) and Scale of Measurement (L_s).

Reference	Relationship	Origin	Saturated Longitudinal Macrodispersivity Estimate (m) for a Scale ≈ 100 m
Neuman (1990)	$\alpha_L \approx 0.017\, L_s^{1.5}$	"Universal relationship" established considering both field and laboratory data (excluding modeling results)	17
Schulze-Makuch (2005)	$\alpha_L \approx 0.085\, L_s^{0.81}$	Established considering field and modeling results (all reliabilities) and excluding laboratory data	3.5
Xu and Eckstein (1995)	$\alpha_L \approx 0.94 (\log_{10} L_s)^{2.693}$	Established considering the same data set as Neuman (1990) including numerical model results	6

References:

Neuman, S. P., 1990, "Universal Scaling of Hydraulic Conductivities and Dispersivities in Geologic Media," *Water Resources Research*, Vol. 26, No. 8, pp. 1749–1758.

Schulze-Makuch, D., 2005, "Longitudinal Dispersivity Data and Implications for Scaling Behavior," *Ground Water*, Vol. 43, No. 3, pp. 443–456.

Xu, M. and Y. Eckstein, 1995, "Use of Weighted Least-Squares Method in Evaluation of the Relationship Between Dispersivity and Field Scale," *Ground Water*, Vol. 33, No. 6, pp. 905–908.

The approach identified in USEPA Soil Screening Level (SSL) document (EPA/540/R-95/128, *Soil Screening Guidance: Technical Background Document*) and WAC 173-340-747, "Deriving Soil Concentrations for Groundwater Protection" indicates that the cross-section of the aquifer volume is usually prescribed to be a unit width of 1 m (3.28 ft) because the equations are developed on the basis of a unit width. This implies that the cross-section width is equal to the width of contamination entering the aquifer. Consistent with this reasoning, other performance assessments conducted at Hanford and other DOE facilities have used an aquifer mixing width equal to the width of the facility (e.g., WCH-520, *Performance Assessment for the Environmental Restoration Disposal Facility, Hanford Site, Washington*; WSRC-MS-2003-00582, *Performance Assessment/Composite Analysis Modeling to Support a Holistic Strategy for the Closure of F Area, a Large Nuclear Complex at the Savannah River Site*).

To calculate the highest groundwater concentration, the base case evaluated the average concentration in the aquifer within nine segments along the line perpendicular to and 100 meters beyond the southeast edge of WMA C (Figure 3-6). Concentrations calculated in the nine segments of the aquifer are assumed to be comparable to concentrations that would be measured by sampling a monitoring well at that location. The nine segments are approximately 30 m long (Table 3-8) and aligned such that the centerlines of the plumes in the groundwater resulting from the residuals released from a single line of 100-series tanks parallel to the direction of groundwater flow, e.g., the centerline of the plumes resulting from the tank residuals in 241-C-102, 241-C-105, 241-C-108, and 241-C-111 intersect the perpendicular line within the same segment.

Table 3-7. Waste Management Area C Performance Assessment Unconfined Aquifer Flow and Transport Properties (Appendix C).

Property	Waste Management Area C
Water Table Elevation (m NAVD88)[a,b]	119.5
Horizontal saturated hydraulic conductivity (m/day)[c]	11,000
Ratio of vertical to horizontal saturated hydraulic conductivity	0.1
Specific storage (1/m)[d]	1.1×10^{-3}
Effective porosity (dimensionless)	0.20 (Hanford Gravel)
Hydraulic gradient (m/m)[e]	2.0×10^{-5}
Depth to water table (m)	80
Aquifer Thickness (m)[f]	12
Longitudinal macrodispersivity (m)	10.5
Longitudinal to transverse macrodispersivity ratio	10

[a]NAVD88 = *North American Vertical Datum of 1988*, National Geodetic Survey, U.S. Department of Commerce.

[b]Water table elevation derived from Central Plateau Groundwater Model (CPGWM) based estimate of post-closure steady state conditions; see Figure 3-4(b).

[c]Thickness-weighted average conductivity estimate derived from CPGWM based on Equivalent Homogeneous Media approach adopted for representing the aquifer in the model.

[d]Using the assumed values of an aquifer compressibility of 1.0×10^{-7} 1/Pa (STOMP© default), a water compressibility of 0.0046 1/atm (CRC Handbook of Chemistry and Physics), and a water density of 1,000 kg/m^3 (CRC Handbook of Chemistry and Physics).

[e]Thickness-weighted gradient estimate derived from CPGWM based on Equivalent Homogeneous Media approach adopted for representing the aquifer in the model.

[f]Aquifer thickness estimated from RPP-RPT-56356, *Development of Alternative Digital Geologic Models of Waste Management Area C* and the Model Grid.

References:

Haynes, W. M. and D. R. Lide, 2011, CRC Handbook of Chemistry and Physics, 92nd Edition, CRC Press, Taylor & Francis Group, Boca Raton, Florida.

Subsurface Transport Over Multiple Phases (STOMP)© is copyrighted by Battelle Memorial Institute, 1996.

The WAC specifies a 5-m mixing zone in groundwater that is consistent with a 5-m vertical interval corresponding to a conceptual groundwater monitoring well with the 15-ft well screen length (and mixing zone dimension) associated with state monitoring well descriptions (e.g., see Equation 747-4 in WAC 173-340-747). The aquifer mixing zone extends into the upper 5 m of the aquifer for the purpose of the evaluations. DOE M 435.1-1 does not specify the level of protection required for water resources and there are no applicable parameterization requirements or guidelines indicated in DOE G 435.1-1, Chapter 4.

Figure 3-6. Points of Calculation 100 Meters Downgradient of Waste Management Area C.

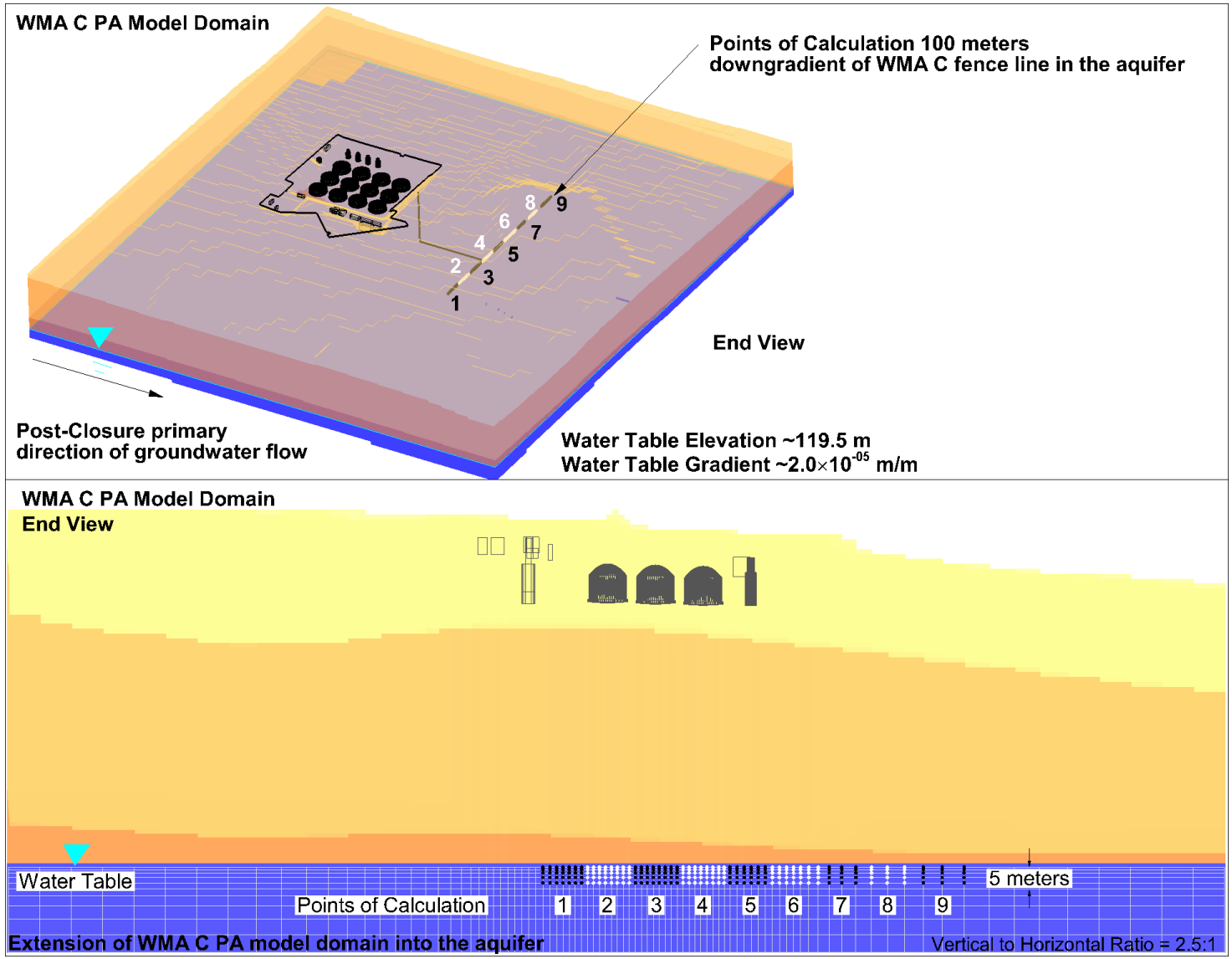

PA = performance assessment WMA = Waste Management Area

Table 3-8. Dimension of Widths for Point of Calculation Segments 100 meters Downgradient of Waste Management Area C.

Point of Calculation Segment	1	2	3	4	5	6	7	8	9
Width (m)	28.8	30.5	30.4	29.6	27	34.5	36	34	28

The compliance timeframe is defined as 1,000 years following closure of the facility (DOE G 435.1-1, Chapter IV Section P). The sensitivity-uncertainty analysis along with NRC draft guidance (NUREG-1854, *NRC Staff Guidance for Activities Related to U.S. Department of Energy Waste Determinations – Draft Final Report for Interim Use*) extends the evaluation to 10,000 years, which is sufficient to evaluate the peak dose from all of the radionuclides that the screening analysis indicates may not impact groundwater within the compliance period. DOE G 435.1-1, Chapter IV Section P states that the sensitivity-uncertainty analysis timeframe should include calculation of the maximum dose regardless of the time at which the maximum occurs as a means of increasing confidence in the outcome of the modeling and increasing the understanding of the models used. However, EPA-SAB-RAC-ADV-99-006, *An SAB Advisory: Modeling of Radionuclide Releases from Disposal of Low Activity Mixed Waste* warns that extending the modeling time frame beyond 10,000 years could make the results irrelevant and hinder public acceptance of the results because of the inherent scientific and social uncertainties associated with such an extended timeframe. The 10,000-year timeframe is sufficient to address uncertainty associated with radionuclides that impact groundwater during the compliance period (NUREG-1573, *A Performance Assessment Methodology for Low-Level Radioactive Waste Disposal Facilities: Recommendations of NRC's Performance Assessment Working Group*).

DOE G 435.1-1, Chapter 4 states that DOE low-level waste disposal facilities must comply with legally applicable requirements for water resource protection. The protectiveness metric determined to be most appropriate for the evaluation of impacts to groundwater during the compliance period from the radionuclide and contaminant inventory in WMA C are the MCLs. MCLs represent the "allowable concentrations" and/or "acceptable limits" of a radionuclide for minimizing further degradation of groundwater in accordance with the conditions identified in State and Federal anti-degradation goals [e.g., EPA/540/R-92/003, *Guidance for Data Useability in Risk Assessment (Part A) Final*; EPA/530-SW-87-017, *Alternate Concentration Limit Guidance Part I ACL Policy and Information Requirements Interim Final*; DOE/RL-2002-59, *Hanford Site Groundwater Strategy Protection, Monitoring, and Remediation*].

Defining the protection of groundwater in the context of vadose zone fate and transport requires consideration of the soil and groundwater media as a hybrid or coupled pathway. This pathway involves the determination of future concentrations in the groundwater medium that result from the transport of the radionuclide and contaminant inventory existing in the WMA C tank residuals. The working definition of protectiveness for the protection of groundwater pathway is considered achieved if the radionuclide and contaminant levels in the WMA C tank residuals do not cause groundwater concentrations to exceed MCLs at the points of calculation within 1,000 years after the assumed closure date of 2020.

3.2 NATURE AND EXTENT OF CONTAMINATION

The WMA C PA addresses the radionuclide and non-radiological contaminant inventory contained in waste residuals in tanks and ancillary equipment in WMA C at the assumed time of closure. Tank waste can be grouped into three types based on physical properties: supernate, salt, and sludge (RPP-RPT-42323). The C Farm contains only a small amount of salt type waste, and with the supernate having been pumped out as part of interim stabilization, the tanks now contain mainly sludge (RPP-RPT-42323). As of the summer of 2015, retrieval has been completed in all but three tanks.

The residual waste volume for tanks not yet retrieved is unknown; therefore assumptions about the inventory have been made based on current threshold requirements. Most constituents' inventory uncertainties vary by a factor of 5 or less, but may vary by as much as a factor of 10 for certain constituents in tanks not yet retrieved. For tanks already retrieved, uncertainty in residual waste estimates is on the order of 20 to 30% for most constituents, assuming no additional retrieval is required.

Specific information about the residual inventory and the release of the radionuclide and non-radiological contaminant inventory from the tanks, ancillary equipment, and pipelines is presented in Section 3.1.3 and RPP-RPT-58948.

4 MODEL IMPLEMENTATION

The 3-D model incorporates spatial heterogeneity and temporal changes of geologic and recharge conditions with the ability to include lateral spreading, comingling of plumes, and preferential flow. The gridding scheme and extent of the domain intend to minimize the numerical error and impact that the boundary conditions have on the model calculations in the areas of interest, i.e., the points of calculation. The discretization scheme allows the distinct representation of the different sources within WMA C such that no sources, with the exception of the pipelines, overlap one another.

This MPR includes discussion of the results of certain simulations conducted to assess the adequacy of the model domain size and discretization during the construction of the model. The results of one simulation provide a check that the model domain is sufficient to prevent the boundary conditions from inappropriately affecting the solution in the area of interest. A comparison of results obtained using different Courant numbers provides a check on numerical dispersion caused by time-step size and a comparison of results using different dispersivity values provides a check that numerical dispersion is not obscuring the solution.

4.1 DISCRETIZATION

The 3-D model incorporates spatial heterogeneity and temporal changes of geologic and recharge conditions, with the ability to include lateral spreading, comingling of plumes, and preferential flow. The gridding scheme and extent of the domain intend to minimize the numerical error and impact that the boundary conditions have on the model calculations in the areas of interest, i.e., the points of calculation. The discretization scheme allows the distinct representation of the different sources within WMA C such that no sources, with the exception of the pipelines, overlap one another.

The horizontal node spacing varies between 3.0 and 20 meters to optimize the discretization in the areas attempting to approximate the slopes associated with construction of WMA C and the 100-series tanks without overwhelming the available computational resources. Within the confines of WMA C, the horizontal grid cell dimensions ranged between 3 and 4 meters to align the nodes with the tanks, vault, and other ancillary equipment (Figure 4-1). Outside of WMA C, the grid cells expanded in size such that no adjoining grids differed in length by more than a factor of 1.5. Table 4-1 presents the pattern of the spacing of the finite difference cells. Vertical spacing in the vadose zone ranged between 1 and 1.25 meters except around the water table where the spacing decreased to 0.5 meters to capture the impact of the capillary fringe above the water table (Figure 4-2).

The total number of nodes in the modeled rectangular prism equals 736,653. During the pre-operational phase, WMA C does not exist and the number of active nodes equals 640,565 with 96,088 inactive. During the operational and post-closure phases, WMA C backfill replaces Hanford H1 Gravel, and the number of active nodes equals 637,543 with 99,110 inactive. The increase in inactive nodes is attributed to the inactivation of the tank and ancillary equipment nodes within the WMA C excavation.

Figure 4-1. Horizontal Alignment of Three-Dimensional Model Computational Nodes with Waste Management Area C Single-Shell Tanks, 241-C-301 Catch Tank, 244-CR Vault, and Other Waste Management Area C Ancillary Equipment.

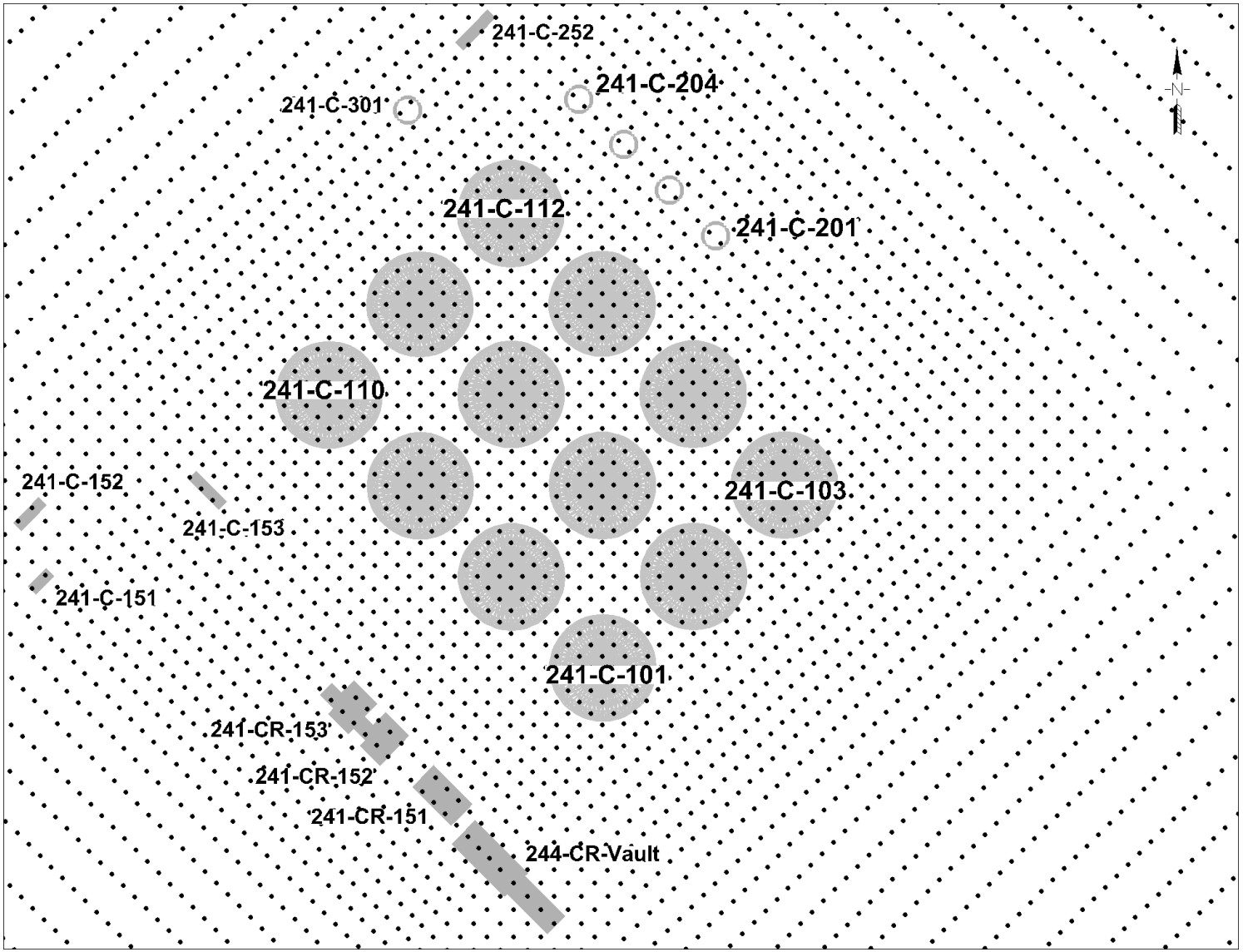

Table 4-1. Horizontal and Vertical Spacing of the Finite Difference Cells in the Three-Dimensional Waste Management Area C Flow and Transport Model Domain.

West to East Spacing; Southeastern Boundary Coordinate = 574656 m (Lambert Coordinate System[1] Easting)						
4@ 20.00 m	2@ 16.00 m	2@ 12.00 m	2@ 10.00 m	2@ 8.00 m	2@ 6.00 m	7@ 4.50 m
1@ 3.70 m	6@ 3.80 m	2@ 3.85 m	14@ 3.80 m	2@ 3.85 m	6@ 3.80 m	1@ 3.00 m
7@ 4.50 m	3@ 6.00 m	4@ 8.00 m	10@ 10.00 m	2@ 12.00 m	1@ 16.00 m	9@ 20.00 m
South to North Spacing; Southwestern Boundary Coordinate = 136454 m (Lambert Coordinate System[1] Northing)						
8@ 20.00 m	3@ 16.00 m	2@ 12.00 m	4@ 10.00 m	3@ 8.00 m	2@ 6.00 m	11@ 4.50 m
4@ 4.00 m	8@ 3.80 m	1@ 3.90 m	15@ 3.80 m	1@ 3.00 m	11@ 4.50 m	2@ 6.00 m
2@ 8.00 m	3@ 10.00 m	3@ 12.00 m	4@ 16.00 m	6@ 20.00 m		
Vertical Spacing; Bottom Elevation = 95 m (NAVD88[2])						
1@ 5.00 m	2@ 4.00 m	1@ 3.00 m	1@ 2.00 m	2@ 1.50 m	1@ 1.25 m	1@ 1.00 m
1@ 0.75 m	3@ 0.50 m	1@ 0.75 m	12@ 1.00 m	40@ 1.25 m	4@ 1.00 m	19@ 1.25 m

[1]NOAA Manual NOS NGS 5, *State Plane Coordinate System of 1983*.

[2]*North American Vertical Datum of 1988*, National Geodetic Survey, U.S. Department of Commerce.

Note: The sequences read left to right. The number preceding the "@" symbol indicates the number of columns (west to east), rows (south to north), or vertical layers (bottom to top) that have the length indicated by the distance following it.

To evaluate any unintended impact of the boundary conditions in the areas of interest, recharge within WMA C follows the base case timeline, but recharge in all areas outside WMA C remains 0.5 mm/yr indefinitely. This recharge scheme provides the greatest contrast between the areas inside and outside of WMA C. According to the boundary conditions, the moisture content at the boundaries should remain unchanged; therefore the magnitude of any change at the boundaries provides an indication of numerical error. Figure 4-3 shows the relative change in moisture content from the pre-Hanford steady-state condition at the four vertical boundaries of the model at three times of interest: at Year 2020 at the end of the WMA C operational period, at Year 2520 at the end of the design life of the WMA C surface barrier, and at Year 3020, which is the end of the compliance time frame and when the system has reacquired or nearly reacquired steady-state conditions. In general, the effects are contained within a relatively small segment along the boundaries near the water table and appear to be minor. The changes in moisture content are negligibly small in magnitude, which indicates that the boundaries are far enough removed from the area of interest to avoid unintentional impacts to the model solution. Consequently, they are not considered to adversely affect the evaluation of radionuclide transport and groundwater impacts associated with the radionuclide and non-radiological contaminant inventory in WMA C.

Figure 4-2. Horizontal and Vertical Alignment and Distribution of Waste Management Area C Performance Assessment Three-Dimensional Model Computational Nodes.

(a) Alternative Geology I

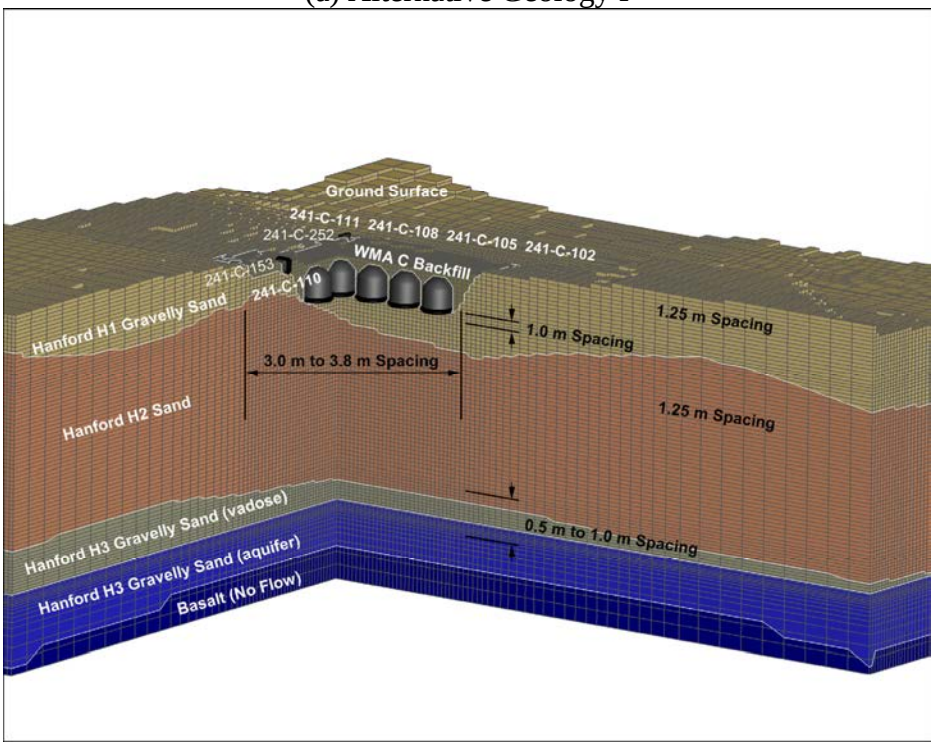

(b) Alternative Geology II

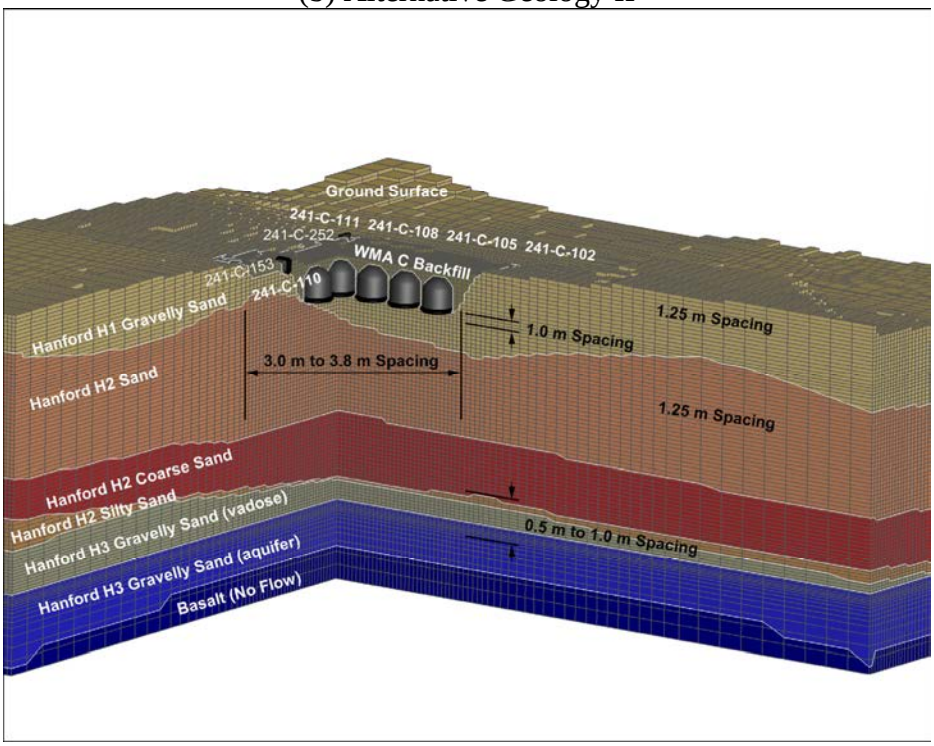

WMA = Waste Management Area

Figure 4-3. Relative Change in Moisture Content (Volume %) from the Pre-Hanford Steady-State Condition at the Four Vertical Boundaries of the Model at Three Times of Interest: Year 2020, Year 2520, and Year 3020.

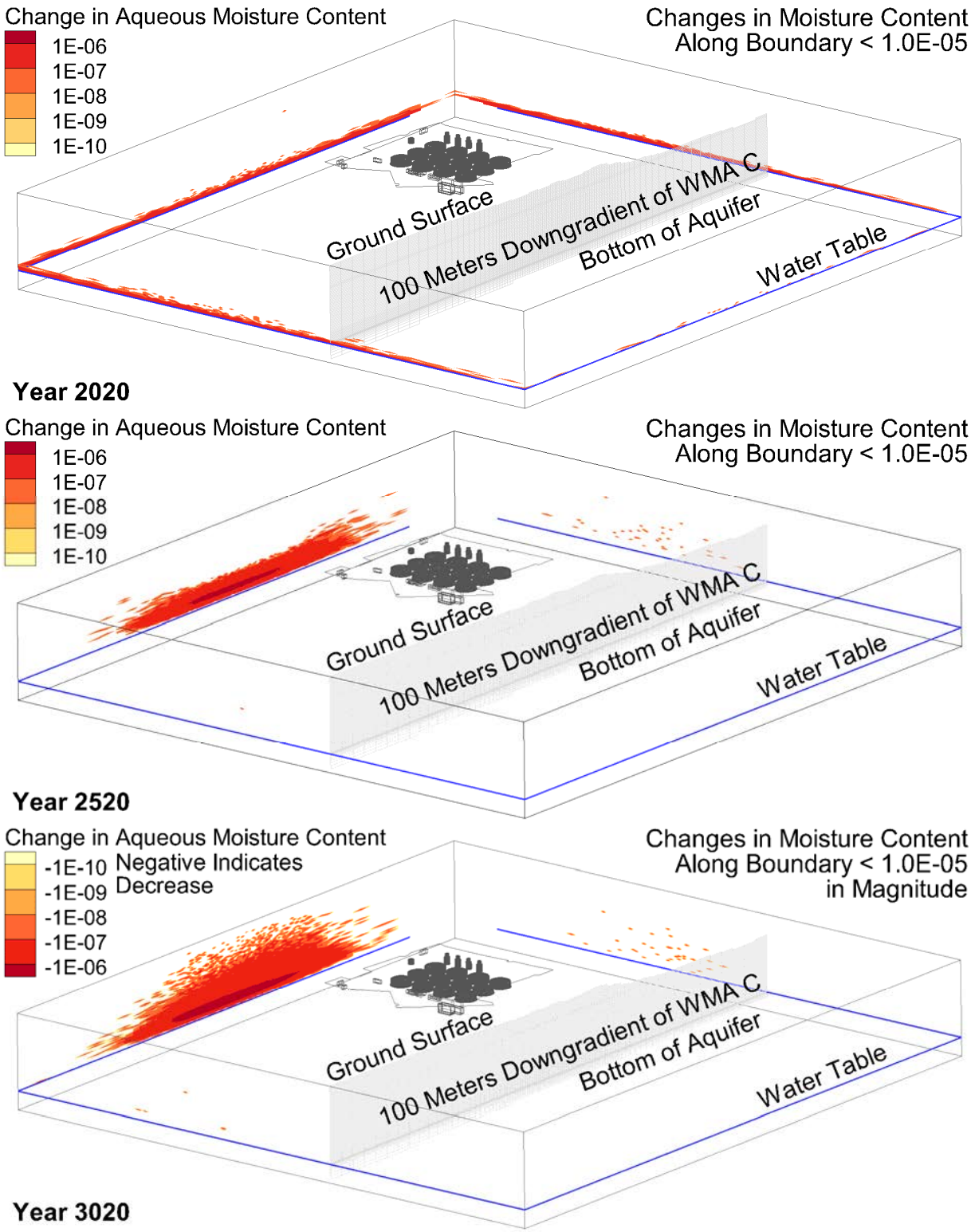

WMA = Waste Management Area

The Peclet number represents the ratio between the movement of contaminants caused by dispersion and diffusion. The Courant number represents the ratio of advective flow to the grid size. In numerical gridding schemes, the Peclet and Courant numbers also provide some insight into numerical dispersion that may be affecting the solution. For the base case, the vadose zone Peclet number equaled approximately 6 (1.25 meters / 0.20 m), with an imposed Courant [number] restriction of 10. While the value of 1 for both these numbers is often considered ideal, it has been demonstrated that acceptably small numerical oscillations may be obtained with local Peclet numbers as high as 10 (Computational Methods in Subsurface Flow [Huyakorn and Pinder 1983]). It is difficult to assess numerical impacts on the solution caused by the grid spacing apart from consideration of the Peclet criteria. The total number of nodes in the model is close to the maximum that the computer hardware and solver can accommodate, so evaluating solution stability through grid refinement is not feasible. Other comparably scaled models indicate that the WMA C PA grid size and spacing is sufficient. DOE/EIS-0391 Appendix N indicates that the horizontal grid size and spacing of 5 meters within WMA C, and vertical spacing of 2 meters, are small enough in that 3-D model to provide accurate simulation of flow and transport.

To determine the impact of any numerical dispersion, a simulation with dispersivity values close the maximum estimates for the different HSUs was evaluated (Appendix B). Numerical dispersion tends to mask the dispersion indicated by the dispersivity coefficient. Therefore, changes in the peak concentration and shape of the breakthrough curves indicates that the numerical dispersion is not impacting the solution in an unacceptable manner. Figure 4-4 shows a comparison of the ^{99}Tc concentration at the nine points of calculation located 100 m downgradient between the base case dispersivity values and dispersivity values intended to test numerical dispersion (Table 4-2). These test case dispersivity values represent the approximate maximum values associated with the different HSUs. The maximum concentration observed in the base case results increases perceptibly compared to the numerical dispersion test case results. This increase indicates that any numerical dispersion that may be occurring is not substantial enough to obscure the contaminant transport calculations, and that the Peclet criteria for the grid is adequate.

The vertical Courant numbers in the vadose zone tend to be small (e.g., 10 yr time step × 0.0035 m/yr recharge / 0.05 moisture content / 1 m grid spacing = 0.7), but the Courant numbers become large near the water table and capillary fringe where the horizontal velocity approaches 400 m/yr. These few layers impose an impractical limit on the time step while the Courant numbers remain small elsewhere else. Table 4-3 presents the results of a Courant criteria evaluation which evaluated the maximum concentration of ^{99}Tc at the points of calculation associated with a subset of the WMA C sources: 241-C-105, 241-C-203, and the pipelines. The negligible differences in the results indicates that an overly strict Courant restriction does not affect the solution and appears to be unwarranted, especially considering the improved efficiency in solution time when the Courant restriction is relaxed to 10. These evaluations indicate that the Courant criteria for the grid is adequate and that the grid is adequately discretized.

Figure 4-4. Comparison at the Nine Points of Calculation Located 100 meters Downgradient for the Technetium-99 Concentration between the Base Case Dispersivity Values and the Numerical Dispersion Test Case Dispersivity Values.

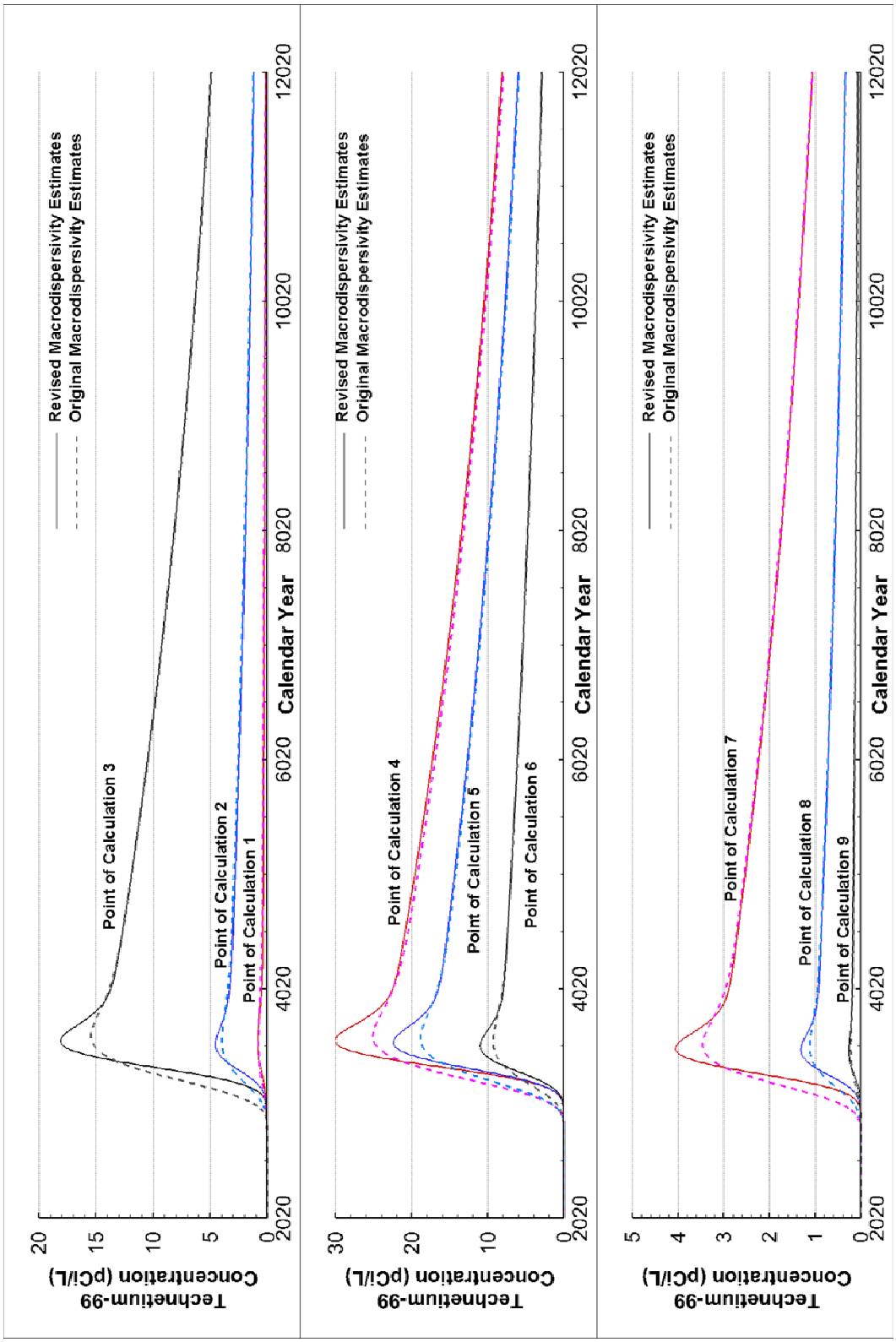

Table 4-2. Comparison Using Vadose Zone Dispersivity Values and Numerical Dispersion Test Case Dispersivity Values.

Hydrostratigraphic Unit	Numerical Dispersion Test Case Longitudinal Macrodispersivity (cm) (Appendix B)	Base Case Longitudinal Macrodispersivity (cm) (Table 3-2)
Backfill	150	20
Hanford H1	100	20
Hanford H2	200	25
Hanford H3	100	20
Point of Calculation 100 meters Downgradient of Waste Management Area C	**Maximum Concentration (pCi/L)**	**Maximum Concentration (pCi/L)**
1	0.80	0.83
2	4.0	4.5
3	15	18
4	25	30
5	19	22
6	9.2	11
7	3.4	4.1
8	1.1	1.3
9	0.22	0.26

4.2 PARAMETERIZATION

Table 4-4 presents a summary of the model parameters and values assigned, including boundary and initial conditions, and identifies the section where the data sources and data quality are discussed. Parameters and values that are already tabularized in the subsections of Section 3.1 are simply referenced by the applicable table number.

4.3 MODELING STAGES

The WMA C tank residual simulations using STOMP© require running three separate stages of the model in sequence. The first stage is a long-term transient simulation of only water flow resulting from historic recharge conditions. This stage is needed to obtain near steady-state soil moisture conditions throughout the model domain at the start time for the second stage. The second stage begins with the initial moisture distribution provided from the first stage and simulates only water flow during the operational period of WMA C, which is the time between the construction of WMA C in 1945 and its assumed closure in 2020. The STOMP©

nomenclature refers to this as a "restart." The contaminant transport stage (stage 3) begins with the moisture distribution provided from the second stage, and simulates flow and transport for 10,000 years, from 2020 to 12020. Each tank, ancillary equipment, and pipeline residual source is simulated individually. The groundwater concentrations resulting from each source are summed according to the principle of superposition to produce time series concentration breakthrough curves at the points of calculation identified in Section 3.1.8. The principle of superposition also applies to the spatial distribution of the pore water concentrations in the vadose zone resulting from each source. The superposition and summing of the concentration results occurs outside of STOMP© and is not addressed in this section.

Table 4-3. Waste Management Area C Performance Assessment Vadose Zone Courant Criteria and Numerical Dispersion Evaluation.

	Numerical Dispersion Test Case Courant Number = 1 (pCi/L)			Base Case Courant Number = 10 (pCi/L)		
Simulation Duration and Time to Complete	4,000 years completed in 112.51 hours			10,000 years completed in 32.08 hours		
Point of Calculation 100 meters Downgradient of Waste Management Area C	**Maximum Concentration (pCi/L)**			**Maximum Concentration (pCi/L)**		
	Source			**Source**		
	241-C-105	**241-C-203**	**Pipelines**	**241-C-105**	**241-C-203**	**Pipelines**
1	0.02	0	0.36	0.02	0	0.36
2	0.86	0	0.53	0.86	0	0.53
3	10	0.000003	0.74	10	0.000003	0.73
4	21	0.0001	0.94	21	0.0001	0.92
5	13	0.002	1.0	13	0.002	1.0
6	4.1	0.006	0.74	4.1	0.006	0.73
7	0.92	0.007	0.34	0.91	0.007	0.34
8	0.22	0.004	0.12	0.22	0.004	0.12
9	0.03	0.001	0.03	0.03	0.001	0.03

4.4 CALIBRATION

DOE G 435.1-1 and Federal risk assessment guidelines [e.g., EPA/540/1-89/002, *Risk Assessment Guidance for Superfund Volume I Human Health Evaluation Manual (Part A) Interim Final*] acknowledge that the assessment of uncertainties associated with how well models approximate actual relationships and conditions in the field (i.e., field validation), is desirable, but that field data for model calibration is generally not available or attainable for vadose zone models.

Table 4-4. Summary of Key Elements and Base Case Parameters Associated with Site-Specific Model Components for Waste Management Area C. (2 sheets)

Model Domain and Boundary Conditions	Rectangular Prism: 737.9 m (2,421 ft) × 795.3 m (2,609 ft) × 116 m (381 ft) (Model Grid Calculation) Prescribed flux across the top (Recharge); no-flow along vertical side boundaries in the vadose zone; prescribed flux and head along the up-gradient and down-gradient vertical side boundaries in the aquifer, respectively; no-flow along the bottom of the model (aquifer). The prescribed volumetric water flux boundary condition is calculated to maintain mass conservation in the aquifer independent of recharge.

Geologic Setting	The Waste Management Area (WMA) C cross-section includes the following anthropogenic or natural units that occur from surface to groundwater (RPP-RPT-56356, *Development of Alternative Digital Geologic Models of Waste Management Area C*):
	• WMA C Backfill (~10 m)
	• Hanford H1 (gravel-dominated, generally identified as gravel or very coarse sand; ~10 m)
	• Hanford H2 Sand (sand-dominated facies generally identified as fining upward sequences of gravel, sandy/gravel to sand to very fine sand; ~40-50 m)
	• Hanford H3 (coarse-grained open framework gravel to sandy gravel; in the vicinity of WMA C is often referred to as undifferentiated H3 gravels, Cold Creek, and Ringold; ~0-20 m)
	• In Alternative Geologic Model II, the Hanford H2 Sand includes following two additional subunits
	  o Hanford H2 Coarse (gravel/coarse-grained facies that underlies the H2 fines; ~15 m)
	  o Hanford H2 Silty Sand (a silty sand unit that is only observed in deep groundwater wells and a mappable unit may not be readily identified; ~0-3 m)

Groundwater Domain and Characteristics	WMA C post-closure water table elevation ~119.5 m NAVD88 and average hydraulic gradient ~0.00002 m/m (Central Plateau Groundwater Model [CPGWM], CP-47631, 2015, *Model Package Report: Central Plateau Groundwater Model Version 6.3.3*) Aquifer Hydraulic Conductivity = 11,000 m/day Aquifer area along northwest cross-section boundary = 6,151.04 m^2 (Model Grid Calculation) Aquifer area along southeast cross-section boundary = 13,997.55 m^2 (Model Grid Calculation) Average aquifer area along all aquifer cross-sections = 9,439.56 m^2 (Model Grid Calculation) Prescribed flux along northwest cross-section boundary (saturated K = 11,000 m/d); 11,000 m/d × 0.2000E-04 × 365.25 d/yr = 0.80355E+02 m/yr; 0.80355E+02 m/yr × 9,439.56 m^2 / 6,151.04 m^2 = 0.12331E+03 m/yr Prescribed head along southeast cross-section boundary = 119.49 m (CPGWM, CP-47631, 2015 and Model Grid Calculation) Groundwater thickness is ~12 m (39 ft) in the aquifer (CPGWM, CP-47631, 2015 and Model Grid Calculation); Groundwater concentrations evaluated for upper 5 m (16 ft) of the aquifer (rationale for aquifer depth presented in section 3.1.8, "Point of Calculation, Protectiveness Metric, and Timeframe Considerations") Aquifer Hydraulic Conductivity Horizontal to Vertical Anisotropy **10:1** Aquifer Dispersivity Horizontal to Vertical Anisotropy **10:1**

Table 4-4. Summary of Key Elements and Base Case Parameters Associated with Site-Specific Model Components for Waste Management Area C. (2 sheets)

Source Term/ Inventory	WMA C Base Case inventory presented in Appendices B.2 (i.e., residual inventories in retrieved tanks), C.2 (i.e., residual inventories in retrieved tanks), and C.3 (i.e., residual inventories in ancillary equipment) in RPP-RPT-42323, Rev. 3. Diffusion controlled release from the grouted tanks and advection controlled release from the pipelines along with equilibrium sorption-desorption processes (i.e., K_d control). More information on these release mechanisms are provided in RPP-RPT-58948, *Model Package Report System Model for the WMA C Performance Assessment and RCRA Closure Analysis Version 1.0*.
Vadose Zone Hydrogeology and Fluid Transport	WMA C Base Case hydrogeologic properties presented in Tables 3-3 through 3-5. Vadose Zone Hydraulic Conductivity and Anisotropy allowed to vary as a function of the moisture content in accordance with the Polmann model (Application of Stochastic Methods to Transient Flow and Transport in Heterogeneous Unsaturated Soils [Polmann 1990]). Vadose Zone Dispersion Horizontal to Vertical Anisotropy **10:1**
Recharge	WMA C Base Case recharge estimates for various soil types, condition of the vegetation cover, and soil integrity during the pre-construction, operational, and post-closure periods are presented in Table 3-4.
Sorption Characteristics	K_d-control for radionuclide transport in the vadose zone and groundwater. WMA C Base Case K_d values (partition coefficients) presented in Table 3-5.

*Applies to all subfacies of this unit.

NAVD88 = *North American Vertical Datum of 1988*, National Geodetic Survey, U. S. Department of Commerce.

NP = Not present

No specific effort to calibrate the WMA C PA flow and transport model has been made, but the base case hydraulic properties were used to simulate a vadose zone flow field and the simulation results were cross-checked against WMA C field-measured moisture contents. WMA C site characterization has included the collection of an extensive database of moisture content measurements of the various HSUs present. A summary of these measurements for the WMA C area and associated statistics presented in Appendix B is provided in RPP-CALC-60450, *Process for Determining the Volumetric Moisture Content for the Vadose Zone Geologic Units Underlying Waste Management Area C*. The comparison of observed and simulated moisture content is presented in Appendix B, Section B.2.1.1. H2 Sand comprises most of the vadose zone, and overall the simulated H2 Sand moisture content of ~6 (% volume) is in agreement with the average WMA C H2 moisture of ~5.15 (% volume).

4.5 SCREENING

The screening analysis uses the 3-D model to determine the maximum K_d value of contaminants in the WMA C tank residuals that reach the water table in 1,000 and 10,000 years. The purpose of this screening phase was to streamline the PA modeling by identifying those contaminants sufficiently mobile to impact groundwater during the compliance, sensitivity and uncertainty

analysis timeframes. This analysis was performed to considerably reduce the computation time required to conduct the PA modeling by limiting the number of radionuclides evaluated in the model. According to the facility performance requirements in DOE O 435.1, performance objectives must be met for 1,000 years, and post-closure evaluations must extend out to 10,000 years to clarify long-term impacts. Given the combination of low infiltration rates and a deep vadose zone below the facility, it is evident that contaminants that are highly sorptive on the soils may not reach the water table within 10,000 years,[4] even for combinations of input parameters that are highly conservative. If the travel time exceeds 10,000 years, even for conservative combinations of input parameters, the contaminant will not affect any of the calculated results in the PA, and can reasonably be screened from the analysis.

The screening methodology and analysis includes vadose zone hydraulic property values and recharge rates developed for the uncertainty analysis, which are discussed in RPP-RPT-58948. In particular, the screening analysis applies the maximum recharge rates associated with each period for each surface type (Table 4-5), assigns the vadose zone hydraulic properties that produce the fastest pore water velocity for each HSU as determined for the uncertainty analysis (Table 4-6), and implements an advection release function for the radionuclides. Other parameters, e.g., dispersivity, distribution coefficient gravel correction, and aquifer hydraulic properties, remain the same as the base case parameters. The use of these parameter values prevents the occurrence of a false negative, i.e., that a radionuclide or non-radioactive contaminant that could impact groundwater within the 1,000- or 10,000-year simulation time frames is screened from the fate and transport evaluations. Model results indicating the time of first arrival at the water table for contaminants with distribution coefficients ranging between 0.1 and 2.0 mL/g are summarized in Table 4-7 and presented in graphical form in Figure 4-5.

Table 4-5. Maximum Net Infiltration (Recharge) Estimates Used in the Screening Analysis for Pre-Construction Period, Operational Period, and Post-Closure of Waste Management Area C.

Surface Status	Pre-Construction (mm/yr)	Operational Period (mm/yr)	Post Closure	
			Until End of Barrier Design Life (500 yr after closure) (mm/yr)	After End of Barrier Design Life (mm/yr)
Waste Management Area C	5.2	140	1.0	5.2
Undisturbed	5.2	5.2	5.2	5.2
Disturbed	5.2	22	5.2	5.2
Reworked	5.2	63	5.2	5.2
Waste Management Area A	5.2	140	1.0	5.2

[4] In this analysis, the travel time to the aquifer is defined as the time to first arrival of the contaminant at the aquifer, taking into account advection, diffusion, and dispersion. This metric will tend to screen fewer contaminants than using the arrival of the peak concentration.

Table 4-6. van Genuchten-Mualem Parameters Associated with the Maximum Pore Water Velocity at Specific Tension Ranges Based on Cumulative Distribution Functions.

Strata	θ_s	θ_r	α (1/cm)	n	Fitted K_s (cm/s)
Hanford H1 (gravelly sand)	0.100	0.0006	0.0190	1.789	5.07E-04
Hanford H2 (sand-dominated)	0.239	0.0006	0.0743	2.042	8.84E-04
Hanford H3 (gravelly sand)	0.100	0.0006	0.0190	1.789	5.07E-04
Backfill	0.100	0.0003	0.0116	1.601	9.42E-05
Aquifer	0.20	0.016	0.0190	1.789	3.49E-03*

* The vertical aquifer hydraulic conductivity value is determined from the horizontal hydraulic conductivity value and the aquifer anisotropy.

The results of the screening analysis, indicate that even when using parameter estimates biased to produce the greatest pore water velocity in the vadose zone, contaminants with a K_d in the fine fraction > 0.15 mL/g do not reach groundwater within the 1,000-year compliance time frame, and radionuclides with a K_d > 1.5 mL/g do not reach groundwater within the 10,000-year post-compliance period (Table 4-7). The screening evaluation helps in reducing the number of radionuclides to be evaluated using 3-D modeling analysis.

Table 4-7. First-Arrival Time (in Calendar Year) of Radionuclides for Various K_d Values Based on Screening Analysis Using Subsurface Transport Over Multiple Phases.

Contaminant Kd (mL/g)				Calendar Year of First Arrival at the Water Table	Time of Arrival (Years after the Assumed Closure Date of 2020)
Fine Fraction	Backfill	Hanford H1 and H3	Hanford H2		
0.10	0.05	0.06	0.08	2517.5	497.5
0.15	0.07	0.09	0.12	3022.5	1,002.5
0.20	0.09	0.12	0.16	3505	1,485
0.25	0.12	0.15	0.20	3900	1,880
0.30	0.14	0.17	0.24	4210	2,190
0.40	0.18	0.23	0.32	4840	2,820
0.60	0.28	0.35	0.48	6110	4,090
0.80	0.37	0.46	0.64	7390	5,370
1.0	0.46	0.58	0.80	8680	6,660
1.5	0.69	0.87	1.2	11900	9,880
2.0	0.92	1.2	1.6	>12020	>10,000

Reference: RPP-CALC-60448, *WMA C Performance Assessment Contaminant Fate and Transport Model to Evaluate Impacts to Groundwater*.

Figure 4-5. Groundwater Pathway Screening Analysis Indicating the Arrival Time of Radionuclides and Non-Radiological Contaminants at the Water Table.

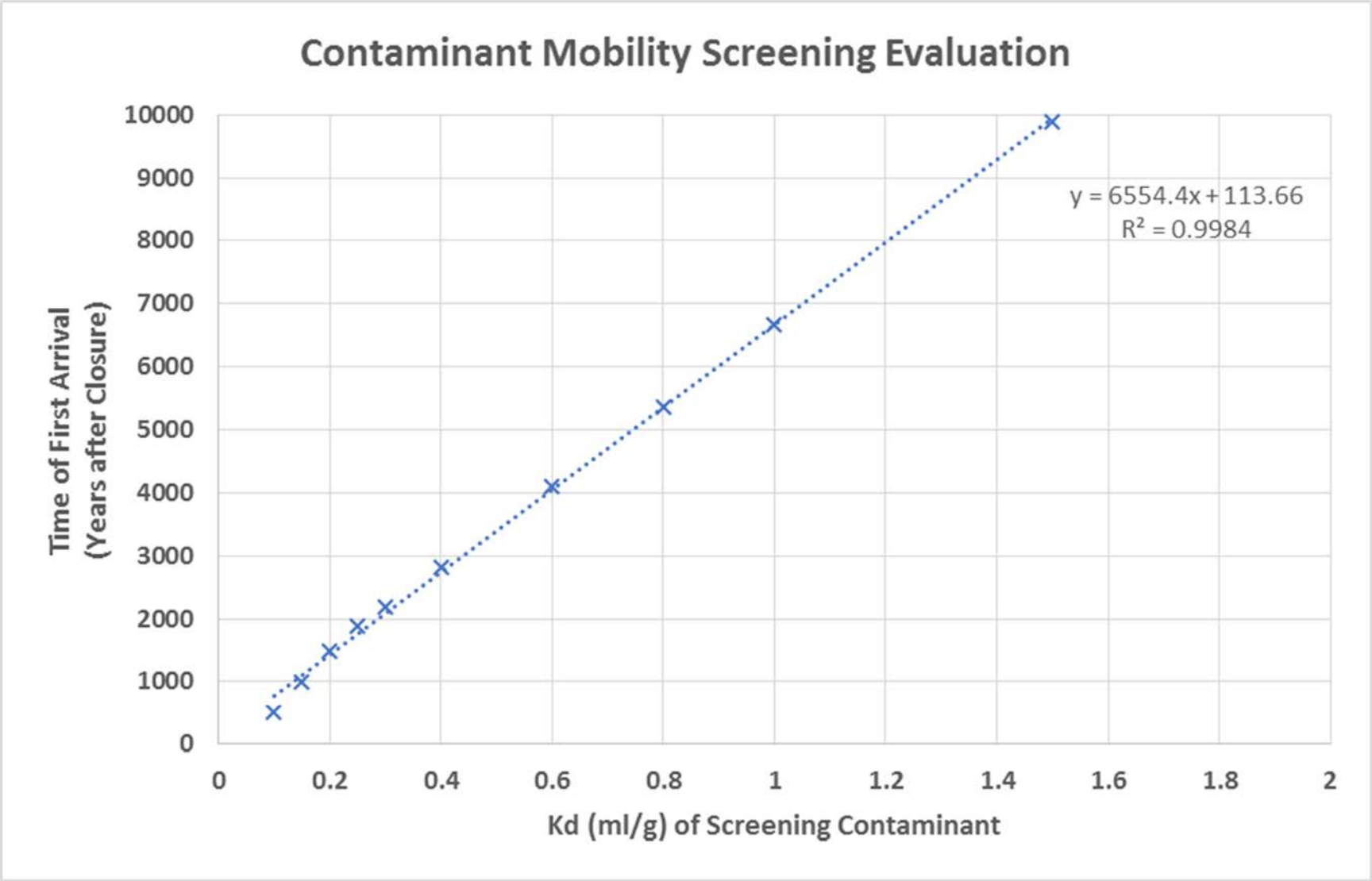

Of the list of radionuclides in the WMA C residuals inventory and on the basis of the results of the screening phase, only 12 (Table 4-8) appear to be sufficiently mobile to arrive at groundwater during the compliance period, with 6 others sufficiently mobile to arrive at groundwater during the sensitivity and uncertainty analysis timeframe. During the sensitivity and uncertainty analysis time frame, even some contaminants that undergo appreciable retardation in the vadose zone, e.g., ^{129}I, ^{14}C, and ^{238}U, are sufficiently mobile to arrive at groundwater within the sensitivity and uncertainty analysis timeframe. The other contaminants in the WMA C residual inventory are not included in further groundwater impact analysis because they do not reach the water table within the evaluation time frames.

Table 4-8. Radionuclides that Arrive at the Water Table within the 1,000-Year Compliance and 10,000-Year Sensitivity and Uncertainty Timeframe Based on the Screening Analysis Conducted Using Subsurface Transport Over Multiple Phases.

Contaminant	K_d [Fine Fraction] (mL/g)	K_d [Backfill] (mL/g)	K_d [Hanford H1 and H3] (mL/g)	K_d [Hanford H2] (mL/g)
Radionuclides and non-radiological contaminants that may arrive at the water table within 1,000 years				
CN	0	0	0	0
Co/Co-60	0	0	0	0
Cr	0	0	0	0
F	0	0	0	0
H-3	0	0	0	0
Hg	0	0	0	0
Nb-93m	0	0	0	0
NO_2	0	0	0	0
NO_3	0	0	0	0
Rn-222	0	0	0	0
Tc-99	0	0	0	0
Se/Se-79	0.1	0.05	0.06	0.08
Radionuclides and non-radiological contaminants that may arrive at the water table within 10,000 years				
I-129	0.2	0.09	0.12	0.16
Sn/Sn-126	0.5	0.23	0.29	0.40
U-238	0.6	0.28	0.35	0.48
U Total	0.6	0.28	0.35	0.48
C-14	1.0	0.46	0.58	0.80
Tributyl Phosphate	1.89	0.87	1.1	1.5

Reference: RPP-CALC-60448, *WMA C Performance Assessment Contaminant Fate and Transport Model to Evaluate Impacts to Groundwater*.

4.6 BASE CASE ANALYSIS

As discussed in Section 2 and Section 3.1.3, the base case analysis evaluates the contribution of individual sources on the peak concentration in groundwater and identifies at which Point of Calculation that peak concentration occurs. This approach was taken specifically to address the need to compare model results with groundwater MCLs. The use of the model to perform base case calculations is documented in separate environmental calculation files. Base case results are not included in this MPR, with the exception of those evaluations that are necessary to demonstrate the soundness of the model.

4.7 SENSITIVITY AND UNCERTAINTY ANALYSIS

This model package focuses on the 3-D numerical flow and transport model and its applicability. The use of the model to perform sensitivity and uncertainty calculations is documented in separate environmental calculation files. Sensitivity and uncertainty results are not included in this MPR, with the exception of those evaluations that are necessary to demonstrate the soundness of the model. The input parameters associated with Alternative Model II are included in this MPR because Alternative Model II represents an alternative conceptualization of the entire geologic model, and not just a single parameter sensitivity test.

5 MODEL APPLICATION

The WMA C PA 3-D VSZ model results apply to the estimation of the increase in groundwater contaminant concentrations from tank and ancillary equipment residual waste in WMA C. The model results do not account for interaction with waste or discharges from waste sites outside WMA C, or cumulative impacts from earlier UPRs from WMA C sources. The results are limited to calculations consistent with the assumption of a porous media continuum and approximate the bulk-flow processes through the vadose zone to estimate the arrival time and concentration of contaminants in groundwater.

5.1 WASTE MANAGEMENT AREA C PERFORMANCE ASSESSMENT MODEL LIMITATIONS

DOE/RL-2011-50 identifies generalized model and code limitations associated with the relevant FEPs for the 200 Areas vadose zone. Other limitations specific to WMA C were considered during FEPs process working sessions conducted from 2009 to 2011, and additional discussions with regulators in 2013 and 2014. The description of the limitations involves a summary of those FEPs considered and not considered in the model along with possible consequences of their omission on the model results. The limitations also address or involve uncertainties in the model results.

For the purposes of establishing that the requirements of DOE O 435.1 are being met, these limitations appear to be acceptable because the results represent reasonable (upper) bounding or limiting conditions. The risk implications of the results are not sensitive to the limitations apart from those identified through the sensitivity analysis. The limitations are considered acceptable because they do not affect the conclusions pertinent to DOE O 435.1 regarding protecting the public and environment from exposure to radiation from radioactive materials.

5.2 WASTE MANAGEMENT AREA C PERFORMANCE ASSESSMENT MODEL RECOMMENDATIONS

None as this time.

This page intentionally left blank.

6 SUBSURFACE TRANSPORT OVER MULTIPLE PHASES SOFTWARE

The STOMP© software is licensed by CH2M HILL Plateau Remediation Company (CHPRC) for use under the terms of a limited government license from Pacific Northwest National Laboratory (PNNL), which developed the code to meet American Society of Mechanical Engineers (ASME) NQA-1-2000, *Quality Assurance Requirements for Nuclear Facility Applications* and DOE O 414.1C, *Quality Assurance* software requirements when those were applicable orders and standards. Specifically and currently, PNNL manages STOMP© under a Configuration Management Plan [PNNL-SA-92584, *Subsurface Transport Over Multiple Phases (STOMP) Software Configuration Management Plan*] in conjunction with a Software Test Plan (PNNL-SA-92579, *STOMP Software Test Plan*), that detail the procedures used to test, document and archive modifications to the source code. PNNL maintains specific operational modes of STOMP© as qualified Safety Software, Level C, per the DOE O 414.1D, *Quality Assurance* definition for safety software and ASME NQA-1-2008 *Quality Assurance Requirements for Nuclear Facility Applications* with NQA-1a-2009 addenda (PNNL-24118, *STOMP/eSTOMP Software Quality Assurance Plan*).

STOMP© is used to solve the Richards equation (the water mass conservation equation in PNNL-12030) and the Advection-Dispersion equation (the solute mass conservation equation in PNNL-12030) that govern water flow and solute transport, respectively, under variably saturated conditions in the vadose zone and groundwater. STOMP© (PNNL-11216; PNNL-12030; PNNL-15782, *STOMP Subsurface Transport Over Multiple Phases Version 4.0 User's Guide*) was selected to simulate the transport of contaminants in the vadose zone of the 200 Area in and around WMA C because STOMP© fulfills the following specifications:

- The STOMP© simulator operational modes needed for implementation of this model is available free for government use under a limited government-use agreement
- The STOMP© simulator solves the necessary governing equations (i.e., Richards' equation and conservation of mass)
- It is capable of directly simulating the principal FEPs that are relevant (see Section 3.1)
- The STOMP© simulator is well documented (PNNL-11216, PNNL-12030, PNNL-15782)
- The STOMP© simulator development meets NQA-1-2008 with NQA-1a-2009 addenda software requirements and is compliant with DOE O 414.1D requirements for Safety Software (PNNL-SA-92579; PNNL-SA-92584; PNNL-24122, *Software Requirements Document for STOMP and eSTOMP*)
- The STOMP© simulator is distributed with source code, enhancing transparency
- The modeling team implementing this model has expertise in use of this simulator
- There is an extensive history of application of STOMP© at Hanford and elsewhere including verification, benchmarking, and data comparisons (DOE/RL-2011-50)

- Use of STOMP© is in keeping with DOE direction for simulation of integrated vadose and saturated zone flow and transport at the Hanford Site (Letter 06-AMCP-0133, "Contract No. DE-AC06-05RL14655 – Hanford Groundwater Modeling Integration").

6.1 SUBSURFACE TRANSPORT OVER MULTIPLE PHASES SOFTWARE QUALITY ASSURANCE

The use of STOMP© to implement the WMA C PA model and perform calculations is performed in a manner that satisfies and complies with environmental quality assurance requirements indicated by Title 10, *Code of Federal Regulations* (CFR), Part 830, "Nuclear Safety Management," and Subpart A—Quality Assurance (10 CFR 830); DOE O 414.1D; and State and Federal environmental regulations. EM-QA-001, *EM Quality Assurance Program*, Attachment G – "Software Quality Requirements" and Attachment H – "Model Development, Use, and Validation" list DOE management expectations for compliance, including configuration control, evaluation, implementation, verification and validation, and operation and maintenance.

Quality assurance project planning for STOMP© modeling follows the guidance in EPA/240/R-02/007, *Guidance for Quality Assurance Project Plans for Modeling, EPA QA/G-5M*. Model project planning includes documenting specific model development efforts and applications. It addresses as relevant and important all nine "Group A" elements presented in EPA/240/B-01/003, *EPA Requirements for Quality Assurance Project Plans, EPA QA/R-5*. The nine elements include problem definition and background, quality objectives and criteria for measurements and data acquisition leading to model inputs and outputs, data validation and usability, references, documentation and records management, special training requirements and certifications for modelers, and assessments and reports to management.

6.2 SUBSURFACE TRANSPORT OVER MULTIPLE PHASES CONTROLLED CALCULATION SOFTWARE

The following describes the STOMP© controlled calculation software and its computational platform.

- Software Title: STOMP-W (a scientific tool for analyzing single- and multiple-phase subsurface flow and transport using the integrated finite volume discretization technique with Newton-Raphson iteration).

- Software Version: STOMP-W was provided by PNNL on January 30, 2013, and was tested and approved for use by CHPRC as "CHPRC Build 4."

- Hanford Information System Inventory Identification Number: 2471 (Safety Software S3, graded Level C).

- Computational Platform: Tellus Subsurface Modeling Platform (Tellus) hosted by Mission Support Alliance for CHPRC
    - Server Chassis: Dell PowerEdge®[5] M1000e Blade Enclosure
    - Compute Nodes: 16 Dell PowerEdge® M610 Blade Servers
        - Intel Xeon® X5670 CPU (x2), 6 Cores/CPU, 2.93 GHz, 12MB Cache
        - 96 GB RAM; DDR3; 1333 MHz
        - 10Gbps Ethernet Mezzanine Card – Dual Port – X520DA2 x 2
    - Storage: internal hard drives on management (frontend) server includes 4 SAMSUNG 830 Series MZ-7PC512D/AM 2.5" SATAIII MLC Internal Solid State Drives
    - Operating System and Version
        - Red Hat Enterprise Linux®[6] 5 (Tikanga), Release 5.8
        - Rocks Cluster/Ganglia open source software operating system.
- Approved User: W. J. (Bill) McMahon.

6.3 SOFTWARE INSTALLATION AND CHECKOUT

After receipt of the STOMP© source code from PNNL, CHPRC commits the code to the MKS Integrity™[7] configuration management system that ensures traceability and precludes loss of information. Successful acceptance and installation includes confirming that the software is operating correctly by benchmarking results produced on the local computer system to those presented for selected problems from the STOMP© Application Guide (PNNL-11216). The CHPRC software owner maintains the configuration-managed copies in MKS Integrity™ and grants access to the executable files to users upon request in accordance with the approved software installation and checkout forms.

Receipt of the current STOMP© source code occurred January 2013, and testing of CHPRC Build 4 on Tellus successfully concluded April, 2013. Approved users are registered in the Hanford Information System Inventory for safety software, which identifies W. J. (Bill) McMahon as an authorized user of STOMP© on the Tellus Platform as of May 6, 2013.

6.4 STATEMENT OF VALID SOFTWARE APPLICATION

The WMA C PA requires calculations of the potential long-term impact on groundwater of post-retrieval SST waste residuals and waste left in ancillary equipment, including pipelines.

---

[5] Dell® and PowerEdge® are registered trademarks of Dell Products, Inc.

[6] Linux® is the registered trademark of Linus Torvalds in the U.S. and other countries.

[7] MKS Integrity, Integrity, and all other PTC product names and logos are trademarks or registered trademarks of Parametric Technology Corporation or its subsidiaries in the United States and in other countries.

STOMP© was developed for these type of applications, among others, and is used to solve the Richards equation and the Advection-Dispersion equation that govern water flow and solute transport, respectively, under variably saturated conditions in the vadose zone and groundwater. The WMA C PA implementation of STOMP© to perform calculations satisfies and complies with environmental quality assurance requirements indicated by 10 CFR 830, Subpart A, "Quality Assurance"; DOE O 414.1D; and State and Federal environmental regulations. Successful acceptance and installation of STOMP© on Tellus concluded in April 2013, and the Hanford Information System Inventory for safety software lists W. J. (Bill) McMahon as an authorized user of Build 4 of STOMP© on the Tellus Platform.

The quality assurance project planning for STOMP© modeling follows the guidance in EPA/240/R-02/007, and the conduct of implementation is shown to comply with DOE management expectations for compliance. Therefore, for this application, STOMP© is an appropriate software code to use. Using it to implement the WMA C PA model described in this report is consistent with STOMP©'s intended use, and its use is shown to comply with applicable quality assurance requirements.

7 MODEL CONFIGURATION MANAGEMENT

All inputs and outputs for the development of WMA C PA models are archived to the CHPRC Environmental Model Management Archive (EMMA) to maintain and preserve models, input files and select output files under configuration management. Inputs include the input files used in the STOMP© simulations and the files called by the input files such as the zonation and boundary node list files. Basis information (that information collected to form the basis for model input parameterization) is also stored in the EMMA for traceability purposes. Use of the STOMP© software for implementing the model described in this report is consistent with its intended use for CHPRC, as indicated in Section 6.4 “Statement of Valid Software Application.”

This page intentionally left blank.

8 REFERENCES

06-AMCP-0133, 2006, "Contract No. DE-AC06-05RL14655 – Hanford Groundwater Modeling Integration" (letter from K. A. Klein to P. L. Pettiette, Washington Closure Hanford, March 9), U.S. Department of Energy, Richland Operations Office, Richland, Washington.

10 CFR 830, "Nuclear Safety Management," *Code of Federal Regulations*, as amended.

10 CFR 830, "Nuclear Safety Management," Subpart A—Quality Assurance Requirements, *Code of Federal Regulations*, as amended.

ASME NQA-1, 2000, *Quality Assurance Requirements for Nuclear Facility Applications*, American National Standards Institute/American Society of Mechanical Engineers, New York, New York.

ASME NQA-1-2008, 2009, *Quality Assurance Requirements for Nuclear Facility Applications*, with the NQA-1a-2009 addenda, American National Standards Institute/American Society of Mechanical Engineers, New York New York.

Comprehensive Environmental Response, Compensation, and Liability Act of 1980, 42 USC 9622, et seq.

CP-47631, 2015, *Model Package Report: Central Plateau Groundwater Model Version 6.3.3*, Rev. 2, INTERA, Inc., Richland, Washington.

Dagan, G., 1984, "Solute transport in heterogeneous porous formations," *Journal of Fluid Mechanics*, Vol. 145, pp. 151–157.

DOE/EIS-0391, 2012, *Final Tank Closure and Waste Management Environmental Impact Statement for the Hanford Site, Richland, Washington*, U.S. Department of Energy, Office of River Protection, Richland, Washington.

DOE G 435.1-1, 1999, *Implementation Guide for Use with DOE M 435.1-1, Radioactive Waste Management Manual*, U.S. Department of Energy, Washington, D.C.

DOE M 435.1-1, 1999, *Radioactive Waste Management Manual*, U.S. Department of Energy, Washington, D.C.

DOE O 414.1C, 2005, *Quality Assurance*, U.S. Department of Energy, Washington, D.C.

DOE O 414.1D, 2011, *Quality Assurance*, U.S. Department of Energy, Washington, D.C.

DOE O 435.1, 1999, *Radioactive Waste Management*, U.S. Department of Energy, Washington, D.C.

DOE/EIS-0391, 2012, *Final Tank Closure and Waste Management Environmental Impact Statement for the Hanford Site, Richland, Washington*, U.S. Department of Energy, Washington, D.C.

DOE/ORP-2005-01, 2006, *Initial Single-Shell Tank System Performance Assessment for the Hanford Site*, Rev. 0, U.S. Department of Energy, Office of River Protection, Richland, Washington.

DOE/ORP-2008-01, 2010, *RCRA Facility Investigation Report for Hanford Single-Shell Tank Waste Management Areas*, Rev. 1, U.S. Department of Energy, Office of River Protection, Richland, Washington.

DOE/RL-92-04, 1993, *PUREX Source Aggregate Area Management Study Report*, Rev. 0, U.S. Department of Energy, Richland Operations Office, Richland, Washington.

DOE/RL-2002-59, 2004, *Hanford Site Groundwater Strategy Protection, Monitoring, and Remediation*, Rev. 0, U.S. Department of Energy, Richland Operations Office, Richland, Washington.

DOE/RL-2007-27, 2011, *Feasibility Study for the Plutonium/Organic-Rich Process Condensate/Process Waste Group Operable Unit: Includes the 200-PW-1, 200-PW-3, and 200-PW-6 Operable Units*, Rev. 0, U.S. Department of Energy, Richland Operations Office, Richland, Washington.

DOE/RL-2011-01, 2011, *Hanford Site Groundwater Monitoring Report for 2010*, Rev. 0, U.S. Department of Energy, Richland Operations Office, Richland, Washington.

DOE/RL-2011-50, 2012, *Regulatory Basis and Implementation of a Graded Approach to Evaluation of Groundwater Protection*, Rev. 1, U.S. Department of Energy, Richland Operations Office, Richland, Washington.

DOE/RL-93-33, 1996, *Focused Feasibility Study of Engineered Barriers for Waste Management Units in the 200 Areas*, Rev. 1, U.S. Department of Energy, Richland Operations Office, Richland, Washington.

Ecology, EPA, and DOE, 1989, *Hanford Federal Facility Agreement and Consent Order – Tri-Party Agreement*, 2 vols., as amended, State of Washington Department of Ecology, U.S. Environmental Protection Agency, and U.S. Department of Energy, Olympia, Washington.

EM-QA-001, 2012, *EM Quality Assurance Program (QAP)*, Rev. 1, Office of Environmental Management, U.S. Department of Energy, Washington, D.C.

EPA/240/B-01/003, 2001, *EPA Requirements for Quality Assurance Project Plans, EPA QA/R-5*, U.S. Environmental Protection Agency, Office of Environmental Information, Washington, D.C.

EPA/240/R-02/007, 2002, *Guidance for Quality Assurance Project Plans for Modeling, EPA QA/G-5M*, U.S. Environmental Protection Agency, Office of Environmental Information, Washington, D.C.

EPA 402-R-94-012, 1994, *A Technical Guide to Ground-Water Model Selection At Sites Contaminated with Radioactive Substances*, U.S. Environmental Protection Agency, Office of Radiation and Indoor Air, Washington, D.C.

EPA/530-SW-87-017, 1987, *Alternate Concentration Limit Guidance Part I ACL Policy and Information Requirements Interim Final*, OSWER Directive 9481.00-6C, Office of Solid Waste, Waste Management Division, U.S. Environmental Protection Agency, Washington, D.C.

EPA/540/1-89/002, 1989, *Risk Assessment Guidance for Superfund Volume I Human Health Evaluation Manual (Part A) Interim Final*, Office of Emergency and Remedial Response, U.S. Environmental Protection Agency, Washington, D.C.

EPA/540/F-95/041, 1996, *Soil Screening Guidance: Fact Sheet*, Publication 9355.4-14FSA, U.S. Environmental Protection Agency, Office of Solid Waste and Emergency Response, Washington, D.C.

EPA/540/R-92/003, 1991, *Guidance for Data Useability in Risk Assessment (Part A) Final*, U.S. Environmental Protection Agency, Office of Emergency Response, Washington, D.C.

EPA/540/R-95/128, 1996, *Soil Screening Guidance: Technical Background Document*, Second Edition, U.S. Environmental Protection Agency, Washington, D.C.

EPA/600/2-91/065, 1991, *The RETC Code for Quantifying the Hydraulic Functions of Unsaturated Soils*, Office of Research and Development, U.S. Environmental Protection Agency, Washington, D.C.

EPA-SAB-RAC-ADV-99-006, 1999, *An SAB Advisory: Modeling of Radionuclide Releases from Disposal of Low Activity Mixed Waste*, U.S. Environmental Protection Agency, Science Advisory Board, Washington, D.C.

ERDA-1538, 1975, *Final Environmental Impact Statement, Waste Management Operations, Hanford Reservation, Richland, Washington*, U.S. Department of Energy, Richland Operations Office, Richland, Washington.

Fayer, M. J. and G. W. Gee, 2006, "Multiple-Year Water Balance of Soil Covers in a Semiarid Setting," *Journal of Environmental Quality*, Vol. 35, No. 2, pp. 366–377.

Gelhar, L. W. and C. L. Axness, 1983, "Three-dimensional analysis of macrodispersion in a stratified aquifer," *Water Resources Research*, Vol. 19, pp. 161–180.

Haynes, W. M. and D. R. Lide, 2011, CRC Handbook of Chemistry and Physics, 92nd Edition, CRC Press, Taylor & Francis Group, Boca Raton, Florida.

HNF-5294, 1999, *Computer Code Selection Criteria for Flow and Transport Code(s) To Be Used in Vadose Zone Calculations for Environmental Analyses in the Hanford Site's Central Plateau*, Rev. 0, CH2M HILL Hanford Group, Inc., Richland, Washington.

HNF-EP-0182, 2014, *Waste Tank Summary Report for Month Ending June 30, 2014*, Rev. 318, Washington River Protection Solutions, LLC, Richland, Washington.

Huyakorn, P. S. and G. F. Pinder, 1993, Computational Methods in Subsurface Flow, Academic Press, Salt Lake City, Utah.

HW-60601, 1959, *Aquifer Characteristics and Ground-Water Movement at Hanford*, Hanford Atomic Products Operation, General Electric Company, Richland, Washington.

Khaleel, R., J. F. Relyea, and J. L. Conca, 1995, "Evaluation of van Genuchten-Mualem Relationships to Estimate Unsaturated Hydraulic Conductivity at Low Water Contents," *Water Resources Research*, Vol. 31, Issue 11, pp. 2659–2668.

Millington, R. J. and J. P. Quirk, 1961, "Permeability of Porous Solids," *Transactions of the Faraday Society*, Vol. 57, pp. 1200–1207.

Mualem, Y., 1976, "A New Model for Predicting the Hydraulic Conductivity of Unsaturated Porous Media," *Water Resources Research*, Vol. 12, No. 3, pp. 513–522.

NAVD88, 1988, *North American Vertical Datum of 1988*, National Geodetic Survey, U.S. Department of Commerce, National Oceanic and Atmospheric Administration, Silver Spring, Maryland.

NCRP Report No. 152, 2005, *Performance Assessment of Near-Surface Facilities for Disposal of Low-Level Radioactive Waste*, National Council on Radiation Protection and Measurements, Bethesda, Maryland.

Neuman, S. P., 1990, "Universal Scaling of Hydraulic Conductivities and Dispersivities in Geologic Media," *Water Resources Research*, Vol. 26, No. 8, pp. 1749–1758.

NOAA Manual NOS NGS 5, 1990, *State Plane Coordinate System of 1983*, National Geodetic Survey, U.S. Department of Commerce, National Oceanic and Atmospheric Administration, Rockville, Maryland.

NUREG-1573, 2000, *A Performance Assessment Methodology for Low-Level Radioactive Waste Disposal Facilities: Recommendations of NRC's Performance Assessment Working Group*, U.S. Nuclear Regulatory Commission, Office of Nuclear Material Safety and Safeguards, Washington, D.C.

NUREG-1854, 2007, *NRC Staff Guidance for Activities Related to U.S. Department of Energy Waste Determinations – Draft Final Report for Interim Use*, U.S. Nuclear Regulatory Commission, Office of Federal and State Materials and Environmental Management Programs, Washington, D.C.

OSWER No. 9200.4-18, 1997, "Establishment of Cleanup Levels for CERCLA Sites with Radioactive Contamination" (Memorandum from S. D. Luftig and L. Weinstock to Addressees, August 22), Office of Solid Waste and Emergency Response, U.S. Environmental Protection Agency, Washington, D.C.

PNNL-11216, 1997, *STOMP Subsurface Transport Over Multiple Phases: Application Guide*, Pacific Northwest National Laboratory, Richland, Washington.

PNNL-12030, 2000, *STOMP Subsurface Transport Over Multiple Phases Version 2.0 Theory Guide*, Pacific Northwest National Laboratory, Richland, Washington.

PNNL-13033, 1999, *Recharge Data Package for the Immobilized Low-Activity Waste 2001 Performance Assessment*, Pacific Northwest National Laboratory, Richland, Washington.

PNNL-13895, 2003, *Hanford Contaminant Distribution Coefficient Database and Users Guide*, Rev. 1, Pacific Northwest National Laboratory, Richland, Washington.

PNNL-14702, 2006, *Vadose Zone Hydrogeology Data Package for Hanford Assessments*, Rev. 1, Pacific Northwest Laboratory, Richland, Washington.

PNNL-15782, 2006, *STOMP Subsurface Transport Over Multiple Phases Version 4.0 User's Guide*, Pacific Northwest National Laboratory, Richland, Washington.

PNNL-16663, 2007, *Geochemical Processes Data Package for the Vadose Zone in the Single-Shell Tank Waste Management Areas at the Hanford Site*, Pacific Northwest National Laboratory, Richland, Washington.

PNNL-16688, 2007, *Recharge Data Package for Hanford Single-Shell Tank Waste Management Areas*, Pacific Northwest National Laboratory, Richland, Washington.

PNNL-17154, 2008, *Geochemical Characterization Data Package for the Vadose Zone in the Single-Shell Tank Waste Management Areas at the Hanford Site*, Pacific Northwest National Laboratory, Richland, Washington.

PNNL-17176, 2008, *200-BP-1 Prototype Hanford Barrier Annual Monitoring Report for Fiscal Years 2005 Through 2007*, Pacific Northwest National Laboratory, Richland, Washington.

PNNL-24118, 2015, *STOMP/eSTOMP Software Quality Assurance Plan*, Rev. 2.1, Pacific Northwest National Laboratory, Richland, Washington.

PNNL-24122, 2015, *Software Requirements Document for STOMP and eSTOMP*, Rev. 3.0, Pacific Northwest National Laboratory, Richland, Washington.

PNNL-SA-92579, 2012, *STOMP Software Test Plan*, Rev. 2, Pacific Northwest National Laboratory, Richland, Washington.

PNNL-SA-92584, 2012, *Subsurface Transport Over Multiple Phases (STOMP) Software Configuration Management Plan*, Rev. 1.5, Pacific Northwest National Laboratory, Richland, Washington.

Polmann, D. J., 1990, Application of Stochastic Methods to Transient Flow and Transport in Heterogeneous Unsaturated Soils, Ph.D. Thesis, Massachusetts Institute of Technology, Department of Civil Engineering, Cambridge, Massachusetts.

PRC-PRO-IRM-309, "Controlled Software Management," CH2M HILL Plateau Remediation Company, Richland, Washington.

RCW 70.105D, "Hazardous Waste Cleanup—Model Toxics Control Act," *Revised Code of Washington*, as amended.

Resource Conservation and Recovery Act of 1976, 42 USC 6901, et seq.

RPP-7494, 2001, *Historical Vadose Zone Contamination from A, AX, and C Tank Farm Operations*, Rev. 0, Fluor Federal Services, Richland, Washington.

RPP-14430, 2003, *Subsurface Conditions Description of the C and A-AX Waste Management Areas*, Rev. 0, CH2M HILL Hanford Group, Inc., Richland, Washington.

RPP-17209, 2006, *Modeling Data Package for an Initial Assessment of Closure of the S and SX Tank Farms*, Rev. 1, CH2M HILL Hanford Group, Inc., Richland, Washington.

RPP-35484, 2008, *Field Investigation Report for Waste Management Areas C and A-AX*, Rev. 1, CH2M HILL Hanford Group, Inc., Richland, Washington.

RPP-CALC-60448, 2016, *WMA C Performance Assessment Contaminant Fate and Transport Model to Evaluate Impacts to Groundwater*, Rev. 0, CH2M HILL Plateau Remediation Company for Washington River Protection Solutions, LLC, Richland, Washington.

RPP-CALC-60450, 2016, *Process for Determining the Volumetric Moisture Content for the Vadose Zone Geologic Units Underlying Waste Management Area C*, Rev. 0, Washington River Protection Solutions, LLC, Richland, Washington.

RPP-ENV-33418, 2011, *Hanford C-Farm Leak Assessments Report*, Rev. 2A, Washington River Protection Solutions, LLC, Richland, Washington.

RPP-ENV-33418, 2015, *Hanford C-Farm Leak Inventory Assessments Report*, Rev. 3, Washington River Protection Solutions, LLC, Richland, Washington.

RPP-PLAN-39114, 2012, *Phase 2 RCRA Facility Investigation/Corrective Measures Study Work Plan for Waste Management Area C*, Rev. 2, Washington River Protection Solutions, LLC, Richland, Washington.

RPP-PLAN-47559, 2012, *Single-Shell Tank Waste Management Area C Pipeline Feasibility Evaluation*, Rev. 1, Washington River Protection Solutions, LLC/Cenibark International, Inc., Richland, Washington.

RPP-RPT-41918, 2010, *Assessment Context for Performance Assessment for Waste in C Tank Farm Facilities after Closure*, Rev. 0, Washington River Protection Solutions, LLC, Richland, Washington.

RPP-RPT-42294, 2015, *Hanford Waste Management Area C Soil Contamination Inventory Estimates*, Rev. 2, Washington River Protection Solutions, LLC, Richland, Washington.

RPP-RPT-42323, 2010, *Hanford C-Farm Tank and Ancillary Equipment Residual Waste Inventory Estimates*, Rev. 1, Washington River Protection Solutions, LLC, Richland, Washington.

RPP-RPT-42323, 2015, *Hanford C-Farm Tank and Ancillary Equipment Residual Waste Inventory Estimates*, Rev. 3, Washington River Protection Solutions, LLC, Richland, Washington.

RPP-RPT-44042, 2010, *Recharge and Waste Release within Engineered System in Waste Management Area C*, Rev. 0, Washington River Protection Solutions, LLC, Richland, Washington.

RPP-RPT-46088, 2010, *Flow and Transport in the Natural System at Waste Management Area C*, Rev. 1, Washington River Protection Solutions, LLC/GSI Water Solutions, Inc., Richland, Washington.

RPP-RPT-46879, 2011, *Corrosion and Structural Degradation within Engineered System in Waste Management Area C*, Rev. 2, Washington River Protection Solutions, LLC, Richland, Washington.

RPP-RPT-48490, 2011, *Technical Approach and Scope for Flow and Contaminant Transport Analysis in the Initial Performance Assessment of Waste Management Area C*, Rev. 1, Washington River Protection Solutions, LLC, Richland, Washington.

RPP-RPT-49425, 2011, *Ecological Risk Assessment Approach for Hanford Waste Management Area C*, Rev. 1, Washington River Protection Solutions, LLC, Richland, Washington.

RPP-RPT-56356, 2014, *Development of Alternative Digital Geologic Models of Waste Management Area C*, Rev. 0, Freestone Environmental Services Inc./Washington River Protection Solutions, LLC, Richland, Washington.

RPP-RPT-58948, 2016, *Model Package Report System Model for the WMA C Performance Assessment and RCRA Closure Analysis Version 1.0*, Rev. 0, Washington River Protection Solutions, LLC, Richland, Washington.

Schulze-Makuch, D., 2005, "Longitudinal Dispersivity Data and Implications for Scaling Behavior," *Ground Water*, Vol. 43, No. 3, pp. 443–456.

van der Kamp, G., L. D. Luba, J. A. Cherry, and H. Maathuis, 1994, "Field Study of a Long and Very Narrow Contaminant Plume," *Ground Water*, Vol. 32, No. 6, pp. 1008–1016.

van Genuchten, M.Th., 1980, "A Closed-form Equation for Predicting the Hydraulic Conductivity of Unsaturated Soils" *Soil Science Society of America Journal*, Vol. 44, No. 5, pp. 892–898.

WAC 173-340-747 "Deriving Soil Concentrations for Groundwater Protection," *Washington Administrative Code*, Olympia, Washington, as amended.

WAC 246-290 "Group A Public Water Supplies," *Washington Administrative Code*, Olympia, Washington, as amended.

WAC 246-290-310 "Maximum Contaminant Levels (MCLs) and Maximum Residual Disinfectant Levels (MRDLs)," *Washington Administrative Code*, Olympia, Washington, as amended.

WCH-520, 2013, *Performance Assessment for the Environmental Restoration Disposal Facility, Hanford Site, Washington*, Rev. 1, Washington Closure Hanford, Richland, Washington.

WHC-SD-WM-EE-004, 1995, *Performance Assessment of Grouted Double-Shell Tank Waste Disposal at Hanford*, Rev. 1, Westinghouse Hanford Company, Richland, Washington.

WSRC-MS-2003-00582, 2003, *Performance Assessment/Composite Analysis Modeling to Support a Holistic Strategy for the Closure of F Area, a Large Nuclear Complex at the Savannah River Site*, Rev. 1, Savannah River Technology Center, Aiken, South Carolina.

Xu, M. and Y. Eckstein, 1995, "Use of Weighted Least-Squares Method in Evaluation of the Relationship Between Dispersivity and Field Scale," *Ground Water*, Vol. 33, No. 6, pp. 905–908.

Ye, M., R. Khaleel, and T.-C. J. Yeh, 2005, "Stochastic analysis of moisture plume dynamics of a field injection experiment," *Water Resources Research*, Vol. 41, W03013.

Yeh, T.-C. J., M. Ye, and R. Khaleel, 2005. "Estimation of effective unsaturated hydraulic conductivity tensor using spatial moments of observed moisture plume," *Water Resources Research*, Vol. 41, W03014.

APPENDIX A

KEY ASSUMPTIONS IN THE PERFORMANCE ASSESSMENT

This page intentionally left blank.

LIST OF TERMS

Abbreviations and Acronyms

DOE	U.S. Department of Energy
RCRA	*Resource Conservation and Recovery Act of 1976*
WMA	Waste Management Area

This page intentionally left blank.

APPENDIX A

KEY ASSUMPTIONS IN THE PERFORMANCE ASSESSMENT

In this Appendix, a set of key assumptions used in the base case analysis of the Performance Assessment are listed. However, it is emphasized that the structure of the Performance Assessment is founded on the extensive use of sensitivity and uncertainty analyses that explore the consequences if alternative assumptions are used. The alternative analyses include sensitivity cases evaluating conditions well outside the range of the base case analysis. In all cases the calculations produced results that are below the performance measures. Therefore, it is not possible to identify key assumptions or design variables that must be met in order to meet the regulatory goals of DOE O 435.1, *Radioactive Waste Management*.

- It has been assumed that the landfill closure of Waste Management Area (WMA) C occurs in 2020, consistent with planning assumptions in the Tank Closure and Waste Management Environmental Impact Statement (DOE/EIS-0391, *Final Tank Closure and Waste Management Environmental Impact Statement for the Hanford Site, Richland, Washington*). The results of the performance assessment are not significantly affected by alternative assumptions about closure timing.

- The Central Plateau has been designated Industrial-Exclusive for the indefinite future, based on several Records of Decision [64 FR 61615, "Record of Decision: Hanford Comprehensive Land-Use Plan Environmental Impact Statement (HCP EIS)"; 73 FR 55824, "Amended Record of Decision for the Hanford Comprehensive Land-Use Plan Environmental Impact Statement"]. This area, which includes the 200 East and 200 West Areas, includes WMA C. There is no stated intention to release the Central Plateau from this designation or from U.S. Department of Energy (DOE) control at any time in the future. Despite this designation, it is assumed in this analysis that institutional control and societal memory of the disposal activities are lost 100 years after site closure, for consistency with DOE O 435.1 requirements. This assumption is necessary to allow future hypothetical individuals to come onto the Central Plateau and engage in activities that might result in exposure.

- In the base case, the land use and land cover, including the barrier, remain shrub steppe indefinitely after closure. Alternative infiltration rates in the future are included in alternative analysis cases, which are intended to address a variety of potential future conditions, including progression to different land uses and land covers.

- The engineered cover for WMA C is not yet designed but is assumed to be similar to the Modified *Resource Conservation and Recovery Act of 1976* (RCRA) Subtitle C Barrier that limits infiltration through the waste primarily by evapotranspiration processes (i.e., surface barrier) based on the work done for the Hanford Prototype barrier (DOE/ORP-2008-01, *RCRA Facility Investigation Report for Hanford Single-Shell Tank Waste Management Areas*, Appendix C). These processes are not modeled directly for this report, but those processes have been studied through field measurements, tracer studies, and numerical models to estimate net infiltration (PNNL-14744, *Recharge Data*

Package for the 2005 Integrated Disposal Facility Performance Assessment; PNNL-14960, *200-BP-1 Prototype Hanford Barrier Annual Monitoring Report for Fiscal Year 2004*; "Multiple-Year Water Balance of Soil Covers in a Semiarid Setting" [Fayer and Gee 2006]). Instead, the recommended net infiltration rates from those reports are applied to the area under the engineered cover and are varied spatially and temporally as appropriate according to the estimated or assumed time-dependent performance of a surface barrier.

- The design life of the cover is assumed to be 500 years in the base case, following which the infiltration through the cover is assumed to return to the site-wide average infiltration rate for undisturbed soil. Alternative infiltration rates in the future are included in alternative analysis cases, which are intended to address a variety of potential future conditions, including progression to different land uses and land covers.

- It is assumed the tanks will be filled with grout according to the basic assumptions outlined for landfill closure in DOE/EIS-0391 (2012). The specific formulation of the grout has not yet been established, but consistent with DOE/EIS-0391 (2012), it is assumed the fill material for the tanks will be similar to the cold-cap grout formulation developed by the U.S. Army Corps of Engineers for the Hanford Grout Vault Program. This type of grout is assumed to behave chemically like ordinary cementitious material. It has been assumed that the grout formulation does not provide any specific or unusual chemical conditions, such as reducing conditions.

- Radionuclide and chemical release mechanisms from the sources are assumed to occur by one of two mechanisms: (a) the entire inventory of the residual waste is assumed to be instantly available for release and transport out of the tanks, or (b) a semi-empirical release function is applied based on leach tests performed on residual waste from WMA C.

- Transport of contamination from the tanks is assumed to be primarily controlled by diffusion from the grouted tanks through the base mat below the tank. Alternative assumptions are included as sensitivity cases that evaluate the consequences of hydraulic failure (i.e., fracturing) of the grouted tanks and base mat.

- The specific formulation of the grout has not yet been established, and site-specific measurements of the chemical influence of the grout have not been performed. The chemical effect of the grout is represented by contaminant-specific distributions of distribution coefficients (K_d), which have been developed from international literature on sorption of radionuclides on cementitious materials. These values are generally consistent with or more conservative than comparable values used for the facility-specific grout at the Savannah River F and H tank farm performance assessments [WSRC-STI-2007-00369, *Hydraulic and Physical Properties of Tank Grouts and Base Mat Surrogate Concrete for FTF Closure* and WSRC-STI-2007-00607, *Chemical Degradation Assessment of Cementitious Materials for the HLW Tank Closure Project (U)*].

- Release from one WMA C solute source and migration are independent of other solute transport and source terms in the model.

- The post-retrieval inventory of contaminants in WMA C is assumed to be uniformly distributed throughout the waste residual volume. The residual volume in the tanks is assumed to be a uniform layer distributed at the bottom of the tanks. In pipelines and ancillary equipment, the residual waste is assumed to be distributed in a homogeneous layer across the WMA C at the depth and area of the pipelines.

- Progeny radionuclides with a half-life of less than two years are assumed to be in secular equilibrium with their parent, which allows a reduction in the number of species tracked but still accounts for the radiological effects of the progeny.

- Inventories of contaminants in retrieved tanks are based on post-retrieval sampling and measurements. It is assumed that the sampling results are representative of the entire waste residual. Inventories for tanks that have not yet completed retrieval use the best estimates of post-retrieval conditions available at this time. These data have been estimated as of September 30, 2014. Additional sensitivity cases were executed based on alternative inventories in the 2009 to 2011 working sessions.

- The vadose zone is modeled as an aqueous-gas porous media system where flow and transport through the gas phase are assumed to be negligible.

- Hydraulic property heterogeneity is assumed to be insignificant within geologic units. Hence, each geologic unit within the vadose zone is assigned upscaled, effective hydraulic properties. These properties have been updated from the input parameters presented in the 2009 and 2011 data packages based on consideration of field data for moisture content, as discussed in Appendix B.

- Post-closure groundwater flow beneath WMA C is assumed to be northwest to southeast and parallel to the four tank arrays of 100-series tanks in WMA C. The justification for this assumption is found in RPP-RPT-46088, *Flow and Transport in the Natural System at Waste Management Area C*. Groundwater flow parameters have been derived from the Central Plateau groundwater model (CP-47631, *Model Package Report: Central Plateau Groundwater Model Version 6.3.3*).

- Distribution coefficients (K_d) are used to represent sediment-contaminant chemical interaction that best represent plausible levels of reactivity. The K_d values are chosen assuming low-salt, near-neutral waste chemistry in the vadose and saturated zone. Justification for the selected parameter values is found in RPP-RPT-46088; PNNL-16663, *Geochemical Processes Data Package for the Vadose Zone in the Single-Shell Tank Waste Management Areas at the Hanford Site*; and PNNL-17154, *Geochemical Characterization Data Package for the Vadose Zone in the Single-Shell Tank Waste Management Areas at the Hanford Site*. In addition, uncertainties in K_d values have been assessed as part of the uncertainty analysis.

- The point of calculation used in the calculation of the groundwater concentrations corresponds to the location 100 m (328 ft) downgradient from the facility per DOE O 435.1. For the purpose of calculating groundwater concentrations for comparison with groundwater protection requirements, it is necessary to identify the peak location in space at which the concentration occurs. The approach for identifying the peak location is described below.

- For volatiles released from the residual wastes, it is assumed that transport through the tank infill grout material and the soil overburden is controlled by diffusion.

- Once volatile radionuclides reach the ground surface, a simplified Gaussian plume model with uniform velocity and atmospheric conditions is assumed for the air transport analysis.

- Assumptions used in the exposure scenarios to define input parameter values are based on appropriate regulatory guidance as detailed in RPP-ENV-58813, *Exposure Scenarios for Risk and Performance Assessments in Tank Farms at the Hanford Site, Washington*. These values represent conservative inputs to the exposure scenario calculations characteristic of a highly exposed individual.

- Age- and gender-weighted intake rates are generally developed for a Representative Person in accordance with the recommendations described in DOE-STD-1196-2011, *Derived Concentration Technical Standard*. The 95th percentile intake rates were obtained from EPA/600/R-090/052F, *Exposure Factors Handbook: 2011 Edition, National Center for Environmental Assessment*, based on available information. Even though mean intake rates were available, the 95th percentile values from the underlying distribution were chosen conservatively to maximize the likely exposure. Typically, the 95th percentile intake rates weighted by age and gender are calculated (Appendix P of RPP-ENV-58813). The exceptions to this approach were the indoor inhalation rate (taken directly from a reference source) and the soil ingestion rates (where simple age weighting is performed for children and adults).

- The following assumptions are specific to inadvertent human intrusion.

    - The only credible intrusion event is a drilling event. Both depth of disposal and the existence of concrete and grout intrusion barriers limit credible intrusion scenarios.

    - Although results are provided for intrusion into individual single-shell tanks, the most credible intrusion event is assumed to be into the ancillary equipment rather than a tank. This type of event is more credible than a tank intrusion, since the tank dome and grout form a substantial intruder protection barrier.

    - For the analysis of intrusion into the pipelines, the driller is assumed to penetrate a transfer line at 100 years after closure. Sensitivity analyses have investigated intrusion into a cascade line, which would release a larger inventory relative to other pipeline locations in WMA C.

- For the intrusion analysis for the 100- and 200-series tanks, the C-301 catch tank, and the 244-CR Process Tank Vault, the intruder is assumed to penetrate the tank dome, tank shell, grout, and residual waste at 500 years after closure.

- The acute exposure to the driller is calculated using representative local assumptions about the duration of the drilling.

- Acute exposures are limited to a well driller that is exposed to waste exhumed by the drill bit during the drilling.

- Chronic post-intrusion exposures are calculated for several alternative exposure scenarios. In these scenarios, waste exhumed by the intrusion event is assumed to be mixed with a surface soil layer. In each scenario, the volume of soil in this layer represents the minimum area consistent with the assumed activities of the scenario. For instance, the residential garden scenario mixes the contamination in an area of a garden sufficient to grow vegetables, whereas the rural pasture scenario mixes the contamination in an area sufficient for cattle grazing. The effect of this assumption is that different post-intrusion chronic scenarios have different soil concentrations, and the relative importance of the scenarios is strongly dependent on the assumed area of contamination.

REFERENCES

64 FR 61615, 1999, "Record of Decision: Hanford Comprehensive Land-Use Plan Environmental Impact Statement (HCP EIS)," *Federal Register*, Vol. 64, pp. 61615–61625 (November 12).

73 FR 55824, 2008, "Amended Record of Decision for the Hanford Comprehensive Land-Use Plan Environmental Impact Statement," *Federal Register*, Vol. 73, pp. 55824–55826 (September 26).

CP-47631, 2015, *Model Package Report: Central Plateau Groundwater Model Version 6.3.3*, Rev. 2, INTERA, Inc., Richland, Washington.

DOE/EIS-0391, 2012, *Final Tank Closure and Waste Management Environmental Impact Statement for the Hanford Site, Richland, Washington*, U.S. Department of Energy, Washington, D.C.

DOE O 435.1, 2001, *Radioactive Waste Management*, U.S. Department of Energy, Washington, D.C.

DOE/ORP-2008-01, 2010, *RCRA Facility Investigation Report for Hanford Single-Shell Tank Waste Management Areas*, Rev. 1, U.S. Department of Energy, Office of River Protection, Richland, Washington.

DOE-STD-1196-2011, 2011, *Derived Concentration Technical Standard*, U.S. Department of Energy, Washington, D.C.

EPA/600/R-090/052F, 2011, *Exposure Factors Handbook: 2011 Edition, National Center for Environmental Assessment*, Office of Research and Development, U.S. Environmental Protection Agency, Washington, D.C.

Fayer, M. J., and G. W. Gee, 2006, "Multiple-Year Water Balance of Soil Covers in a Semiarid Setting," *Journal of Environmental Quality*, Vol. 35, No. 2, pp. 366–377.

PNNL-14744, 2004, *Recharge Data Package for the 2005 Integrated Disposal Facility Performance Assessment*, Pacific Northwest National Laboratory, Richland, Washington.

PNNL-14960, 2005, *200-BP-1 Prototype Hanford Barrier Annual Monitoring Report for Fiscal Year 2004*, Pacific Northwest National Laboratory, Richland, Washington.

PNNL-16663, 2007, *Geochemical Processes Data Package for the Vadose Zone in the Single-Shell Tank Waste Management Areas at the Hanford Site*, Pacific Northwest National Laboratory, Richland, Washington.

PNNL-17154, 2008, *Geochemical Characterization Data Package for the Vadose Zone in the Single-Shell Tank Waste Management Areas at the Hanford Site*, Pacific Northwest National Laboratory, Richland, Washington.

Resource Conservation and Recovery Act of 1976, 42 USC 6901, et seq.

RPP-ENV-58813, 2016, *Exposure Scenarios for Risk and Performance Assessments in Tank Farms at the Hanford Site, Washington*, Rev. 0, Washington River Protection Solutions, LLC, Richland, Washington.

RPP-RPT-46088, 2010, *Flow and Transport in the Natural System at Waste Management Area C*, Rev. 1, Washington River Protection Solutions, LLC/GSI Water Solutions, Inc., Richland, Washington.

WSRC-STI-2007-00369, 2007, *Hydraulic and Physical Properties of Tank Grouts and Base Mat Surrogate Concrete for FTF Closure*, Rev. 0, Savannah River National Laboratory, Aiken, South Carolina.

WSRC-STI-2007-00607, 2007, *Chemical Degradation Assessment of Cementitious Materials for the HLW Tank Closure Project (U)*, Rev. 0, Washington Savannah River Company/ Savannah River National Laboratory, Aiken, South Carolina.

APPENDIX B

BASIS FOR DEVELOPMENT OF VADOSE ZONE HYDRAULIC PROPERTIES AT WASTE MANAGEMENT AREA C

This page intentionally left blank.

TABLE OF CONTENTS

APPENDIX B – BASIS FOR DEVELOPMENT OF VADOSE ZONE HYDRAULIC PROPERTIES AT WASTE MANAGEMENT AREA C B-1

B.1 MOISTURE CONTENT MEASUREMENTS AT WASTE MANAGEMENT AREA C B-1

B.1.1 Moisture Content Measurements for Hanford H2 Sand-Dominated Unit B-2

B.1.2 Moisture Content Measurements for Hanford H1, Hanford H3 and Backfill Gravelly Units B-13

B.2 LABORATORY-SCALE MEASUREMENTS FOR HYDRAULIC PROPERTIES B-22

B.2.1 Properties of the Hanford H2 Sand Unit B-22

B.2.2 Properties of the Hanford H1 and H3 Gravelly Units B-28

B.2.3 Properties for the Backfill Gravelly Unit B-33

B.3 EFFECTIVE (UPSCALED) FLOW PARAMETERS FOR VADOSE ZONE B-33

B.3.1 Composite Macroscopic Relationships and Effective Parameters B-34

B.3.2 Stochastic Model for Macroscopic Anisotropy B-36

B.3.3 Macroscopic Anisotropy Relations B-41

B.4 EFFECTIVE TRANSPORT PARAMETERS B-43

B.4.1 Bulk Density and K_d B-44

B.4.2 Diffusivity B-44

B.4.3 Vadose Zone Macrodispersivities B-44

B.5 REFERENCES B-55

LIST OF FIGURES

Figure B-1. Distribution of Moisture Content Measurements Collected in and around Waste Management Area C (a) Plan View with all Moisture Content Data, (b) Plan View with all Moisture Content Data Inside the Single-Shell Tank Footprint, (c) Plan View with all Moisture Content Data Outside the Single-Shell Tank Footprint and (d) a Side View Looking Northwest. B-3

Figure B-2a. Waste Management Area C Moisture Content Histogram for All H2 Data (Includes the Data from Both Inside and Outside of the Single-Shell Tank Footprint). B-4

Figure B-2b. Waste Management Area C Moisture Content Histogram for H2 Data Within the Single-Shell Tank Footprint. B-5

Figure B-2c. Waste Management Area C Moisture Content Histogram for H2 Data Outside of the Single-Shell Tank Footprint. B-6

Figure B-3. Location of Sisson and Lu Site, Integrated Disposal Facility and Selected Boreholes in 200 Area. B-7

Figure B-4. (a) Pre- and (b) Post-Injection Moisture Plumes for the Field Injection Experiment in the 200 East Area. B-8

Figure B-5. Borehole Location Map for Waste Management Area C. B-9

Figure B-6a. Borehole C4297 Lithology and Gravimetric Moisture Content Measurements (the shaded areas in light blue and gray are regions of increased moisture). B-10

Figure B-6b. Borehole 299-E27-22 Lithology and Gravimetric Moisture Content Measurements (the shaded areas in light blue and gray are regions of increased moisture). B-11

Figure B-7a. Matric Potentials Measured by Filter Paper Technique on Core Samples from Borehole C4297. ..... B-14

Figure B-7b. Matric Potentials Measured by Filter Paper Technique on Core Samples from Borehole 299-E27-22. ..... B-15

Figure B-8a. Comparison of Gravimetric Moisture Content Measurements for Boreholes C4297 and 299-E27-22. ..... B-17

Figure B-8b. Comparison of Soil Moisture Tension Measurements for Boreholes C4297 and 299-E27-22. ..... B-18

Figure B-9a. Waste Management Area C Moisture Content Histogram for All H1 Data (Includes the Data from Both Inside and Outside of the Single-Shell Tank Footprint). B-19

Figure B-9b. Waste Management Area C Moisture Content Histogram for H1 Data Within the Single-Shell Tank Footprint. B-19

Figure B-9c. Waste Management Area C Moisture Content Histogram for H1 Data Outside of the Single-Shell Tank Footprint. B-20

Figure B-10a. Waste Management Area C Moisture Content Histogram for All Backfill Data (Includes the Data from Both Inside and Outside of the Single-Shell Tank Footprint). B-20

Figure B-10b. Waste Management Area C Moisture Content Histogram for Backfill Data Inside of the Single-Shell Tank Footprint. B-21

Figure B-10c. Waste Management Area C Moisture Content Histogram for Backfill Data Outside the Single-Shell Tank Footprint. B-22

Figure B-11. Waste Management Area C Hanford H2 Sand-Dominated Core. B-23

Figure B-12. Moisture Retention Data for H2 Unit (44 Samples). B-28

Figure B-13. Unsaturated Hydraulic Conductivity Data for H2 Unit (44 Samples). B-29

Figure B-14. Comparison of Simulated (Blue) and Observed (Circle) Moisture Content for Hanford H2 Sand-Dominated Unit. B-30

Figure B-15. Moisture Retention Curves for Various Hydrostratigraphic Units and Selected Properties for Alternative Geologic Model II. B-31

Figure B-16. Unsaturated Hydraulic Conductivity Curves for Various Hydrostratigraphic Units and Selected Properties for Alternative Geologic Model II. B-32

Figure B-17. Unsaturated Hydraulic Conductivity Measurements for Sand-Dominated and Gravel-Dominated Samples. B-33

Figure B-18. Moisture Retention Data for H1 and H3 Units (17 Samples). B-36

Figure B-19. Unsaturated Hydraulic Conductivity Data for H1 and H3 Units (17 Samples). B-37

Figure B-20. Moisture Retention Data for Backfill Unit (10 Samples). B-39

Figure B-21. Unsaturated Hydraulic Conductivity Data for Backfill Units (10 Samples). B-40

Figure B-22. Experimental (Triangles) and Fitted Theoretical (Squares) Variogram for Saturated Hydraulic Conductivity (LnKs)..... B-42

Figure B-23. Calculated Macroscopic Anisotropy as a Function of Mean Matric Potential for the H2 Sand-Dominated Unit..... B-43

Figure B-24. Calculated Macroscopic Anisotropy as a Function of Mean Matric Potential for the H1 and H3 Gravelly Units. B-45

Figure B-25. Calculated Macroscopic Anisotropy as a Function of Mean Matric Potential for Backfill Gravelly Unit..... B-46

Figure B-26. (a) Ks, (b) α, and (c) n Random Distribution for a Single Realization. B-47

Figure B-27. Simulated Concentration Distribution for a Single Realization at (a) 400 days, (b) 700 days, and (c) 1,000 days and (d) the Averaged Concentration Profile at Those Times for Flow Perpendicular to Bedding for a Mean Pressure Head (H) of -1 m. B-49

Figure B-28. Simulated Concentration Distribution for a Single Realization at (a) 400 days, (b) 700 days, and (c) 1,000 days and (d) the Averaged Concentration Profile at Those Times for Flow Parallel to Bedding for a Mean Pressure Head (H) of -1 m. B-52

Figure B-29. Longitudinal Laboratory- and Field-Scale Dispersivities in Unsaturated Media as a Function of Overall Problem Scale. B-54

LIST OF TABLES

Table B-1. Summary Statistics for Waste Management Area C Moisture Content (% Volume) Database. B-4

Table B-2. Mean Moisture and Matric Potentials for Borehole Samples Inside and Outside of Waste Management Area C. B-16

Table B-3. van Genuchten Parameters (Based on the Multistep Method) and Saturated Hydraulic Conductivity Data for 44 Integrated Disposal Facility Borehole Samples from the H2 Sandy Sequence. B-25

Table B-4. Wet Sieve Particle Size Distribution for Borehole 299-E27-22 Sediments. B-27

Table B-5. van Genuchten Parameters, Fitted Saturated Hydraulic Conductivity, and Measured Bulk Density Data for H1/H3 Units (17 Samples). B-35

Table B-6. van Genuchten Parameters, Fitted Saturated Hydraulic Conductivity, and Measured Bulk Density Data for Backfill Unit (10 Samples). B-38

Table B-7. Composite van Genuchten-Mualem Parameters for Waste Management Area C Hydrostratigraphic Units. B-40

Table B-8. Simulated Average Tension Ranges for Polmann Anisotropy Model. B-42

Table B-9. Variable, Macroscopic Anisotropy Parameter Estimates for Various Waste Management Area C Units. B-43

Table B-10. Effective Bulk Density (g/cm^3) Estimates for Waste Management Area C Hydrostratigraphic Units. B-46

Table B-11. Longitudinal Macrodispersivity Estimates (cm). B-55

LIST OF TERMS

Abbreviations and Acronyms

ACM-I/ACM1	Alternative Geologic Model I
ACM-II/ACM2	Alternative Geologic Model II
EHM	equivalent homogeneous medium
ERDF	Environmental Restoration Disposal Facility
HSU	hydrostratigraphic unit
IDF	Integrated Disposal Facility
MC	Monte Carlo
MPa	megapascal
PA	performance assessment
RCRA	*Resource Conservation and Recovery Act of 1976*
RETC	RETention Curve
S&L	Sisson and Lu
SST	single-shell tank
WMA	Waste Management Area

APPENDIX B

BASIS FOR DEVELOPMENT OF VADOSE ZONE HYDRAULIC PROPERTIES AT WASTE MANAGEMENT AREA C

This appendix provides a description of the basis for the selection of hydraulic properties for hydrostratigraphic units (HSUs) identified at Waste Management Area (WMA) C. No WMA C site-specific data are available that can be used to directly develop estimates of hydraulic properties needed for the performance assessment (PA). As a result, a process has been developed for identifying surrogate hydraulic properties based on samples collected at other sites within the 200 Areas that are considered to be representative of sediments characteristic of the major HSUs identified at WMA C. The selected properties were then used to simulate a WMA C vadose zone flow field and the simulation results were cross-checked against field moisture contents for different WMA C units. This step allowed an updating of the properties by incorporating data sets developed from data collected at other nearby sites within the 200 Areas that are consistent with WMA C field data.

The following information is included in this Appendix:

- WMA C moisture content database, its consistency with nearby field data, and a summary of available data on 241-C Tank Farm (C Farm) soil-water matric potential and their impact on the selection of moisture characteristic data for PA modeling (see Section B.1)

- Evaluation of laboratory measurements for vadose zone soil moisture retention, saturated and unsaturated hydraulic conductivity for samples in the vicinity of C Farm and 200 Areas (see Section B.2 below) as the basis for the selection of hydraulic properties for the major HSUs identified at WMA C (see Section B.2)

- Comparison of observed and simulated moisture content using selected hydraulic properties (see Section B.2.1.1)

- Moisture characteristic curves for major HSUs identified for Alternative Geologic Models I and II (see Section B.2.1.2)

- Effective (upscaled) moisture retention, saturated and unsaturated hydraulic conductivity, bulk density, diffusivity, and macrodispersivity estimates for various strata (see Sections B.3 and B.4).

B.1 MOISTURE CONTENT MEASUREMENTS AT WASTE MANAGEMENT AREA C

As part of WMA C site characterization, an extensive database of moisture content information is available for various HSUs. The moisture content database was developed as part of a direct push campaign conducted at WMA C in 2008, and understood as being long after the occurrence

of past leaks and discharges at the farm. A summary of these measurements for the WMA C area and associated statistics presented in this Appendix is provided in RPP-CALC-60450, *Process for Determining the Volumetric Moisture Content for the Vadose Zone Geologic Units Underlying Waste Management Area*.

The spatial distribution of all moisture measurements collected in and around WMA C is shown in Figure B-1(a); the database includes moisture content data collected both within the footprint of the single-shell tanks (SSTs) (i.e., where the backfill is thickest) [Figure B-1(b)] and outside this area (where the backfill is thin or non-existent) [Figure B-1(c)]. The green line on Figure B-1(b) and (c) reflects the approximate demarcation of areas inside and outside of the SST footprint. In each of the four plots on Figure B-1, the size of the circles depicted at each borehole is indicative of the magnitude of moisture content. The larger-diameter circles (higher moisture content) are more prevalent in the shallower units and outside the farm. Figure B-1(d) is a perspective view looking north-northwest, showing both the vertical direct pushes, dry wells, groundwater well, characterization borehole, and slant direct pushes.

A summary of the statistics of the moisture content measurements by major HSUs is provided in Table B-1. Overall, the moisture content data show considerable variability: the range varies from a low of 0.11 (% volume) for backfill to as high as 30.64 (% volume) for H1 unit (Table B-1).

B.1.1 Moisture Content Measurements for Hanford H2 Sand-Dominated Unit

The Hanford H2 (sand-dominated) unit is the dominant unit at WMA C in terms of vadose zone thickness. The largest number of the moisture content measurements is associated with the Hanford H2 unit (Table B-1).

Figure B-1(a) and (b) show the location of where moisture content measurements were made in the Hanford H2 unit relative to the green line that marks the boundary of where the backfill is thickest (i.e., within the footprint of the SSTs). Figure B-2a shows the histogram for H2 moisture data for all measurements inside and outside of the SST footprint. Figure B-2b shows the histogram for measurements inside the SST footprint, whereas Figure B-2c shows the histogram for measurements outside the SST footprint. While the average for all H2 measurements (inside as well as outside of SST footprint) is ~5.15 (% volume) (Figure B-2a), inside the tank farm, the average is 5.09 (% volume), with the range varying from ~1.86% to 19.9% and a variance of 3.03% (Figure B-2b). Outside the SST footprint, the average is 5.17 (% volume), with the range varying from ~1.06% to 26.32% and a variance of 3.39% (Figure B-2c). The statistics suggest that the averages for moisture content measurements inside and outside the SST footprint are not significantly different. The variance for measurements inside the SST footprint is lower, compared to variance for measurements outside the SST footprint. This may simply be a reflection of a smaller sample size (a count of 5,143 inside of the SST footprint versus a count of 15,733 outside of the SST footprint), or may reflect differences in media heterogeneities within the H2 unit.

Figure B-1. Distribution of Moisture Content Measurements Collected in and around Waste Management Area C (a) Plan View with all Moisture Content Data, (b) Plan View with all Moisture Content Data Inside the Single-Shell Tank Footprint, (c) Plan View with all Moisture Content Data Outside the Single-Shell Tank Footprint and (d) a Side View Looking Northwest.

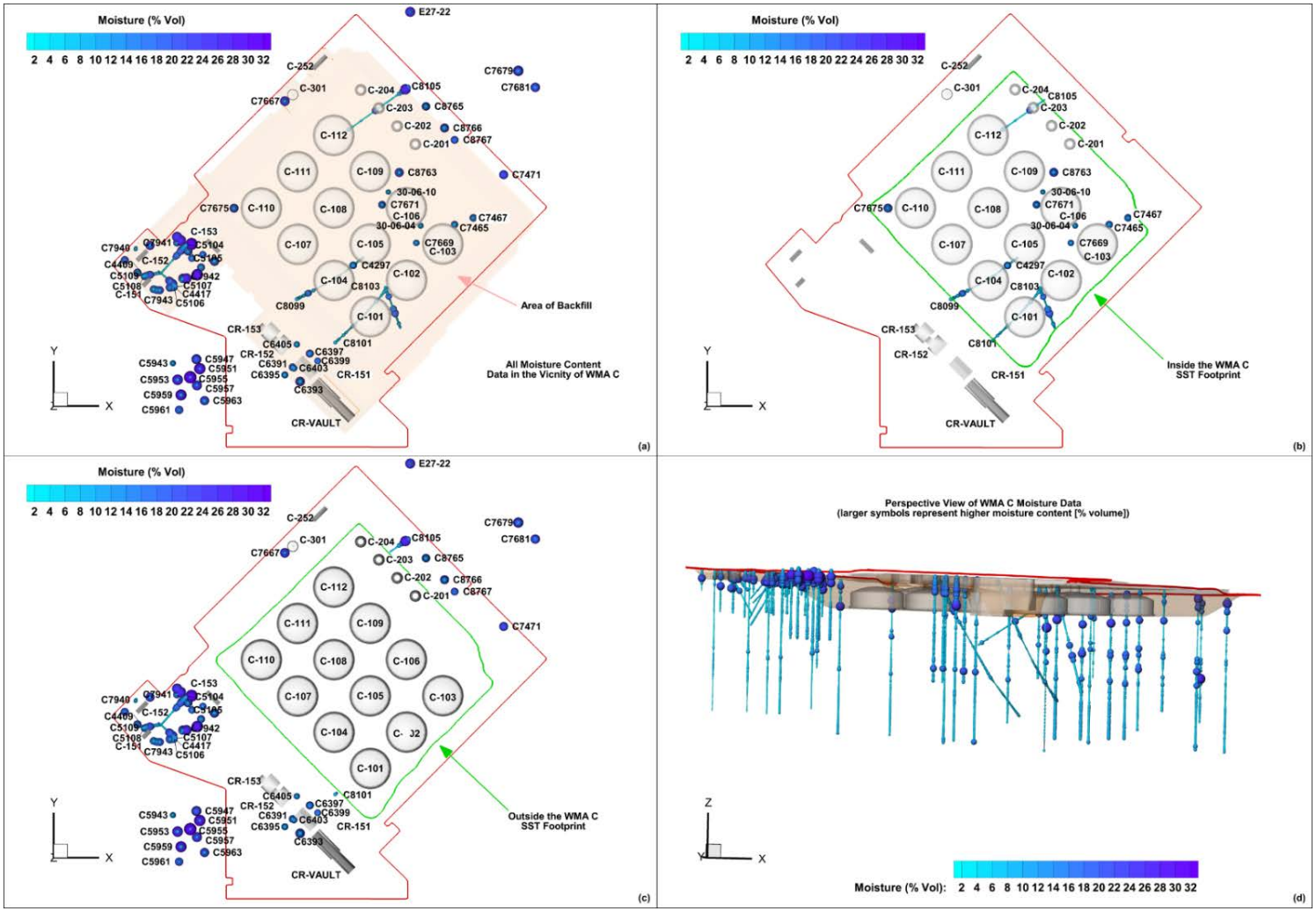

SST = single-shell tank WMA = waste management area

Table B-1. Summary Statistics for Waste Management Area C Moisture Content (% Volume) Database.

Unit	Count	Minimum	Maximum	Average
Backfill	4,052	0.11	30.61	8.09
H1	7,977	0.13	30.64	5.88
H2	20,876	1.06	26.32	5.15
H3	7	5.54	7.09	6.18
All Units	32,912	0.11	30.64	5.69

Figure B-2a. Waste Management Area C Moisture Content Histogram for All H2 Data (Includes the Data from Both Inside and Outside of the Single-Shell Tank Footprint).

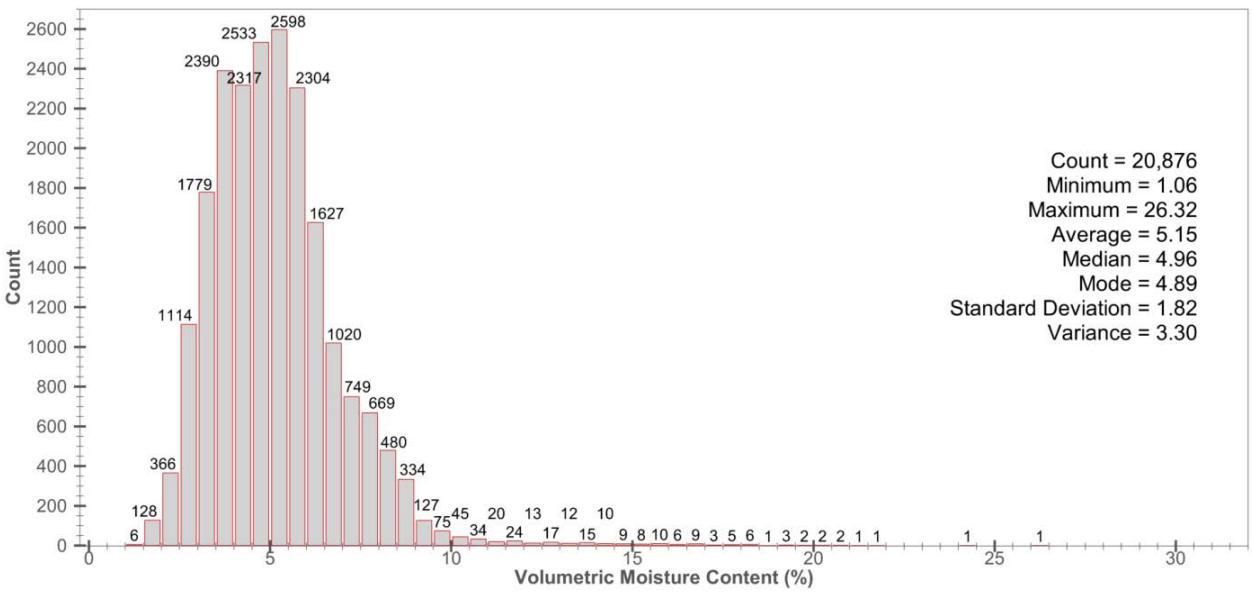

B.1.1.1 Comparison with Sisson and Lu Site Moisture Content Measurements. In this section of the Appendix, the moisture content measurements for the Hanford H2 unit at WMA C is compared to, and checked for consistency against, another extensive set of moisture content measurements collected at the nearby Sisson and Lu (S&L) field injection site in 200 East Area (Figure B-3). Unlike WMA C, soil hydraulic properties data are available for the S&L site (PNNL-14284, *Laboratory Measurements of the Unsaturated Hydraulic Properties at the Vadose Zone Transport Field Study Site*; "Evaluation of van Genuchten-Mualem relationships to estimate unsaturated hydraulic conductivity at low water contents" [Khaleel et al. 1995]). Furthermore, unlike WMA C, moisture content measurements are available before and after application of anthropogenic recharge at the S&L site. Thus, the S&L site serves as a backdrop for WMA C moisture measurements for Hanford H2 unit. Details of the S&L site, field injections and the spatio-temporal distribution of observed moisture plume are described elsewhere ("Stochastic analysis of moisture plume dynamics of a field injection experiment"

[Ye et al. 2005]; PNNL-13795, *Vadose Zone Transport Field Study: Soil Water Content Distributions by Neutron Moderation*).

Figure B-2b. Waste Management Area C Moisture Content Histogram for H2 Data Within the Single-Shell Tank Footprint.

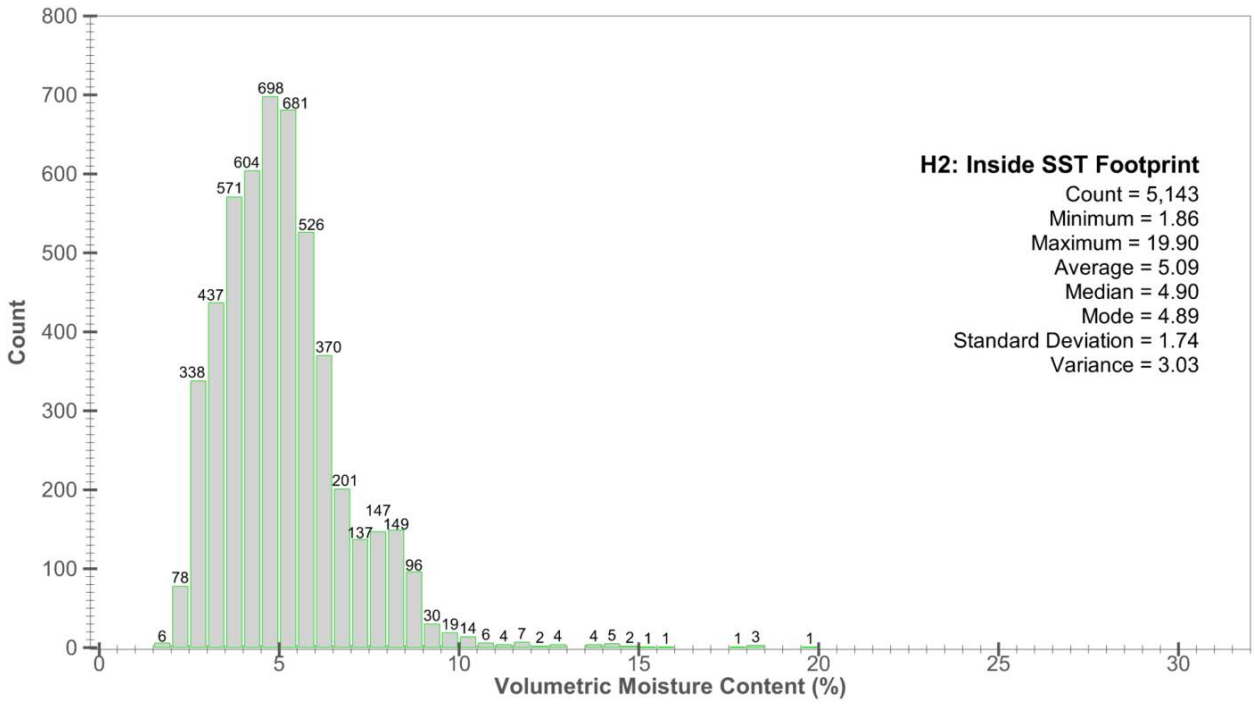

SST = single-shell tank

Figure B-4 shows the composite set of all moisture content measurements collected before and after injection at the S&L site. The S&L site initial moisture content data were collected on May 5, 2000 [Figure B-4(a)] and post-injection and post-redistribution data were collected about two months later [Figure B-4(b)]. These measurements are all within an HSU that would correlate with the Hanford H2 sand unit identified at WMA C. The S&L moisture content profiles are in general agreement with the known stratigraphic cross-section (Ye et al. 2005), with larger moisture content values being associated with the fine-textured sediments and smaller values being associated with the coarse textured sediments. In addition to the 2000 S&L field experiment, data also exist on the 1980 field experiment conducted at the same site (RHO-ST-46P, *Field Calibration of Computer Models for Application to Buried Liquid Discharges: A Status Report*). Although not shown here, the 1980 moisture content measurements are nearly identical to the 2000 moisture content measurements. The consistency in the moisture content profiles over the 20-year time interval suggests that, in the absence of anthropogenic recharge, the moisture content distribution is under a state of natural equilibrium with meteoric recharge. The S&L moisture content profiles (Figure B-4) clearly illustrate the impact of media heterogeneities and natural capillary breaks ("Simulating field-scale moisture flow using a combined power-averaging and tensorial connectivity-tortuosity approach" [Zhang and Khaleel 2010]; Ye et al. 2005). During and following field injections, the capillary breaks created due to textural discontinuities allow flow to occur laterally until the pressure head in the fine layer is sufficient to overcome the entry pressure head of the underlying coarse layer.

Nonetheless, as indicated in Figure B-4, the pre- and post-injection moisture plumes are essentially confined within three layers (i.e., two fine textured layers and a coarse-textured layer that is sandwiched in between the two fine-textured layers).

Figure B-2c. Waste Management Area C Moisture Content Histogram for H2 Data Outside of the Single-Shell Tank Footprint.

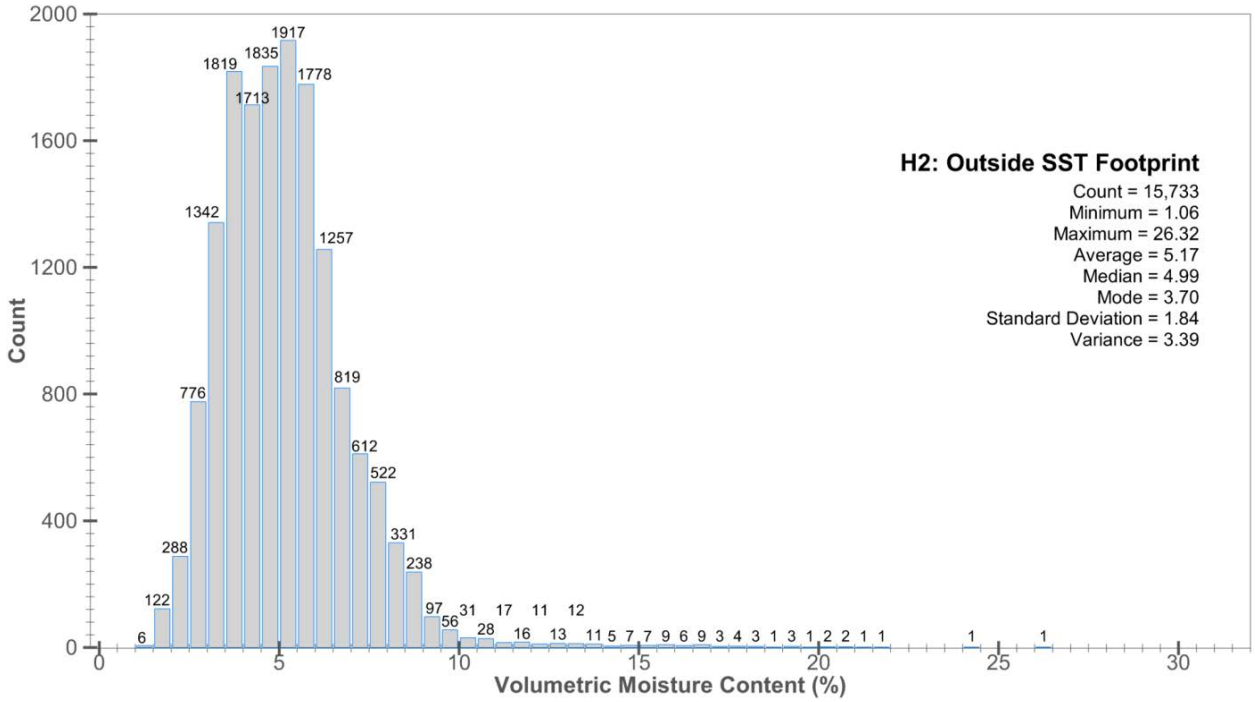

SST = single-shell tank

At WMA C, the volumetric moisture content for the Hanford H2 unit inside the tank farm (see Figure B-2c) ranges from 1.86 to 19.90 with a mean of 5.09 (% volume), whereas at the S&L site the volumetric moisture content ranges from 4.60 to 24.50 with a mean of 8.92 (% volume) (Ye at al. 2005). Even though the natural recharge at the two sites are not identical and the sediment textural data are different, the WMA C H2 unit moisture contents compare well and show similar trends relative to variability with field-measured H2 moisture contents at the nearby S&L site (i.e., higher moisture contents for fine-textured units and lower moisture contents for coarse-textured units as illustrated in Figure B-4). However, the S&L mean moisture content is much higher than the WMA C (inside the tank farm) mean value. This is consistent with the ubiquitous occurrence of fine textured units at the S&L site (Ye at al. 2005), and the apparent non-occurrence of such units at WMA C. These data show that the field measurements at both WMA C and S&L sites are significantly impacted by small-scale heterogeneities. However, if the moisture content data is used as a surrogate for characterizing media heterogeneities, the higher mean (~8.92 [% volume]) moisture values at the S&L site suggests that the Hanford H2 unit is much coarser at WMA C than at the nearby S&L site. Therefore, while the comparison with the S&L site generally corroborates the understanding of the WMA C H2 unit, the S&L site is not a useful surrogate for development of hydraulic properties for the Hanford H2 sand unit at WMA C. Furthermore, the comparison demonstrates that substantial variability can occur in the H2 unit over fairly short spatial distances.

Figure B-3. Location of Sisson and Lu Site, Integrated Disposal Facility and Selected Boreholes in 200 Area.

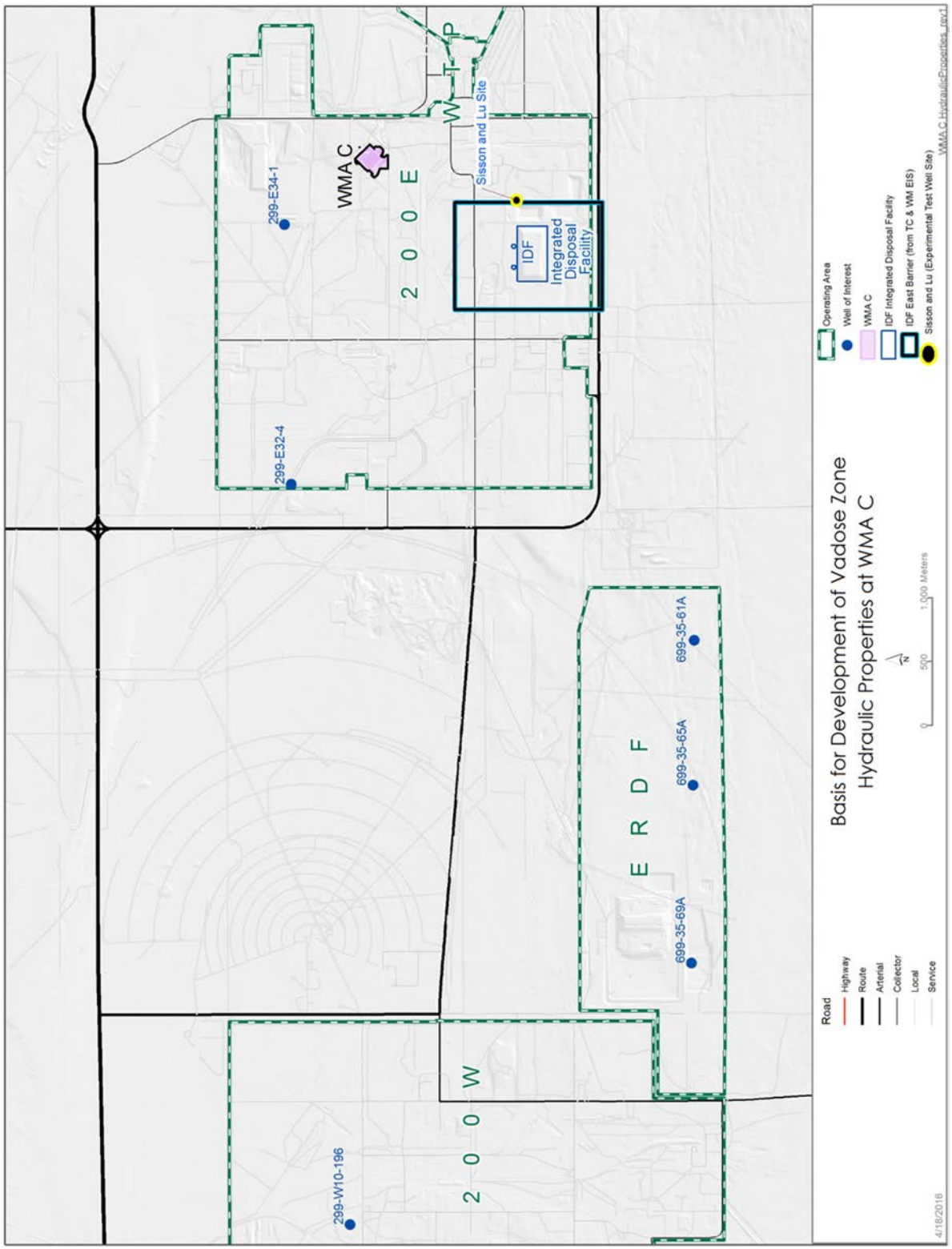

ERDF = Environmental Restoration Disposal Facility
WMA = Waste Management Area
TC & WM EIS = Tank Closure and Waste Management Environmental Impact Statement

Figure B-4. (a) Pre- and (b) Post-Injection Moisture Plumes for the Field Injection Experiment in the 200 East Area.

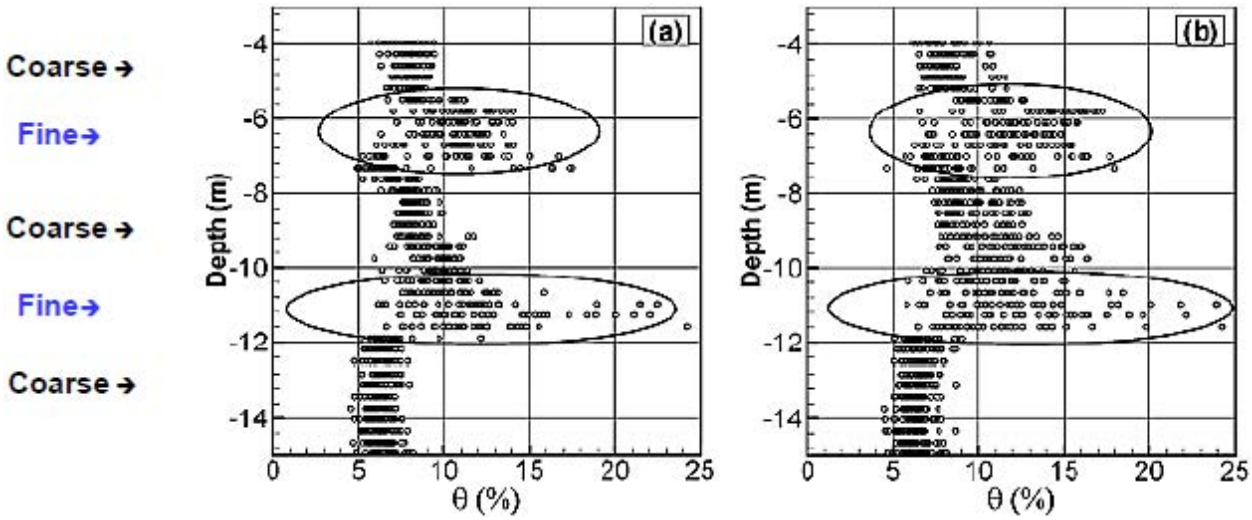

Profiles of volumetric moisture content (%) measured on (a) May 5, 2000, and (b) July 31, 2000. The figures illustrate the fact that, in the absence of anthropogenic recharge, moisture contents at the field site are in equilibrium with natural recharge at the site.
Reference: "Stochastic analysis of moisture plume dynamics of a field injection experiment" (Ye et al. 2005).

B.1.1.2 Soil-Moisture and Matric Potential Data for Borehole Samples Inside and Outside the Tank Farm. In addition to the moisture content measurements developed from neutron logging of direct push boreholes presented in Section B.1, additional moisture content data as well as matric potential information are available for two individual boreholes. Boreholes C4297 (inside the tank farm near tank C-105) and 299-E27-22 (*Resource Conservation and Recovery Act of 1976* [RCRA] borehole just outside the tank farm) (Figure B-5) provide moisture content (gravimetric) measurements as well as matric potential (using filter paper) data (PNNL-15503, *Characterization of Vadose Zone Sediments Below the C Tank Farm: Borehole C4297 and RCRA Borehole 299-E27-22*). The two sets of data on moisture content and matric potential were collected to evaluate differences between one being outside the farm (a lower expected average moisture content and a more negative matric potential) and the other inside the farm (a higher expected average moisture content and a less negative matric potential indicative of a draining soil profile). However, as stated earlier (Section B.1.1), the averages for moisture content measurements inside and outside the SST footprint were not significantly different.

The moisture content profiles for the two boreholes are shown in Figures B-6a and B-6b, respectively. Zones with relatively high moisture are illustrated via a light blue bar immediately to the right of the lithologic log in these diagrams. The moisture content and lithological data are generally consistent; the elevated levels of moisture in the vadose zone at C Farm are associated with fine-grained lenses of fine sand and/or silt. Most of these occur within the Hanford formation H2 unit, although there is also one at the base of the backfill in borehole C4297, and within the H1 unit in RCRA borehole 299-E27-22, which is consistent with the concentration of moisture at an abrupt, large contrast in grain size. This is illustrated at the 82-ft depth in RCRA borehole 299-E27-22 (Figure B-6b), where there is a sharp contact between gravelly sand overlying fine to coarse sand (PNNL-15503).

Figure B-5. Borehole Location Map for Waste Management Area C.

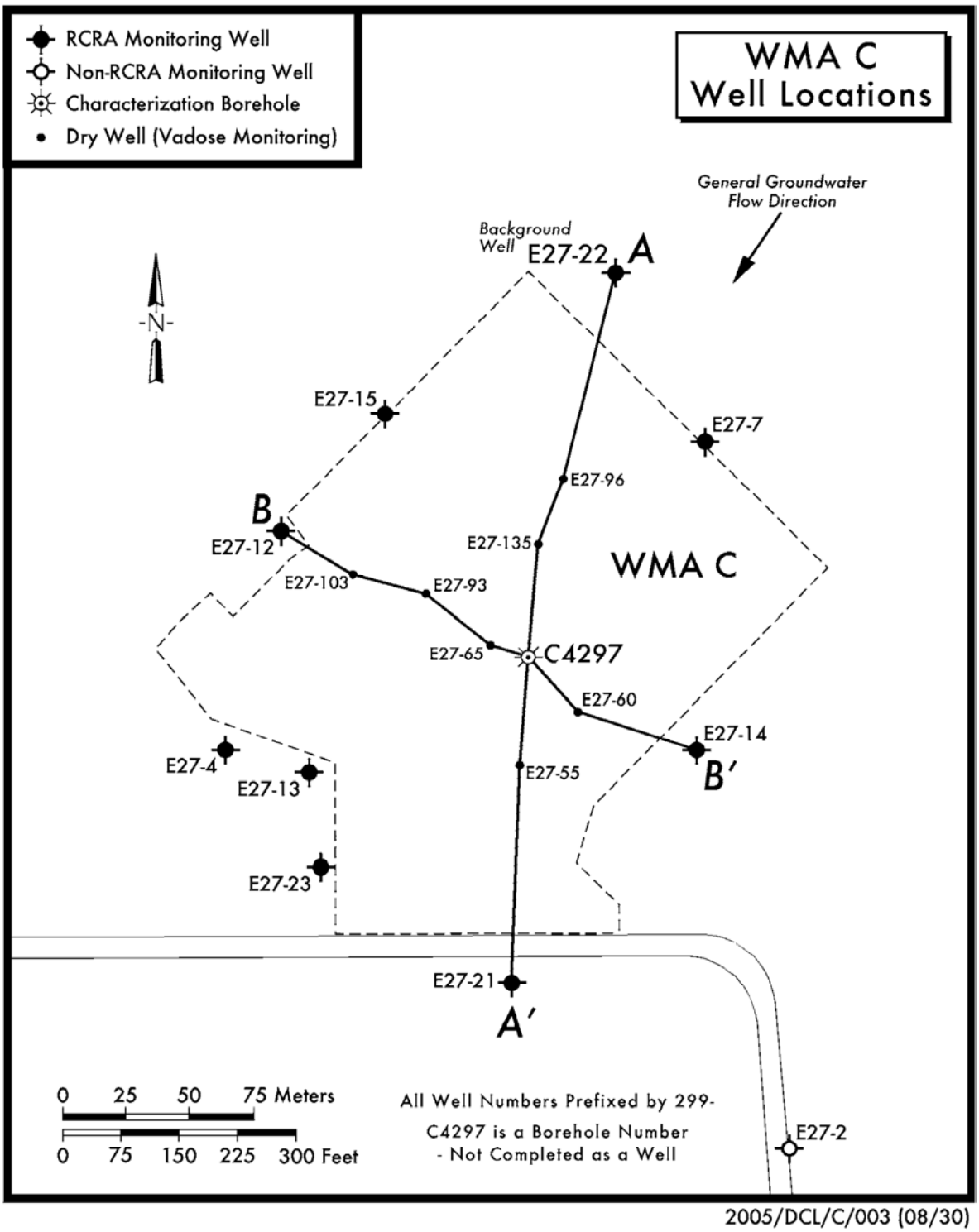

RCRA = *Resource Conservation and Recovery Act of 1976* WMA = Waste Management Area

Source: PNNL-15503, *Characterization of Vadose Zone Sediments Below the C Tank Farm: Borehole C4297 and RCRA Borehole 299-E27-22*.

Note: Cross-sections AA' and BB' are Figures 2.4 and 2.5, respectively, in PNNL-15503.

Figure B-6a. Borehole C4297 Lithology and Gravimetric Moisture Content Measurements (the shaded areas in light blue and gray are regions of increased moisture).

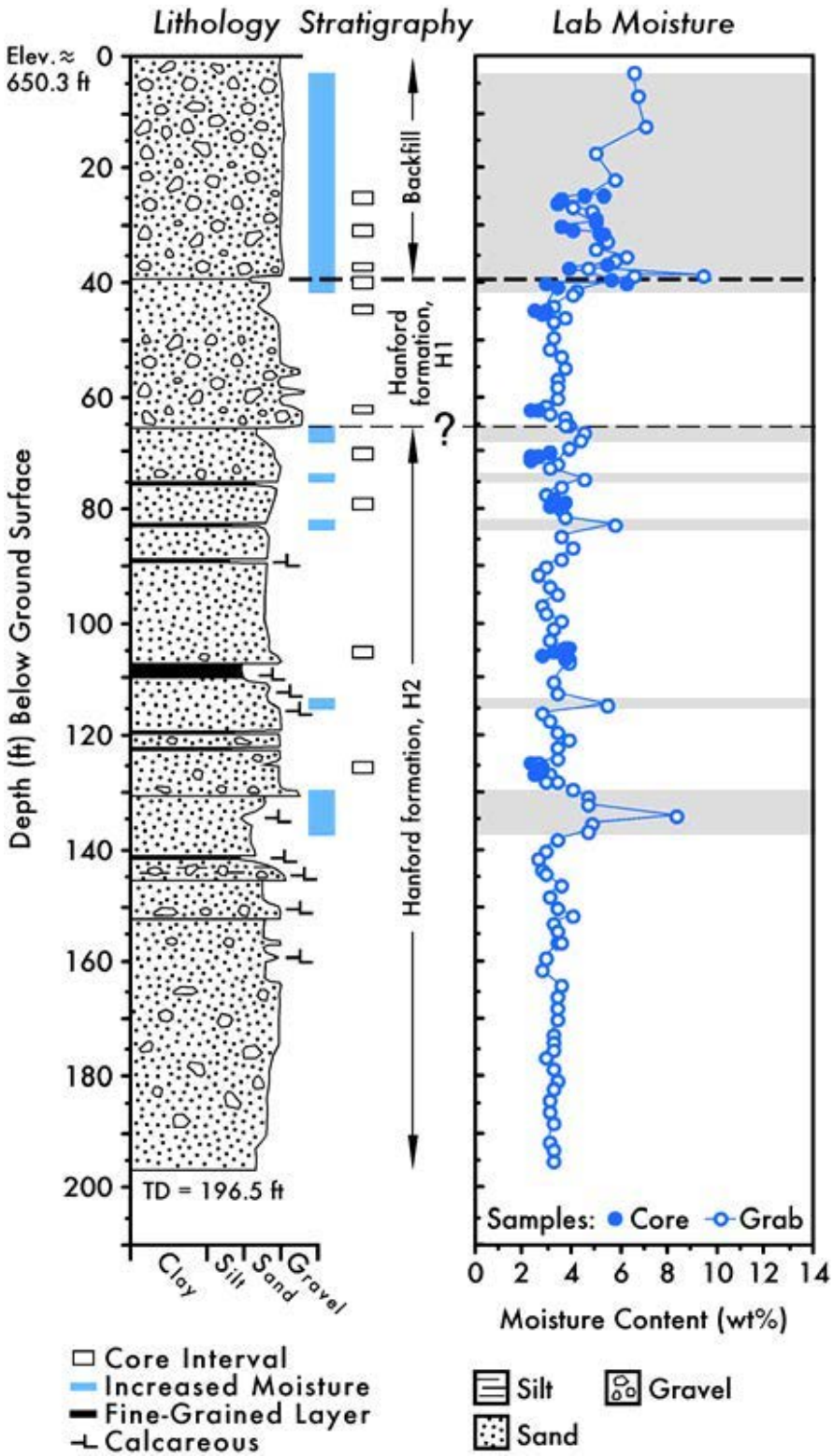

Reference: PNNL-15503, *Characterization of Vadose Zone Sediments Below the C Tank Farm: Borehole C4297 and RCRA Borehole 299-E27-22.*

Figure B-6b. Borehole 299-E27-22 Lithology and Gravimetric Moisture Content Measurements (the shaded areas in light blue and gray are regions of increased moisture).

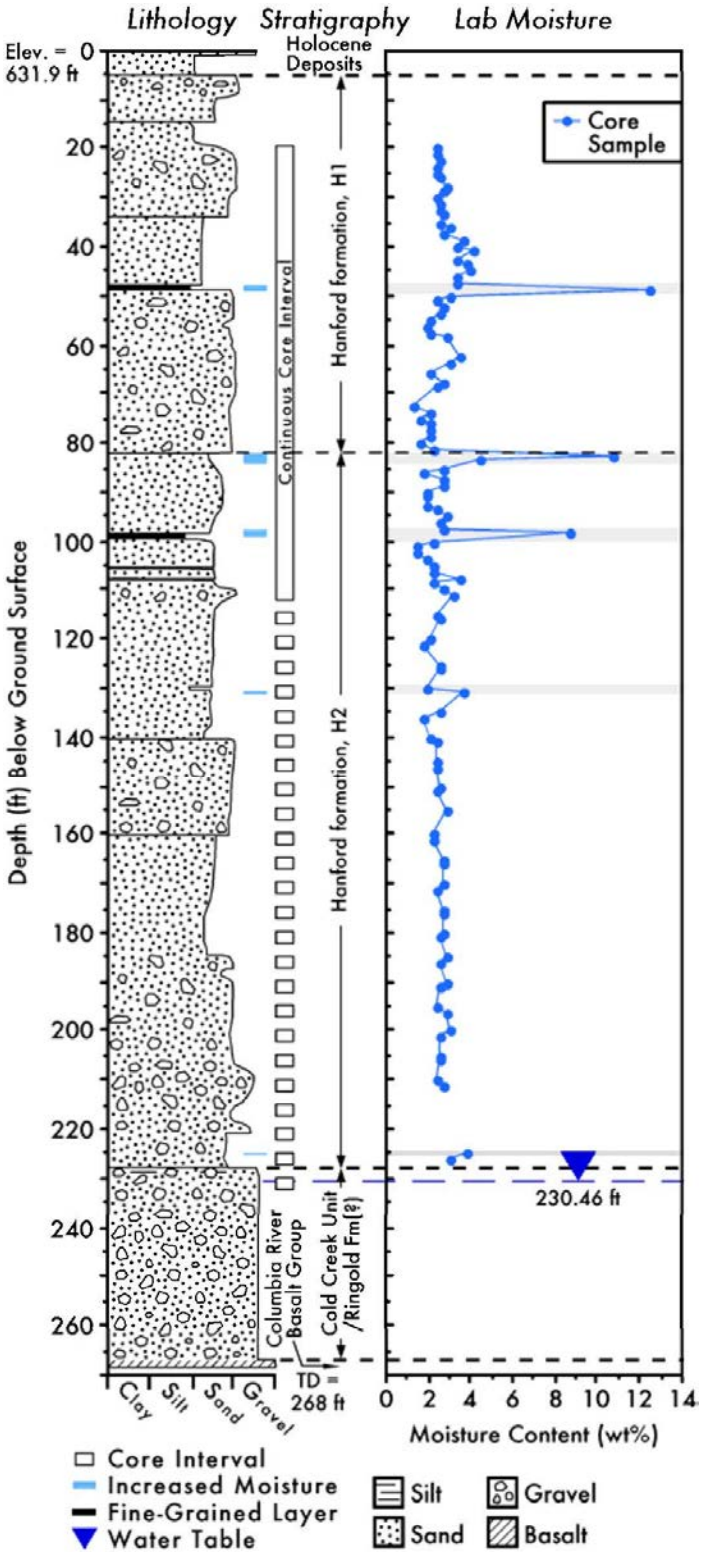

Reference: PNNL-15503, *Characterization of Vadose Zone Sediments Below the C Tank Farm: Borehole C4297 and RCRA Borehole 299-E27-22.*

The distribution of moisture in the vadose zone at these two borehole locations was developed by gravimetric moisture measured directly from core samples in the laboratory (Figures B-6a and B -6b). Moisture data based on grab sampling is only available for one of the two boreholes (C4297), and these data generally corroborate the laboratory-measured moisture content measurements (Figure B-6a). However, several pronounced spikes that appear on the laboratory-moisture plot do not appear in the moisture log. This is likely the result of a number of thin (a few inches or less) fine-grained layers that were preferentially sampled during core processing. These thin layers are not visible on the geophysical log because the neutron flux is averaged over a larger area beyond the limits of the fine-grained layer, including adjacent relatively dry layers. Thus, the resulting field logging signal is dampened. In general, the neutron-moisture log appears to accurately reflect the relative bulk moisture content, and can confidently be used as a substitute to estimate bulk moisture conditions when core samples are unavailable. However, most thin (<6 in.) moist zones go undetected on neutron-moisture logs (PNNL-15503).

While the moisture content profiles provide useful information, the moisture profiles, by themselves, cannot be used to describe the soil-water energy status and the vadose zone flow dynamics. Data on soil-moisture matric potentials are needed to establish the energy level and the subsequent flow status. A simple measure of direction of flow can be approximated by plotting field-measured matric potentials versus the height above the water table. The hydraulic potential at any given elevation is given by the sum of matric potential and gravitational potential and the flux is calculated from the Darcy-Buckingham law (Soil Physics [Jury and Horton 2004]).

Figures B-7a and B-7b illustrate the respective filter paper-based matric potential measurements, as a function of depth for sediment samples from the two boreholes: C4297 (inside the farm) and 299-E27-22 (outside the farm), with the potentials (MPa) shown as absolute values (PNNL-15503). With the filter paper technique, the moisture in a filter material reaches equilibrium with the surrounding environment. In both figures, the red line, labeled “theoretical value” is the theoretical line that represents the steady-state equilibrium condition. Matric potential values to the left of the theoretical line suggest a draining profile. The general trend for the data is that the measured potentials for both boreholes are consistent with those of a draining profile.

For borehole 299-E27-22 (Figure B-7b), matric potentials for three of the samples (27.0, 72.0, and 74.5 ft below ground surface) suggest very dry conditions; these appear to be erroneous because of inadvertent drying of the samples or weighing errors (PNNL-15503). The matric suction values are generally below 0.5 MPa (~5,000 cm) for the sediment profile in borehole 299-E27-22 as well as borehole C4297.

Filter paper-based soil matric potentials are point measurements, and are not consistent with the use of averaged upscaled (effective) properties (Section 6) for the large blocks used in the PA simulations. In addition, the error bar for filter paper measurements is rather large (0.1 to 0.2 MPa). Soil moisture measurements are typically more accurate than matric potential measurements, and the matric potential variability is typically larger than the soil moisture

variability (PNNL-15503). Overall, however, the WMA C moisture and tension data appear to be internally consistent and represent a relatively dry moisture regime.

Table B-2 summarizes the mean moisture content and mean filter paper-based matric potential measurements for the two borehole samples. The data show a drier moisture content for measurements outside the farm compared to those inside the farm. A comparison of the moisture and matric potential profiles for the two boreholes is shown in Figures B-8a and B-8b, respectively.

As stated earlier, matric potential measurements for both boreholes suggest a draining soil profile (PNNL-15503). Intuitively, it might be postulated that the higher mean observed moisture and a less negative mean matric potential inside the farm is due to the combined effects of both natural recharge and the operational use of water during the period of past tank farm operations. However, whereas the mean moisture contents for the two borehole samples suggest a slightly higher moisture content from measurements inside the tank farm, the much more negative mean matric potential for outside borehole samples (Table B-2) could simply be a reflection of differences in moisture retention characteristics for the two datasets, albeit being of similar lithology. A comparison of the field-measured and simulated moisture contents for the sand-dominated H2 unit is provided in Section B.2.1.1.

B.1.2 Moisture Content Measurements for Hanford H1, Hanford H3 and Backfill Gravelly Units

The statistics of moisture content measurement for Hanford H1 and H3 gravelly units and backfill gravelly unit are summarized in Table B-1. As indicated in Table B-1, unlike moisture content measurements made in the H1 gravelly unit, the sample size of moisture content measurements made in the H3 gravelly unit is too small to generate any meaningful statistics.

B.1.2.1 Hanford H1 Gravelly Unit. Figure B-9a shows the histogram for all moisture content measurements made in the H1 gravelly unit inside and outside the tank farm (Figure B-2c). Figure B-9b shows the histogram for measurements inside the SST footprint, whereas Figure B-9c shows the histogram for measurements outside the SST footprint. While the average for all H1 measurements is about 5.88% on a volume basis (Figure B-9a), inside the tank farm the average is 4.24 (% volume), with the range varying from ~1.47% to 23.11% and a variance of 3.76% (Figure B-9b). Outside of the SST footprint the average is 6.41 (% volume), with the range varying from ~0.13% to 30.64% and a large variance of 15.42% (Figure B-9c). Once again, similar to H2 data and contrary to expectation, the statistics suggest a considerably higher H1 average moisture content for measurements outside the SST footprint, compared with the average for measurements inside the SST footprint. The variance for H1 measurements outside the SST footprint is higher, compared to variance for measurements inside the SST footprint. This might simply be a reflection of a smaller sample size (a count of 1,921 inside versus a count of 6,056 outside), and/or media heterogeneities that are prevalent within the H1 unit.

Figure B-7a. Matric Potentials Measured by Filter Paper Technique on Core Samples from Borehole C4297. Matric potentials are presented as absolute values.

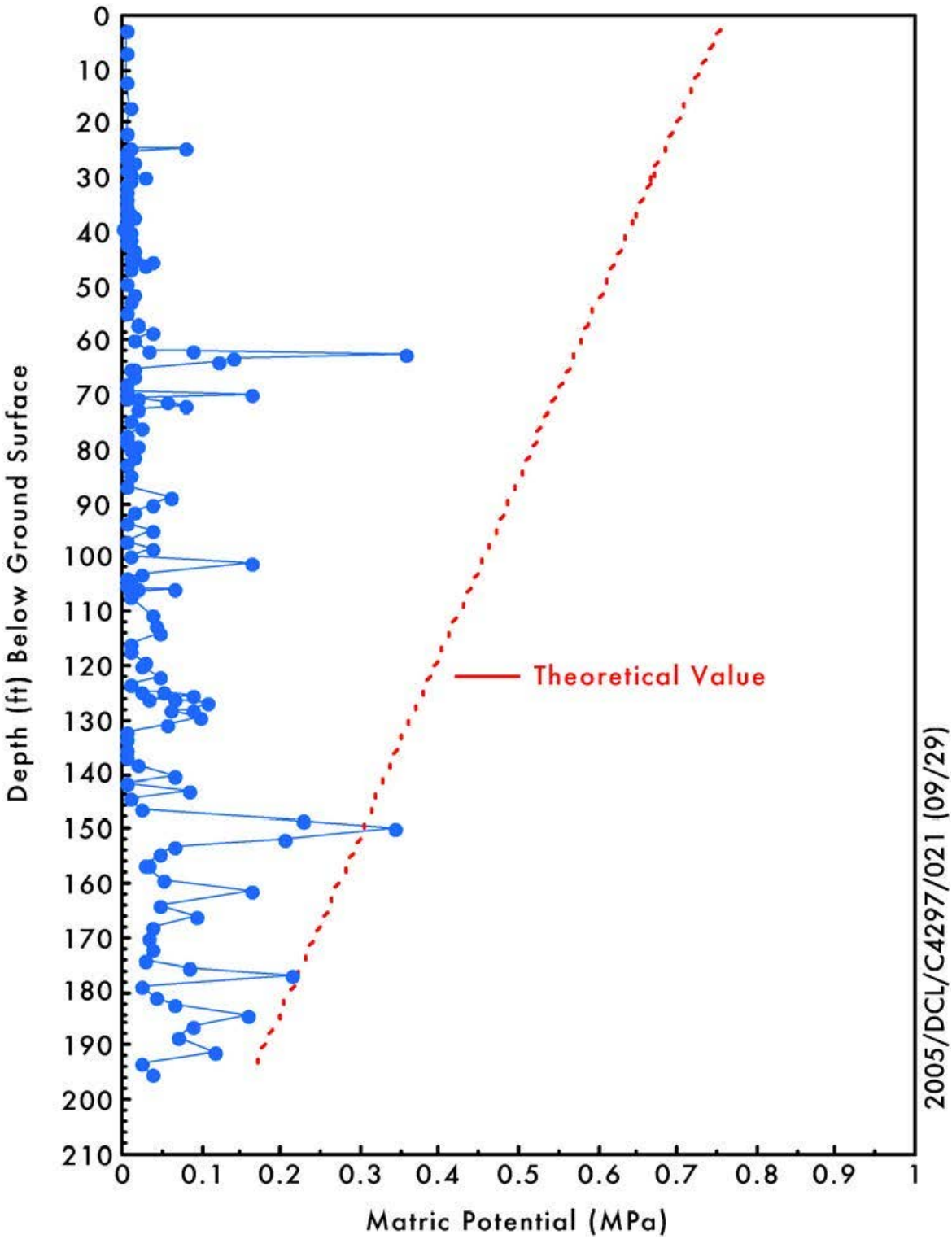

Reference: PNNL-15503, *Characterization of Vadose Zone Sediments Below the C Tank Farm: Borehole C4297 and RCRA Borehole 299-E27-22*.

Figure B-7b. Matric Potentials Measured by Filter Paper Technique on Core Samples from Borehole 299-E27-22.
Matric potentials are presented as absolute values.

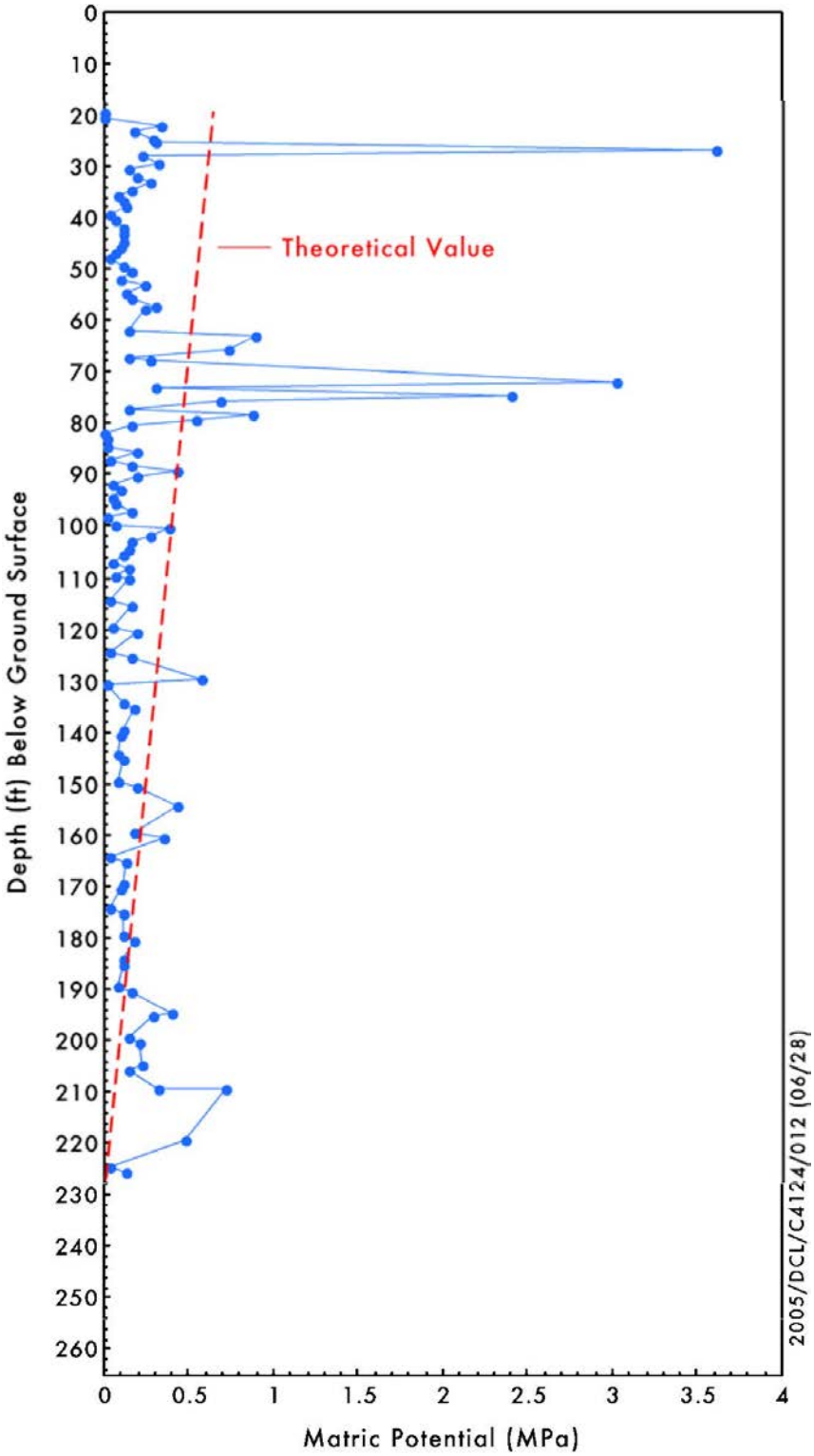

Reference: PNNL-15503, *Characterization of Vadose Zone Sediments Below the C Tank Farm: Borehole C4297 and RCRA Borehole 299-E27-22.*

Table B-2. Mean Moisture and Matric Potentials for Borehole Samples Inside and Outside of Waste Management Area C.

Borehole	C4297 (inside tank farm)	299-E27-22 (outside tank farm)
Mean moisture content (% volume)*	6.00	4.60
Mean matric potential (-cm)	498.45	1,616.43

*Gravimetric data were converted to volumetric moisture content using an assumed sediment bulk density of 1.7 g cm^{-3}.

Reference: PNNL-15503, *Characterization of Vadose Zone Sediments Below the C Tank Farm: Borehole C4297 and RCRA Borehole 299-E27-22*.

It is questionable as to whether the observed high moisture contents (e.g., 30.64 [% volume] for the gravel-dominated H1 unit) are reflective of the natural moisture regime. As discussed earlier, other moisture data in the nearby S&L test site suggest that, in the absence of anthropogenic recharge, the moisture profiles are typically in equilibrium with meteoric recharge. Furthermore, in the absence of anthropogenic recharge, moisture contents correlate with sediment texture (i.e., coarse-textured sediments have a lower moisture content and fine textured sediments have a higher moisture content) (Figure B-4). Nonetheless, none of the S&L moisture content measurements for the fine-textured horizons approach as high as 30.64% (% volume); such an unusually high value for the gravel-dominated H1 unit is considered an outlier.

B.1.2.2 Backfill Gravelly Unit. In general, tank farm backfill materials consist of unstructured, poorly-sorted mixtures of gravel, sand, and silt removed during tank excavation, and then later used as fill around the tanks. Backfill materials extend to depths of ~50 ft (~15.24 m) within the tank farms. Most or all of the recent deposits of eolian sand and silt material found elsewhere across the Hanford Site have been removed and replaced with backfill in the immediate vicinity of the tank farms.

For the backfill unit, the average moisture content is 8.08 (% volume) (Table B-1), and is the highest among averages for all the units. The backfill unit also has the lowest measured moisture content of 0.11 (% volume) among all units. The maximum measured moisture content for backfill is 30.61 (% volume).

Figure B-10a shows the histogram for all moisture content measurements made in the backfill gravelly unit inside and outside the tank farm (Figure B-2c). Figure B-10b shows the histogram for measurements inside the SST footprint, whereas Figure B-10c shows the histogram for measurements outside the SST footprint. While the average for all backfill measurements is ~8.09% (% volume) (Figure B-10a), inside the tank farm, the average is 6.61 (% volume), with the range varying from ~0.31% to 23.05% and a variance of 7.69% (Figure B-10b). Outside of the SST footprint, the average is considerably higher (9.30 [% volume]), with the range varying from ~0.11% to 30.61% and a large variance of 15.47% (Figure B-10c).

Figure B-8a. Comparison of Gravimetric Moisture Content Measurements for Boreholes C4297 and 299-E27-22.

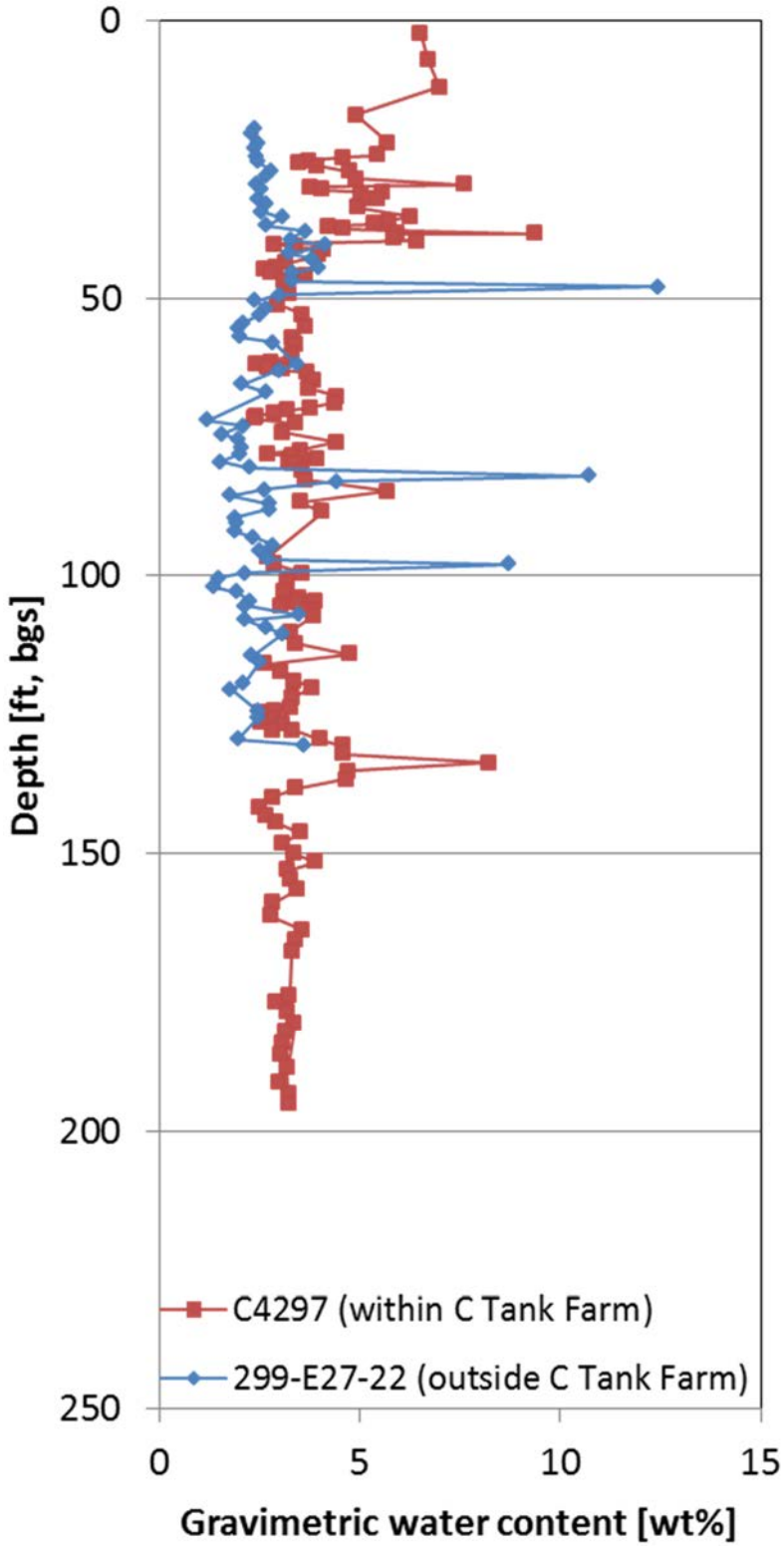

Reference: PNNL-15503, *Characterization of Vadose Zone Sediments Below the C Tank Farm: Borehole C4297 and RCRA Borehole 299-E27-22*.

Figure B-8b. Comparison of Soil Moisture Tension Measurements for Boreholes C4297 and 299-E27-22.

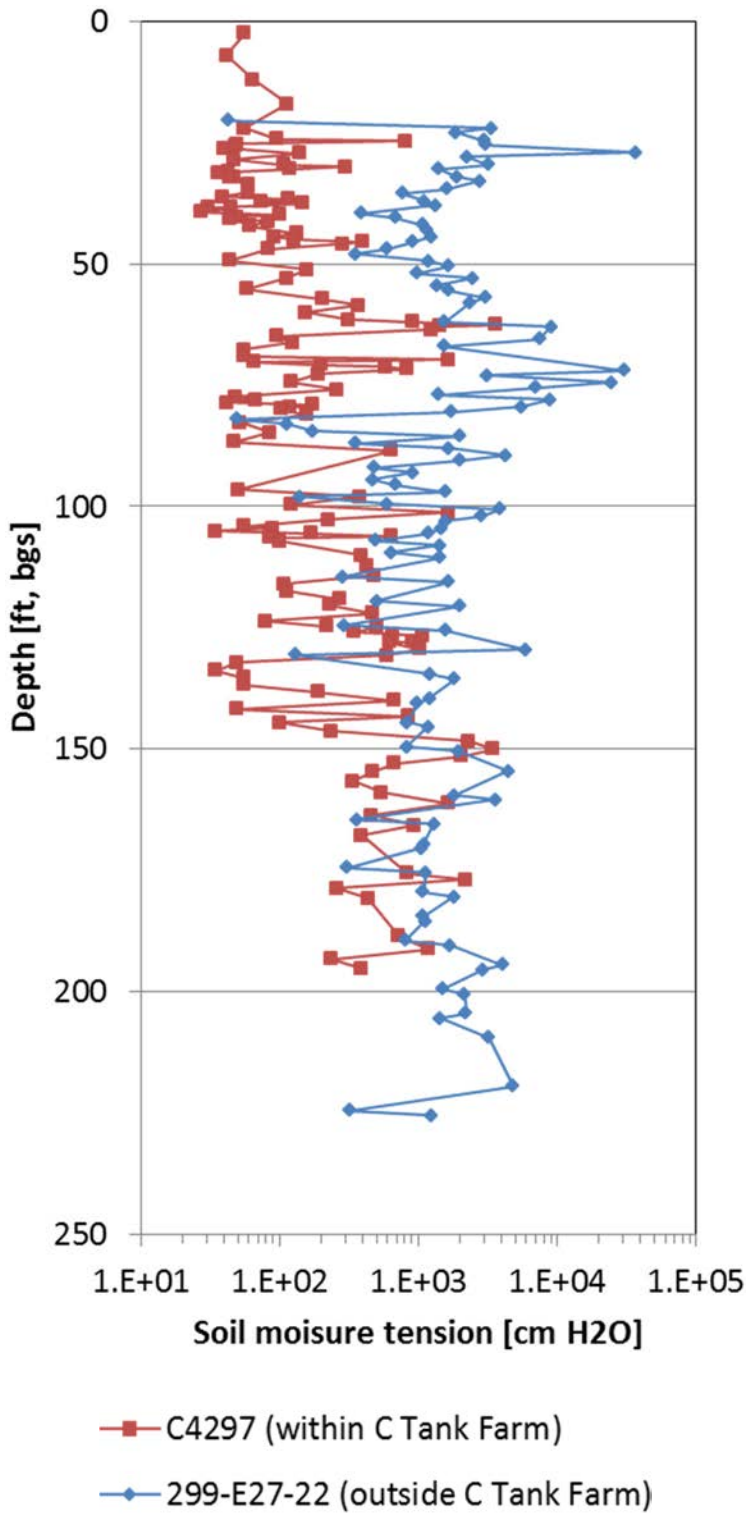

Reference: PNNL-15503, *Characterization of Vadose Zone Sediments Below the C Tank Farm: Borehole C4297 and RCRA Borehole 299-E27-22.*

Figure B-9a. Waste Management Area C Moisture Content Histogram for All H1 Data (Includes the Data from Both Inside and Outside of the Single-Shell Tank Footprint).

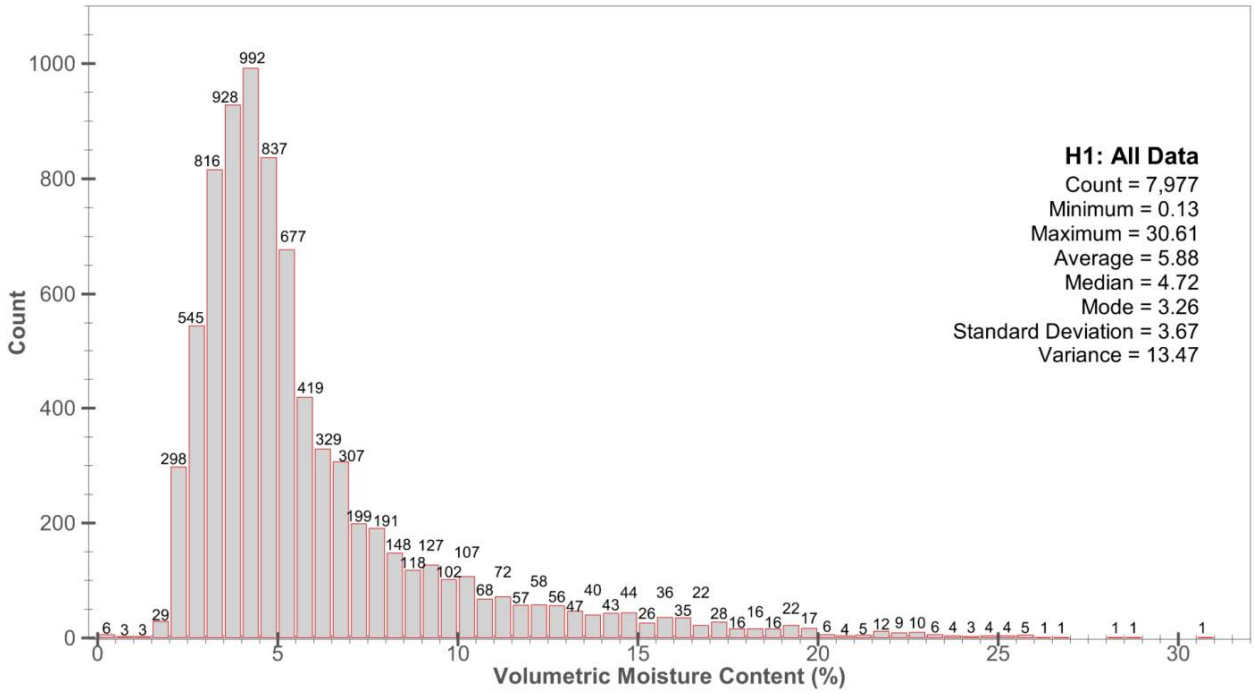

Figure B-9b. Waste Management Area C Moisture Content Histogram for H1 Data Within the Single-Shell Tank Footprint.

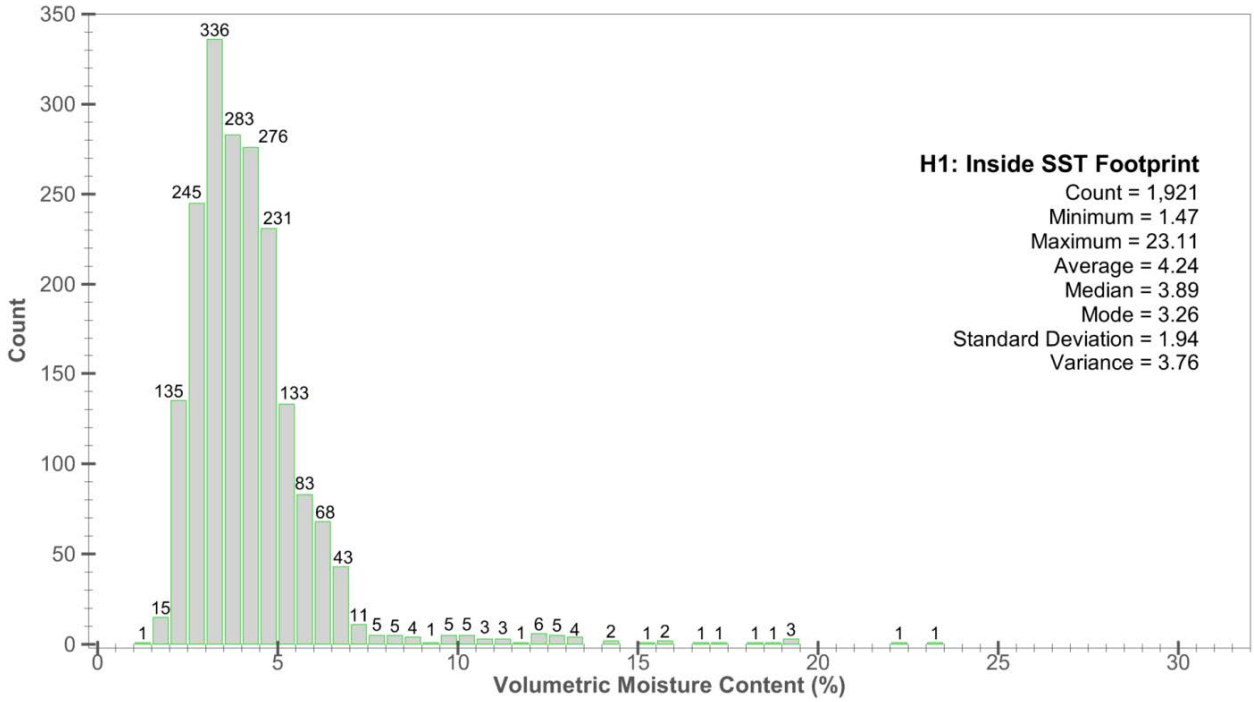

SST = single-shell tank

Figure B-9c. Waste Management Area C Moisture Content Histogram for H1 Data Outside of the Single-Shell Tank Footprint.

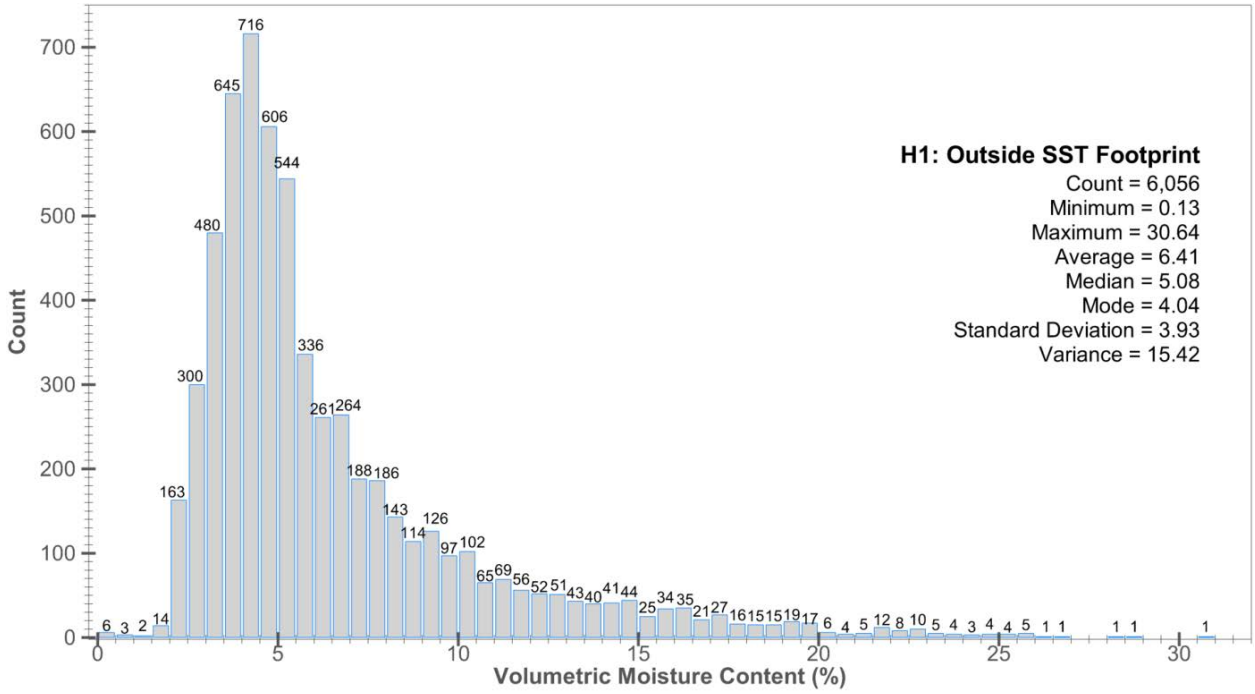

SST = single-shell tank

Figure B-10a. Waste Management Area C Moisture Content Histogram for All Backfill Data (Includes the Data from Both Inside and Outside of the Single-Shell Tank Footprint).

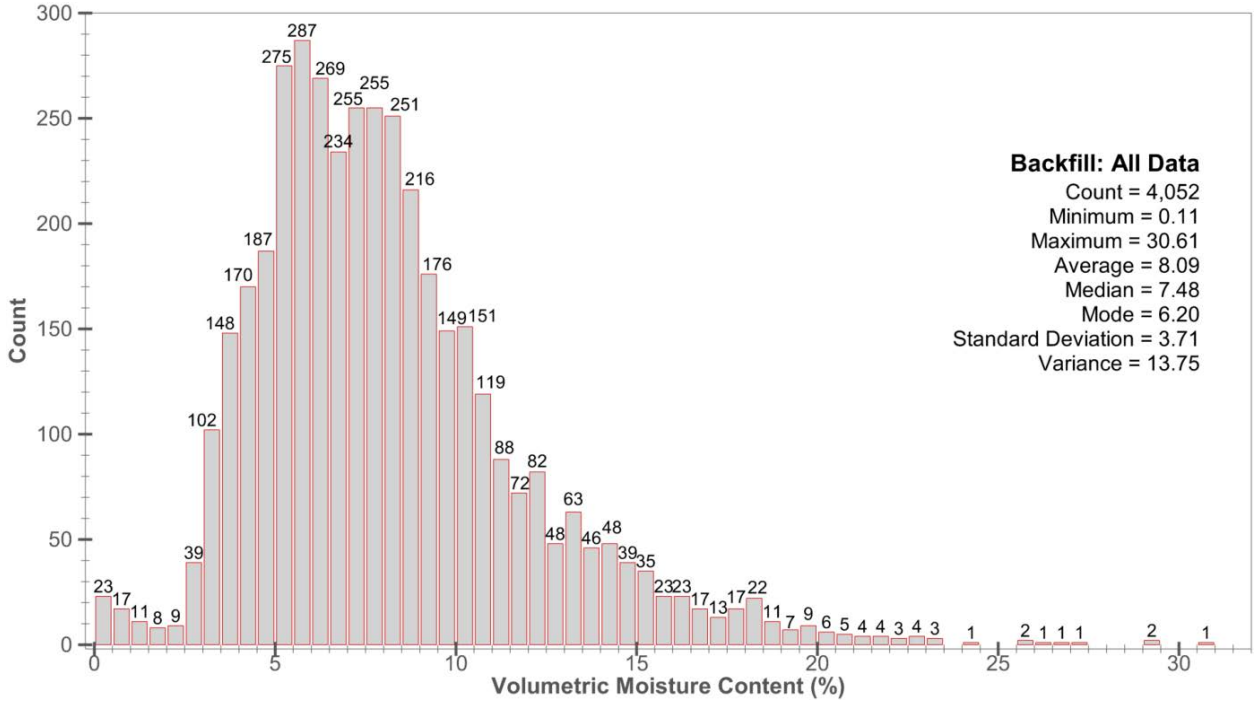

Figure B-10b. Waste Management Area C Moisture Content Histogram for Backfill Data Inside of the Single-Shell Tank Footprint.

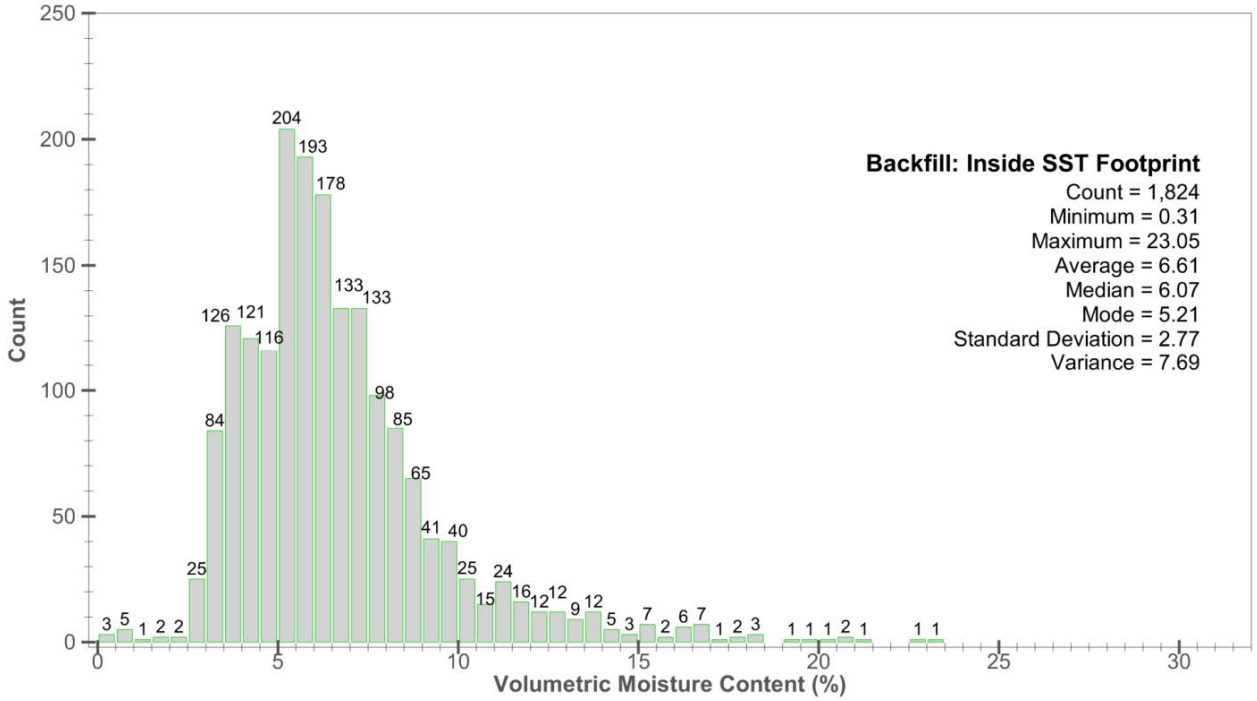

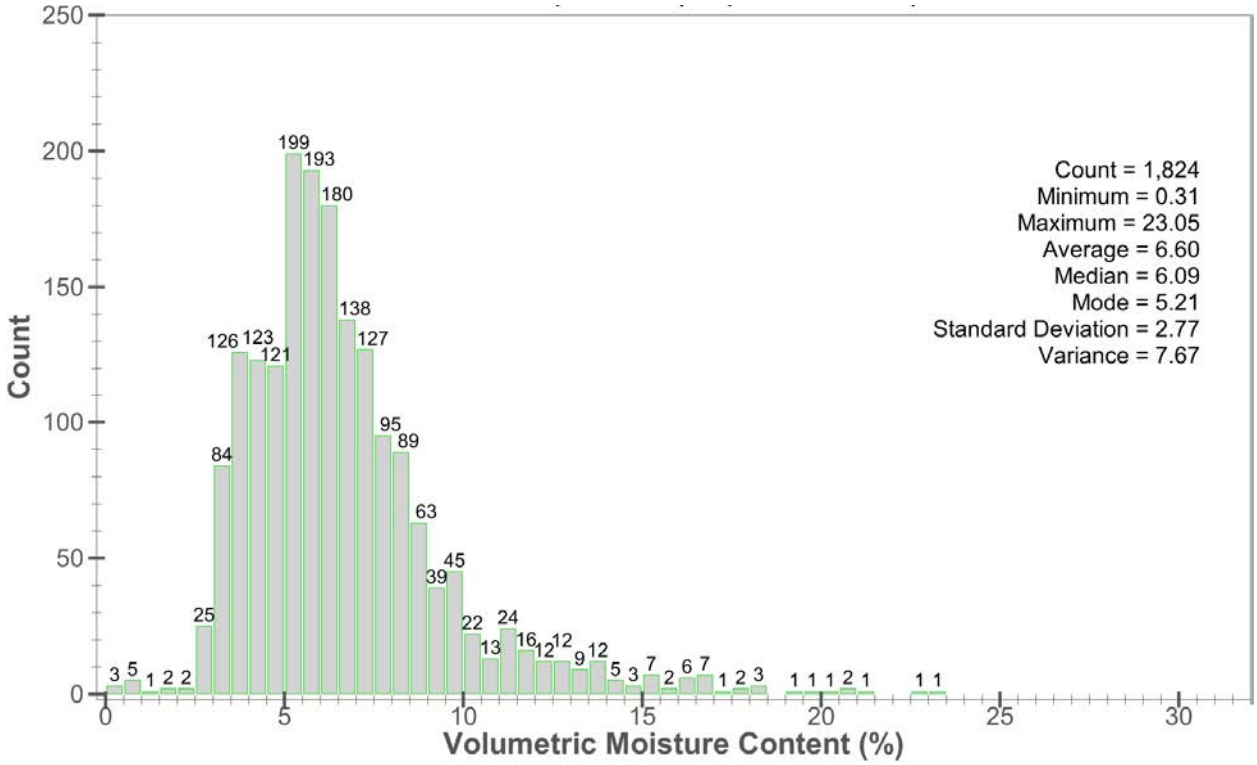

SST = single-shell tank

Figure B-10c. Waste Management Area C Moisture Content Histogram for Backfill Data Outside the Single-Shell Tank Footprint.

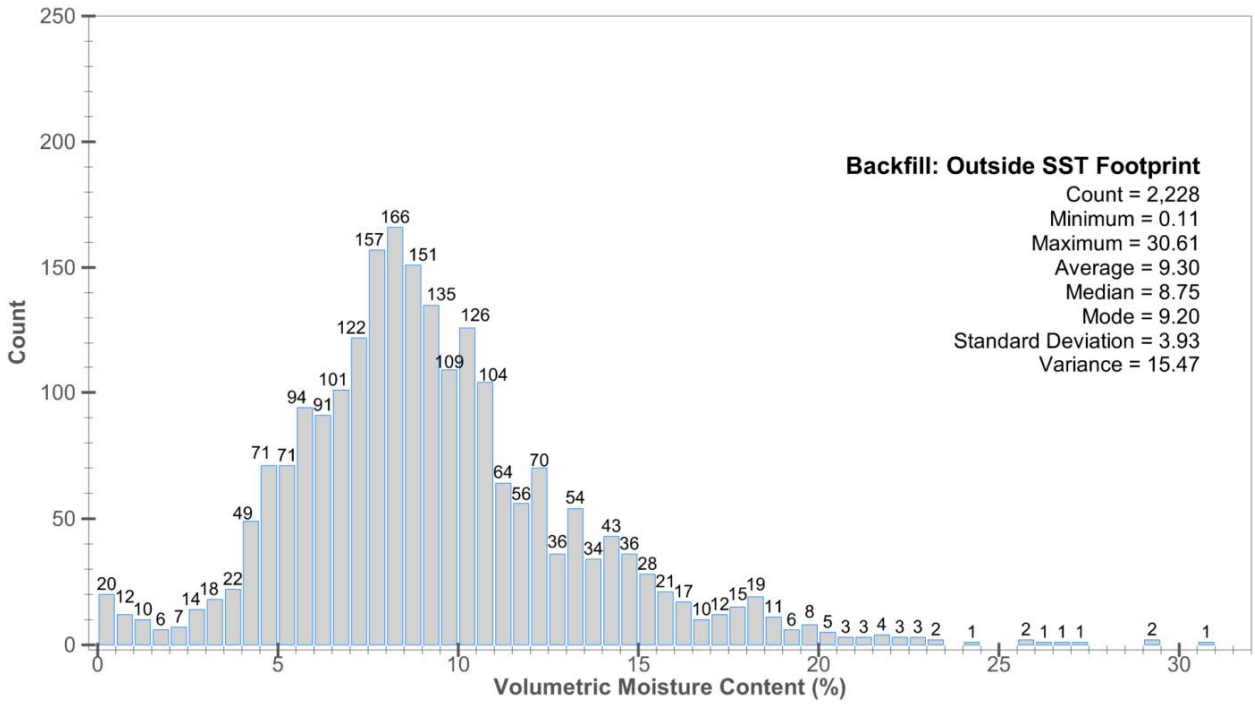

SST = single-shell tank

B.2 LABORATORY-SCALE MEASUREMENTS FOR HYDRAULIC PROPERTIES

The purpose of this section is to summarize data sources and laboratory measurements of core scale sample properties for different HSUs; these are later upscaled for use in WMA C PA modeling (Section B.3 below). Core-scale measurements and their parameterization are described below for the following HSUs:

- Hanford H2 Sand Unit
- Hanford H1 and H3 Gravelly Units
- Backfill Gravelly Unit.

B.2.1 Properties of the Hanford H2 Sand Unit

Figure B-11 shows a representative sample of sediments associated with the Hanford H2 sand dominated unit identified at WMA C. Because site-specific hydraulic properties data are unavailable, the available hydraulic properties database for coarse sands as well as the WMA C moisture content distribution were used to identify and characterize hydraulic properties for the Hanford H2 sand unit identified at WMA C. Soils used to characterize the WMA C Hanford H2 unit properties were similar to those shown in Figure B-11. Using moisture as a proxy, the nearby 200 East Area Integrated Disposal Facility (IDF) site (Figure B-3) coarse sand unit correlates well with the Hanford H2 sand unit identified at WMA C; the IDF coarse sands were

thus used as surrogate for the WMA C H2 sands. The primary mission of RCRA-permitted IDF (Figure B-3) is disposal of low-level wastes, mixed low-level wastes, and Immobilized Low-Activity Waste (i.e., the Hanford tank waste that has undergone separations treatment to remove the bulk of the radionuclides and then solidified at the Hanford Waste Treatment and Immobilization Plant).

Figure B-11. Waste Management Area C Hanford H2 Sand-Dominated Core.

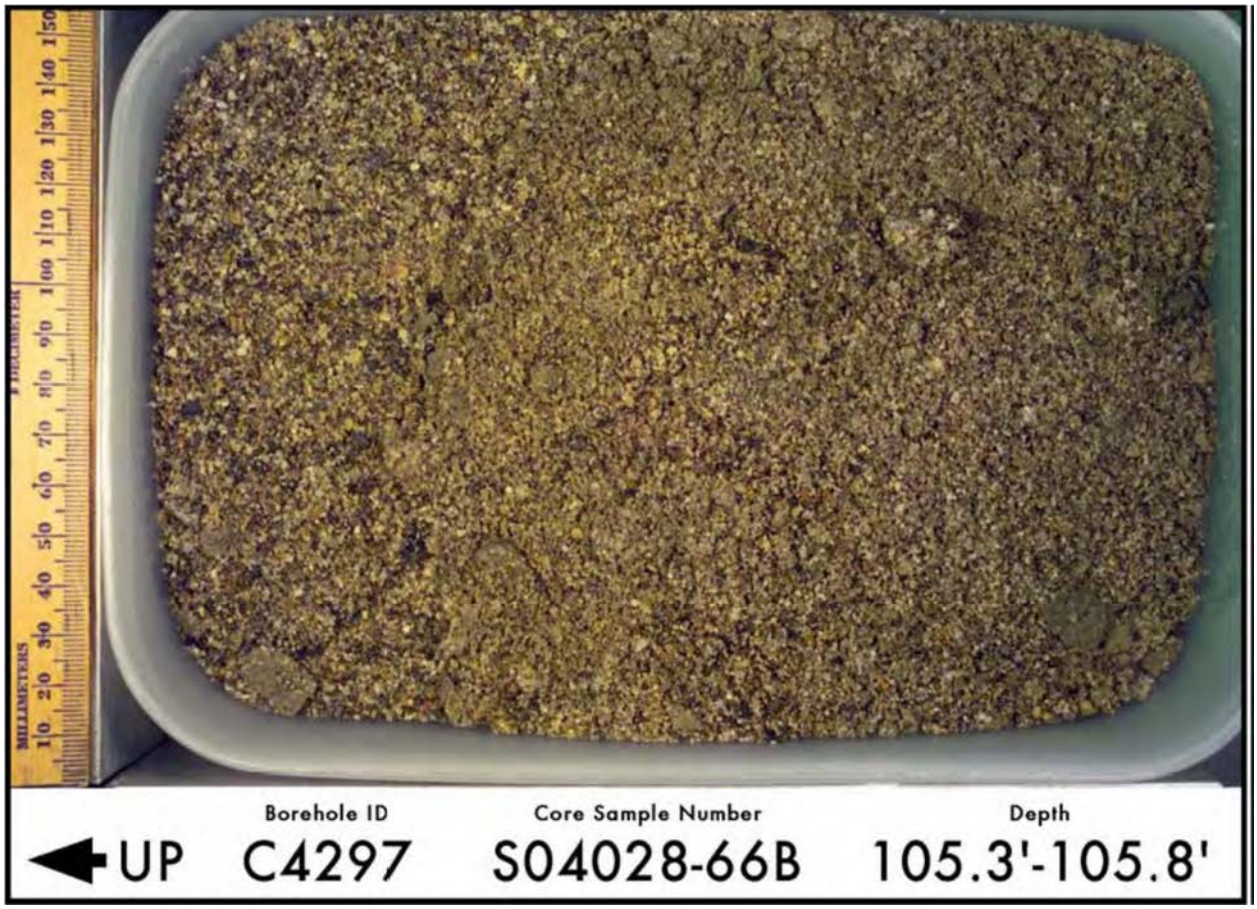

Reference: PNNL-15503, *Characterization of Vadose Zone Sediments Below the C Tank Farm: Borehole C4297 and RCRA Borehole 299-E27-22*.

As part of site characterization for IDF, sediment samples were obtained in fiscal years 1998, 2001 and 2002 via a borehole drilling and sampling program. The Hanford formation sandy H2 sequence identified at the IDF site is ~200 ft (~61 m) thick and, like WMA C, is the dominant facies at the site.

The laboratory procedures used to analyze the IDF H2 borehole samples and analysis of samples from the three boreholes are described in appendices found in RPP-20621, *Far-Field Hydrology Data Package for the Integrated Disposal Facility Performance Assessment*. Briefly, the multistep and steady-state methods were used to obtain moisture retention and unsaturated conductivity data. The specific details for the two methods are described in RPP-20621 appendices. Both methods were performed on the same core using the same sensor locations. In

addition to cumulative outflow, the multistep method provides water content-matric potential (θ-ψ) pairs. These data were used in conjunction with a numerical inversion procedure ("Optimization of Hydraulic Functions from Transient Outflow and Soil Water Pressure Data" [Eching and Hopmans 1993]) to determine the optimal set of van Genuchten model ("A Closed-form Equation for Predicting the Hydraulic Conductivity of Unsaturated Soils" [van Genuchten 1980]) parameters (RPP-20621). The steady-state method, described in "Hydraulic Conductivity and Diffusivity: Laboratory Methods" (Klute and Dirksen 1986), provides water content-matric potential-unsaturated conductivity (θ-ψ-K) triplets; the method was primarily used as a check on the multistep method.

RPP-20621 (Tables 1 through 3) provides the van Genuchten model parameters determined using the numerical inversion procedure and data from the multistep test. The pore-size distribution parameter ℓ ("A New Model for Predicting the Hydraulic Conductivity of Unsaturated Porous Media" [Mualem 1976]) was kept fixed at 0.5. The fitted van Genuchten-Mualem parameters for the IDF H2 sandy sequence (44 samples) are reproduced in Table B-1.

The IDF H2 samples contain very little gravel (>2-mm size) (RPP-20621). To account for the presence of gravel fraction for WMA C samples, the IDF H2 moisture retention data (Table B-3) were corrected ("Correcting laboratory-measured moisture retention data for gravels" [Khaleel and Relyea 1997]). Table B-4 data suggest that the gravel fraction for the H2 unit can range from less than 1% to about 25%. Also, borehole logs (PNNL-15503) suggest the presence of a high gravel fraction, and many WMA C H2 samples are characterized as "sandy pebble gravel" and "pebbly sand." A gravel fraction of 20% was assumed and applied to correct the IDF retention data. The fitted moisture retention curves and unsaturated conductivity curves for H2 sandy sequence as well as the WMA C H2 composite curves are shown in Figures B-12 and B-13, respectively. To obtain the composite curves, all measurements for an equivalent homogeneous medium (EHM) were pooled and the composite van Genuchten parameters were obtained via RETC (RETention Curve) code (EPA/600/2 91/065, The RETC Code for Quantifying the Hydraulic Functions of Unsaturated Soils) and a simultaneous fit of both moisture retention and unsaturated conductivity data. The composite curves account for gravel correction (Khaleel and Relyea 1997).

B.2.1.1 Comparison of Simulated and Observed Moisture Content. As stated earlier, the selected properties were used to simulate a vadose zone flow field and the simulation results were cross-checked against WMA C field-measured moisture contents. Figure B-14 shows a comparison of measured moisture profile for borehole C4297 (Figure B-5) and the simulated steady-state moisture profile for WMA C. As indicated, for an expected long-term recharge estimate of 3.5 mm/yr, the simulated H2 moisture profile compares well with the measurements. Overall, the simulated H2 moisture content of ~6 (% volume) is in agreement with the average WMA C H2 moisture of ~5.15 (% volume) (Table B-1). As stated in Section B.1.1, the averages for moisture content measurements for H2 inside and outside the SST footprint were not significantly different even though the recharge conditions outside the farm are different (lower infiltration) from those inside the farm (higher infiltration). As expected, the field-measured moisture contents are significantly impacted by small-scale heterogeneities and exhibit considerable variability (Figure B-14). To the contrary, the PA simulations are based on upscaled or effective hydraulic properties; each heterogeneous formation is replaced by its

homogeneous equivalent, and the upscaled or effective flow parameters are used to represent the EHM. This effectively results in a smoothing of the model estimates (Figure 6-3). Therefore, the variability of field-measured moisture contents, induced by media heterogeneities, is inherently larger in comparison to that based on PA simulations using homogenized upscaled properties, and the ensemble average, embedded in EHM approximation, cannot capture the field-scale variability.

Table B-3. van Genuchten Parameters (Based on the Multistep Method) and Saturated Hydraulic Conductivity Data for 44 Integrated Disposal Facility Borehole Samples from the H2 Sandy Sequence. (2 sheets)

Sample	θ_s (cm^3/cm^3)	θ_r (cm^3/cm^3)	α (1/cm)	n (-)	Saturated Hydraulic Conductivity (cm/s)
7A[1]	0.377	0.0404	0.0290	1.825	1.04E-03
10A[1]	0.413	0.0279	0.1161	1.784	2.95E-03
12A[1]	0.363	0.0309	0.0650	1.755	2.15E-03
14A[1]	0.416	0.0324	0.0445	1.728	1.99E-03
15A[1]	0.380	0.0254	0.0487	1.844	2.09E-03
16A[1]	0.420	0.0228	0.0682	1.710	9.57E-03
17A[1]	0.423	0.0382	0.0689	1.899	1.99E-03
19A[1]	0.444	0.0279	0.2010	1.542	4.31E-03
20A[1]	0.419	0.0321	0.0305	2.081	2.54E-03
21A[1]	0.403	0.0276	0.0545	1.926	2.94E-03
22A[1]	0.352	0.0252	0.1078	1.585	5.06E-03
23A[1]	0.371	0.0411	0.0079	1.553	2.65E-04
24A[1]	0.321	0.0413	0.0130	1.684	5.69E-04
25A[1]	0.345	0.0267	0.0842	2.158	5.40E-03
27A[1]	0.377	0.0354	0.0830	1.532	8.14E-03
29A[1]	0.359	0.0317	0.0784	1.732	3.75E-03
31A[1]	0.418	0.0444	0.0058	2.012	8.21E-04
32A[1]	0.359	0.0401	0.0931	1.703	6.71E-03
34A[1]	0.316	0.0324	0.0819	2.398	1.32E-02
35A[1]	0.299	0.0428	0.0897	2.160	1.06E-02
45L[2]	0.385	0.008	0.1039	1.737	3.24E-2
45U[2]	0.385	0.005	0.088	1.664	3.24E-2

Table B-3. van Genuchten Parameters (Based on the Multistep Method) and Saturated Hydraulic Conductivity Data for 44 Integrated Disposal Facility Borehole Samples from the H2 Sandy Sequence. (2 sheets)

Sample	θ_s (cm^3/cm^3)	θ_r (cm^3/cm^3)	α (1/cm)	n (-)	Saturated Hydraulic Conductivity (cm/s)
50L[2]	0.420	0.025	0.073	1.710	1.75E-3
50U[2]	0.420	0.013	0.045	1.667	1.75E-3
80L[2]	0.359	0.031	0.0403	2.368	1.05E-3
80U[2]	0.359	0.033	0.0313	2.572	1.05E-3
85L[2]	0.406	0.023	0.1074	1.697	3.84E-2
85U[2]	0.406	0.027	0.0847	1.595	3.84E-2
110L[2]	0.412	0.039	0.0362	2.328	5.16E-4
110U[2]	0.412	0.046	0.0268	3.182	5.16E-4
130L[2]	0.358	0.032	0.0940	2.003	1.97E-2
130U[2]	0.358	0.036	0.0674	1.934	1.97E-2
150L[2]	0.431	0.015	0.0992	1.547	7.48E-3
150U[2]	0.431	0.024	0.0703	1.514	7.48E-3
200L[2]	0.410	0.002	0.0995	2.162	4.93E-2
215L[2]	0.370	0.028	0.0448	1.918	2.24E-3
215U[2]	0.370	0.023	0.0333	1.815	2.24E-3
230L[2]	0.309	0.040	0.0472	1.658	3.56E-3
230U[2]	0.309	0.038	0.0400	1.658	3.56E-3
251L[2]	0.427	0.032	0.084	1.845	1.43E-2
261L[2]	0.390	0.045	0.0191	2.485	5.54E-4
C3826-171[3]	0.382	0.0226	0.0390	1.840	7.96E-3
C3827-63.5[3]	0.444	0.0	0.0914	1.500	2.23E-2
C3827-221[3]	0.361	0.0220	0.0660	1.770	7.30E-3

[1]Fiscal year 1998 borehole.
[2]Fiscal year 2001 borehole.
[3]Fiscal year 2002 borehole.

Reference: RPP-20621, *Far-Field Hydrology Data Package for the Integrated Disposal Facility Performance Assessment*.

Table B-4. Wet Sieve Particle Size Distribution for Borehole 299-E27-22 Sediments.

Depth (ft bgs)	Stratigraphic Unit (Hanford formation)	Weight Percent		
		Gravel	Sand	Silt/Clay
28.0	H1	28.2	62.9	8.78
40.5	H1	0.104	85.1	14.3
45.5	H1	0.136	88.9	10.5
48.0	H1	0	61.6	36.3
50.5	H1	22.1	72.3	5.58
78.0	H1	11.0	77.6	11.2
82.0	H2	0.165	87.5	11.9
85.5	H2	1.74	89.6	8.61
95.5	H2	1.10	88.4	10.4
100.5	H2	0.424	90.8	8.62
139.5	H2	0.112	88.4	11.0
145.5	H2	24.7	66.1	9.09
160.5	H2	15.9	68.8	15.2
164.5	H2	3.21	89.1	7.53
185.5	H2	18.9	60.9	20.0
200.5	H2	17.3	73.5	9.12
210.5	H2	17.1	68.5	14.2
225.5	H2	11.7	76.2	11.9

Reference: PNNL-15503, *Characterization of Vadose Zone Sediments Below the C Tank Farm: Borehole C4297 and RCRA Borehole 299-E27-22.*

Similar comparison was also made for other units using their selected properties (presented below); for a recharge estimate of 3.5 mm/yr, the steady-state simulated moisture contents and the field measured average moisture contents (Table B-1) compared well.

B.2.1.2 Alternative Geologic Model Properties. The preceding sections have identified parameters for the soils in Alternative Geologic Model I (ACM-I). Alternative Geologic Model II (ACM-II) is a slight variation (see Section 6) of ACM-I. The primary difference between the two alternative models concerns whether or not a sandy gravel facies followed by a silty sandy layer exist at the bottom of the H2 unit in the vicinity of WMA C. Figure B-15 illustrates the moisture retention curves for ACM-II, whereas Figure B-16 illustrates the unsaturated conductivity curves for ACM-II.

Figure B-12. Moisture Retention Data for H2 Unit (44 Samples). The Waste Management Area C H2 composite curve is shown in red.

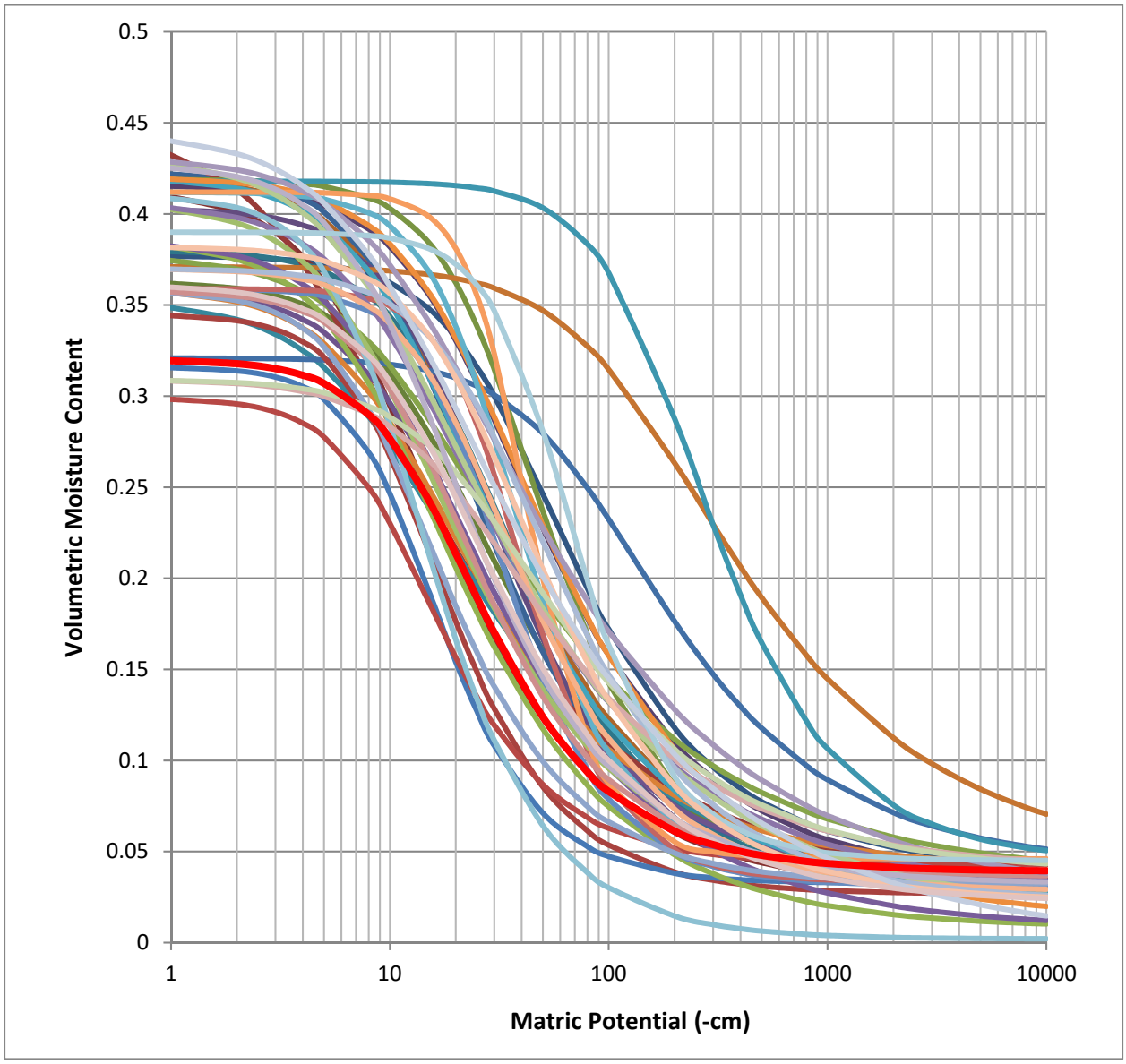

Reference: RPP-20621, *Far-Field Hydrology Data Package for the Integrated Disposal Facility Performance Assessment*.

B.2.2 Properties of the Hanford H1 and H3 Gravelly Units

Similar to Hanford H2 sand-dominated unit, no site-specific data are available for the WMA C Hanford H1 and H3 gravelly units. However, as part of other Hanford Site projects, particle-size distribution, bulk density, saturated hydraulic conductivity, moisture retention, and unsaturated conductivity data have been collected for several borehole samples (Figure B-3) at other sites in the vicinity of C Farm and within 200 Areas. These sites include the 218-E-12B and 218-E-10 low-level solid waste burial grounds in 200 East Area, the Environmental Restoration Disposal Facility site located in between the 200 West and 200 East Areas, and the 241-T-106 tank site

located in 200 West Area. Borehole sediment samples from these sites were used as surrogates to represent the hydraulic properties for WMA C H1 and H3 gravel-dominated units.

Figure B-13. Unsaturated Hydraulic Conductivity Data for H2 Unit (44 Samples). The Waste Management Area C H2 composite curve is shown in red.

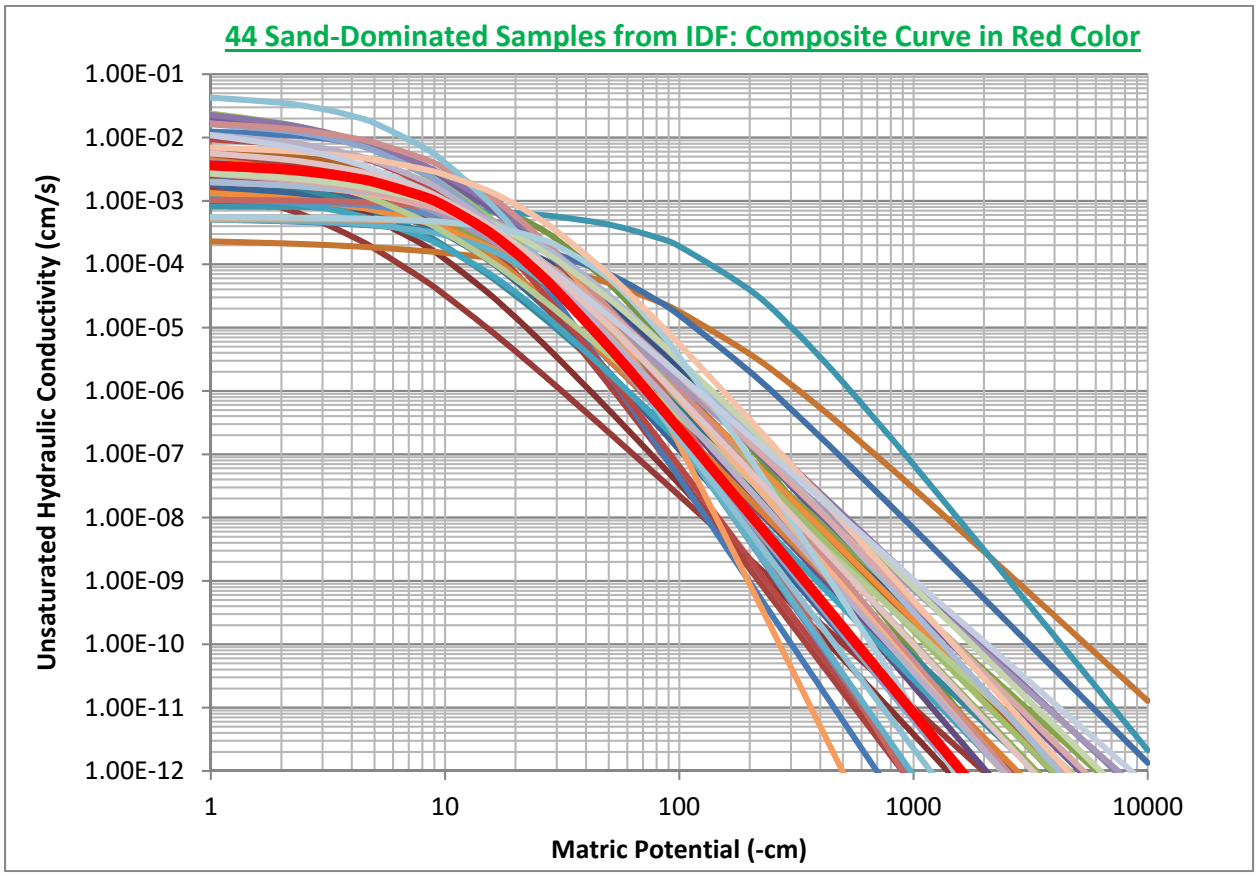

Reference: RPP-20621, *Far-Field Hydrology Data Package for the Integrated Disposal Facility Performance Assessment*.

Unlike H2 sediments, both H1 and H3 sediments are comprised of a significant gravel (>2 mm size) fraction. To explore the impact of gravelly sediments for the drier moisture regime, a separate study was conducted ("Variability of Gardner's α for coarse-textured sediments" [Khaleel and Relyea 2001]); a total of 79 gravelly and sandy samples were analyzed in the laboratory. The gravel fraction for 41 samples ranged from 20 to 71% (by weight); the remaining 38 samples were sandy with very little gravel fraction (Figure B-17). A noteworthy feature of Figure B-17 is the fact that the variability in saturated conductivity is much greater than the variability in unsaturated conductivity near saturation. Furthermore, the measured unsaturated conductivities for the gravelly samples showed less variability for the drier moisture regime, fell within a narrower range, and were well within the range of measured unsaturated conductivities for the sandy samples (see Figure B-17). Such a generic behavior for the gravelly sediments for the drier moisture regime prompted assigning similar properties for both H1 and H3 units.

Figure B-14. Comparison of Simulated (Blue) and Observed (Circle) Moisture Content for Hanford H2 Sand-Dominated Unit.

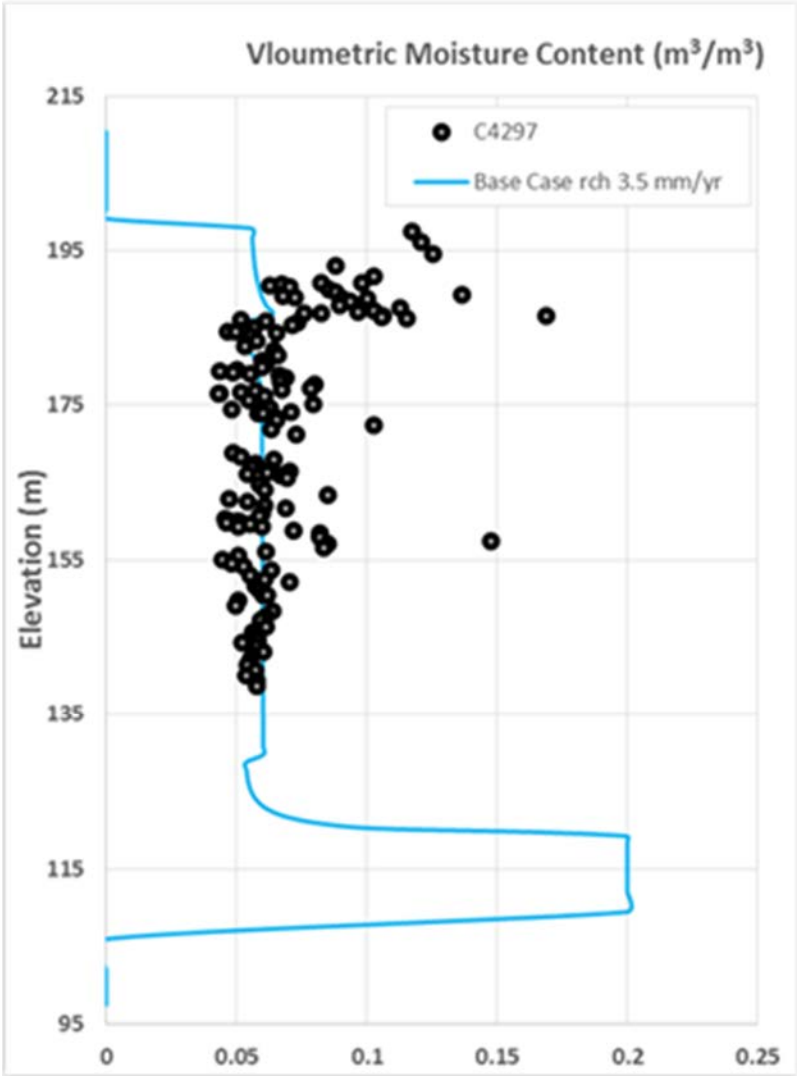

Standard laboratory and Westinghouse Hanford Company quality assurance procedures (WHC-IP-0635, *Geotechnical Engineering Procedure Manual*) were used to analyze the H1 and H3 sediment samples. The moisture retention data for the fine fraction (<2 mm) and the drainage cycle of up to -1,000 cm of pressure head were measured using "Tempe" pressure cells; the rest of the drainage data up to -15,000 cm was measured using the pressure plate extraction method ("Water Retention: Laboratory Methods" [Klute 1986]). A variation of the unit gradient method (Klute and Dirksen 1986; Khaleel et al. 1995) was used to measure unsaturated hydraulic conductivities for the bulk samples. The laboratory measured data on <2 mm size fraction were corrected for the gravel fraction ("Water Content" in Methods of Soils Analysis, Part 1—Physical and Mineralogical Methods [Gardner 1986]; Khaleel and Relyea 1997). No correction was needed for the saturated and unsaturated conductivities, since these were measured on the bulk sample.

Figure B-15. Moisture Retention Curves for Various Hydrostratigraphic Units and Selected Properties for Alternative Geologic Model II.

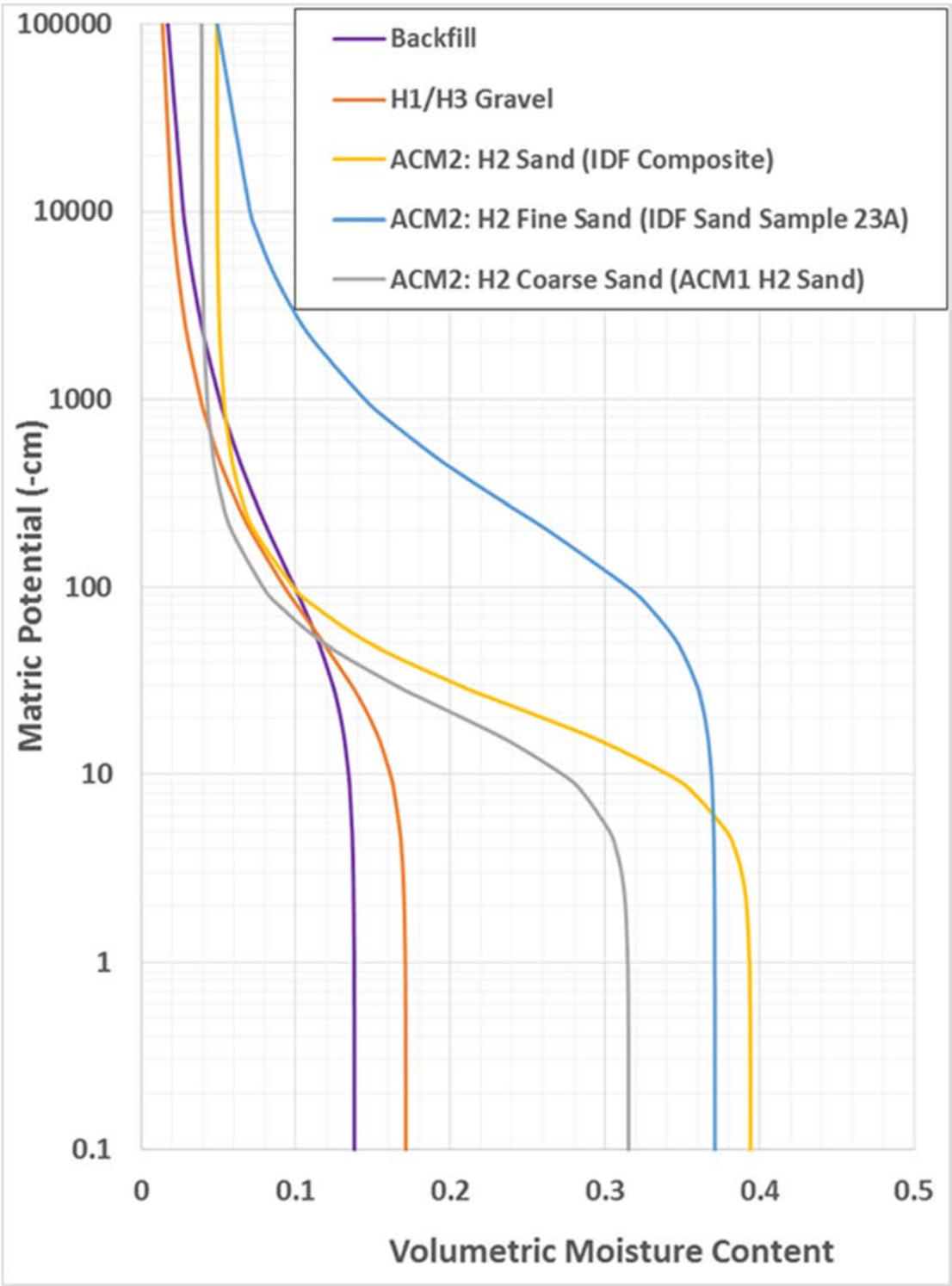

ACM1 = Alternative Geologic Model I
ACM2 = Alternative Geologic Model II
IDF = Integrated Disposal Facility

Figure B-16. Unsaturated Hydraulic Conductivity Curves for Various Hydrostratigraphic Units and Selected Properties for Alternative Geologic Model II.

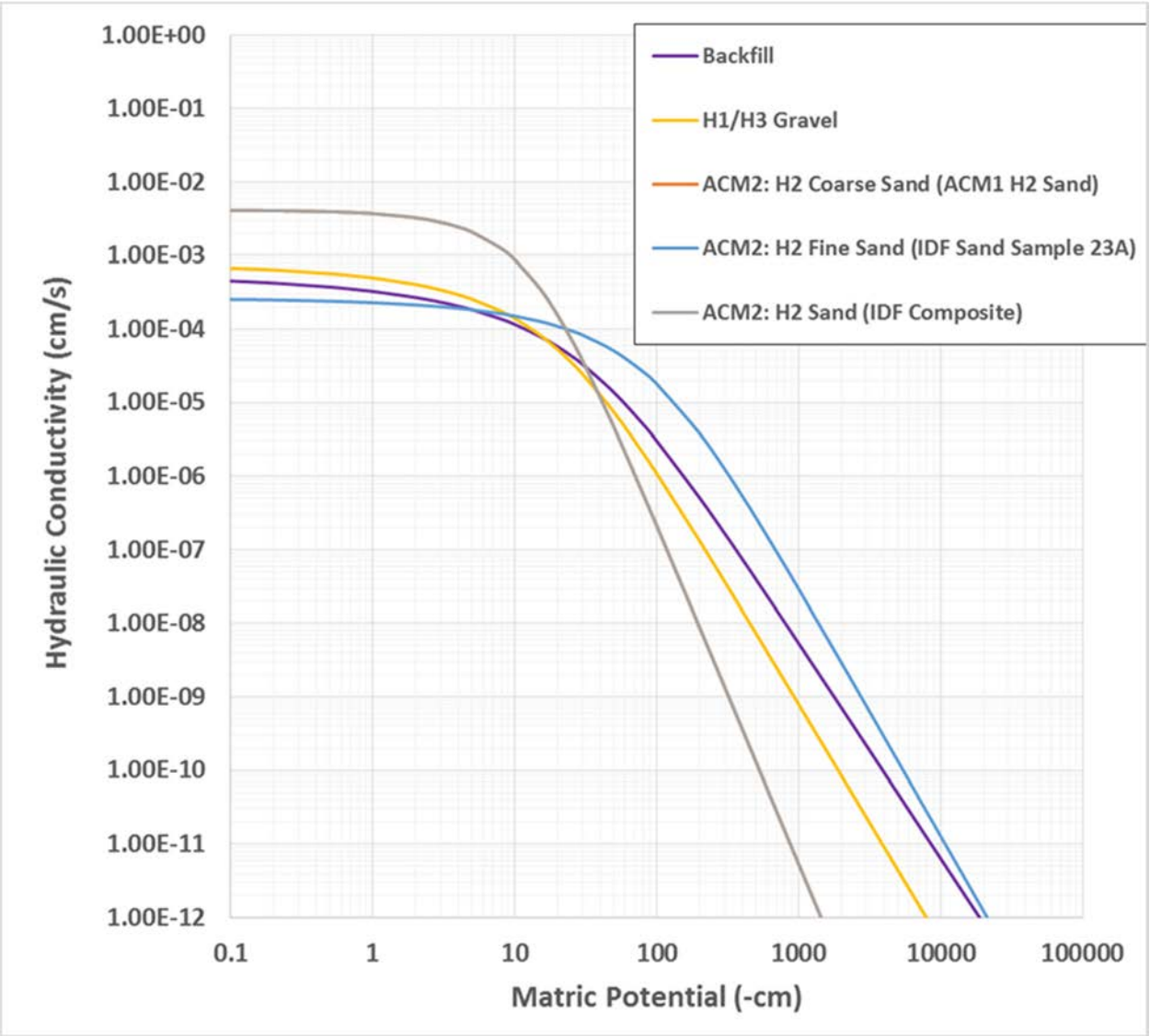

ACM1 = Alternative Geologic Model I
ACM2 = Alternative Geologic Model II
IDF = Integrated Disposal Facility

As was done for the Hanford H2 sandy unit, a simultaneous fit of both laboratory-measured moisture retention and unsaturated conductivity data was used; and all five unknown parameters (i.e., θr, θ_s, α, n, and K_s), with m=1 1/n (van Genuchten 1980), were fitted to the data via RETC (EPA/600/2-91/065, *The RETC Code for Quantifying the Hydraulic Functions of Unsaturated Soils*). The pore size distribution factor, ℓ (Mualem 1976), was kept fixed at 0.5 during the simultaneous fitting. The fitted parameters, based on moisture retention and unsaturated conductivity measurements for H1 and H3 units, are shown in Table B-5. The fitted retention and conductivity curves for H1 and H3 units are shown in Figure B-18 and Figure B-19, respectively.

Figure B-17. Unsaturated Hydraulic Conductivity Measurements for Sand-Dominated and Gravel-Dominated Samples.

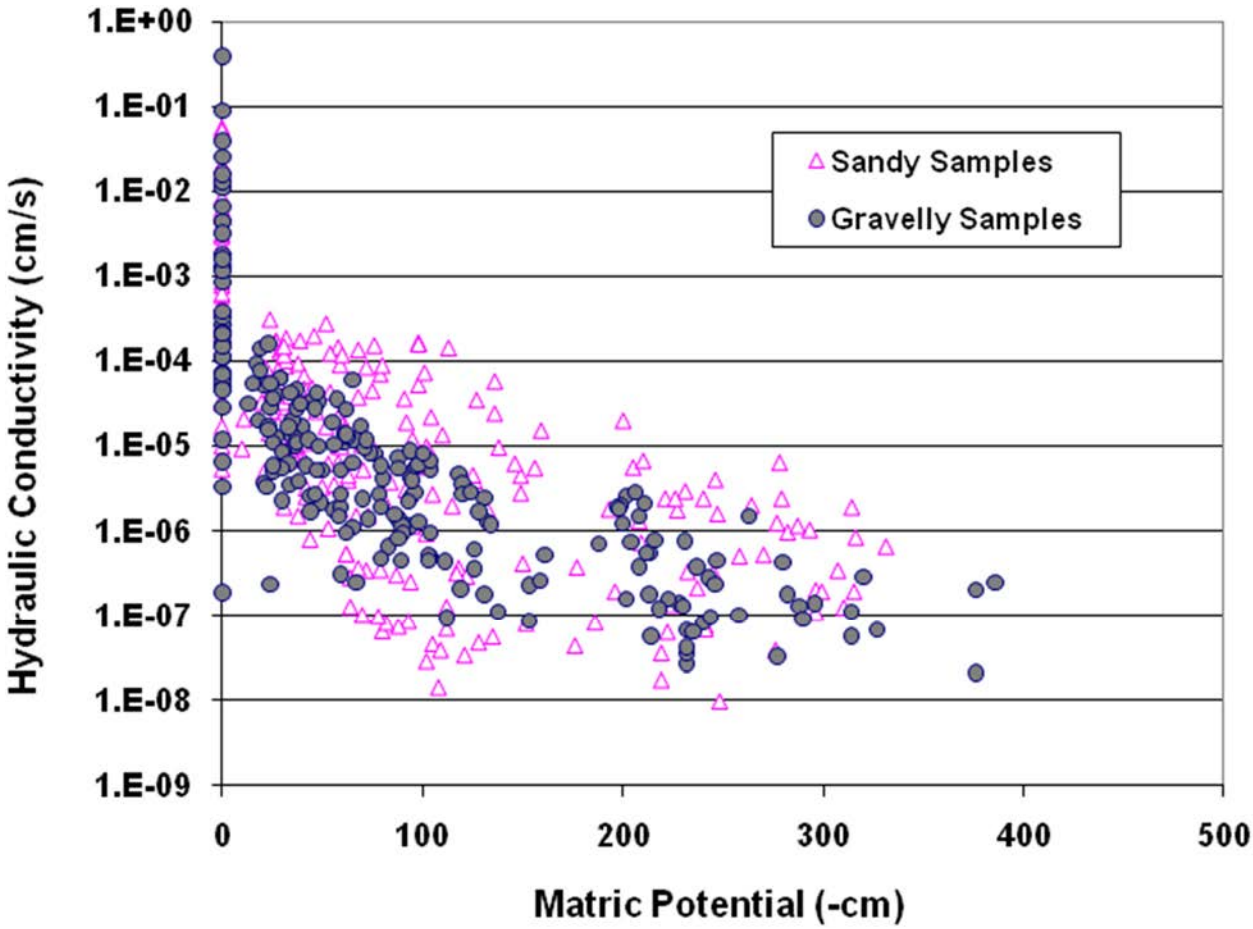

Reference: "Variability of Gardner's α for coarse-textured sediments" (Khaleel and Relyea 2001).

B.2.3 Properties for the Backfill Gravelly Unit

Because of high gravel content, the backfill hydraulic properties are expected to be similar to H1 and H3 gravelly media properties. Table B-6 catalogs the van Genuchten-Mualem parameters for samples that were selected from the 200 Areas database to represent the WMA C tank farm backfill sediments. Because the backfill includes a significant gravel fraction, most of the samples (Table B-6) are the same as the 17 samples used to represent the H1 and H3 gravelly units. The fitted retention and conductivity curves for the backfill unit are shown in Figure B-20 and Figure B-21, respectively.

B.3 EFFECTIVE (UPSCALED) FLOW PARAMETERS FOR VADOSE ZONE

Data on hydraulic properties, described in the preceding sections, were obtained via laboratory tests on core samples (scales of the order of a few centimeters). However, numerical models of fluid flow and contaminant transport in the unsaturated zone require specifying hydraulic

properties for each discretized grid block (scales of the order of meters), which are much larger than the core scale at which the unsaturated properties are measured. The process of defining large-scale properties for the numerical grid blocks based on small, core-scale measurements is called upscaling ("Upscaled Flow and Transport Properties for Heterogeneous Unsaturated Media" [Khaleel et al. 2002]).

For stratified sediments such as those existing in the 200 Areas, the effective hydraulic conductivity tensor is anisotropic with a moisture-dependent (or tension-dependent) degree of anisotropy. The anisotropy ratio of horizontal hydraulic conductivity to vertical hydraulic conductivity increases with decreasing moisture content. Theoretical work on variable anisotropy include, for example, "Stochastic Analysis of Unsaturated Flow in Heterogeneous Soils, 2. Statistically Anisotropic Media with Variable α" (Yeh et al. 1985), "Stochastic Modeling of Large-Scale Transient Unsaturated Flow Systems" (Mantoglou and Gelhar 1987), and "Estimation of effective unsaturated hydraulic conductivity tensor using spatial moments of observed moisture plume" (Yeh et al. 2005). Experimental studies supporting variable anisotropy include, for example, "Dependence of Anisotropy on Saturation in a Stratified Sand" (Stephens and Heermann 1988), "Effective Unsaturated Hydraulic Conductivity of Layered Sands" (Yeh and Harvey 1990), and "Hysteresis and State-Dependent Anisotropy in Modeling Unsaturated Hillslope Hydrologic Processes" (McCord et al. 1991). Variable, moisture-dependent anisotropy in unsaturated soils, in effect, is an effective, large-scale (macroscopic) flow property which results from media heterogeneities at a smaller scale, and provides a framework for upscaling laboratory-scale measurements to delineate the effective or upscaled properties for the large-scale vadose zone. A stochastic model (i.e., Application of Stochastic Methods to Transient Flow and Transport in Heterogeneous Unsaturated Soils [Polmann 1990]) is used to describe moisture- or tension-dependent anisotropy for WMA C sediments. Such an upscaling process recognizes the spatial variability inherent in heterogeneous media such as those existing at WMA C.

Effective or upscaled values of flow parameters for the WMA C vadose zone are presented in Section B.3.1. Specific upscaled flow parameters include moisture retention, saturated, and unsaturated hydraulic conductivity. Transport parameters (e.g., bulk density, diffusivity, sorption coefficients, and macrodispersivity) are discussed later in Section B.4.

B.3.1 Composite Macroscopic Relationships and Effective Parameters

The WMA C composite parameters for moisture characteristics are derived based on laboratory measurements presented in preceding sections. The fitted moisture retention curves (e.g., Figure B-12 for H2 unit) show spatial variability, albeit the degree of variation at a given tension is more modest than that of hydraulic conductivity (e.g., Figure B-13 for H2 unit). For both sandy (e.g., H2 unit) and gravelly (e.g., H1, H3, and backfill units) sediments, the composite van Genuchten parameters were obtained via RETC (EPA/600/2-91/065) and a simultaneous fit of both moisture retention and unsaturated conductivity data. The pore size distribution factor ℓ (van Genuchten 1980) was kept constant at 0.5 during the simultaneous fitting.

Table B-5. van Genuchten Parameters, Fitted Saturated Hydraulic Conductivity, and Measured Bulk Density Data for H1/H3 Units (17 Samples).

Sample	Site/Operable Unit	Borehole Number	Depth m	Percent Gravel	Θs cm^3/cm^3	Θr cm^3/cm^3	α 1/cm	n	Fitted Ks cm/s	Bulk Density g/cm^3
5-0150	218-E-12B	299-E34-1	24.84	17	0.240	0.023	0.030	1.7077	1.47E-03	1.95
5-0157	218-E-10	299-E32-4	3.50	13	0.293	0.033	0.027	2.1675	7.77E-03	1.88
5-0152	218-E-12B	299-E34-1	65.50	26	0.280	0.025	0.044	1.3253	2.43E-03	1.85
5-0158	218-E-10	299-E32-4	71.50	44	0.214	0.013	0.008	1.4226	1.38E-04	2.15
5-0148	218-E-12B	299-E34-1	15.25	54	0.148	0.013	0.021	1.5589	2.72E-04	2.16
4-1080	ERDF	699-35-61A	93.50	43	0.178	0.000	0.007	1.3819	8.11E-06	2.00
4-0791	ERDF	699-35-65A	63.20	0	0.338	0.026	0.023	2.2565	6.81E-04	1.60
4-0792	ERDF	699-35-65A	75.40	71	0.100	0.008	0.030	1.5858	3.42E-04	2.32
4-1076	ERDF	699-35-61A	76.40	0	0.357	0.000	0.029	1.7015	1.23E-03	1.74
4-1079	ERDF	699-35-61A	90.90	61	0.163	0.000	0.014	1.3079	1.18E-04	2.06
4-1013	ERDF	699-35-69A	77.90	65	0.139	0.013	0.007	1.5656	1.06E-06	2.20
4-1012	ERDF	699-35-69A	73.90	55	0.147	0.000	0.008	1.5109	4.50E-05	2.19
3-0668	241-T-106	299-W10-196	38.90	62	0.175	0.000	0.019	1.6124	1.63E-04	2.13
3-0682	241-T-106	299-W10-196	46.10	51	0.224	0.000	0.017	1.6577	2.37E-04	2.14
3-0210	241-T-106	299-W10-196	3.10	48	0.186	0.029	0.014	1.7674	1.96E-04	2.11
3-0688	241-T-106	299-W10-196	48.50	49	0.199	0.000	0.004	1.5321	2.60E-05	2.17
3-0690	241-T-106	299-W10-196	53.7	53	0.182	0.018	0.005	1.5410	4.19E-05	2.19

ERDF = Environmental Restoration Disposal Facility

Figure B-18. Moisture Retention Data for H1 and H3 Units (17 Samples). The composite curve is shown in red.

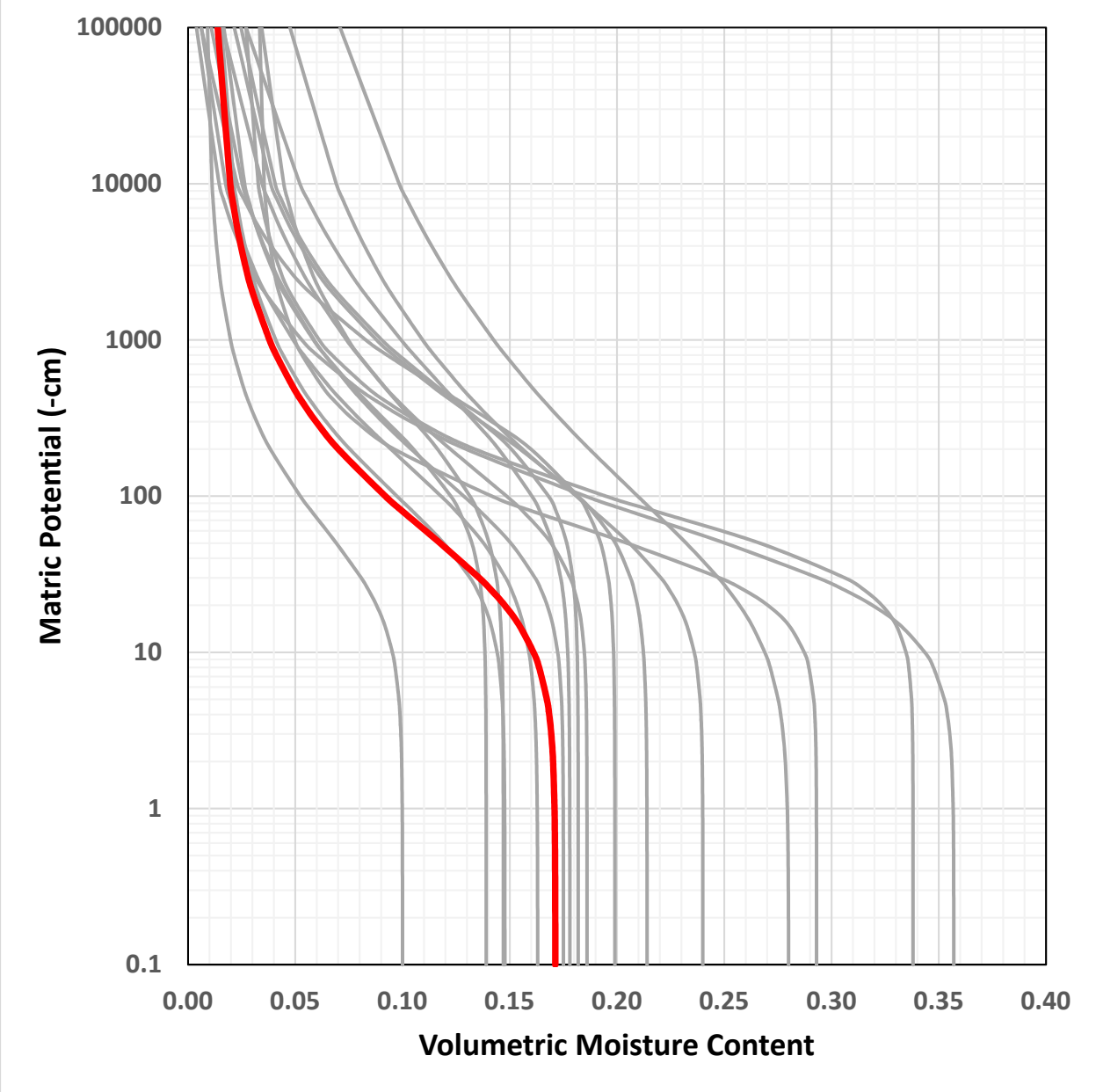

The fitted composite van Genuchten-Mualem parameters for different HSUs are shown in Table B-7. Estimates for the equivalent horizontal and vertical hydraulic conductivities are discussed in Section B.3.2.

B.3.2 Stochastic Model for Macroscopic Anisotropy

As discussed earlier, variable, tension-dependent anisotropy provides a framework for upscaling small-scale measurements to the effective or upscaled properties for the large-scale vadose zone. A stochastic model is used to describe tension-dependent anisotropy for sediments at the C Farm.

Figure B-19. Unsaturated Hydraulic Conductivity Data for H1 and H3 Units (17 Samples). The composite curve is shown in red.

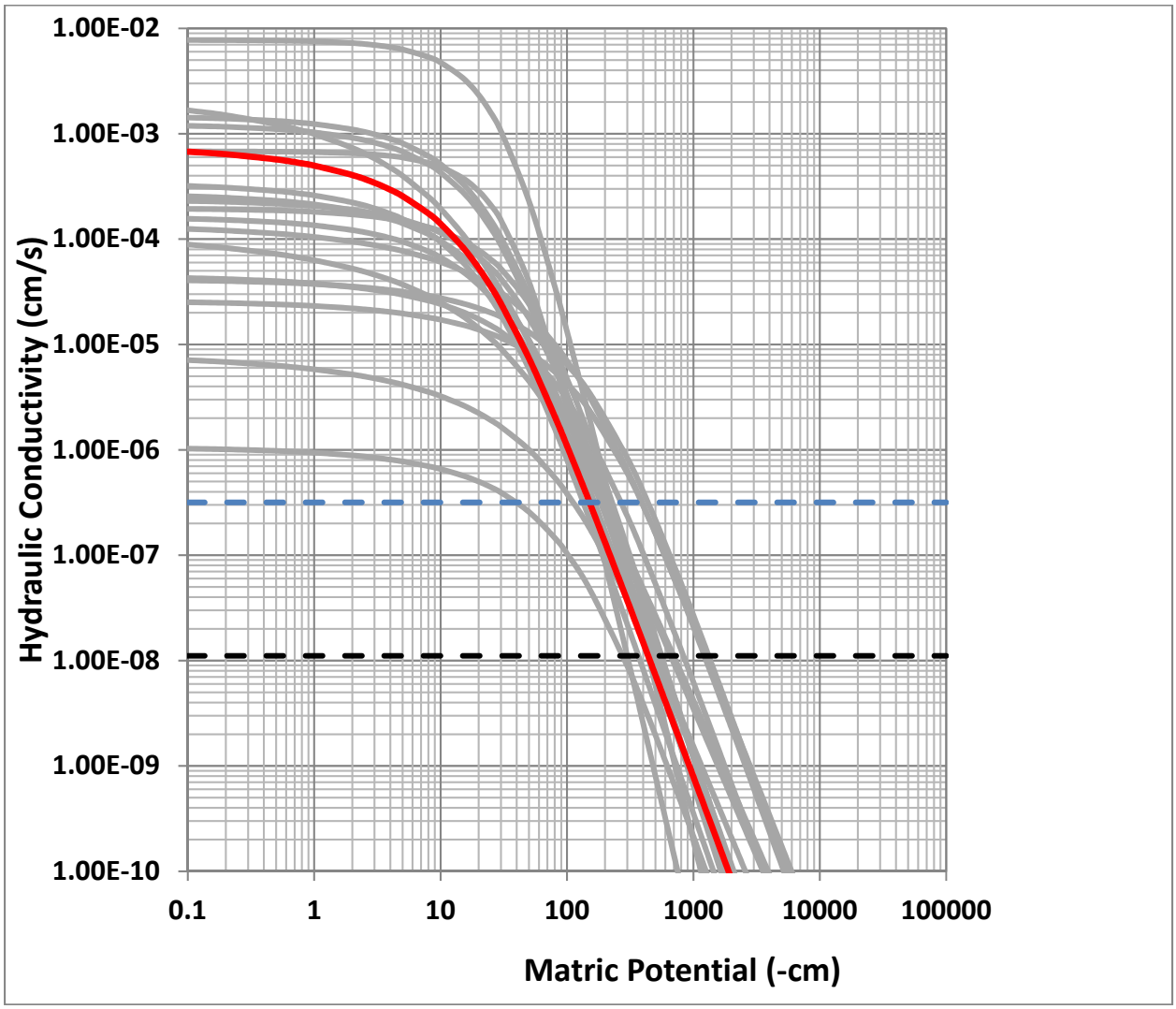

Yeh et al. (1985) analyzed steady unsaturated flow through heterogeneous porous media using a stochastic model. Parameters such as hydraulic conductivity are treated as random variables rather than as deterministic quantities. The Gardner relationship ("Some Steady-State Solutions of the Unsaturated Moisture Flow Equation with Application to Evaporation from a Water Table" [Gardner 1958]) was used by Yeh et al. (1985) to describe unsaturated hydraulic conductivity (K) as a function of saturated hydraulic conductivity (Ks) and tension (h), as shown in Equations B-1 and B-2.

$$K(h) = K_s \, exp(-\beta h) \tag{B-1}$$

Where β is a fitting parameter.

Table B-6. van Genuchten Parameters, Fitted Saturated Hydraulic Conductivity, and Measured Bulk Density Data for Backfill Unit (10 Samples).

Sample	Site	Borehole Number	Depth (m)	Percent Gravel	θ_s (cm^3/cm^3)	θ_r (cm^3/cm^3)	α (1/cm)	n (-)	Fitted K_s (cm/s)	Bulk Density (g/cm^3)
4-0792	ERDF	699-35-65A	75.4	71	0.100	0.0084	0.03	1.5858	3.42E-04	2.32
4-1012	ERDF	699-35-69A	73.9	55	0.147	0	0.0076	1.5109	4.50E-05	2.19
4-1013	ERDF	699-35-69A	77.9	65	0.139	0.0127	0.0065	1.5656	1.06E-06	2.20
4-1079	ERDF	699-35-61A	90.9	61	0.163	0	0.014	1.3079	1.18E-04	2.06
4-1080	ERDF	699-35-61A	93.5	43	0.178	0	0.0074	1.3819	8.11E-06	2.00
3-0668	241-T-106	299-W10-196	38.9	62	0.175	0	0.0192	1.6124	1.63E-04	2.13
3-0682	241-T-106	299-W10-196	46.1	51	0.224	0	0.0166	1.6577	2.37E-04	2.14
3-0688	241-T-106	299-W10-196	48.5	49	0.199	0	0.0043	1.5321	2.60E-05	2.17
3-0689	241-T-106	299-W10-196	52.2	28	0.236	0	0.0025	1.4747	4.58E-05	1.93
3-0690	241-T-106	299-W10-196	53.7	53	0.1819	0.0177	0.0046	1.541	4.19E-05	2.19

ERDF = Environmental Restoration Disposal Facility

Figure B-20. Moisture Retention Data for Backfill Unit (10 Samples). The composite curve is shown in red.

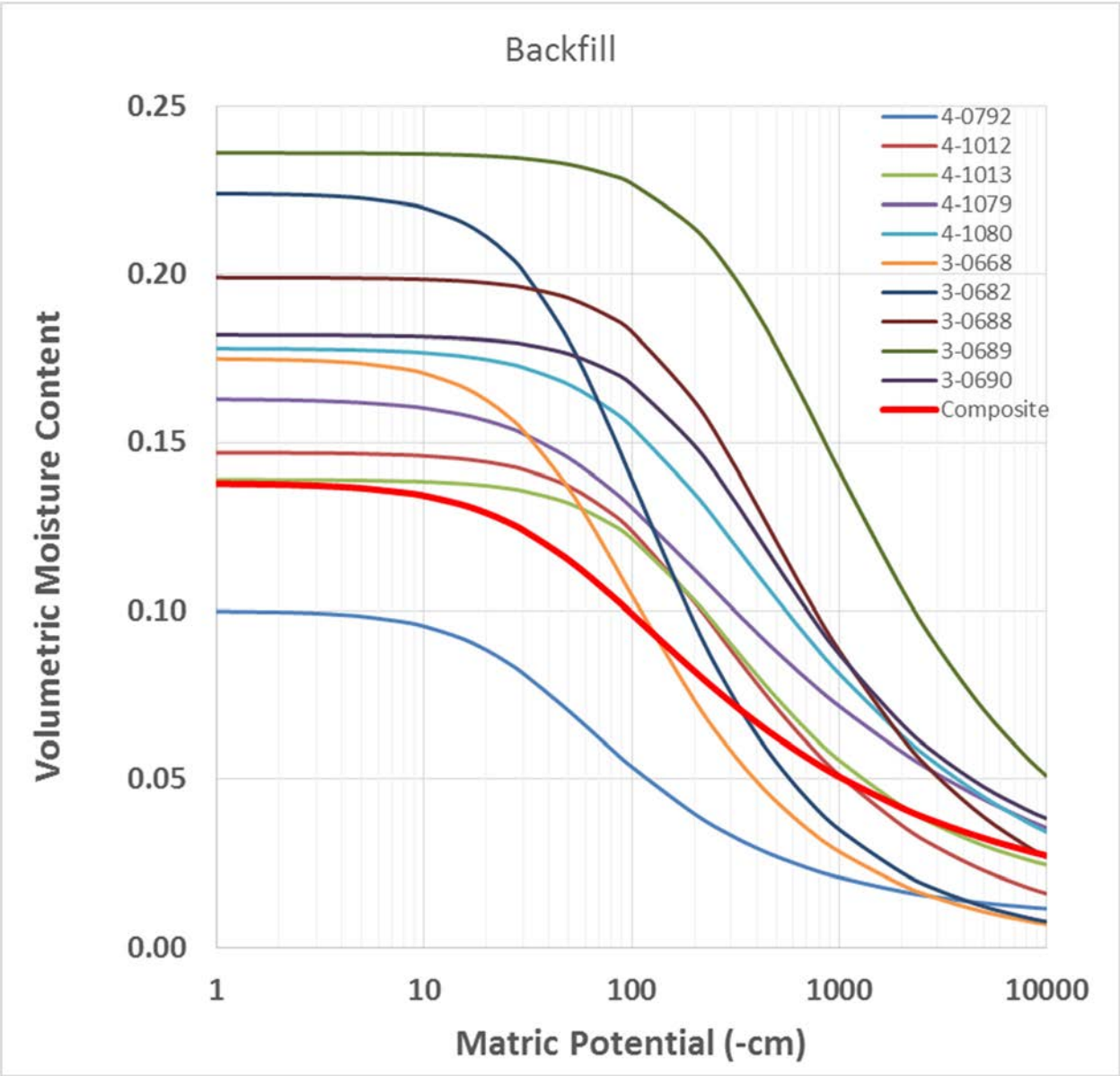

Equation B-1 can be written as

$$ln(K(h)) = ln(K_s) - \beta h \qquad \text{(B-2)}$$

Equation B-2 is referred to as the log-linear model, since ln(K(h)) is linearly related to h through the constant slope β. However, such a constant slope is often inadequate in describing ln(K(h)) over ranges of tension of practical interest for field applications. As an alternative, the slope β can be approximated locally by straight lines over a fixed range of tension. The pseudo "ln(K_s)" term in Equation B-2 can then be derived by extrapolating the local slopes back to zero tension.

Figure B-21. Unsaturated Hydraulic Conductivity Data for Backfill Units (10 Samples). The composite curve is shown in red.

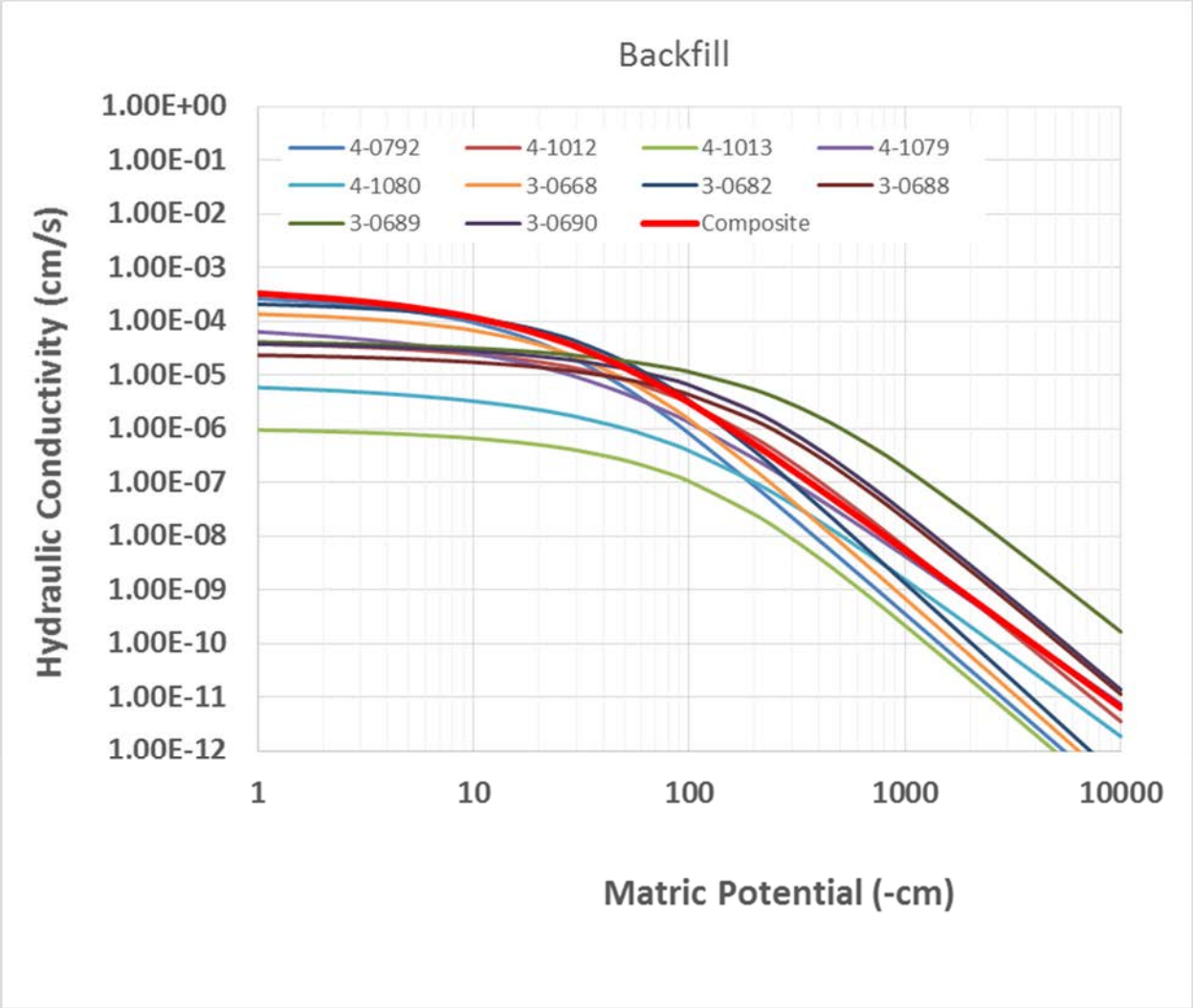

Table B-7. Composite van Genuchten-Mualem Parameters for Waste Management Area C Hydrostratigraphic Units.

Hydrostratigraphic Unit	Number of samples	θ_s	θ_r	α (1/cm)	n	ℓ	Fitted K_s (cm/s)
Backfill Gravelly Unit	10	0.138	0.010	0.021	1.374	0.5	5.60E-04
H1 and H3 Gravelly Units	15	0.171	0.011	0.036	1.491	0.5	7.70E-04
H2 Sand-Dominated Unit	44	0.315	0.0392	0.0631	2.047	0.5	4.15E-03

Using a linear correlation model between the log-conductivity zero-tension intercept and β, Polmann (1990) presents a generalized model that accounts for the cross-correlation of the local

soil property [i.e., ln(K_s) and β] residual fluctuations. When compared with the uncorrelated ln(K_s) - β model, a partial correlation of the properties is shown to have a significant impact on the magnitude of the effective parameters derived from the stochastic theory. The Polmann (1990) equations for deriving the effective parameters are shown in Equation B-3.

$$
\begin{aligned}
&< LnK > = < LnK_s > - A < h > - \sigma^2_{LnKs}\lambda[p - p^2 < h > - \zeta^2 < h >]/(1 + A\lambda) \\
&\sigma^2_{LnK} = \sigma^2_{LnKs}[(1 - p < h >)^2 + \zeta^2 < h >^2]/(1 + A\lambda) \\
&K_h^{eq} = \exp[< LnK > + (\sigma^2_{LnK}/2)] \\
&K_v^{eq} = \exp[< LnK > - (\sigma^2_{LnK}/2)]
\end{aligned}
\qquad \text{(B-3)}
$$

Where:

σ^2_{LnK}	=	variance of log unsaturated conductivity (which depends on mean tension)
$<h>$	=	mean tension (positive) = |ψ|
ψ	=	matric potential (negative)
σ^2_{LnKs}	=	variance of pseudo "log saturated conductivity"
$<LnK_s>$	=	mean of ln(K_s)
p	=	slope of the β versus ln(K_s) regression line, where β is the slope of the unsaturated conductivity curve and approximated locally based on Gardner's (1958) exponential model
ζ	=	$\sigma_\delta/\sigma_{\ln(Ks)}$
σ_δ	=	standard deviation of the residuals in the β versus ln(K_s) regression
A	=	mean slope, β, for ln(K) vs. h
λ	=	vertical correlation lengths for ln(K_s) (assumed to be same as that of β)
K_h^{eq}	=	equivalent unsaturated horizontal conductivity
K_v^{eq}	=	equivalent unsaturated vertical conductivity.

B.3.3 Macroscopic Anisotropy Relations

Results of application of Equation B-3 for variable anisotropy are presented below. The data for individual HSUs (Tables B-3, B-5 and B-6) are used to obtain the Polmann parameters < ln(K_s)>, σ^2_{LnKs}, p, ζ, and A (Equation B-3). The slope and pseudo ln(K_s) estimates, discussed in the preceding section, are evaluated for the expected moisture regime of interest (i.e., relatively high tension range) (Table B-8). However, it should be noted that often no experimental data are available for unsaturated conductivities in the tension range of interest; β and ln(K_s) estimates are then based on the fitted van Genuchten-Mualem curves.

An estimate of correlation length λ is needed for anisotropy calculations. Most of the measurements in the 200 Area have been obtained at sampling intervals that are too coarse to yield a reasonable estimate for the correlation length. However, one data set is available that provides saturated conductivity estimates at about 30-cm intervals for a depth of 18 m within the Hanford formation; the site is located about 0.5 mi east of the IDF site (Figure B-3) in the

200 East Area. Figure B-22 shows the experimental variogram and the fitted theoretical variogram for saturated conductivities. The fitted variogram suggests a correlation length λ of about 50 cm (i.e., the distance at which the variogram drops to [1-(1/e)] times the sill) (Figure B-22). Correlation length λ for both ln(K_s) and β were assumed to be equal.

Table B-8. Simulated Average Tension Ranges for Polmann Anisotropy Model.

Hydrostratigraphic Unit	Simulated Average Tension (cm)
Backfill Gravelly Unit	400 – 750
H1 and H3 Gravelly Units	150 – 400
H2 Sand-Dominated Unit	80 – 300

Figure B-22. Experimental (Triangles) and Fitted Theoretical (Squares) Variogram for Saturated Hydraulic Conductivity (LnK$_s$).

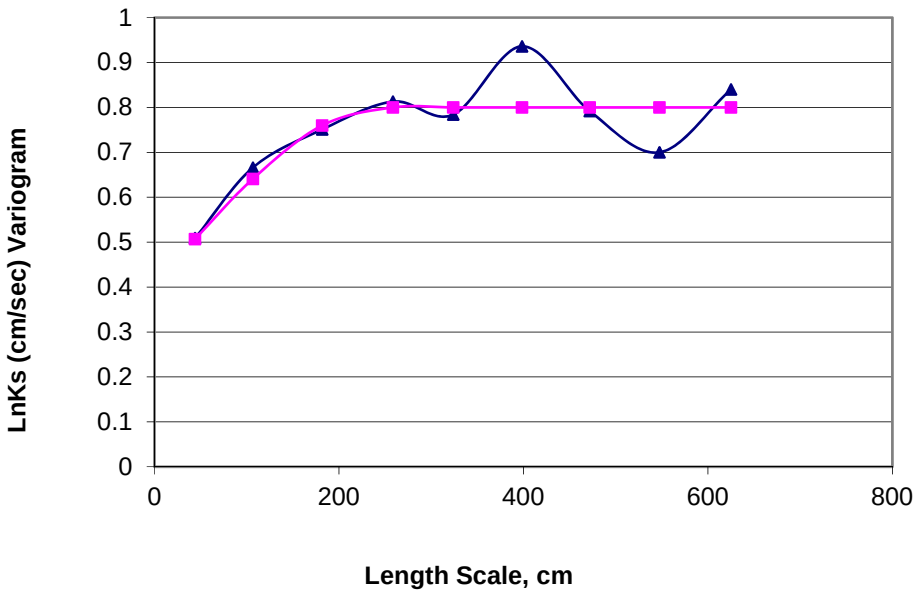

Reference: RPP-20621, *Far-Field Hydrology Data Package for the Integrated Disposal Facility Performance Assessment*.

Table B-9 lists the variable, macroscopic anisotropy parameter estimates for various WMA C units. The calculated macroscopic variable anisotropy relations for various HSUs are shown in Figures B-23, B-24, and B-25. A supporting document presents the anisotropy calculations (RPP-CALC-60452, *Moisture Dependent Anisotropy Calculations Supporting WMA C PA*).

Note that values listed in Table B-7 are the composite van Genuchten-Mualem parameters for different units. Equation B-3 is used to assign the variable Polmann anisotropy (i.e., the ratio of

equivalent unsaturated horizontal conductivity to equivalent unsaturated vertical conductivity) as a function of saturation. The van Genuchten-Mualem parameters in Table B-7 are then used to assign the actual unsaturated hydraulic conductivity estimates. The fitted K_s values in Table B-7 represent the vertical components.

Table B-9. Variable, Macroscopic Anisotropy Parameter Estimates for Various Waste Management Area C Units.

Hydrostratigraphic Unit	Number of samples	$<LnK_s>$	$\sigma^2_{LnK_s}$	p	ζ	λ (cm)	A
Backfill Gravelly Unit	10	-14.60	2.98	-2.28E-04	3.53E-04	30	0.00534
H1 and H3 Gravelly Units	17	-12.34	1.41	1.04E-03	2.68E-03	30	0.01249
H2 Sand-Dominated Unit	44	-11.79	2.50	-7.45E-04	3.33E-03	50	0.02415

Figure B-23. Calculated Macroscopic Anisotropy as a Function of Mean Matric Potential for the H2 Sand-Dominated Unit.

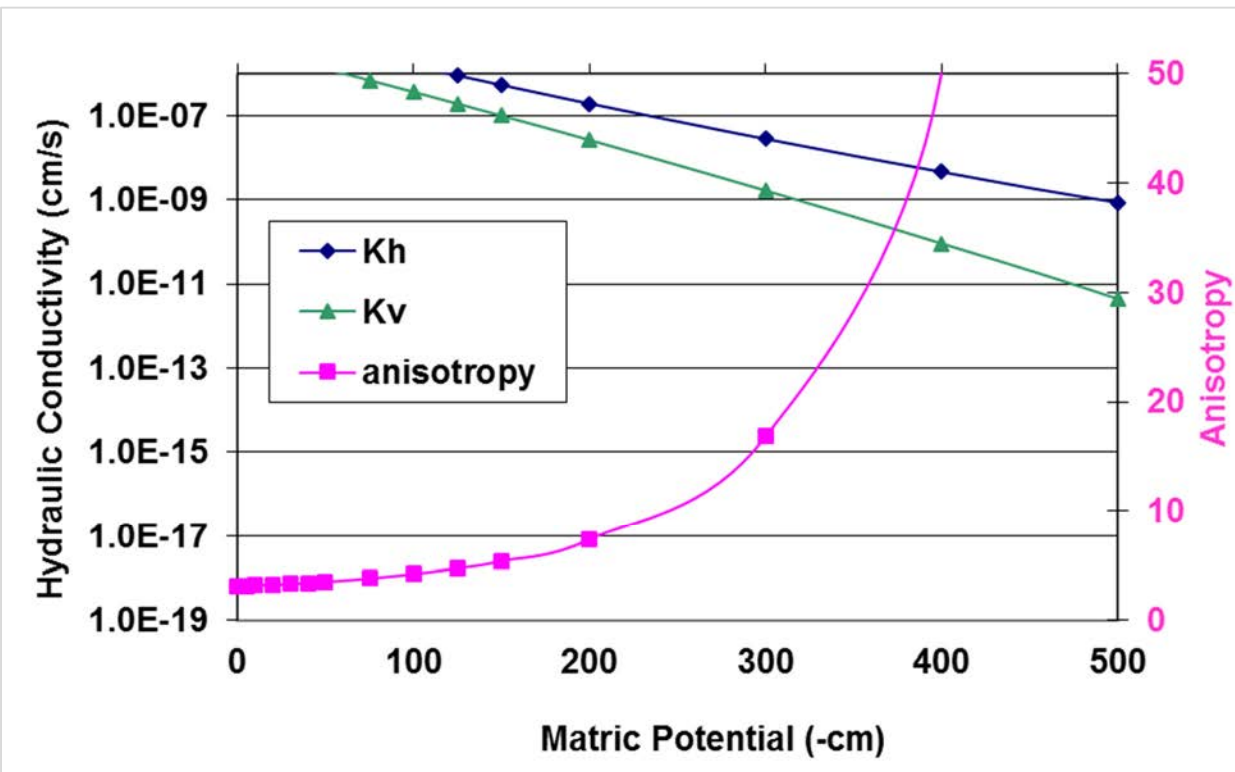

B.4 EFFECTIVE TRANSPORT PARAMETERS

Base case effective transport parameter (bulk density, diffusivity, and dispersivity) estimates are presented in this section. Because of natural variability, the transport parameters are all spatially

variable. The purpose is again, similar to the flow parameters, to evaluate the effect of such variability on the large-scale transport process.

B.4.1 Bulk Density and K_d

Both bulk density (ρ_b) and Kd estimates are needed to calculate retardation factors for different species. The effective, large-scale estimate for bulk density is the average of the small-scale laboratory measurements for bulk density (Stochastic Subsurface Hydrology [Gelhar 1993]). Table B-10 provides the effective, large-scale bulk density estimates for WMA C HSUs. The K_d values, presented in Section 6, were corrected for the gravel (>2-mm size) fraction, and are not repeated here. The correction procedure followed is described in PNNL-17154, *Geochemical Characterization Data Package for the Vadose Zone in the Single-Shell Tank Waste Management Areas at the Hanford Site*. For materials that contain significant amounts of gravel (notably H1 and H3), K_d values are typically lower than those determined with <2 mm size material because the surface area and the corresponding quantity of adsorption sites is lower (PNNL-17154).

B.4.2 Diffusivity

It is assumed that the effective, large-scale diffusion coefficients for all HSUs are a function of volumetric moisture content, θ and can be estimated based on an empirical relation ("Permeability of Porous Solids" [Millington and Quirk 1961]):

$$D_e(\theta) = D_0 \frac{\theta^{10/3}}{\theta_s^2} \tag{B-4}$$

where $D_e(\theta)$ is the effective diffusion coefficient of an ionic species, and D_0 is the effective diffusion coefficient for the same species in free water. The molecular diffusion coefficient for all species in pore water is assumed to be 2.5×10^{-5} cm^2/sec (WHC-SD-WM-EE-004, *Performance Assessment of Grouted Double-Shell Tank Waste Disposal at Hanford*).

B.4.3 Vadose Zone Macrodispersivities

Field-scale dispersivities are referred to as macrodispersivities. The terms macrodispersivity and dispersivity are used interchangeably in this section. Readers can go directly to Section B.4.3.4 for the macrodispersivity values recommended for WMA C PA calculations. Details on how the selections are made using different methods are provided in Section B.4.3.1 (numerical simulations), Section B.4.3.2 (stochastic theory) and Section B.4.3.3 (experimental observations).

Field observations indicate that the dispersion coefficients required to describe the large-scale transport processes, at field scales of tens or hundreds of meters, are much different from those observed in small-scale laboratory experiments (Gelhar 1993). In fact, field-scale dispersivities may often be orders of magnitude larger than those observed in the laboratory. Consequently, laboratory scale dispersivities, which are typically ~1 cm or less, are of little use in estimating field-scale dispersivities.

Figure B-24. Calculated Macroscopic Anisotropy as a Function of Mean Matric Potential for the H1 and H3 Gravelly Units.

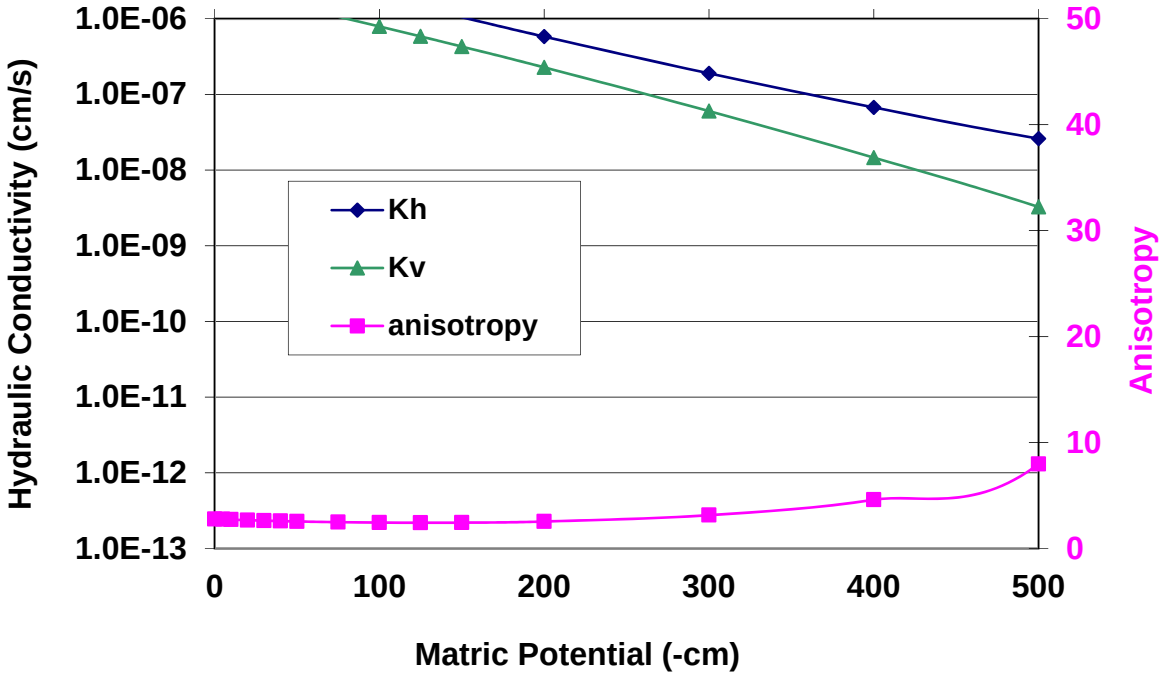

There is general agreement in hydrology literature that hydraulic conductivity variations induced by field-scale heterogeneities play an important role in field-scale transport processes. However, there does not appear to be a clear consensus about how best to describe such processes quantitatively (Gelhar 1993). While well-designed, large-scale tracer experiments would provide useful information, limited field data are available at this time to quantify macrodispersivities in unsaturated media.

Dispersivities are a function of matric potential (or soil moisture content) in unsaturated media (Mantoglou and Gelhar 1987). As with saturated media, heterogeneities that exist at various length scales result also in a scale dependence of macrodispersivities in unsaturated media ("A Critical Review of Data on Field-Scale Dispersion in Aquifers" [Gelhar et al. 1992]). Dispersivities increase with time, or equivalently with distance, until they tend to converge on their unique asymptotic (large-time) values. However, it can take a long time (e.g., years or decades) for the asymptotic Fickian approximation to take hold. Nonetheless, the second-moment evolution or the time-dependent, preasymptotic dispersivities are of marginal interest in simulations involving long-times or large-mean travel distances such as those in the WMA C PA modeling. This well-known behavior is usually attributed to heterogeneity-induced spreading and mixing until the point at which all of the heterogeneity has effectively been "sampled" by the contaminant plume such that dispersion becomes constant. The use of a constant (asymptotic) macrodispersivity is thus considered appropriate in PA simulations (NUREG/CR-6114, *Auxiliary Analyses in Support of Performance Assessment of a Hypothetical Low-Level Waste Facility: Groundwater Flow and Transport Simulation*, Vol. 3; NUREG/CR-5965, *Modeling Field Scale Unsaturated Flow and Transport Processes*).

Figure B-25. Calculated Macroscopic Anisotropy as a Function of Mean Matric Potential for Backfill Gravelly Unit.

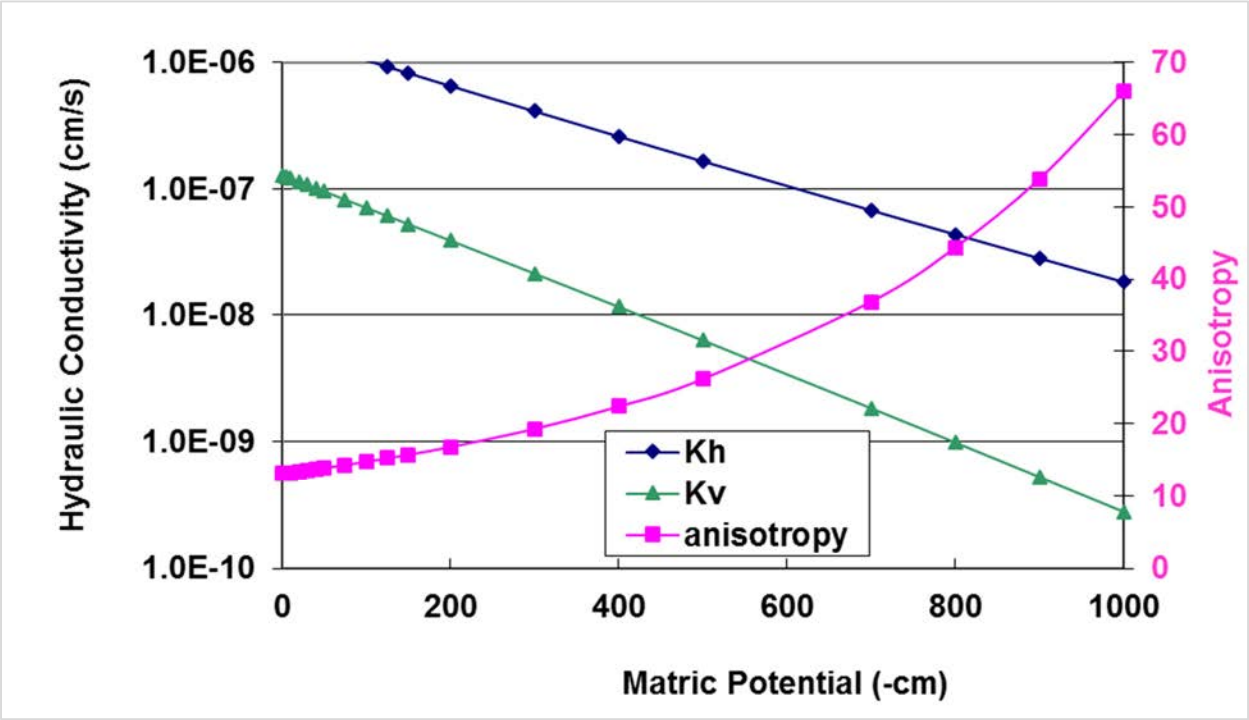

Table B-10. Effective Bulk Density (g/cm3) Estimates for Waste Management Area C Hydrostratigraphic Units.

Hydrostratigraphic Unit	E[ρ_b]*
Backfill Gravelly Unit	2.13
Hanford H2 Sand-dominated Unit	1.71
Hanford H1 and H3 Gravelly Units	2.05

*E = Expectation.

Note that, because of the relatively dry moisture regime, unsaturated media macrosdispersivity estimates are expected to be smaller, compared to saturated media estimates. Below, a range of estimates on the basis of numerical simulations (Section B.4.3.1), stochastic theory (Section B.4.3.2) and experimental observations (Section B.4.3.3) is provided. To obtain macrodispersivity, the local pore-scale dispersivities, which are typically small (<1 cm), are not included either in numerical simulations or stochastic solutions. This is consistent with the approach used by other investigators ("Stochastic analysis of adsorbing solute transport in three-dimensional, heterogeneous, unsaturated soils" [Yang et al. 1997]; Gelhar 1993; "Three-Dimensional Stochastic Analysis of Macrodispersion in Aquifers" [Gelhar and Axness 1983]).

B.4.3.1 Numerical Simulations. Details of the numerical simulation approach are described in Khaleel et al. (2002). Briefly, Monte Carlo (MC) simulations are used to obtain upscaled (effective) properties. The simulations mimic steady state, gravity infiltration for 50 realizations in two-dimensional (20 m × 20 m) heterogeneous flow regions. Constitutive relations for unsaturated media at the mesh-size scale are based on the van Genuchten-Mualem relationships. A realization of the flow field is shown in Figure B-26. The sediment properties are based on laboratory measurements of moisture retention and unsaturated *K* for coarse-textured sandy samples from the upper Hanford formation (HNF-4769, *Far-Field Hydrology Data Package for Immobilized Low-Activity Tank Waste Performance Assessment*); these data show somewhat less variability when compared to the 44 Hanford formation H2 samples discussed earlier. A unit mean-gradient approach is used to derive upscaled properties for flow perpendicular to bedding. For a specified infiltration rate, the simulated pressure head distributions for 50 realizations are averaged to yield a mean pressure head, H. Because the simulated flow field is under a unit mean gradient condition, the infiltration rate is equal to the effective conductivity at the calculated H.

Figure B-26. (a) Ks, (b) α, and (c) n Random Distribution for a Single Realization.

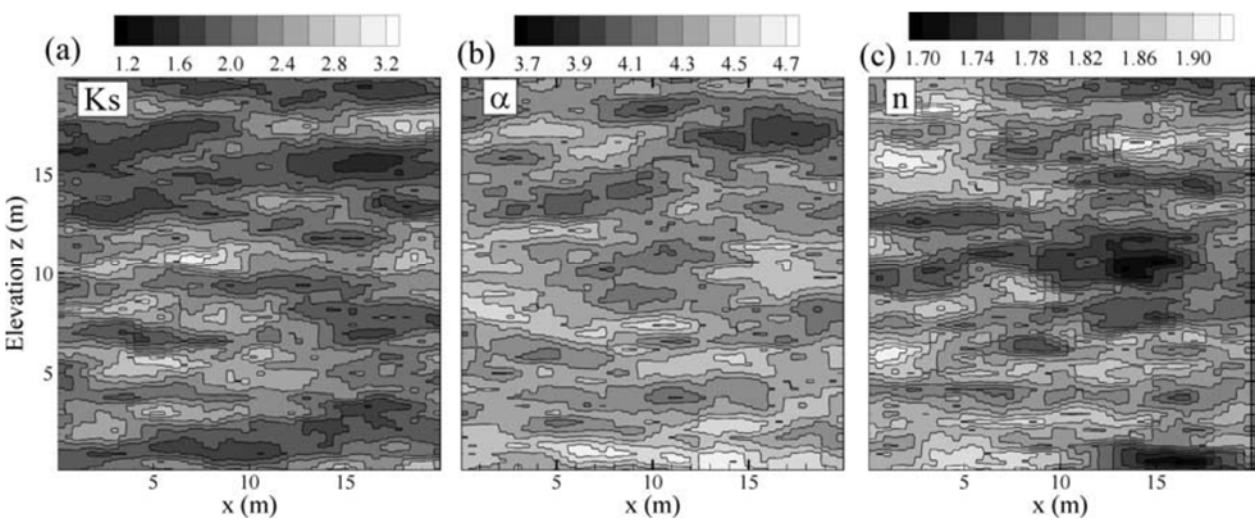

Reference: "Upscaled Flow and Transport Properties for Heterogeneous Unsaturated Media" (Khaleel et al. 2002).

Following flow simulations, macrodispersivities are calculated on the basis of spatial moments of the ensemble-mean plume (Khaleel et al. 2002). For a given steady flow and a prescribed flux, the migration and spread of a slug of simulated tracer is simulated. Snapshots are taken of the two dimensional plume distribution at different times. The snapshot at each sampling time is then averaged over the length across the flow domain to obtain the solute concentration profiles as a function of depth. The concentration profiles for all realizations are averaged to obtain the ensemble mean profile; these profiles are then used to evaluate their spatial moments. The calculated second spatial moment of the plume about the center of mass (i.e., spatial variance) over time allows estimation of the longitudinal macrodispersivity.

Figures B-27a, B-27b and B-27c are snapshots, for a mean pressure head of -1.0 m, of the simulated plume for a single realization and for flow perpendicular to bedding at 400, 700, and 1,000 days after simulating the release of a conservative tracer across the top boundary of a

mildly heterogeneous media (Figure B-26). The averaged concentration profiles for the flow regime and for the corresponding sampling times are illustrated in Figure B-27d. Bedding perpendicular to flow direction enhances lateral mixing and prevents growth of irregular flow paths. Consequently, the averaged concentration profiles for flow perpendicular to bedding (Figure B-27d) exhibit the typical bell-shaped distribution as described by the classical Fickian advection-dispersion equation. The computed longitudinal macrodispersivity for a mean pressure head (H) of -2 m was ~25 cm, ranging from ~15 cm to ~40 cm for the 50 realizations. On the other hand, for a mean H of -20 m, the macrodispersivity was ~100 cm, ranging from ~70 cm to ~130 cm for the 50 realizations. As the MC simulations indicate, considerable variability in longitudinal macrodispersivity estimates is expected depending on the mean matric potential. Nonetheless, results show a clear dependence of longitudinal macrodispersivity on the moisture regime; longitudinal macrodispersivity estimates are higher for the drier moisture regime.

To evaluate directional dependence, simulations were also run for flow parallel to geologic bedding for the same flow domain. Figures B-28a, B-28b, and B-28c are snapshots of the plume at identical times for flow parallel to bedding for the same realization and for H=-1 m; Figure B-28d shows the averaged profile. A comparison of Figures B-27 and B-28 shows that the two-dimensional concentration distribution is more irregular in case of flow parallel to bedding than for flow perpendicular to bedding (Figures B-28a, B-28b, and B-28c versus Figures B-27a, B-27b, and B-27c). Compared with flow perpendicular to bedding, the concentration profiles for flow parallel to bedding are highly skewed and characterized by multiple peaks, and spread out over greater distances, characteristics of a non-Fickian behavior. Thus, while the averaged concentration profiles for flow perpendicular to bedding show “textbook like” Fickian behavior, the averaged profiles for flow parallel to bedding are highly skewed and non-Fickian. At H=-2 m, the computed longitudinal macrodispersivity for flow parallel to bedding is considerably higher (~120 cm) than for flow perpendicular to bedding (~25 cm). For a mean H of -20 m, the macrodispersivity is ~180 cm for flow parallel to bedding versus ~100 cm for flow perpendicular to bedding.

In summary, the numerical results for Hanford H2 sands having mild heterogeneity (HNF-4769) show that the longitudinal dispersivities for flow parallel to bedding are higher than those for flow perpendicular to bedding (Khaleel et al. 2002). For both perpendicular and parallel to bedding, macrodispersivities increase as the mean matric potential becomes more negative. However, the Fickian regime is reached much earlier for cases with flow perpendicular to bedding than parallel to bedding (Khaleel et al. 2002). For WMA C PA modeling, the flow is mostly perpendicular to geologic bedding; nonetheless, the preceding analysis provides estimates in situations where the flow is not necessarily perpendicular to bedding.

B.4.3.2 Stochastic Models. For unsaturated media, in addition to the size of flow domain and media heterogeneities, macrodispersivities are expected to be a function of soil moisture content (or matric potential). Furthermore, as demonstrated via preceding MC simulations, macrodispersivities are larger for flow parallel to bedding than for flow perpendicular to bedding. The following describes two stochastic models to estimate WMA C longitudinal macrodispersivities for flow perpendicular to the geologic bedding.

Figure B-27. Simulated Concentration Distribution for a Single Realization at (a) 400 days, (b) 700 days, and (c) 1,000 days and (d) the Averaged Concentration Profile at Those Times for Flow Perpendicular to Bedding for a Mean Pressure Head (H) of -1 m.

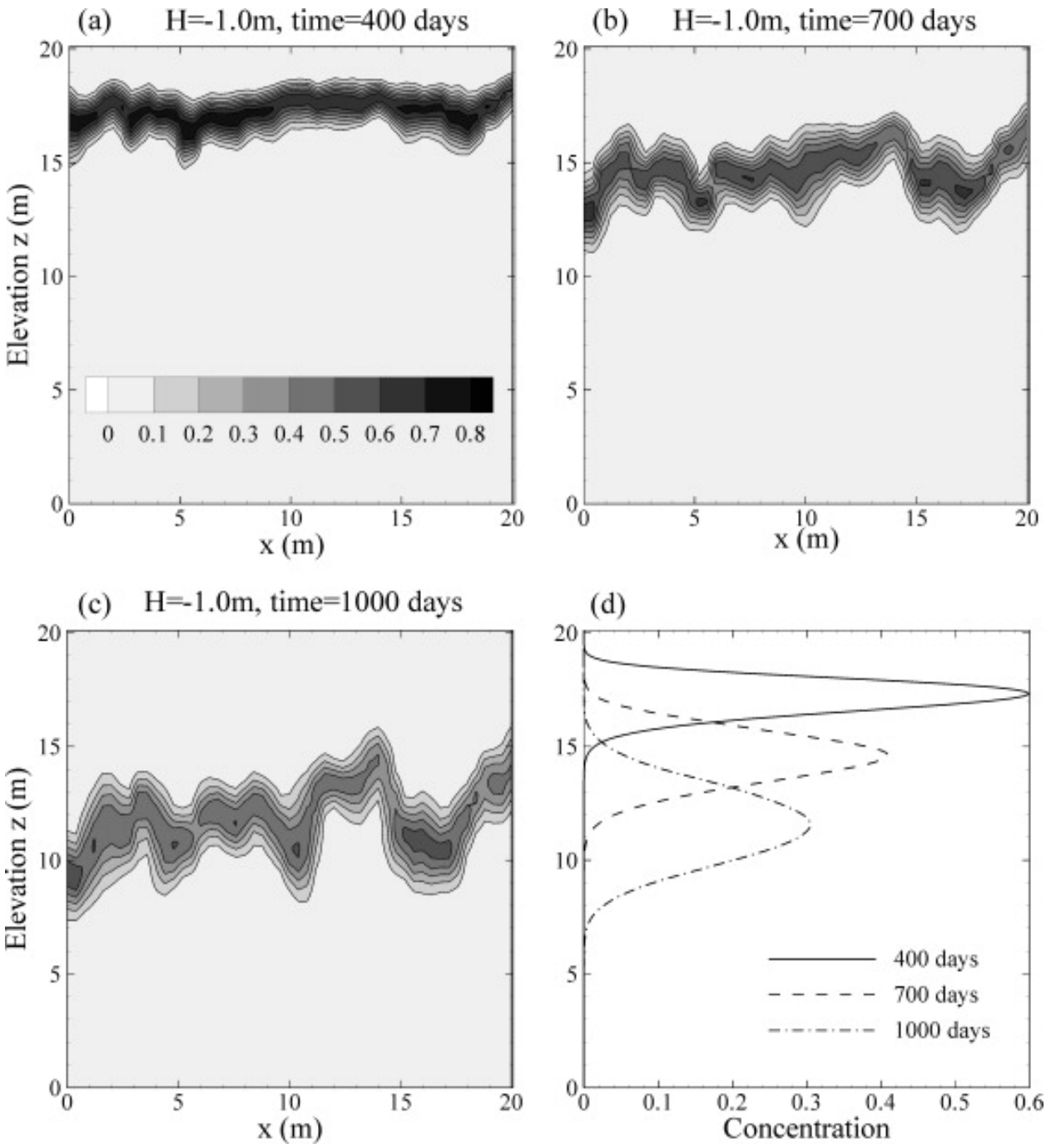

Reference: "Upscaled Flow and Transport Properties for Heterogeneous Unsaturated Media" (Khaleel et al. 2002).

B.4.3.2.1 Mantoglou Model. Using spectral perturbation techniques (Gelhar and Axness 1983; Gelhar 1993), an approximate equation was derived for macrodispersivities in unsaturated media for flow perpendicular to bedding (Large-Scale Models of Transient Unsaturated Flow

and Contaminant Transport Using Stochastic Methods [Mantoglou 1984]). Mantoglou showed that the asymptotic value of tension-dependent longitudinal macrodispersivity, $A_{\perp}$ under unit mean gradient condition, for flow perpendicular to bedding, is

$$A_{\perp}(H) = \frac{\sigma^2_{LnK_u}\lambda_u}{\gamma^2} \tag{B-5}$$

where $A_{\perp}$ depends on the mean pressure head *H*, σ^2_{LnKu} is the variance in log unsaturated *K*, λ_u is the correlation length scale for unsaturated hydraulic conductivity, and γ is a flow factor that depends on the direction of mean flow and the orientation of heterogeneity (Gelhar and Axness 1983).

Equation B-5 represents the asymptotic macrodispersivity estimate for steady-state uniform flow with uniform mean tension. Because macrodispersivity modeled by Equation B-5 is an asymptotic parameter, it applies only when the concentration plume has traveled a large distance in a geologic unit and has encountered numerous heterogeneities in the formation. Furthermore, it is important to note that similar to other stochastic perturbation approaches (Gelhar 1993), the validity of Equation B-5 relies on the variance of hydraulic properties being relatively small (i.e., $\sigma^2_{LnKu} < 1$).

Mantoglou (1985; Figure 5.9) presents longitudinal macrodispersivity estimates, based on Equation B-5, for Maddock sandy loam ("Spatial Variability of in Situ Unsaturated Hydraulic Conductivity of Maddock Sandy Loam" [Carvallo et al. 1976]) and Panoche silty clay loam ("Spatial Variability of Field-Measured Soil-Water Properties" [Nielsen et al. 1973]) soil types. Mantoglou results show considerable variability even for mild tensions. Based on the Mantoglou model (Equation B-5), for Maddock soil type, the asymptotic longitudinal macrodispersivity was 2.4 m at a mean tension of 50 cm. For Panoche soil type, the estimate was 0.8 m at a mean tension of 300 cm.

B.4.3.2.2 Russo Model. Using the Lagrangian framework in conjunction with the Yeh et al (1985) velocity covariance, theoretical expressions were developed for evolution of contaminant plume spatial moments in unsaturated heterogenous media under steady-state conditions ("Stochastic Analysis of Simulated Vadose Zone Solute Transport in a Vertical Cross Section of Heterogeneous Soil During Nonsteady Water Flow" [Russo 1991]). The spatial moments were then used to assess the preasymptotic evolution of macrodispersivity.

$$A_{zz}(t) = \sigma^2_{LnK_u}\lambda_u\left\{1 - 3(2\tau)^{-1} - 3(\tau)^{-2}\exp(-\tau) + 3(\tau)^{-3}[1-\exp(-\tau)]\right\} \tag{B-6}$$

where A_{zz} is the longitudinal macrodispersivity (i.e., similar to $A_{\perp}$), *z* denotes vertical direction, *t* is time, λ_u is vertical correlation length, and $\tau = z_c(t)/\lambda_u$. The unsaturated conductivity variance σ^2_{LnKu} was derived by Russo (1991) using the Gardner (1958) exponential model for

unsaturated conductivity. At large times, $\tau \rightarrow \infty$; the longitudinal asymptotic macrodispersivity is therefore

$$A_{zz}(\infty) = \sigma^2_{LnK_u} \lambda_u \,. \tag{B-7}$$

Note that this is the same as Mantoglou Equation B-5 without the flow factor γ in the denominator. For hypothetical vadose zone flow domains having $\sigma^2_{LnK_u}$ = 0.29 and extending 15 m and 10 m in the horizontal and vertical directions, respectively, and a correlation length of 0.12 m in the vertical direction, Russo (1991) computed an asymptotic longitudinal macrodispersivity (Equation B-7) of 3.48 cm. As discussed later, the conductivity variance of 0.29 is, however, much smaller compared to variance for Hanford H2 unsaturated conductivity data.

B.4.3.2.3 Stochastic Theory Based Macrodispersivity Estimates for Waste Management Area C. To apply stochastic Equations B-5 and B-7, an estimate of λ_u for unsaturated K is needed. As discussed earlier, a correlation length of the order of 50 cm was used for saturated conductivity. However, as saturation decreases, an increase in the variance of log unsaturated conductivity is accompanied by a decrease in the correlation scale of log unsaturated K ("Stochastic Modeling of Macrodispersion for Solute Transport in a Heterogeneous Unsaturated Porous Formation" [Russo 1993]). Also, the Equation B-5 flow factor γ (Mantoglou 1984) in a predominantly vertical unsaturated flow through a layered system would be less than 1; it is approximately the ratio of the harmonic and geometric means of unsaturated K (Gelhar 1993; Gelhar and Axness 1983). Assuming a correlation length of 10 cm (approximate measurement scale for small-scale unsaturated K measurements), and γ estimates based on the ratio of the harmonic and geometric means (Khaleel et al. 2002), for H2 sands, Mantoglou's model yields asymptotic macrodispersivity estimates, for flow perpendicular to bedding, that are ~360 cm at relatively low tensions of ~2 m. For the Russo (1991) model (Equation B-7), at ~2 m tension, the asymptotic longitudinal macrodispersivity for H2 sands is ~32 cm. Note that the MC simulations (Khaleel et al. 2002) yielded a longitudinal macrodispersivity of ~25 cm for flow perpendicular to bedding and for H=-2m. However, the favorable comparison with Russo's model is coincidental since σ^2_{LnK} and mean tension values are different.

Reported values have a relatively low tension of 2 m because of the limitation of low perturbation for stochastic models. The variance, σ^2_{LnKu} in Equation B-5 becomes rather large for H2 sands; at a mean tension of 1 m, σ^2_{LnKu} is about 1.96, whereas at a tension of 2 m, σ^2_{LnKu} is about 4.73. Compared to H2 sands, σ^2_{LnKu} for the H1/H3/Backfill gravelly units is significantly lower; at a mean tension of 150 cm, σ^2_{LnKu} is about 1.22, whereas at a mean tension of 400 cm, σ^2_{LnK} is about 2.02. Such variance results are consistent with the unsaturated *K* data reported earlier for sandy and gravelly samples (Figure B-17). Unsaturated *K* for gravelly samples fall within a narrow range, and well within the range of measured *K* for sandy samples. At a matric potential of -1 m, the unsaturated *K* for sandy samples ranges over 4 order of

magnitudes, whereas the unsaturated *K* for gravelly samples ranges over 2 order of magnitudes (Figure B-17).

Figure B-28. Simulated Concentration Distribution for a Single Realization at (a) 400 days, (b) 700 days, and (c) 1,000 days and (d) the Averaged Concentration Profile at Those Times for Flow Parallel to Bedding for a Mean Pressure Head (H) of -1 m.

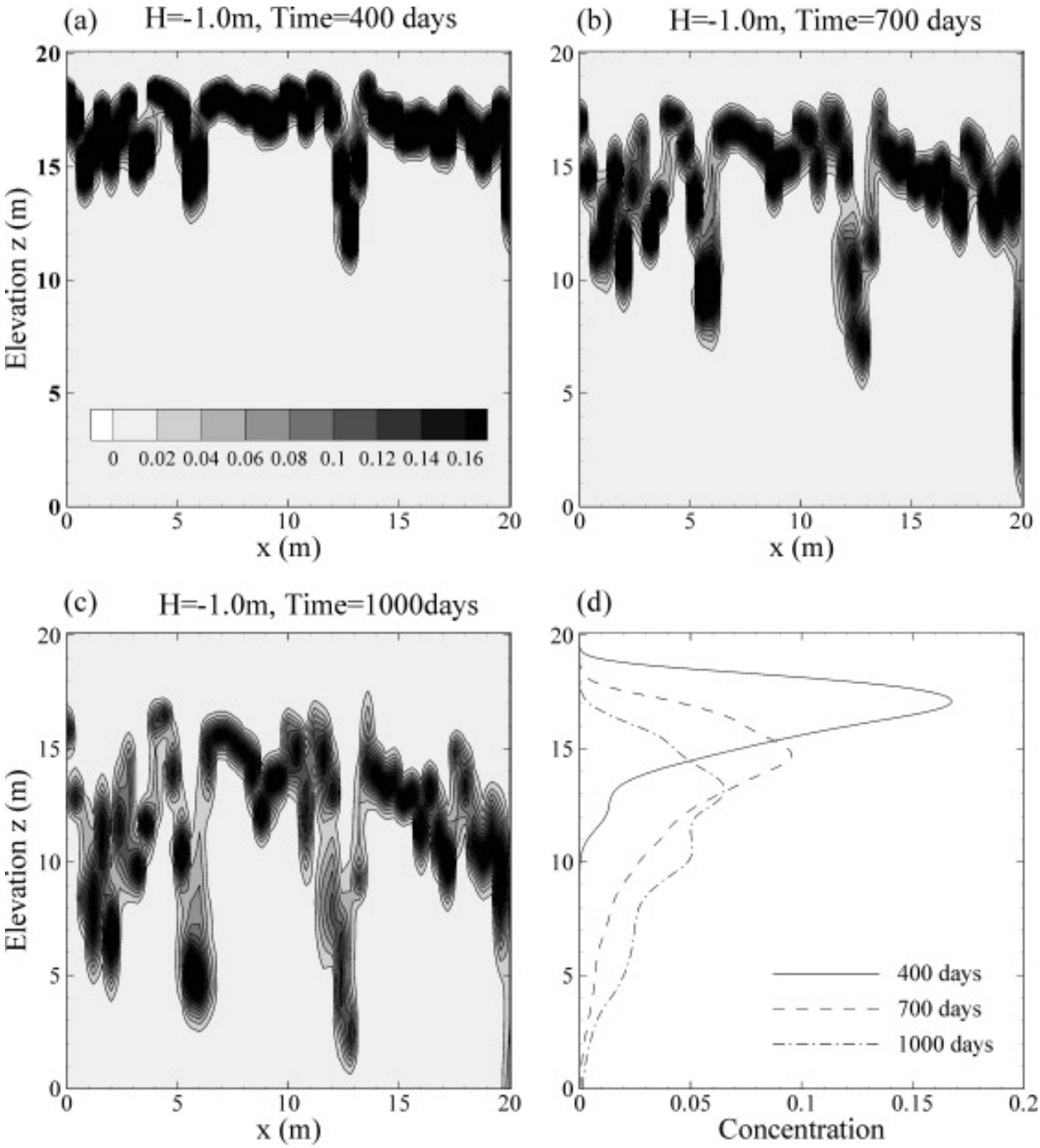

Reference: "Upscaled Flow and Transport Properties for Heterogeneous Unsaturated Media" (after Khaleel et al. 2002).

B.4.3.3 Experimental Data from 200 Areas and Other Sites. Field experiments were conducted at a location in 200 East Area, using potassium chloride as a tracer (RPP-20621 Appendix E, "Hanford Low-Activity Tank Waste Performance Assessment Activity: Determination of in Situ Hydraulic Parameters of the Upper Hanford Formation"). Analysis of the data, using moment analysis, provided dispersivities that ranged from 1.3 cm to 7.8 cm for travel distances ranging from 25 cm to 125 cm. Although these estimates are for the Hanford formation, the transport distance within the vadose zone is indeed of limited extent. Nonetheless, results based on the limited data are consistent with the concept of a scale-dependent dispersivity; it is expected that the asymptotic value will be larger than those based on the small-scale tracer experiment. In fact, extrapolation of the trend line for the data (RPP-20621 Appendix E) suggests that an asymptotic dispersivity estimate of ~1 m is not unlikely if the heterogeneity at the field site is similar to that of the sandy sediments underlying C Farm, and if the entire sandy sequence of the Hanford formation is treated as EHM.

In addition to preceding data, results of artificial tracer experiments are available from several arid/semi-arid regions. Two massively instrumented solute transport experiments were performed in desert soils near Las Cruces, New Mexico ("The Las Cruces Trench Site: Characterization, Experimental Results, and One-Dimensional Flow Predictions" [Wierenga et al. 1991]; "The Second Las Cruces Trench Experiment: Experimental Results and Two-Dimensional Flow Predictions" [Hills et al. 1991]). Drip emitters were used to irrigate a plot adjoining a deep trench in heterogeneous media, with well in excess of one order of magnitude standard deviation in saturated hydraulic conductivity. Monitoring of the trench face showed a spatially uniform progression of the wetting front and did not reveal indications of preferential flow (Wierenga et al. 1991). Hills et al. (1991) found that a dispersivity of 5 cm provided reasonably realistic simulations of tritium and bromine tracer distributions.

One additional study ("Chlorine 36 and Tritium From Nuclear Weapons Fallout as Tracers for Long-Term Liquid and Vapor Movement in Desert Soils" [Phillips et al. 1988]) assessed the degree of mixing in desert soils using the conventional advection-dispersion modeling, yielding a dispersion coefficient of 50 cm^2/yr. This compares with the calculated effective diffusion coefficient of 25 cm^2/yr. A similar study ("Evaluation of Liquid and Vapor Water Flow in Desert Soils Based on Chlorine 36 and Tritium Tracers and Nonisothermal Flow Simulations" [Scanlon 1992]) at another southwestern arid site obtained a dispersion coefficient of about 14 cm^2/yr. These, then, lead to effective dispersivities of about 7 cm and 4 cm at the two arid sites, and Peclet numbers (displacement divided by dispersivity) of 23 and 17. In summary, long-term environmental tracer studies at several arid southwestern sites indicate vadose zone dispersivities being less than 10 cm.

Based on a different survey of literature, Gelhar (1993) presented the longitudinal vadose zone dispersivities as a function of the scale of the experiment (Figure B-29). The figure shows sparse data for scales larger than 2 m. Nonetheless, similar to saturated flow (Gelhar et al. 1992), Figure B-29 shows an increase of dispersivity with an increase in scale. Also, shown in Figure B-29 are results of the 200 East Area field experiment (RPP-20621 Appendix E); the trend line dispersivity estimate at a field scale of ~10 m is in close agreement with "Field Scale Transport of Bromide in an Unsaturated Soil, 2. Dispersion Modeling" (Butters and Jury 1989) field data.

Figure B-29. Longitudinal Laboratory- and Field-Scale Dispersivities in Unsaturated Media as a Function of Overall Problem Scale.

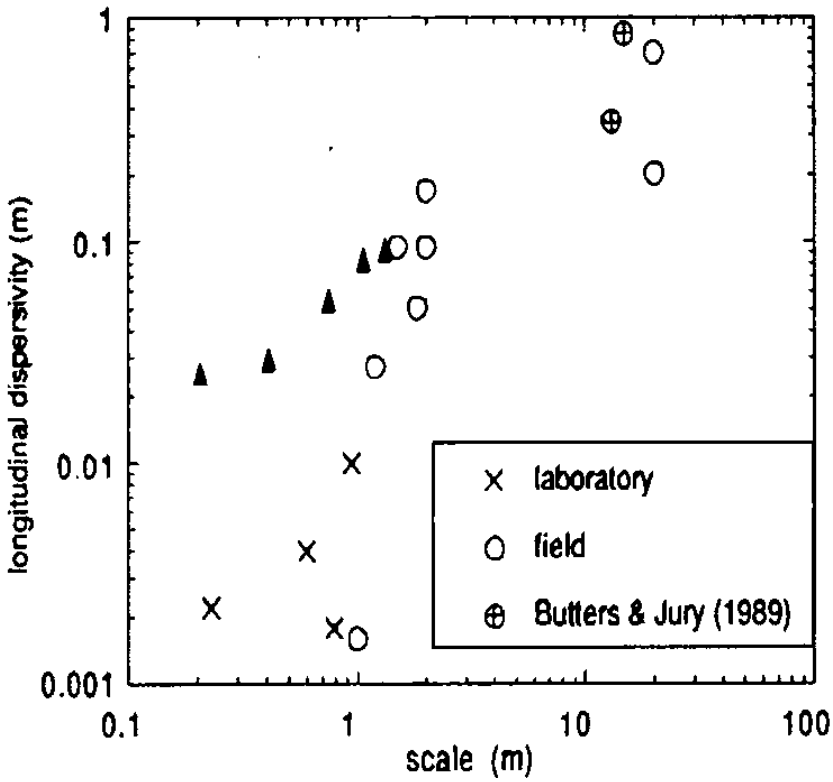

Note: The triangles are data from RPP-20621, *Far-Field Hydrology Data Package for the Integrated Disposal Facility Performance Assessment*, Appendix E, "Hanford Low-Activity Tank Waste Performance Assessment Activity: Determination of In Situ Hydraulic Parameters of the Upper Hanford Formation."

References:
"Field Scale Transport of Bromide in an Unsaturated Soil, 2. Dispersion Modeling" (Butters and Jury 1989).
Stochastic Subsurface Hydrology (Gelhar 1993).

B.4.3.4 Recommended Macrodispersivities for Waste Management Area C Performance Assessment. Table B-11 summarizes the macrodispersivity estimates based on results of numerical simulation, stochastic theory, and 200 Areas experimental data. Table B-11 shows that, for H2 sands, estimates are available by all three methods. For the H2 sand unit, for the PA modeling, the recommendation is to use longitudinal macrodispersivity values ranging from 25 cm (based on numerical simulations) to 100 cm (based on field experiments). For H1/H3/Backfill sediments, the recommendation is to use, based on stochastic theory, longitudinal macrodispersivity values range from 20 cm to 100 cm. The transverse macrodispersivity is typically much lower; in saturated media, it may range from 1 to 10% of the longitudinal macrodispersivity (Gelhar and Axness 1983). In the absence of unsaturated media experimental data, the recommendation is to use a transverse macrodispersivity 1/10th of the longitudinal macrodispersivity. This value appears to be consistent with the measured ^{99}Tc data collected from wells near WMA C.

Table B-11. Longitudinal Macrodispersivity Estimates (cm).

Hydrostratigraphic Unit	Numerical Simulation	Stochastic Theory (Russo and Mantoglou Equations 5 and 7)	200 Area Field Experiments
H2 Sand-Dominated Unit	25	~32[a] – 360[a]	~100[c]
H1, H3, and Backfill Gravelly Units	NA	~20[b] – 100[b]	NA

[a]Evaluated at a mean tension of 2 m.

[b]Evaluated at a mean tension of 4 m.

[c]Extrapolated experimental data (RPP-20621, *Far-Field Hydrology Data Package for the Integrated Disposal Facility Performance Assessment*, Appendix E, "Hanford Low-Activity Tank Waste Performance Assessment Activity: Determination of In Situ Hydraulic Parameters of the Upper Hanford Formation").

NA = Not Available

References:
Large-Scale Models of Transient Unsaturated Flow and Contaminant Transport Using Stochastic Methods (Mantoglou 1984).
"Stochastic Analysis of Simulated Vadose Zone Solute Transport in a Vertical Cross Section of Heterogeneous Soil During Nonsteady Water Flow" (Russo 1991).

B.5 REFERENCES

Butters, G. L., and W. A. Jury, 1989, "Field Scale Transport of Bromide in an Unsaturated Soil, 2. Dispersion Modeling," *Water Resources Research*, Vol. 25, No. 7, pp. 1583–1589.

Carvallo, H. O., D. K. Cassel, J. Hammond, and A. Bauer, 1976, "Spatial Variability of in Situ Unsaturated Hydraulic Conductivity of Maddock Sandy Loam," *Soil Science*, Vol. 121, pp. 1–8.

Eching, S. O. and J. W. Hopmans, 1993, "Optimization of Hydraulic Functions from Transient Outflow and Soil Water Pressure Data," *Soil Science Society of America Journal*, Vol. 57, No. 5, pp. 1167–1175.

EPA/600/2-91/065, 1991, *The RETC Code for Quantifying the Hydraulic Functions of Unsaturated Soils*, Office of Research and Development, U.S. Environmental Protection Agency, Washington, D.C.

Gardner, W. H., 1986, "Water Content," in Methods of Soils Analysis, Part 1—Physical and Mineralogical Methods, pp. 493–544, *American Society of Agronomy-Soil Science Society of America*, Madison, Wisconsin.

Gardner, W. R., 1958, "Some Steady-State Solutions of the Unsaturated Moisture Flow Equation with Application to Evaporation from a Water Table," *Soil Science*, Vol. 85, No. 4, pp. 228–232.

Gelhar, L. W., 1993, Stochastic Subsurface Hydrology, Prentice Hall, New York, New York.

Gelhar, L. W. and C. L. Axness, 1983, "Three-Dimensional Stochastic Analysis of Macrodispersion in Aquifers," *Water Resources Research*, Vol. 19, No. 1, pp. 161–180.

Gelhar, L. W., C. Welty, and K. R. Rehfeldt, 1992, "A Critical Review of Data on Field-Scale Dispersion in Aquifers," *Water Resources Research*, Vol. 28, No. 7, pp. 1955–1974.

HNF-4769, 1999, *Far-Field Hydrology Data Package for Immobilized Low-Activity Tank Waste Performance Assessment*, Rev. 1, Fluor Daniel Northwest, Richland, Washington.

Hills, R. G., P. J. Wierenga, D. B. Hudson, and M. R. Kirkland, 1991, "The Second Las Cruces Trench Experiment: Experimental Results and Two-Dimensional Flow Predictions," *Water Resources Research*, Vol. 27, No. 10, pp. 2707–2718.

Jury, W. A. and R. Horton, 2004, Soil Physics, 6th edition, Wiley and Sons, Inc., New York, New York.

Khaleel, R. and J. F. Relyea, 1997, "Correcting laboratory-measured moisture retention data for gravels," *Water Resources Research*, Vol. 33, No. 8, pp. 1875–1878.

Khaleel, R. and J. F. Relyea, 2001, "Variability of Gardner's α for coarse-textured sediments," *Water Resources Research*, Vol. 37, No. 6, pp. 1567–1575.

Khaleel, R., J. F. Relyea and J. L. Conca, 1995, "Evaluation of van Genuchten-Mualem relationships to estimate unsaturated hydraulic conductivity at low water contents," *Water Resources Research*, Vol. 31, No. 11, pp. 2659–2668.

Khaleel, R., T.-C. J. Yeh, and Z. Lu, 2002, "Upscaled Flow and Transport Properties for Heterogeneous Unsaturated Media," *Water Resources Research*, Vol. 38, No. 5, pp. 11.1–11.12.

Klute, A., 1986, "Water Retention: Laboratory Methods," in Methods of Soil Analysis, Part 1—Physical and Mineralogical Methods, pp. 635–660, *American Society of Agronomy-Soil Science Society of America*, Madison, Wisconsin.

Klute, A. and C. Dirksen, 1986, "Hydraulic Conductivity and Diffusivity: Laboratory Methods," in Methods of Soil Analysis, Part 1—Physical and Mineralogical Methods, pp. 687–734, *American Society of Agronomy-Soil Science Society of America*, Madison, Wisconsin.

Mantoglou, A., 1984, Large-Scale Models of Transient Unsaturated Flow and Contaminant Transport Using Stochastic Methods, Ph.D. Thesis, Massachusetts Institute of Technology, Department of Civil Engineering, Cambridge, Massachusetts.

Mantoglou, A. and L. W. Gelhar, 1987, "Stochastic Modeling of Large-Scale Transient Unsaturated Flow Systems," *Water Resources Research*, Vol. 23, No. 1, pp. 37–46.

McCord, J. T., D. B. Stephens, and J. L. Wilson, 1991, "Hysteresis and State-Dependent Anisotropy in Modeling Unsaturated Hillslope Hydrologic Processes," *Water Resources Research*, Vol. 27, No. 7, pp. 1501–1518.

Millington, R. J. and J. P. Quirk, 1961, "Permeability of Porous Solids," *Transactions of the Faraday Society*, Vol. 57, pp. 1200–1207.

Mualem, Y., 1976, "A New Model for Predicting the Hydraulic Conductivity of Unsaturated Porous Media," *Water Resources Research*, Vol. 12, No. 3, pp. 513–522.

Nielsen, D. R., J. M. Biggar, and K. T. Erh, 1973, "Spatial Variability of Field-Measured Soil-Water Properties," *Hilgardia*, Vol. 42, No. 7, pp. 215–260.

NUREG/CR-5965, 1994, *Modeling Field Scale Unsaturated Flow and Transport Processes*, Nuclear Regulatory Commission, Washington, D.C.

NUREG/CR-6114, 1994, *Auxiliary Analyses in Support of Performance Assessment of a Hypothetical Low-Level Waste Facility: Groundwater Flow and Transport Simulation*, Vol. 3, U.S. Nuclear Regulatory Commission, Washington, D.C.

Phillips, F. M., J. L. Mattick, T. A. Duval, D. Elmore, and P. W. Kubik, 1988, "Chlorine 36 and Tritium From Nuclear Weapons Fallout as Tracers for Long-Term Liquid and Vapor Movement in Desert Soils," *Water Resources Research*, Vol. 24, No. 11, pp. 1877–1891.

PNNL-13795, 2000, *Vadose Zone Transport Field Study: Soil Water Content Distributions by Neutron Moderation*, Pacific Northwest National Laboratory, Richland, Washington.

PNNL-14284, 2003, *Laboratory Measurements of the Unsaturated Hydraulic Properties at the Vadose Zone Transport Field Site*, Pacific Northwest National Laboratory, Richland, Washington.

PNNL-15503, 2008, *Characterization of Vadose Zone Sediments Below the C Tank Farm: Borehole C4297 and RCRA Borehole 299-E27-22*, Rev. 1, Pacific Northwest National Laboratory, Richland, Washington.

PNNL-17154, 2008, *Geochemical Characterization Data Package for the Vadose Zone in the Single-Shell Tank Waste Management Areas at the Hanford Site*, Pacific Northwest National Laboratory, Richland, Washington.

Polmann, D. J., 1990, Application of Stochastic Methods to Transient Flow and Transport in Heterogeneous Unsaturated Soils, Ph.D. Thesis, Massachusetts Institute of Technology, Department of Civil Engineering, Cambridge, Massachusetts.

Resource Conservation and Recovery Act of 1976, 42 USC 6901, et seq.

RHO-ST-46P, 1984, *Field Calibration of Computer Models for Application to Buried Liquid Discharges: A Status Report*, Rockwell Hanford Operations, Richland, Washington.

RPP-20621, 2004, *Far-Field Hydrology Data Package for the Integrated Disposal Facility Performance Assessment*, Rev. 0, CH2M HILL Hanford Group, Inc., Richland, Washington.

RPP-20621, 2004, *Far-Field Hydrology Data Package for the Integrated Disposal Facility Performance Assessment*, Appendix E, "Hanford Low-Activity Tank Waste Performance Assessment Activity: Determination of In Situ Hydraulic Parameters of the Upper Hanford Formation," Rev. 0, CH2M HILL Hanford Group, Inc., Richland, Washington.

RPP-CALC-60450, 2016, *Process for Determining the Volumetric Moisture Content for the Vadose Zone Geologic Units Underlying Waste Management Area*, Rev. 0, Washington River Protection Solutions, LLC, Richland, Washington.

RPP-CALC-60452, 2016, *Moisture Dependent Anisotropy Calculations Supporting WMA C PA*, Rev. 0, Washington River Protection Solutions, LLC, Richland, Washington.

Russo, D., 1991, "Stochastic Analysis of Simulated Vadose Zone Solute Transport in a Vertical Cross Section of Heterogeneous Soil During Nonsteady Water Flow," *Water Resources Research*, Vol. 27, No. 3, pp. 267–283.

Russo, D., 1993, "Stochastic Modeling of Macrodispersion for Solute Transport in a Heterogeneous Unsaturated Porous Formation," *Water Resources Research*, Vol. 29, No. 2, pp. 383–397.

Scanlon, B. R., 1992, "Evaluation of Liquid and Vapor Water Flow in Desert Soils Based on Chlorine 36 and Tritium Tracers and Nonisothermal Flow Simulations," *Water Resources Research*, Vol. 28, No. 1, pp. 285–297.

Stephens, D. B., and S. Heermann, 1988, "Dependence of Anisotropy on Saturation in a Stratified Sand," *Water Resources Research*, Vol. 24, No. 5, pp. 770–778.

van Genuchten, M. Th., 1980, "A Closed-form Equation for Predicting the Hydraulic Conductivity of Unsaturated Soils," *Soil Science Society of America Journal*, Vol. 44, No. 5, pp. 892–898.

WHC-IP-0635, 1991, *Geotechnical Engineering Procedure Manual*, Vols. 1 and 2, Westinghouse Hanford Company, Richland, Washington.

WHC-SD-WM-EE-004, 1995, *Performance Assessment of Grouted Double-Shell Tank Waste Disposal at Hanford*, Rev. 1, Westinghouse Hanford Company, Richland, Washington.

Wierenga, P. J., R. G. Hills, and D. B. Hudson, 1991, "The Las Cruces Trench Site: Characterization, Experimental Results, and One-Dimensional Flow Predictions," *Water Resources Research*, Vol. 27, No. 10, pp. 2695–2705.

Yang, J., R. Zhang, J. Wu, and M. B. Allen, 1997, "Stochastic analysis of adsorbing solute transport in three-dimensional, heterogeneous, unsaturated soils," *Water Resources Research*, Vol. 33, No. 3, pp. 1947–1956.

Ye, M., R. Khaleel, and T.-C. J. Yeh, 2005, "Stochastic analysis of moisture plume dynamics of a field injection experiment," *Water Resources Research*, Vol. 41, W03013, pp. 1–13.

Yeh, T.-C. J., and D. J. Harvey, 1990, "Effective Unsaturated Hydraulic Conductivity of Layered Sands," *Water Resources Research*, Vol. 26, No. 6, pp. 1271–1279.

Yeh, T.-C. J., L. W. Gelhar and A. L. Gutjahr, 1985, "Stochastic Analysis of Unsaturated Flow in Heterogeneous Soils, 2. Statistically Anisotropic Media with Variable α," *Water Resources Research*, Vol. 21, No. 4, pp. 457–464.

Yeh, T.-C. J., M. Ye, and R. Khaleel, 2005, "Estimation of effective unsaturated hydraulic conductivity tensor using spatial moments of observed moisture plume," *Water Resources Research*, Vol. 41, W03014, pp. 1–12.

Zhang, Z. F. and R. Khaleel, 2010, "Simulating field-scale moisture flow using a combined power-averaging and tensorial connectivity-tortuosity approach," *Water Resources Research*, Vol. 46, W09505, pp. 1–14.

This page intentionally left blank.

APPENDIX C

TECHNICAL BASIS FOR WASTE MANAGEMENT AREA C UNCONFINED AQUIFER CONCEPTUAL MODEL: FIELD DATA AND RELATED INVESTIGATIONS

This page intentionally left blank.

TABLE OF CONTENTS

APPENDIX C – TECHNICAL BASIS FOR WASTE MANAGEMENT AREA C UNCONFINED AQUIFER CONCEPTUAL MODEL: FIELD DATA AND RELATED INVESTIGATIONS C-1

C.1 HIERARCHY OF LENGTH SCALES AND SCALE DEPENDENCE OF MEDIA PROPERTIES C-2

C.2 HYDROGEOLOGIC CONDITIONS AND STRUCTURE C-3

C.2.1 Paleochannel Configuration and Flow Paths C-4

C.2.2 Theoretical Basis for Hydraulic Conductivity Estimates of Paleochannel Sediments C-6

C.3 ESTIMATES OF UNCONFINED AQUIFER FLOW AND TRANSPORT PROPERTIES C-7

C.3.1 Groundwater Flow Velocities and Fluxes C-7

C.3.2 Hydraulic Conductivity of Unconfined Aquifer Sediments C-8

C.3.3 Groundwater Flow Directions and Hydraulic Gradients C-12

C.3.4 Anisotropy C-13

C.3.5 Properties for Contaminant Transport C-13

C.4 UNCONFINED AQUIFER FLOW AND TRANSPORT PROPERTIES USED IN THE WASTE MANAGEMENT AREA C PERFORMANCE ASSESSMENT C-16

C.4.1 Flow Properties C-18

C.4.2 Contaminant Transport Properties C-20

C.5 DEVELOPMENT OF UNCERTAINTY IN GROUNDWATER FLUX AND MACRODISPERSIVITY FOR SATURATED ZONE C-21

C.6 REFERENCES C-25

LIST OF FIGURES

Figure C-1. Schematic Illustrating Scale in a Heterogeneous Media and Scale Dependence of Saturated Hydraulic Conductivity. C-2

Figure C-2. Interpreted Extent of a Paleochannel Associated with the Ancestral Columbia River in 200 East Area in the Vicinity of Waste Management Area C. C-5

Figure C-3. Digital Photo Log for Borehole 299-E27-4 with an Expansion Showing the Open Framework Gravel below the Water Table. C-9

Figure C-4. (a) An Idealized Hexagonal Model Approximation of Open-Framework Gravelly Media, and (b) Representative Flow Regions Used to Determine Equivalent Hydraulic Conductivity. C-10

Figure C-5. Plan View of the Central Plateau Groundwater Model Representing the Aquifer and the Volumetric Flux Calculation Window in the Vicinity of Waste Management Area C. C-14

Figure C-6. Hanford Formation Saturated Hydraulic Conductivity Estimates Based on Slug Tests, Pump Tests, and Model Calibration. C-15

Figure C-7. Borehole Log of Well 299-E27-22. ..... C-17

Figure C-8. Pacific Northwest National Laboratory Sitewide Model Calibration of Hydraulic Conductivity of the Unconfined Aquifer with the Location of Waste Management Area C and Magnitude of Hydraulic Conductivity Indicated. C-18

Figure C-9. Central Plateau Groundwater Model Layer Discretization In the Saturated Zone and Extent of Various Hydrostratigraphic Units within the Model Layer in the Vicinity of Waste Management Area C (shown by the Rectangle). C-19

Figure C-10. Longitudinal Macrodispersivity in Saturated Media as a Function of Overall Problem Scale with Data Classified by Reliability. C-21

Figure C-11. Central Plateau Groundwater Model Calibration Results in the Vicinity of Waste Management Area C. C-23

Figure C-12. Low-Gradient Low-Level Waste Management Area 1 Monitoring Network Results. C-24

LIST OF TABLES

Table C-1. Calculation of Weighted Average Hydraulic Conductivity Value and Volumetric Water Flux from the Central Plateau Groundwater Model. C-20

Table C-2. Relationship Between Saturated Longitudinal Macrodispersivity (α_L) and Scale of Measurement (L_s). C-22

Table C-3. Triangular Distribution of Aquifer Flux and Proportional Hydraulic Conductivity Values Applicable to the Uncertainty Analysis. C-24

LIST OF TERMS

CCu	Cold Creek unit
CPGWM	Central Plateau Groundwater Model
EHM	equivalent homogeneous medium
FY	fiscal year
HSU	hydrostratigraphic unit
LLWMA	Low-Level Waste Management Area
PA	Performance Assessment
RCRA	*Resource Conservation and Recovery Act of 1976*
STOMP	Subsurface Transport Over Multiple Phases
TC&WM EIS	Tank Closure and Waste Management Environmental Impact Statement
WMA	Waste Management Area

APPENDIX C

TECHNICAL BASIS FOR WASTE MANAGEMENT AREA C UNCONFINED AQUIFER CONCEPTUAL MODEL: FIELD DATA AND RELATED INVESTIGATIONS

The groundwater pathway analysis is an important aspect of the Waste Management Area C (WMA C) Performance Assessment (PA). As the contaminant mass flux arriving from the vadose zone enters the aquifer it mixes with the groundwater and undergoes dilution, dispersion, and retardation while traveling along the flow path. The amount of dilution is strongly dependent on the ratio of volumetric groundwater flux to contaminant mass flux within the mixing zone. However, groundwater flux is not ordinarily a measurable quantity. Instead, it is inferred from hydraulic head measurements and from hydraulic properties of the aquifer (i.e., estimates of the hydraulic gradients and hydraulic conductivities), which are deduced from a variety of measurement methods, such as pump and slug tests, or derived from inverse modeling of the aquifer to estimate conductivity from measured head values.

Past and present measured field data (hydraulic heads) in observation boreholes in the vicinity of WMA C must be used carefully as the region is recovering from the effects of both surface (ponds, cribs, trenches, and ditches) and subsurface (leaking pipelines, leaking tanks, and injection wells) liquid discharges from Hanford operations for many years. Groundwater mounding continues to dissipate to an equilibrium condition that is likely to be similar to the pre-Hanford operations condition (see Section 3.1.5.4.2 and Figure 3-35). As a result, the post-closure position of the water table, and its hydraulic gradient, can only be estimated through evaluating the current water table and forecasting the anticipated changes. Modeling is a critical tool in this evaluation, as it can be used to estimate both the hydraulic gradient and the recovery of hydraulic heads from the operational liquid discharges. Consequently, this analysis uses modeling tools to calculate the future groundwater flux, based on aquifer hydraulic properties and the projected hydraulic gradient.

This appendix provides a detailed assessment and evaluation of saturated media field data used to estimate the aquifer hydraulic properties, including saturated hydraulic conductivity, groundwater fluxes, and hydraulic gradients, and specifies the technical basis for parameter selection and use in the WMA C PA modeling. Included in this assessment/evaluation is the following:

- A brief review of scale dependence of saturated media parameters (Section C.1)
- A brief overview of the hydrogeologic conditions pertinent to WMA C (Section C.2)
- A summary of measured and theoretically estimated aquifer hydraulic parameter estimates available for the areas near WMA C (Section C.3)
- A summary of how this information is used for the PA (Section C.4), including a discussion of the sensitivity and uncertainties of groundwater flux and flow parameters used in the PA (Section C.5).

C.1 HIERARCHY OF LENGTH SCALES AND SCALE DEPENDENCE OF MEDIA PROPERTIES

A variety of methods exist which can be used to estimate hydraulic conductivity, including permeameter cells, slug tests, pump tests, and model calibration. In general, estimates of saturated hydraulic conductivity, either inferred by aquifer testing or determined from calibrated models, tend to increase as the scale of the flow domain increases (e.g., U.S. Geological Survey Water-Supply Paper 2237, *Regional Flow in the Dakota Aquifer: A Study of the Role of Confining Layers*). The evolving heterogeneities at various length scales result in a scale dependence of effective parameters such as saturated hydraulic conductivity ("An Analysis Platform for Multiscale Hydrogeologic Modeling with Emphasis on Hybrid Multiscale Methods" [Scheibe et al. 2015]). For WMA C PA saturated media modeling, the flow domain size of interest is shown on the right side of Figure C-1, with the characteristic length scale for flow and transport on the order of hundred meters. As the length scale of observation increases, the effective properties increase in discretely hierarchical stages or evolve continuously (Scheibe et al. 2015). The effects of large-scale heterogeneity on flow and determination of media properties can therefore be inferred most effectively by using regional scale groundwater models.

Figure C-1. Schematic Illustrating Scale in a Heterogeneous Media and Scale Dependence of Saturated Hydraulic Conductivity.

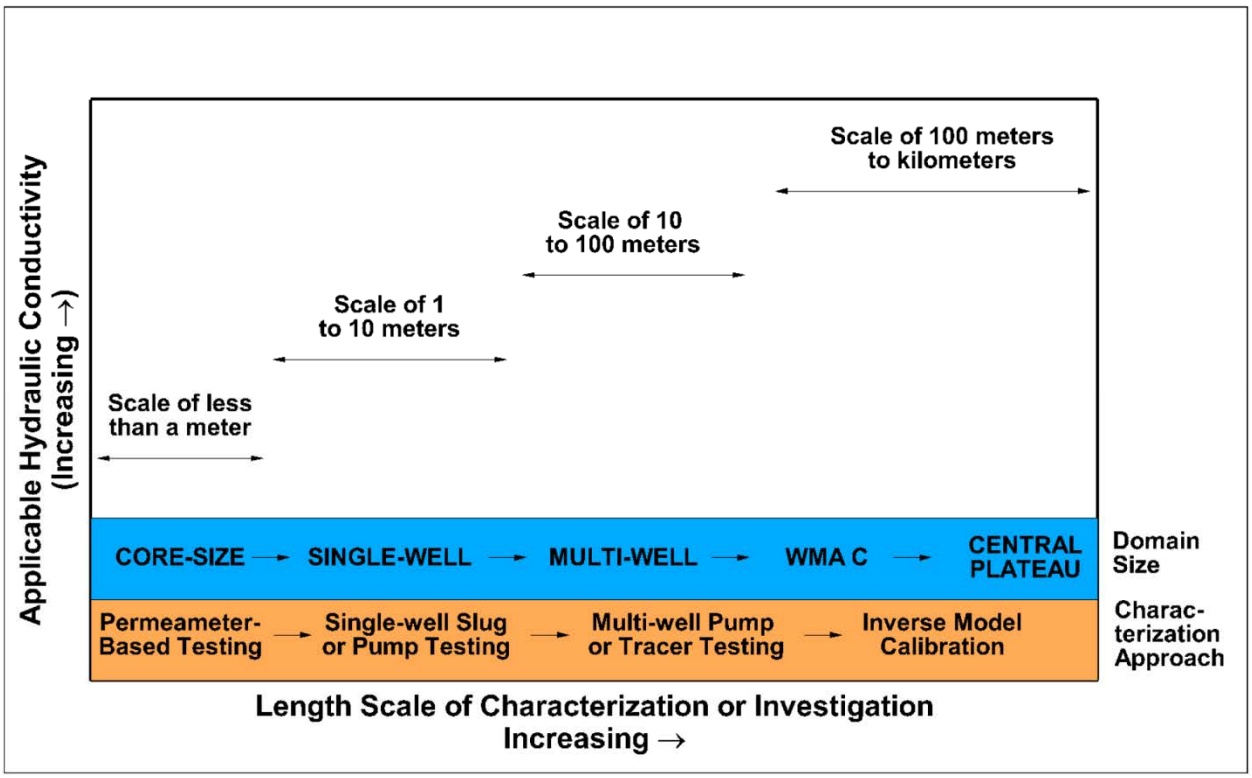

WMA = Waste Management Area

Determining effective hydraulic conductivities applicable to the field scale appears to be best evaluated using inverse modeling conditioned by available data, using appropriate boundary

conditions. Measurements of hydraulic conductivity appear to be dependent on the test scale, and increase as the scale increases, particularly in heterogeneous media ("Scale Dependency of Hydraulic Conductivity Measurements" [Rovey and Cherkauer 1995]; "Scale Dependency of Hydraulic Conductivity in Heterogeneous Media" [Schulze-Makuch et al. 1999]). In-situ measures of aquifer flow and hydraulic properties inferred from hydraulic testing represent relatively small areas (Figure C-1) compared to the overall scale and dimensions of the model domain, and therefore do not provide representative results appropriate for the field scale (*Use and Measurement of Mass Flux and Mass Discharge* [ITRC 2010]). Similarly, individual well-based slug and pump tests provide information at a relatively small scale, albeit larger than core-scale permeameter tests. Permeameter, slug, and pump tests are also limited in their ability to quantify spatial averages or trends, and are less likely to produce central measures of flow magnitudes than a regional model (ITRC 2010). Field estimates for saturated hydraulic conductivity based on slug tests, for example, provide estimates of hydraulic representation at a scale of meters and are not considered generally appropriate to be used directly in the modeling, even though slug and pumping test data are important input for model calibration (ITRC 2010).

Consequently, in evaluating available information for the aquifer at WMA C, hydraulic conductivities derived from a calibrated model are regarded as more reliable than direct measurements by permeameter, slug, or pump tests. This distinction is important because, as Section C.2 will show, substantially different values for hydraulic conductivity have been estimated by various investigators using different methods.

C.2 HYDROGEOLOGIC CONDITIONS AND STRUCTURE

To understand the groundwater flow conditions in the vicinity of WMA C, and in particular the large-scale saturated hydraulic conductivity and hydraulic gradient, it is important to note the regional geology and the hydrogeologic conditions and geologic structure in the 200 Areas. Groundwater in the unconfined aquifer at Hanford generally flows from recharge areas in the elevated region near the western boundary of the Hanford Site, toward the Columbia River on the eastern and northern boundaries. The Columbia River is the primary discharge area for the unconfined aquifer.

The unconsolidated sediments of present-day Central Plateau reflect deposits of ancient Columbia River, and the Pleistocene cataclysmic flooding (Section 3.1.4 and 3.1.9 provide a detailed discussion of the regional and local geology that is not repeated here). Briefly, WMA C lies on the northern flank of the Cold Creek bar, a large compound flood bar formed during Pleistocene cataclysmic flooding, which last occurred about 15,000 years ago (On the Trail of the Ice Age Floods: A Geological Field Guide to the Mid-Columbia Basin [Bjornstad 2006]). The cataclysmic floods caused repeated large erosional and depositional events, which have significantly shaped the Central Plateau and the present WMA C geology. Erosion by Ice-Age flooding and the ancestral Columbia River are believed to have removed much of the Ringold Formation from the area and created a highly transmissive paleochannel. The cataclysmic floods deposited into the channel the gravel-dominated facies of the Hanford formation that consist of coarse-grained basaltic sand and granule- to boulder-size gravel displaying an open framework. These large-scale features significantly influence groundwater flow and plume migration because

the deposits in the channel are much more transmissive than those outside of the channel. The groundwater flow direction in the unconfined aquifer in the vicinity of WMA C trends toward the southeast. This conclusion is based on the following: 1) slightly higher hydraulic heads to the northwest, 2) the orientation of the southeast trending paleochannel in the area, and 3) the configuration of the major contamination plumes.

C.2.1 Paleochannel Configuration and Flow Paths

As discussed above, the paleochannel has a significant influence on flow and contaminant transport under WMA C. The open-framework gravels of the paleochannel are highly conductive, and as such constitute a potential fast pathway for migration of contaminants. It is therefore important to characterize the spatial extent of the paleochannel in the vicinity of WMA C, and to appropriately estimate its permeability.

Based on current understanding of the ancestral Columbia River deposits, a large paleochannel is interpreted extending southeast through Gable Gap (Figure C-2) that bifurcates just south of the gap. One sub-channel trends easterly following along the direction of strike of the Gable Mountain anticline while the other sub-channel trends in a more southerly direction through the eastern portion of the 200 Area Inner Boundary (the paleochannel identified in Figure C-2). The southerly trending paleochannel configuration, flow path, and dimensions have been the subject of numerous studies, owing to their importance to site-wide contaminant transport.

Recent reports providing information supporting the current interpretation of the extent of the paleochannel include the following.

- PNNL-12261, *Revised Hydrogeology for the Suprabasalt Aquifer System, 200-East Area and Vicinity, Hanford Site, Washington*. The report includes detailed interpretations on the paleo and flood channels, and has several cross sections and figures displaying their configuration and flow paths.

- Aero-Metric LiDAR, *RCCC-Hanford Battelle/PNNL/DOE, Digital Orthophotography & LiDAR Surveys Photogrammetric Report*, prepared by Aero-Metric, Seattle, Washington. The report includes LiDAR data; surficial expression of paleochannel outlines are apparent from ground-proofed Aero-Metric LiDAR data collected in 2008.

- Fiscal year (FY) 2013 and 2014 Annual Groundwater Monitoring Reports, CHPRC. Interpretation of tritium and ^{129}I plume extents follow the highly conductive flow paleochannel flow path.

- ECF-Hanford-13-0029, *Development of the Hanford South Geologic Framework Model, Hanford Site, Washington*. The report shows areas where interpolated sediment volumes are not present, suggesting scouring along the paleochannel flow paths. All but two of the wells used in ECF-Hanford-13-0029 in the immediate vicinity of WMA C lie within the paleochannel. Geologic and geophysical logging data from the wells were also used in estimating paleochannel location.

Figure C-2. Interpreted Extent of a Paleochannel Associated with the Ancestral Columbia River in 200 East Area in the Vicinity of Waste Management Area C.

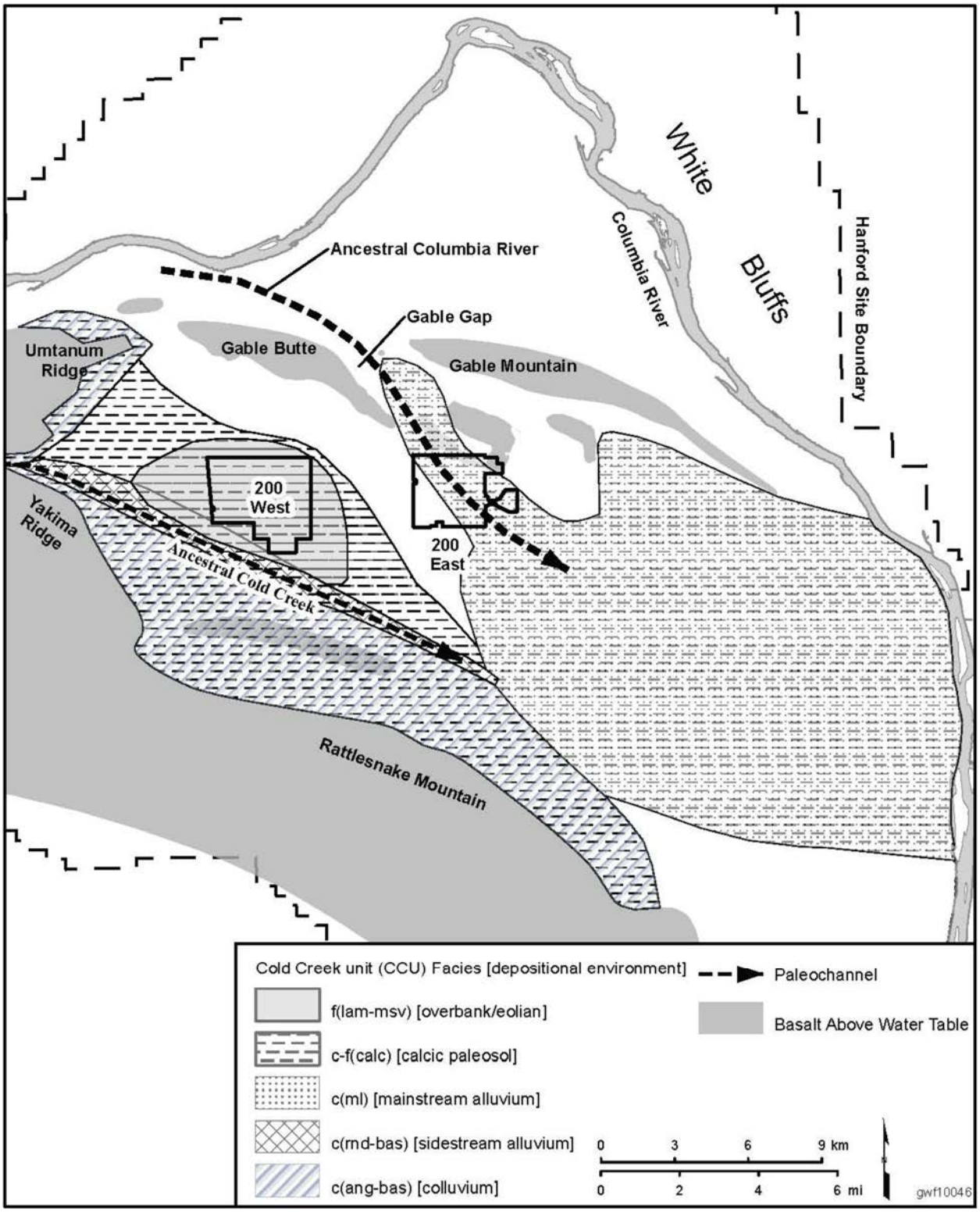

Source: DOE/RL-2011-118, *Hanford Site Groundwater Monitoring for 2011*, Appendix E.

Scouring of suprabasalt sediments in the paleochannels is evident in that, along much of its path, only the Hanford formation overlies the top of the basalt. Hanford formation material makes up almost entirely the material within the paleochannels in general, as well as all of the material within the paleochannel at the WMA C water table. Removal of pre-Hanford formation suprabasalt sediments, with the possible exception of a thin layer of Cold Creek unit (CCu) beneath the eastern half of WMA C, is apparent suggesting a paleochannel width of over 500 m beneath WMA C. Wells 299-E27-14 and 299-E27-15 penetrate the Hanford formation within the paleochannel beneath WMA C. The Hanford formation is ~86 m thick and the saturated thickness from the water table to the top of the basalt is ~13 m.

C.2.2 Theoretical Basis for Hydraulic Conductivity Estimates of Paleochannel Sediments

As discussed above, the paleochannel comprises an open-framework gravelly medium below WMA C. Figure C-3 is a digital photo log for borehole 299-E27-4 showing its proximity to WMA C and the open-framework gravelly media below the water table (the broken blue line is the water table location). The importance of the paleochannel to groundwater transport in the central plateau has led to a number of efforts to characterize its permeability, which can be applied to the WMA C PA.

Permeability measurements in open-framework gravelly media present special challenges, as the permeabilities are so high that they are above the measurement range of most laboratory constant-head permeameters—the head difference is too small to be measured. “Measuring the permeability of open-framework gravel” (Ferreira et al. 2010) addresses the challenge of measuring the high permeability by using a 3-m long permeameter. The head difference over this length was of the order of 10^{-2} to 10^{-3} m, which could be measured to the nearest 10^{-5} m. Measured permeability values varied between 3,456 m/d (for uniform pebbles) to 86,400 m/d (for open-framework gravels).

Figure C-4 illustrates an idealized unit cell model of an open-framework gravelly medium. “Scale Dependence of Continuum Models for Fractured Basalts” (Khaleel 1989) derived an expression (Equation C-1) for the isotropic saturated hydraulic conductivity (K) for such idealized media.

$$K_1 = K_2 = \frac{b^3 g}{12\sqrt{3}\ell\nu} \tag{C-1}$$

where g is the acceleration (LT-2) due to gravity, b is the open space aperture (L), ℓ is the coordinate length (L) along the opening of the unit cell, and ν is the kinematic viscosity (L2T-1) of the fluid. By inspection of equation (C-1) for equivalent isotropic *K*, the aperture size or width *b* is the most sensitive parameter in influencing conductivity estimates. For different aperture widths, and for a hexagon side length of 0.005 m (i.e., representative of 0.01-m (10-mm) diameter pebbles), the calculated equivalent K estimates range from a low of 8 m/d to 65,000 m/d for aperture widths (*b*) ranging from a rather modest spacing of 0.1 mm to as high as 2 mm. In regard to WMA C, according to sieve results of sandy gravel samples collected from near the water table and below at well 299-E27-4, the grain size of approximately 35% to 40% of the material exceeds 10 mm (PNNL-14656, *Borehole Data Package for Four CY 2003 RCRA*

Wells 299-E27-4, 299-E27-21, 299-E27-22, and 299-E27-23 at Single-Shell Tank, Waste Management Area C, Hanford Site, Washington).

A theoretical estimate of the permeability of a uniform pebble network can also be obtained using the Kozeny-Carman equation (Dynamics of Fluids in Porous Media [Bear 1972]):

$$k = \frac{d}{180} \frac{\phi^3}{(1-\phi)^2} \tag{C-2}$$

The 10-mm diameter (*d*) uniform pebble model having a measured porosity ϕ=40% yields a permeability of about 86,000 m/d. Therefore, the two theoretical approaches are the same order of magnitude, and both provide very high estimates of saturated conductivity that are comparable to those based on the large-scale permeameter experiments (Ferreira et al. 2010).

C.3 ESTIMATES OF UNCONFINED AQUIFER FLOW AND TRANSPORT PROPERTIES

Estimation of aquifer flow and transport parameters at WMA C are necessary for evaluating the rate and extent of migration of contaminants arriving from the vadose zone and to assess the groundwater quality as required under the *Resource Conservation and Recovery Act of 1976* (RCRA). The RCRA groundwater quality assessment program requires determination of whether past releases from WMA C are affecting groundwater quality and estimation of the rate and extent of migration of dangerous waste or dangerous waste constituents in the groundwater (DOE/RL-2009-77, *Groundwater Quality Assessment Plan for the Single-Shell Tank Waste Management Area C*; SGW-54508, *WMA C September 2012 Quarterly Groundwater Monitoring Report*).

C.3.1 Groundwater Flow Velocities and Fluxes

Estimates of groundwater flow velocity or Darcy flux can provide valuable information about the hydraulic properties of the aquifer. These estimates can be made by measuring the flow within a borehole (using downhole flowmeters) or by interrogating the local or regional scale flow models.

Few direct measurements of groundwater flow exist in 200 East Area, and none are particularly relevant to the groundwater flow conditions forecast for the unconfined aquifer in the immediate vicinity of WMA C. Measurements of groundwater flow velocity (groundwater flux divided by porosity) in the vicinity of WMA B-BX-BY, collected using a colloidal borescope circa 2001, reflected the impact of the large mound caused by the discharges at 216-B-3 Pond diverting flow from the east or southeast. The results did indicate that the flow velocities appeared to be greater in magnitude in the southern half of WMA B-BX-BY than in the northern half ("Application of the Colloidal Borescope to Determine a Complex Groundwater Flow Pattern" [Narbutovskih et al. 2002]). WHC-SD-EN-WP-012, *Groundwater Screening Evaluation/Monitoring Plan -- 200 Area Treated Effluent Disposal Facility, Project W-049H*, documents the results of an

evaluation conducted using a heat pulse flowmeter used to measure the magnitude and direction of groundwater flow velocity in three wells located east of the 216-B-3 Pond complex. However, during January and February 1994 when the evaluation occurred, the 216-B-3 Pond complex still received effluent and sustained the prominent groundwater mound, and the results of the testing were influenced by the mound created by the 216-B-3 pond discharges.

Groundwater flux information for particular subareas of regional models is often difficult to obtain from previous studies, and often must be inferred from whatever information is available. DOE/EIS-0391, *Final Tank Closure and Waste Management Environmental Impact Statement for the Hanford Site, Richland, Washington* estimated the future steady-state flow velocity in the highly conductive Hanford formation sediments at the 216-BY Cribs to be approximately 2 to 3 m/day toward the southeast, according to figures in Appendix L (i.e., Figures L-55, L-56, and L-57). According to the range of specific yield values presented in Table L-12 of Appendix L of DOE/EIS-0391, the flux in the aquifer is between 0.3 and 0.9 m/day.

Groundwater flux in the aquifer is estimated using the Central Plateau Groundwater Model (CPGWM) (CP-47631, *Model Package Report: Central Plateau Groundwater Model Version 6.3.3*) by evaluating the water budget through a planar rectangular window (300 m × 200 m that encompasses most of WMA C flow domain) over the unconfined aquifer thickness (Figure C-5). The results of the CPGWM include two times of interest, present day and post-closure steady state:

- For Year 2014 (approximating present day conditions), the CPGWM-calculated flow through the window volume is 1,100 m^3/day, which divided by the cross-sectional area of 3,300 m^2 translates to a Darcy flux of 0.33 m/day

- For Year 2100 (approximating post-closure steady state conditions), the CPGWM-calculated flow through the window volume is 580 m^3/day, which divided by the cross-sectional area of 3,300 m^2 translates to a Darcy flux of 0.18 m/day.

C.3.2 Hydraulic Conductivity of Unconfined Aquifer Sediments

The basis for the hydraulic conductivity of the unconfined aquifer used in the PA takes account of the accumulated knowledge and experience of many years of study of the aquifer beneath the Central Plateau, undertaken for a variety of purposes by different investigators, using a variety of measurement and modeling approaches. The hydraulic conductivity estimates from various investigations, with focus on the aquifer within the 200 East Area, are presented in Figure C-6 in such a manner that the length scale of observation increases from left to right. The results presented on the left hand side are from slug tests (small spatial scale measurements), while the pumping test-based measurements are in the middle and the regional scale model-based estimates are on the right hand side. Where multiple results are provided within a single report that cover slug and pump test data, the range of hydraulic conductivity is shown with a vertical line (Figure C-6). The generally increasing estimates of effective hydraulic conductivity moving from left to the right are consistent with Figure C-1 and description in the Section C.1. The results of most hydrologic tests indicate the presence of highly permeable conditions in the unconfined aquifer within the Central Plateau, and measured hydraulic conductivity estimates range as high as 51,500 m/day.

Figure C-3. Digital Photo Log for Borehole 299-E27-4 with an Expansion Showing the Open Framework Gravel below the Water Table.

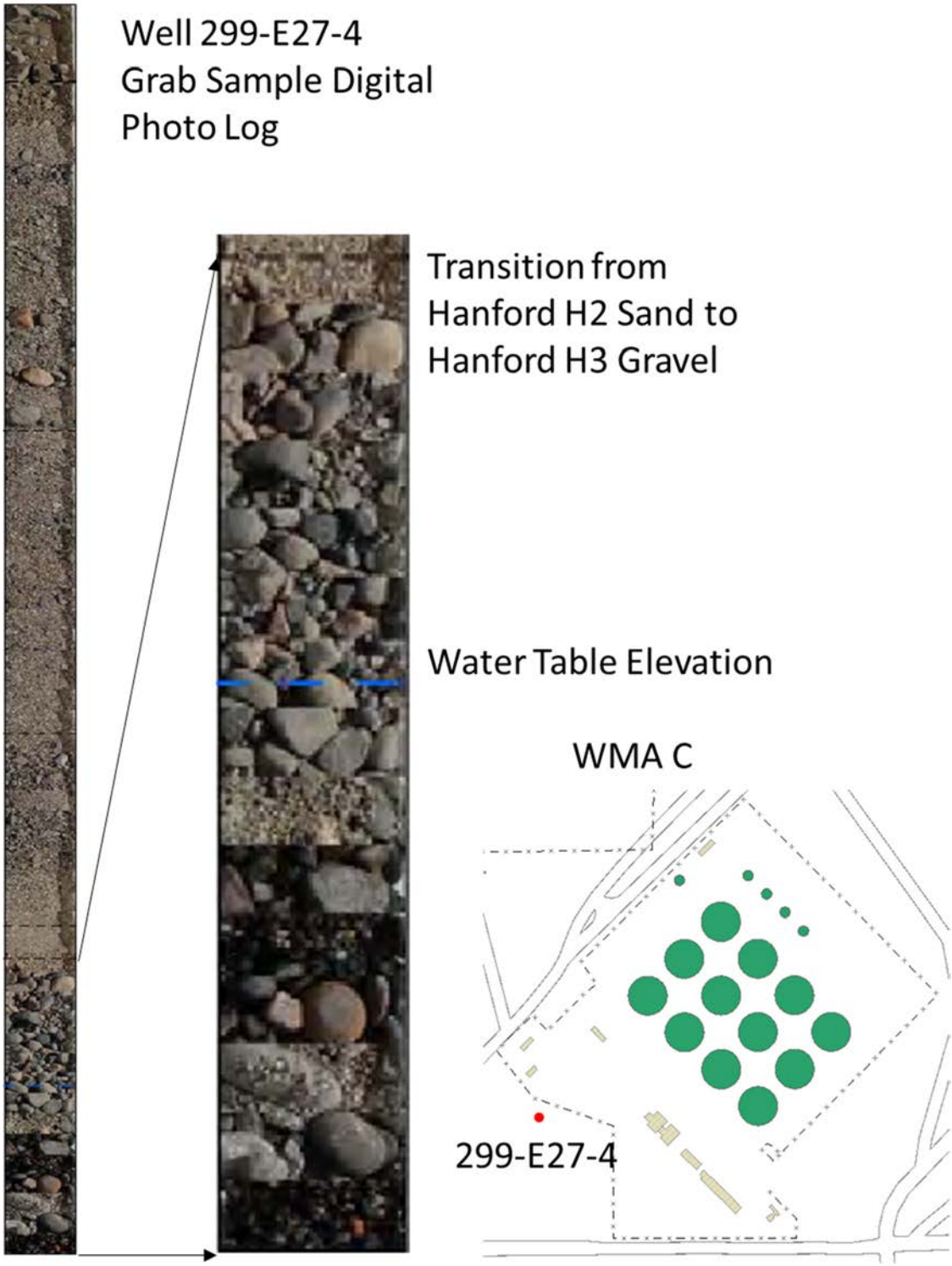

Adapted from PNNL-14656, *Borehole Data Package for Four CY 2003 RCRA Wells 299-E27-4, 299-E27-21, 299-E27-22, and 299-E27-23 at Single-Shell Tank, Waste Management Area C, Hanford Site, Washington.*

WMA = Waste Management Area

Figure C-4. (a) An Idealized Hexagonal Model Approximation of Open-Framework Gravelly Media, and (b) Representative Flow Regions Used to Determine Equivalent Hydraulic Conductivity.

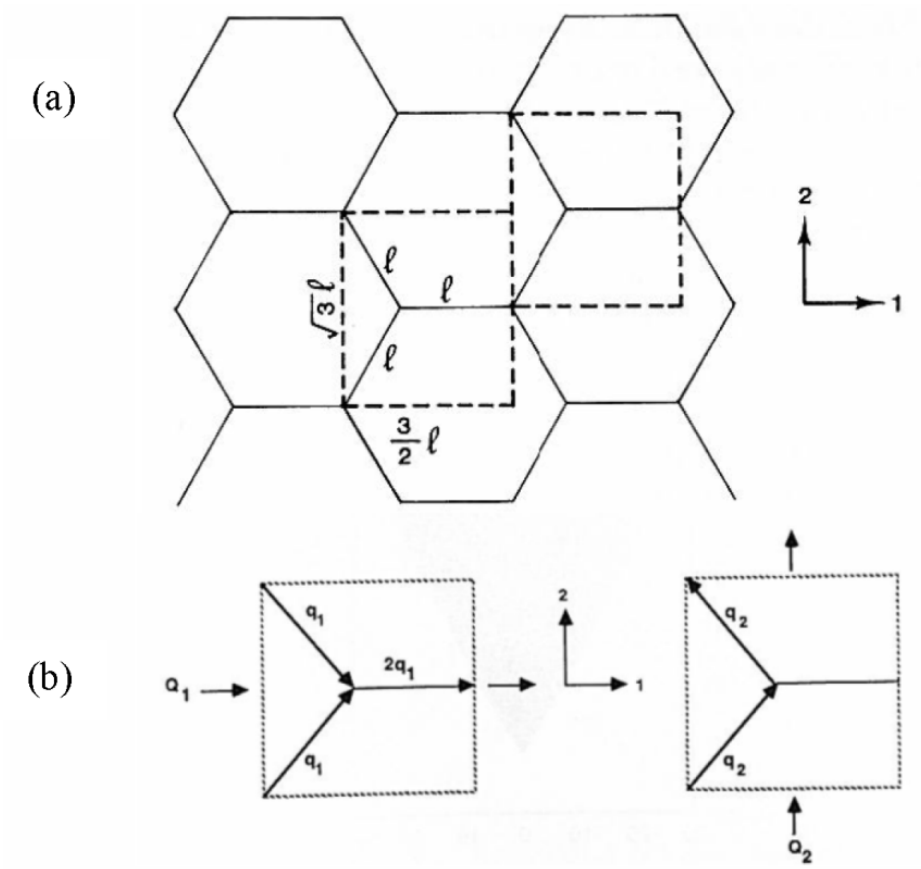

SGW-54508 considers hydraulic conductivity of the Hanford gravel at WMA C to range from 100 to 2,100 m/day on the basis of the results of slug and pumping tests conducted in the immediate vicinity of WMA C. Excluded from this range are unpublished slug test results from well 299-E27-24 that produced hydraulic conductivity estimates ranging from 3,650 to 51,500 m/day, and slug test results from well 299-E27-22 that range from 1,888 to 6,888 m/day (shown in Figure C-6). SGW-54508 discounts the results from well 299-E27-24 because the open interval and well radius were not controlled and sloughing conditions existed before testing. SGW-54508 also discounts the results from well 299-E27-22 because the sediment borehole log description at well 299-E27-22 indicates a more dominant silt matrix with less gravel content than at well 299-E27-23, where slug test results indicated that the hydraulic conductivity measures 100 to 108 m/day. However, the borehole log of well 299-E27-22 (Figure C-7) does indicate the presence of the open-framework gravel in the aquifer, and SGW-54508 does not explain why sloughing would cause hydraulic conductivity estimates derived from a slug test to be overestimated. In addition, the slug test data presented in SGW-48722, *Borehole Summary Report for the ARRA Installation of Five RCRA Groundwater Monitoring Wells in the 200 Areas, FY 2010* collected from wells 299-E27-24 and 299-E27-25 exhibit the oscillatory response indicative of highly permeable conditions. While the summary of data presented in SGW-54508 is appropriate for the purposes of the RCRA groundwater quality assessment program, which

include collecting and analyzing the available data, the data represent measurements made at a much smaller observation scale than is appropriate for developing an effective hydraulic conductivity estimate for WMA C (Figure C-1).

PNNL-14656 indicates that the high values measured at the wells are indicative of and consistent with the geologic interpretation of the open, highly permeable lower Hanford H3 gravels. The slug test and well screen development drawdown data also indicate comparable highly permeable conditions in the aquifer at wells 299-E27-21 and 299-E27-22 (PNNL-14656). Lastly, the results of an aquifer test with multiple observation wells conducted at well 699-55-50 indicate an aquifer hydraulic conductivity of 2,700 m/day (HW-60601, *Aquifer Characteristics and Ground-Water Movement at Hanford*). HW-60601 describes the aquifer as consisting of "Glaciofluviatile sands and gravels," which are described as unconsolidated sands and gravels occurring chiefly as glacial outwash. This description matches that given to the highly permeable gravel contained in the paleochannel.

Past calibration efforts (e.g., PNL-10886, *Development of a Three-Dimensional Ground-Water Model of the Hanford Site Unconfined Aquifer System: FY 1995 Status Report*; PNNL-11801, *Three-Dimensional Analysis of Future Groundwater Flow Conditions and Contaminant Plume Transport in the Hanford Site Unconfined Aquifer System: FY 1996 and 1997 Status Report*) estimated that an upper limit of hydraulic conductivity for coarse-gravel flood deposits found in the central part of the Hanford Site is on the order of several tens of thousands of meters per day (Figure C-8). Figure C-8 shows the influence of the high hydraulic conductivity paleochannel in the aquifer beneath WMA C, as denoted by the swath of red. This swath indicates hydraulic conductivity exceeding 7,000 m/day, extending from the Gable Gap through the southeast corner of 200 East Area. In one calibration effort, the hydraulic conductivity ranged from 271 m/day to 8,840 m/day within the WMA C PA model domain, and a value of 7,020 m/d in the immediate vicinity of WMA C (PNNL-14753, *Groundwater Data Package for Hanford Assessments*). In another effort, the hydraulic conductivity of the Hanford formation sediments ranged up to about 1,000,000 m/d for the Hanford flood deposits (PNNL-13641, *Uncertainty Analysis Framework – Hanford Site-Wide Groundwater Flow and Transport Model*). The Tank Closure and Waste Management Environmental Impact Statement (TC&WM EIS) model estimates the hydraulic conductivity of the highly conductive Hanford gravel present at WMA C to be ~4,000 m/day (DOE/EIS-0391). In a more recent modeling effort, CP-57037, *Model Package Report: Plateau to River Groundwater Transport Model Version 7.1* developed a calibrated estimate of 17,000 m/day for the Hanford formation associated with the paleochannel.

The CPGWM provides calibrated hydraulic conductivity estimates for the hydrostratigraphic units (HSUs) present within the aquifer. The CPGWM represents the most recent culmination of understanding of the unconfined aquifer under the Central Plateau and, given the rigorous nature of the development effort, is deemed to be the most suitable for predicting flow. The thicknesses and extent of the different HSUs within the selected model layers in the vicinity of WMA C for the saturated zone is shown in Figure C-9. The equivalent hydraulic conductivity for a given layer within the rectangular area (approximate extent of WMA C) ranges between 5,802 m/day and 17,000 m/day (Table C-1). Using a layer thickness weighted averaging scheme the effective hydraulic conductivity for an equivalent homogeneous medium (EHM) is estimated to be 11,000 m/day for the entire aquifer (Table C-1). The EHM approach is used for representing the

saturated zone in the three-dimensional WMA C PA model using the Subsurface Transport Over Multiple Phases (STOMP)©[8], as discussed in Appendix D, and therefore the value of 11,000 m/day is used for the aquifer.

C.3.3 Groundwater Flow Directions and Hydraulic Gradients

In the vicinity of WMA C, directions of groundwater flow and hydraulic gradients are inferred from water-level measurements in another part of the 200 East Area, around Low-Level Waste Management Area (LLWMA)-1 (DOE/RL-2013-22, *Hanford Site Groundwater Monitoring Report for 2012*), which is located northwest of WMA C. According to DOE/RL-2014-32, *Hanford Site Groundwater Monitoring Report for 2013*, the hydraulic gradient ranges between 2.2×10^{-5} m/m and 2.9×10^{-5} m/m, with flow moving in a southeastern direction. The average hydraulic gradient estimated from July 2011 through September 2012 was 2.5×10^{-5} ($\pm 0.4 \times 10^{-5}$) m/m toward the south (SGW-54165, *Evaluation of the Unconfined Aquifer Hydraulic Gradient Beneath the 200 East Area, Hanford Site*). SGW-54165 indicates that, while the hydraulic gradient determination represents a spatial average across the entire Low-gradient Monitoring Network in the vicinity of LLWMA-1, mapping of water levels from August 2011 indicates that the flow direction directly beneath LLWMA-1 is more toward the southeast rather than toward the south.

Hydraulic gradient estimates in groundwater based on the CPGWM estimates of future conditions within the Central Plateau are summarized in Table C-1. Although water levels in the 200 East Area continue to decline, an evaluation of current groundwater flow directions and rates at WMA C is difficult due to the very low hydraulic gradient (on the order of 10^{-5} m/m). The hydraulic gradient according to the CPGWM is calculated from the volumetric flux through the window described in Section C.3.1.2 and the hydraulic conductivity value described in Section C.3.1.2. As indicated previously, the results of the CPGWM include two times of interest, present day and post-closure steady state (Table C-1), as follows.

- For Year 2014 (approximating present day conditions), the CPGWM-calculated flow through the window volume is 1,000 m^3/day, which divided by the cross-sectional area of 3,300 m^2 and equivalent hydraulic conductivity of 11,000 m/day translates to a hydraulic gradient of 3×10^{-5}. The direction of flow inferred from the modeling and consistent with plume movements is in a south to southeasterly direction.

- For Year 2100 (approximating post-closure steady state conditions), the CPGWM-calculated flow through the window volume is 730 m^3/day, which divided by the cross-sectional area of 3,300 m^2 and equivalent hydraulic conductivity of 11,000 m/day translates to a hydraulic gradient of 2×10^{-5}. The direction of flow inferred from the model is in a southeasterly direction.

The CPGWM model estimate of 3×10^{-5} m/m for year 2014 is consistent with the average gradient measured during 2013 (2.6×10^{-5} m/m) (DOE/RL-2014-32), and within the range of

[8] Subsurface Transport Over Multiple Phases (STOMP)© is copyrighted by Battelle Memorial Institute, 1996.

what is reported in SGW-54508 and SGW-58561, *WMA C Quarterly October through December 2014 Quarterly Groundwater Monitoring Report* (5.9×10^{-6} to 4.5×10^{-5} m/m).

C.3.4 Anisotropy

Anisotropy in saturated hydraulic conductivity for Hanford H3 Gravels has been estimated from pumping tests, which indicate values ranging from 0.01 to 0.1 (PNL-10886) and 0.015 to 0.5 (DOE/RL-2007-28, *Feasibility Study Report for the 200-ZP-1 Groundwater Operable Unit*) for post-year 2000 testing. Previous modeling analyses (e.g., PNNL-14398, *Transient Inverse Calibration of the Site-Wide Groundwater Flow Model [ACM-2]: FY 2003 Progress Report*, PNNL-14753, DOE/EIS-0391, and CPGWM [CP-47631]) estimate anisotropy to be 0.1.

C.3.5 Properties for Contaminant Transport

The transport of contaminants also requires estimates of the porosity, the volume of pore space in the aquifer, and the macrodispersivity, which accounts for the mixing that occurs because of variations in the flow and velocity caused by heterogeneities.

C.3.5.1 Porosity. According to RPP-14430, *Subsurface Conditions Description of the C and A-AX Waste Management Area*, porosity is generally estimated to be about 30% for unconsolidated coarse-grained sediments, but a value closer to 20% may be more appropriate where boulders and cobbles are present and mixed with sand and gravels, such as at WMA C. Other estimated values include 0.06 determined from an aquifer pumping test at a well (699-62-43) screened within the Hanford gravel sequence similar to that at WMA C (HW-60601); 0.1 derived from laboratory tests of Hanford gravels discussed in PNNL-19277, *Conceptual Models for Migration of Key Groundwater Contaminants Through the Vadose Zone and Into the Unconfined Aquifer Below the B-Complex*, and 0.25 in RPP-RPT-46088, *Flow and Transport in the Natural System at Waste Management Area C*. DOE/EIS-0391 identified 0.15 to 0.30 as a reasonable range for the storage property value (expressed as specific yield values) of the highly conductive Hanford formation present in the paleochannel. CP-57037 estimated porosity of the Hanford formation associated with the paleochannel to be 0.2.

C.3.5.2 Macrodispersivity Estimates. Field-scale dispersivities are referred to as macrodispersivities. Field observations indicate that the dispersion coefficients required to describe the large-scale transport processes, at field scales of tens or hundreds of meters, are much different from those observed in small-scale laboratory experiments (Stochastic Subsurface Hydrology [Gelhar 1993]). In fact, macrodispersivities may often be orders of magnitude larger than those observed in the laboratory. Consequently, laboratory-scale dispersivities, which are typically ~1 cm or less, are of little use in estimating field-scale dispersivities.

There is general agreement in hydrology literature that hydraulic conductivity variations induced by field-scale heterogeneities play an important role in field-scale transport processes. However, there does not appear to be a clear consensus about how best to describe such processes quantitatively (Gelhar 1993). While well-designed, large-scale tracer experiments would provide useful information, limited field data are available at this time to quantify macrodispersivities in unsaturated media.

Figure C-5. Plan View of the Central Plateau Groundwater Model Representing the Aquifer and the Volumetric Flux Calculation Window in the Vicinity of Waste Management Area C.

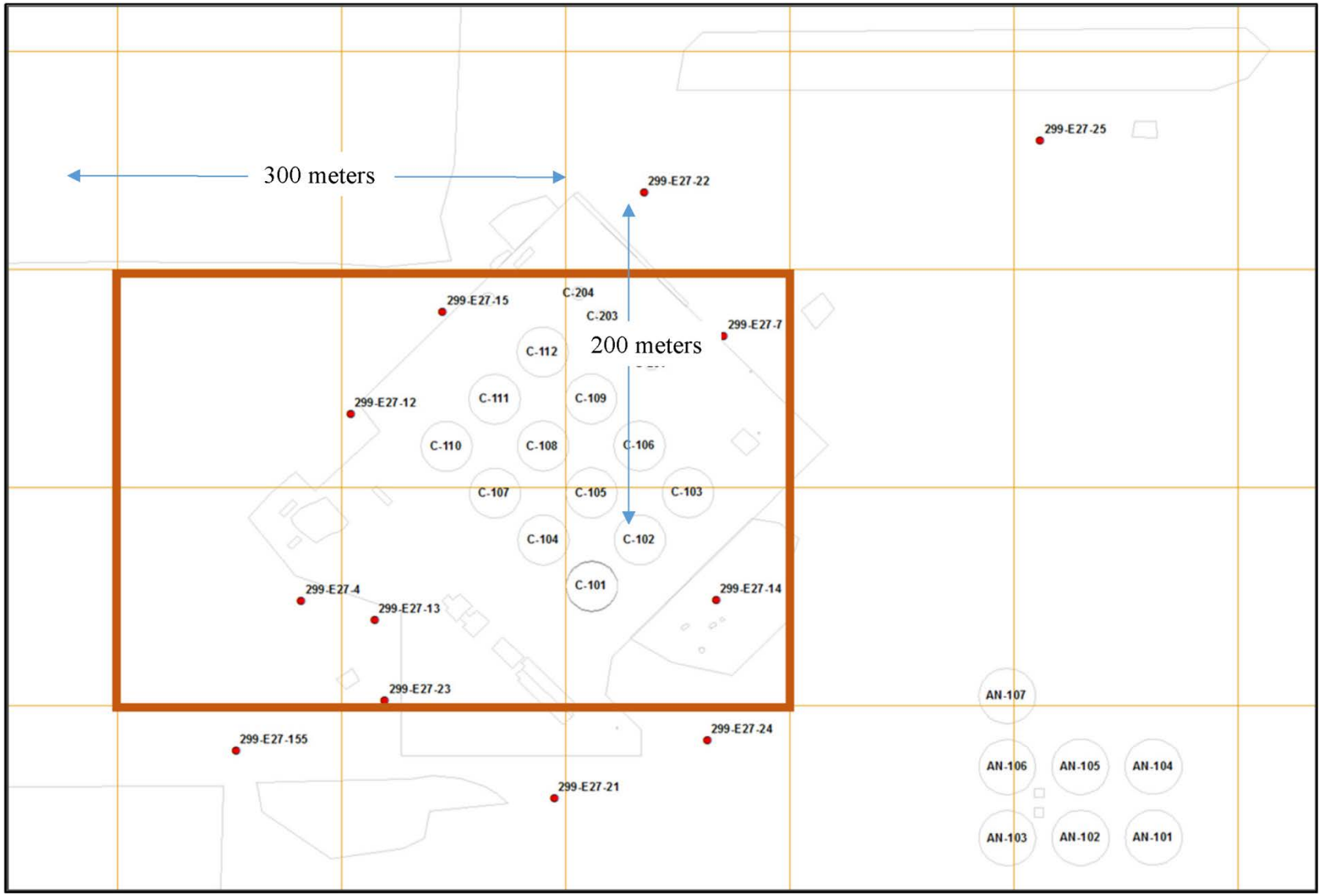

Figure C-6. Hanford Formation Saturated Hydraulic Conductivity Estimates Based on Slug Tests, Pump Tests, and Model Calibration.

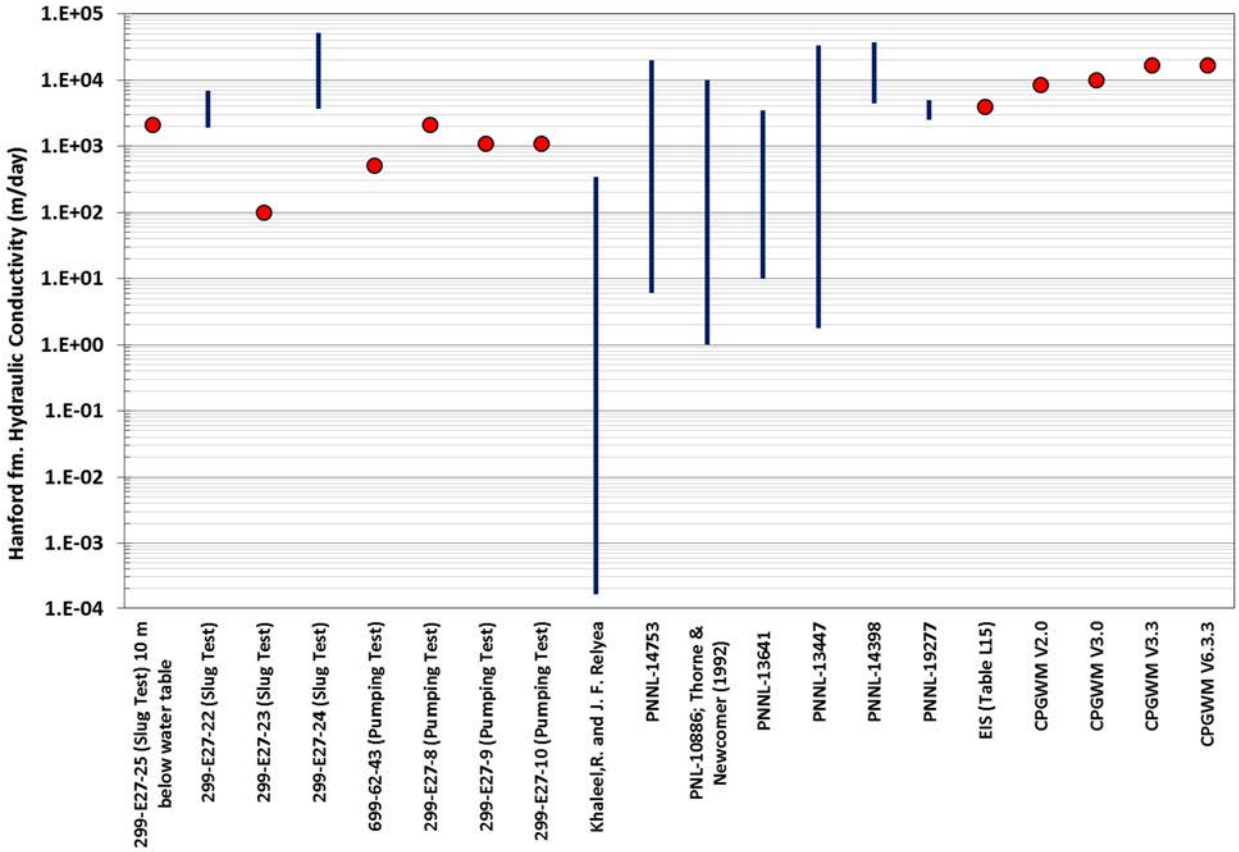

Heterogeneities that exist at various length scales result in a scale dependence of macrodispersivities (Figure C-10; "A Critical Review of Data on Field-Scale Dispersion in Aquifers" [Gelhar et al. 1992]). Dispersivities increase with time, or equivalently with distance, until they tend to converge on their unique asymptotic (large-time) values. However, it can take a long time (e.g., years or decades) for the asymptotic Fickian approximation to take hold. Nonetheless, the second-moment evolution or the time-dependent, preasymptotic dispersivities are of marginal interest in simulations involving long-times or large-mean travel distances such as those in PA modeling. The use of a constant (asymptotic) macrodispersivity is thus considered appropriate in PA simulations (NUREG/CR-6114, *Auxiliary Analyses in Support of Performance Assessment of a Hypothetical Low-Level Waste Facility: Groundwater Flow and Transport Simulation*).

The longitudinal and transverse macrodispersivity estimates in the saturated zone are based on a review of three general relationships ("Universal Scaling of Hydraulic Conductivities and Dispersivities in Geologic Media" [Neuman 1990]; "Longitudinal Dispersivity Data and Implications for Scaling Behavior" [Schulze-Makuch 2005]; and "Use of Weighted Least-Squares Method in Evaluation of the Relationship Between Dispersivity and Field Scale" [Xu and Eckstein 1995]) that quantify the dependence of this parameter on measurement scale (L_s). For the 100 m scale of transport calculations considered in the PA effort, which is the

approximate distance of transport from source areas to a compliance well located in the saturated zone, the calculated values fall within the range of 3.5 to 17 m (Table C-2).

RPP-17209, *Modeling Data Package for an Initial Assessment of Closure of the S and SX Tank Farms*, and "Field Study of a Long and Very Narrow Contaminant Plume" (van der Kamp et al. 1994) indicate that a value of 10 represents a reasonable estimate of the ratio of longitudinal to transverse macrodispersivity.

C.4 UNCONFINED AQUIFER FLOW AND TRANSPORT PROPERTIES USED IN THE WASTE MANAGEMENT AREA C PERFORMANCE ASSESSMENT

The WMA C PA mostly adopted flow and transport properties derived from results developed from the calibrated CPGWM. The CPGWM takes into account the accumulated knowledge and experience of many years of study of the aquifer beneath the Central Plateau. One of the objectives for the CPGWM is to create a common modeling platform that can be used for investigations that support remedial activities and decisions in the four groundwater operable units that exist in the Central Plateau region (CP-47631). As discussed in Section C-1, the scale of the WMA C PA requires aquifer flow property estimates consistent with large area model calibration studies that are on the appropriate spatial scale.

The CPGWM incorporates the large-scale geologic and hydrogeologic features, and provides estimates of water levels, hydraulic gradients, and groundwater flows throughout the 200 West and 200 East Areas for current and expected future groundwater conditions. The model domain includes six suprabasalt HSUs with hydraulic properties established primarily through a transient calibration of the model to historical water level measurements. The CPGWM calibration places emphasis on matching water level data from the 1940s, early 1950s, and first decade of the 21st century to estimate hydraulic properties using flow conditions relatively unperturbed by site operations. Simulated water levels are compared to observed values for wells located upgradient and downgradient of the WMA C (Figure C-11). The observed heads and CPGWM-simulated heads, representing a time span of over 20 years, compare well as indicated in Figure C-11, providing confidence in the predictive capabilities of the CPGWM.

The CPGWM is not a single-time-use tool, but represents the product of ongoing development and continued improvement that began in FY 2009 (CP-47631). The CPGWM represents the most recent culmination of understanding of the unconfined aquifer under the Central Plateau. CP-47631 provides information pertaining to the CPGWM objectives; conceptualization; model implementation; sensitivity, calibration, and uncertainty analyses; configuration control; and limitations of the groundwater flow component of the CPGWM.

The CPGWM has undergone several revisions (currently at Revision 6.3.3) to improve its performance with respect to calibration. CPGWM 6.3.3 takes account of the historical development of understanding the unconfined aquifer, along with current interpretations of the geology (including the extent of the paleochannel), and up-to-date measurements of the recovery of the water table from operational discharges. Hence, it represents the best current understanding of flow under the Central Plateau.

Figure C-7. Borehole Log of Well 299-E27-22.

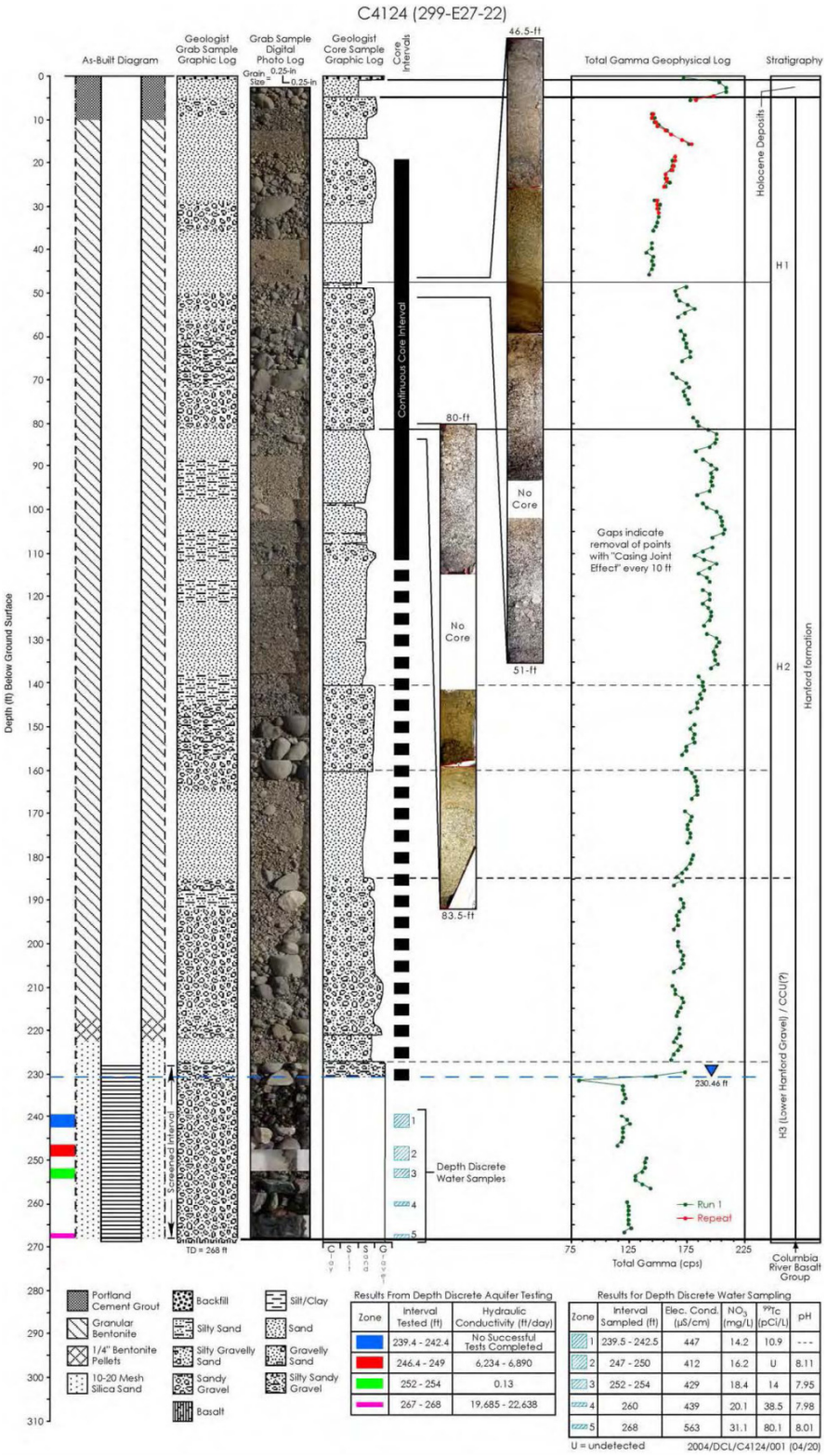

Zone	Interval Tested (ft)	Hydraulic Conductivity (ft/day)
	239.4 - 242.4	No Successful Tests Completed
	246.4 - 249	6,234 - 6,890
	252 - 254	0.13
	267 - 268	19,685 - 22,638

Zone	Interval Sampled (ft)	Elec. Cond. (µS/cm)	NO_3 (mg/L)	^{99}Tc (pCi/L)	pH
1	239.5 - 242.5	447	14.2	10.9	---
2	247 - 250	412	16.2	U	8.11
3	252 - 254	429	18.4	14	7.95
4	260	439	20.1	38.5	7.98
5	268	563	31.1	80.1	8.01

Source: PNNL-14656, *Borehole Data Package for Four CY 2003 RCRA Wells 299-E27-4, 299-E27-21, 299-E27-22, and 299-E27-23 at Single-Shell Tank, Waste Management Area C, Hanford Site, Washington.*

Figure C-8. Pacific Northwest National Laboratory Sitewide Model Calibration of Hydraulic Conductivity of the Unconfined Aquifer with the Location of Waste Management Area C and Magnitude of Hydraulic Conductivity Indicated.

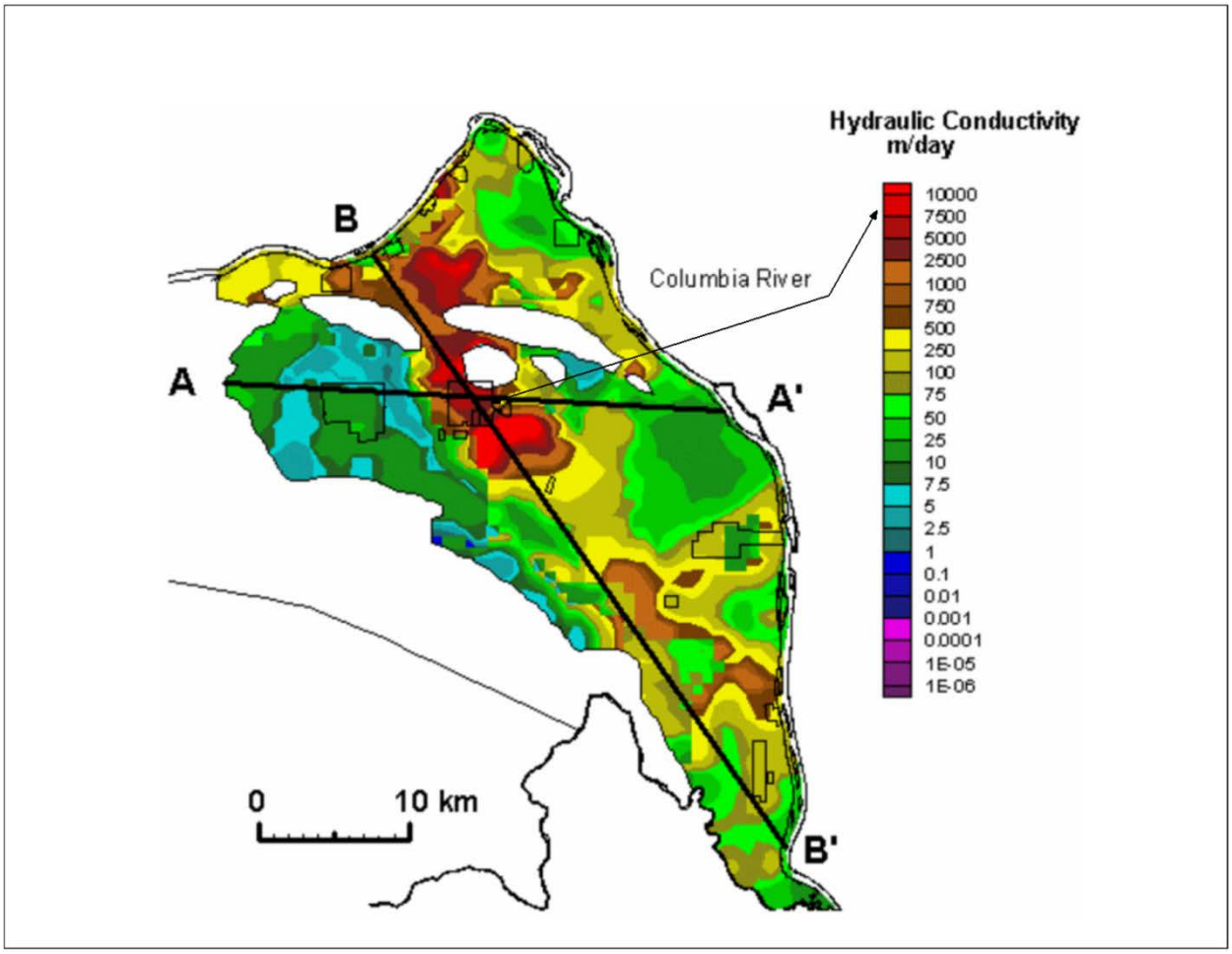

Excerpted and adapted from PNNL-13447, *Transient Inverse Calibration of Hanford Site-Wide Groundwater Model to Hanford Operational Impact – 1943 to 1996.*

C.4.1 Flow Properties

C.4.1.1 Hydraulic Conductivity. As discussed in Section C.3.2, the effective hydraulic conductivity for the entire aquifer at WMA C using an EHM approach is estimated to be 11,000 m/day (Table C-1). This is based on the layer thickness weighted averaging scheme of calibrated hydraulic conductivity of the HSUs in the CPGWM in the vicinity of WMA C flow domain.

C.4.1.2 Hydraulic Gradient. The hydraulic gradient estimate (2×10^{-5} m/m, Table C-1) is based on the CPGWM estimates of future conditions within the Central Plateau. Water levels in the 200 East Area continue to decline, and evaluation of current flow direction and rate of groundwater flow at WMA C is difficult due to the very low hydraulic gradient. However, no appreciable change in hydraulic gradient is expected to occur after about 100 years after closure of WMA C, once the remedial actions in the nearby operable units are completed and the water

table is at or near steady state. It is expected that by the time the contaminants are released from WMA C and reach the water table, several hundred years would have passed and the water table would be at a steady-state condition. These conditions justify the use of a single value of hydraulic gradient for the water table, even though it is known to have changed substantially in the past owing to operational releases.

Figure C-9. Central Plateau Groundwater Model Layer Discretization In the Saturated Zone and Extent of Various Hydrostratigraphic Units within the Model Layer in the Vicinity of Waste Management Area C (shown by the Rectangle).

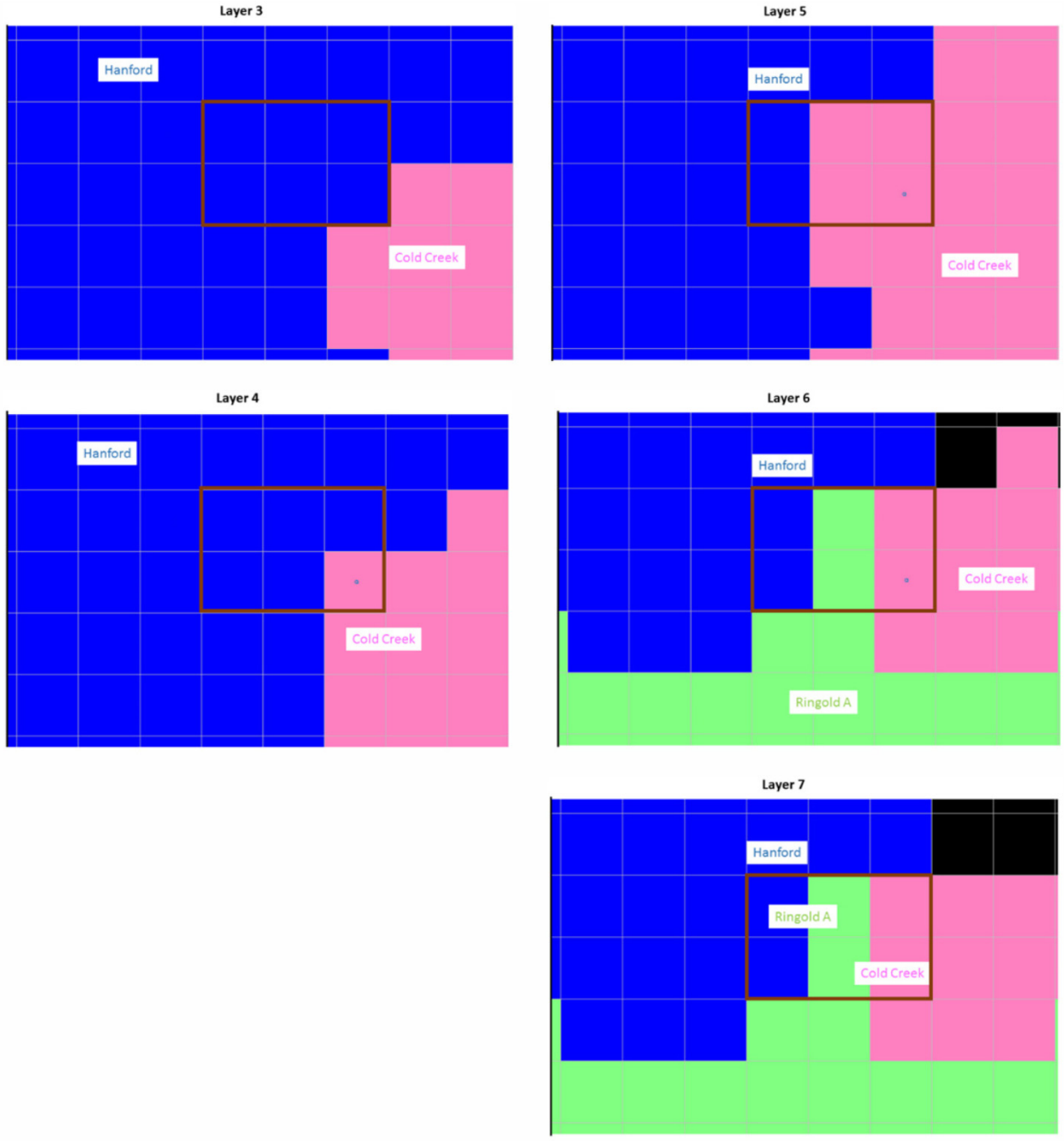

Table C-1. Calculation of Weighted Average Hydraulic Conductivity Value and Volumetric Water Flux from the Central Plateau Groundwater Model.

Year	Model Layer	Predicted Volumetric Water Flux (m^3/day)	Length of Window (m)	Layer Thickness (m)	Hanford Unit Calibrated Horizontal Hydraulic Conductivity (m/day)	Calculated Gradient (m/m)
2014	3	277.1	300	3	17,000	1.81E-05
2014	4	319.1	300	3	14,233	2.49E-05
2014	5	253.4	300	3	5,933	4.75E-05
2014	6	143.1	300	1	5,802	8.22E-05
2014	7	52.5	300	1	5,802	3.02E-05
2100	3	161.3	300	3	17,000	1.05E-05
2100	4	238.4	300	3	14,233	1.86E-05
2100	5	188.7	300	3	5,933	3.53E-05
2100	6	104.6	300	1	5,802	6.01E-05
2100	7	38.5	300	1	5,802	2.21E-05
Layer Thickness Weighted Hydraulic Conductivity (m/day, rounded):						11,000
Hydraulic Gradient 2014 (m/m, rounded):						3E-05
Hydraulic Gradient 2200 (m/m, rounded):						2E-05

C.4.1.3 Anisotropy. The CPGWM estimate of 0.1 (CP-47631) for the anisotropy, which is defined here as the ratio of vertical to horizontal hydraulic conductivity, is consistent with previous modeling analyses (e.g., PNNL-14398, PNNL-14753, and DOE/EIS-0391).

C.4.2 Contaminant Transport Properties

C.4.2.1 Porosity. The CPGWM value of 0.20 is consistent with the conclusion in RPP-14430, the vadose zone value of 0.17 for the Hanford H1 and H3 sediments discussed in Section 6.3.2.2, and with the aquifer test results presented in HW-60601. The porosity value is within the range of other estimated values (e.g., PNNL-19277 and RPP-RPT-46088).

C.4.2.2 Macrodispersivity Estimates. A value of 10.5 m is considered representative and the midpoint of the range of values presented in Section C.3.5.2. The ratio of longitudinal to transverse macrodispersivity is chosen to be 10 based on RPP-17209 and van der Kamp et al. 1994.

Figure C-10. Longitudinal Macrodispersivity in Saturated Media as a Function of Overall Problem Scale with Data Classified by Reliability.

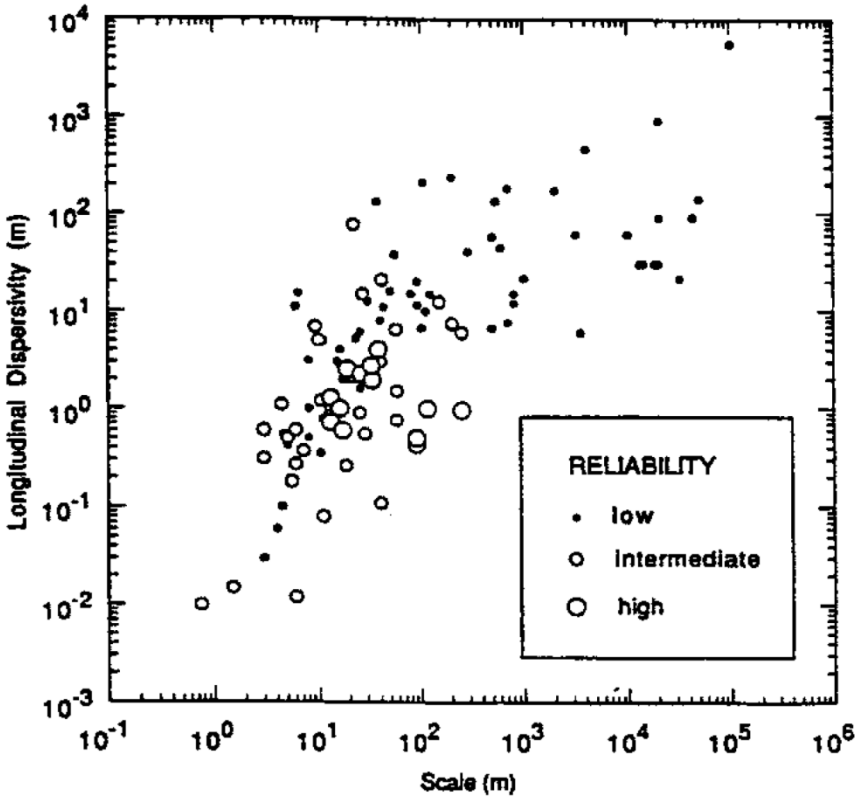

Reference: "A Critical Review of Data on Field-Scale Dispersion in Aquifers" (Gelhar et al. 1992).

C.5 DEVELOPMENT OF UNCERTAINTY IN GROUNDWATER FLUX AND MACRODISPERSIVITY FOR SATURATED ZONE

In the WMA C PA, the contaminant concentrations in the aquifer largely depend on the groundwater flux through the aquifer. While the groundwater flux can vary spatially due to local changes in hydraulic properties, the peak concentration at a particular location appears to correlate strongly to the mean groundwater flux, even in a heterogeneous aquifer (ITRC 2010; NUREG/CR-6767, *Evaluation of Hydrologic Uncertainty Assessments for Decommissioning Sites Using Complex and Simplified Models*).

Groundwater flux is linearly proportional to the hydraulic conductivity and hydraulic gradient. In the vicinity of WMA C, estimates of hydraulic gradient appear to include much less variability than estimates of hydraulic conductivity, as indicated by the results of detailed studies of the hydraulic gradient in 200 East Area (Figure C-12). Because changes in one of the parameters can be negated by reciprocal changes to the other, for the purpose of evaluating uncertainty range in the groundwater flux, only the uncertainty in effective hydraulic conductivity is considered.

Table C-2. Relationship Between Saturated Longitudinal Macrodispersivity (αL) and Scale of Measurement (Ls).

Reference	Relationship	Origin	Saturated Longitudinal Macrodispersivity Estimate (m) for a Scale ≈ 100 m
Neuman (1990)	$\alpha_L \approx 0.017\, L_s^{1.5}$	"Universal relationship" established considering both field and laboratory data (excluding modeling results)	17
Schulze-Makuch (2005)	$\alpha_L \approx 0.085\, L_s^{0.81}$	Established considering field and modeling results (all reliabilities) and excluding laboratory data	3.5
Xu and Eckstein (1995)	$\alpha_L \approx 0.94\left(\log_{10} L_s\right)^{2.693}$	Established considering the same data set as Neuman (1990) including numerical model results	6

References:
"Universal Scaling of Hydraulic Conductivities and Dispersivities in Geologic Media" (Neuman 1990).
"Longitudinal Dispersivity Data and Implications for Scaling Behavior" (Schulze-Makuch 2005).
"Use of Weighted Least-Squares Method in Evaluation of the Relationship Between Dispersivity and Field Scale" (Xu and Eckstein 1995).

The general understanding of the groundwater flux in the aquifer around WMA C was used to evaluate the uncertainty in that parameter. The groundwater flux estimate from the calibrated CPGWM is considered to be the best estimate. The uncertainty in groundwater flux is represented by propagation of uncertainty in hydraulic conductivity (K_s) and by holding the long-term hydraulic gradient constant (2×10^{-5} m/m). A lower bound estimate of K_s is chosen to be 1,000 m/d and the upper bound estimate is chosen to be 21,000 m/d with the best estimate of 11,000 m/d. The lower bound estimate of 1,000 m/day is in the middle of the range of test results presented in DOE/RL-2013-22, but appears to substantially underestimate the regional-scale value estimated using the CPGWM. The upper bound estimate of 21,000 m/d is chosen as a reasonable upper bound given that the hydraulic gradient is kept fixed. Based on this information, the uncertainty distribution for K_s is represented by a triangular distribution with minimum of 1,000 m/d, maximum of 21,000 m/d, and mode of 11,000 m/d.

The base case groundwater flux (Darcy flux) value of 0.22 m/day is calculated from best-estimate hydraulic gradient and hydraulic conductivity. This represents the mode of the triangular distribution with the minimum and maximum values estimated to be 0.02 m/day and 0.42 m/day, respectively. The minimum and maximum values are chosen in the same proportion (relative to the best estimate) as for the K_s, as discussed above. The uncertainty distributions are summarized in Table C-3.

The uncertainty in macrodispersivity within the unconfined aquifer was based on a review of literature-based, scale-dependent relationships for this parameter as discussed in Section C.3.5.2. The range in saturated zone macrodispersivity at the scale of the WMA C model is estimated to be from 1 m to 20 m.

Figure C-11. Central Plateau Groundwater Model Calibration Results in the Vicinity of Waste Management Area C.

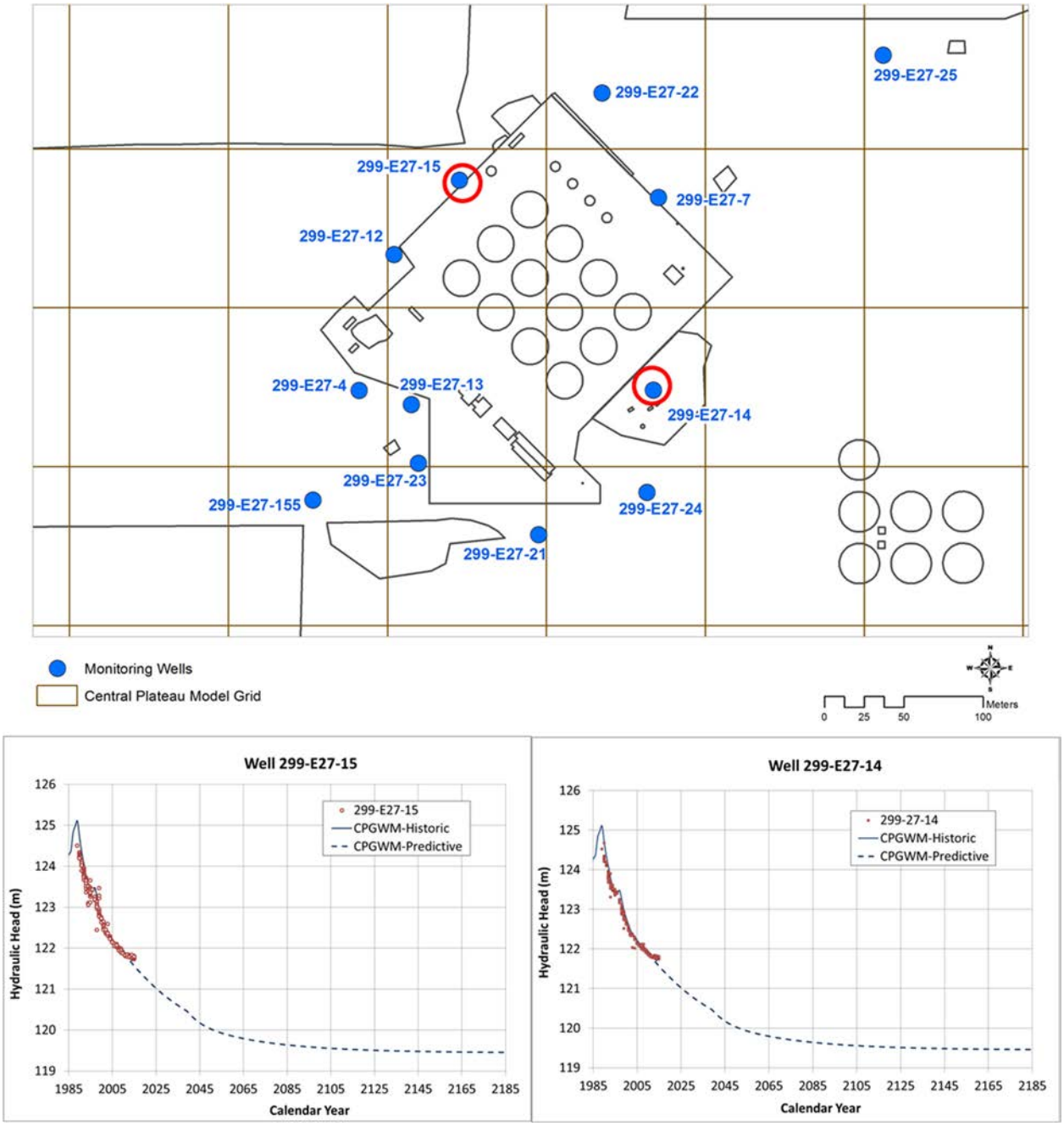

CPGWM = Central Plateau Groundwater Model

Uncertainty in the anisotropy and porosity in the aquifer are not considered as they have small range and are not likely to appreciably impact the contaminant concentrations (WCH-520, *Performance Assessment for the Environmental Restoration Disposal Facility, Hanford Site, Washington*). Furthermore, the uncertainty associated with these effects is considered to be minor and included within the uncertainty in the concentration results associated with the uncertainty in the groundwater flux.

Figure C-12. Low-Gradient Low-Level Waste Management Area 1 Monitoring Network Results.

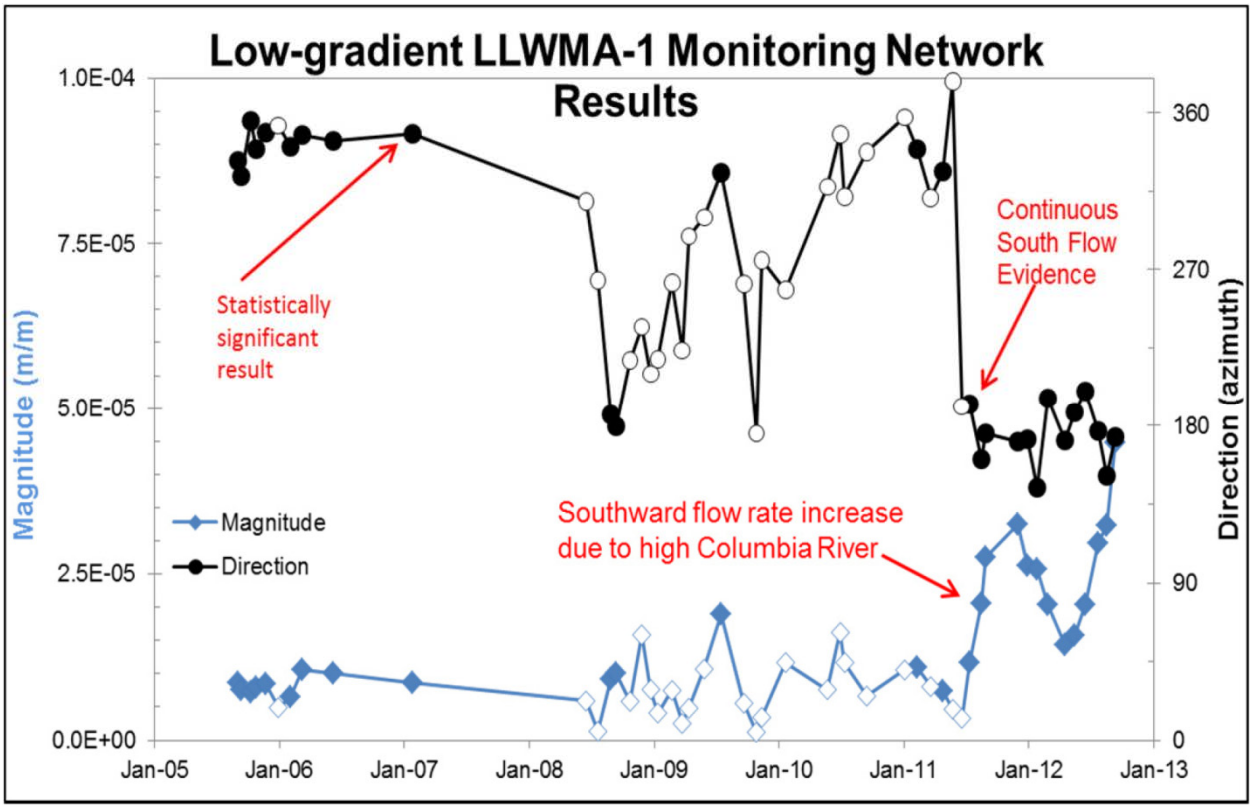

Excerpted from SGW-54165, *Evaluation of the Unconfined Aquifer Hydraulic Gradient Beneath the 200 East Area, Hanford Site*.

LLWMA-1 = Low-Level Waste Management Area 1

Table C-3. Triangular Distribution of Aquifer Flux and Proportional Hydraulic Conductivity Values Applicable to the Uncertainty Analysis.

		Minimum	Mode/Median	Maximum
Aquifer Flux (m/day)	Triangular Distribution	0.02	0.22	0.42
Resultant Hydraulic Conductivity (m/day)	Triangular Distribution	1,000	11,000	21,000

C.6 REFERENCES

Aero-Metric LiDAR, 2008, *RCCC-Hanford Battelle/PNNL/DOE, Digital Orthophotography & LiDAR Surveys Photogrammetric Report*, Aero-Metric, Inc., Seattle, Washington.

Bear, J. 1972, Dynamics of Fluids in Porous Media, American Elsevier Publishing Company, Inc., New York, New York.

Bjornstad, B., 2006, On the Trail of the Ice Age Floods: A Geological Field Guide to the Mid-Columbia Basin, Keokee Co. Publishing, Inc., Sandpoint, Idaho.

CP-47631, 2015, *Model Package Report: Central Plateau Groundwater Model Version 6.3.3*, Rev. 2, INTERA, Inc., Richland, Washington.

CP-57037, 2015, *Model Package Report: Plateau to River Groundwater Transport Model Version 7.1*, Rev. 0, CH2M HILL Plateau Remediation Company, Richland, Washington.

DOE/EIS-0391, 2012, *Final Tank Closure and Waste Management Environmental Impact Statement for the Hanford Site, Richland, Washington*, U.S. Department of Energy, Washington, D.C.

DOE/RL-2007-28, 2008, *Feasibility Study Report for the 200-ZP-1 Groundwater Operable Unit*, Rev. 0, U.S. Department of Energy, Richland Operations Office, Richland, Washington.

DOE/RL-2009-77, 2010, *Groundwater Quality Assessment Plan for the Single-Shell Tank Waste Management Area C*, Rev. 0, U.S. Department of Energy, Richland Operations Office, Richland, Washington.

DOE/RL-2011-118, 2012, *Hanford Site Groundwater Monitoring for 2011*, Rev. 0, U.S. Department of Energy, Richland Operations Office, Richland, Washington.

DOE/RL-2013-22, 2013, *Hanford Site Groundwater Monitoring Report for 2012*, Rev. 0, CH2M HILL Plateau Remediation Company, Richland, Washington.

DOE/RL-2014-32, 2014, *Hanford Site Groundwater Monitoring Report for 2013*, Rev. 0, U.S. Department of Energy, Richland Operations Office, Richland, Washington.

ECF-Hanford-13-0029, 2015, *Development of the Hanford South Geologic Framework Model, Hanford Site, Washington*, Rev. 1, CH2M HILL Plateau Remediation Company, Richland, Washington.

Ferreira, J. T., R. W. Ritzi, and D. F. Dominic, 2010, "Measuring the permeability of open-framework gravel," *Ground Water*, Vol. 48, pp. 593–597.

Gelhar, L. W., 1993, Stochastic Subsurface Hydrology, Prentice Hall, New York, New York.

Gelhar, L. W., C. Welty, and K. R. Rehfeldt, 1992, "A Critical Review of Data on Field-Scale Dispersion in Aquifers," *Water Resources Research*, Vol. 28, pp. 1955–1974.

HW-60601, 1959, *Aquifer Characteristics and Ground-Water Movement at Hanford*, General Electric Company, Hanford Atomic Products Operation, Richland, Washington.

ITRC, 2010, *Use and Measurement of Mass Flux and Mass Discharge*, The Interstate Technology & Regulatory Council, Integrated DNAPL Site Strategy Team, Washington, D.C.

Khaleel, R., 1989, "Scale Dependence of Continuum Models for Fractured Basalts," *Water Resources Research*, Vol. 25, No. 8, pp. 1847–1855.

Narbutovskih, S. M., J. P. McDonald, R. Schalla, M. D. Sweeney, 2002, "Application of the Colloidal Borescope to Determine a Complex Groundwater Flow Pattern," in *Evaluation and Remediation of Low Permeability and Dual Porosity Environments*, pp. 176–190, Symposium on Evaluation and Remediation of Low Permeability and Dual Porosity Environments, Reno, Nevada.

Neuman, S. P., 1990, "Universal Scaling of Hydraulic Conductivities and Dispersivities in Geologic Media," *Water Resources Research*, Vol. 26, No. 8, p. 1749–1758.

NUREG/CR-6114, 1994, *Auxiliary Analyses in Support of Performance Assessment of a Hypothetical Low-Level Waste Facility: Groundwater Flow and Transport Simulation*, Vol. 3, U.S. Nuclear Regulatory Commission, Washington, D.C.

NUREG/CR-6767, 2002, *Evaluation of Hydrologic Uncertainty Assessments for Decommissioning Sites Using Complex and Simplified Models*, PNNL-13832, Pacific Northwest National Laboratory prepared for Division of Systems Analysis and Regulatory Effectiveness, Office of Nuclear Regulatory Research, U.S. Nuclear Regulatory Commission, Washington, D.C.

PNL-10886, 1995, *Development of a Three-Dimensional Ground-Water Model of the Hanford Site Unconfined Aquifer System: FY 1995 Status Report*, Pacific Northwest Laboratory, Richland, Washington.

PNNL-11801, 1997, *Three-Dimensional Analysis of Future Groundwater Flow Conditions and Contaminant Plume Transport in the Hanford Site Unconfined Aquifer System: FY 1996 and 1997 Status Report*, Pacific Northwest National Laboratory, Richland, Washington.

PNNL-12261, 2000, *Revised Hydrogeology for the Suprabasalt Aquifer System, 200-East Area and Vicinity*, Hanford Site, Washington, Pacific Northwest National Laboratory, Richland, Washington.

PNNL-13447, 2001, *Transient Inverse Calibration of Hanford Site-Wide Groundwater Model to Hanford Operational Impact – 1943 to 1996*, Pacific Northwest National Laboratory, Richland, Washington.

PNNL-13641, 2001, *Uncertainty Analysis Framework – Hanford Site-Wide Groundwater Flow and Transport Model*, Pacific Northwest National Laboratory, Richland, Washington.

PNNL-14398, 2003, *Transient Inverse Calibration of the Site-Wide Groundwater Flow Model (ACM-2): FY 2003 Progress Report*, Rev. 0, Pacific Northwest National Laboratory, Richland, Washington.

PNNL-14656, 2004, *Borehole Data Package for Four CY 2003 RCRA Wells 299-E27-4, 299-E27-21, 299-E27-22, and 299-E27-23 at Single-Shell Tank, Waste Management Area C, Hanford Site, Washington*, Pacific Northwest National Laboratory, Richland, Washington.

PNNL-14753, 2006, *Groundwater Data Package for Hanford Assessments*, Rev. 1, Pacific Northwest National Laboratory, Richland, Washington.

PNNL-19277, 2010, *Conceptual Models for Migration of Key Groundwater Contaminants Through the Vadose Zone and Into the Unconfined Aquifer Below the B-Complex*, Rev. 0, Pacific Northwest National Laboratory, Richland, Washington.

Resource Conservation and Recovery Act of 1976, 42 USC 6901, et seq.

Rovey, C. W. II and D. S. Cherkauer, 1995, "Scale Dependency of Hydraulic Conductivity Measurements," *Ground Water*, Vol. 33, No. 5, pp. 769–780.

RPP-14430, 2003, *Subsurface Conditions Description of the C and A-AX Waste Management Area*, Rev. 0, CH2M HILL Hanford Group, Inc., Richland, Washington.

RPP-17209, 2006, *Modeling Data Package for an Initial Assessment of Closure of the S and SX Tank Farms*, Rev. 1, CH2M HILL Hanford Group, Inc., Richland, Washington.

RPP-RPT-46088, 2010, *Flow and Transport in the Natural System at Waste Management Area C*, Rev. 1, Washington River Protection Solutions, LLC/GSI Water Solutions, Inc., Richland, Washington.

Scheibe, T. D., E. M. Murphy, X. Chen, A. K. Rice, K. C. Carroll, B. J. Palmer, A. M. Tartakovsky, I. Battiato, and B. D. Wood, 2015, "An Analysis Platform for Multiscale Hydrogeologic Modeling with Emphasis on Hybrid Multiscale Methods," *Ground Water*, Vol. 53, No. 1, pp. 38–56.

Schulze-Makuch, D., 2005, "Longitudinal Dispersivity Data and Implications for Scaling Behavior," *Ground Water*, Vol. 43, No. 3, p. 443–456.

Schulze-Makuch, D., D. A. Carlson, D. S. Cherkauer, P. Malik, 1999, "Scale Dependency of Hydraulic Conductivity in Heterogeneous Media," *Ground Water*, Vol. 37, No. 6, pp. 904–919.

SGW-48722, 2011, *Borehole Summary Report for the ARRA Installation of Five RCRA Groundwater Monitoring Wells in the 200 Areas, FY 2010*, Rev. 0, Freestone Environmental Services, Inc., Richland, Washington.

SGW-54165, 2014, *Evaluation of the Unconfined Aquifer Hydraulic Gradient Beneath the 200 East Area, Hanford Site*, Rev. 0, CH2M HILL Plateau Remediation Company, Richland, Washington.

SGW-54508, 2013, *WMA C September 2012 Quarterly Groundwater Monitoring Report*, Rev. 0, CH2M HILL Plateau Remediation Company, Richland, Washington.

SGW-58561, 2015, *WMA C Quarterly October through December 2014 Quarterly Groundwater Monitoring Report*, Rev. 0, CH2M HILL Plateau Remediation Company, Richland, Washington.

U.S. Geological Survey Water-Supply Paper 2237, 1983, *Regional Flow in the Dakota Aquifer: A Study of the Role of Confining Layers*, U.S. Government Printing Office, Alexandria, Virginia.

van der Kamp, G., L. D. Luba, J. A. Cherry, and H. Maathuis, 1994, "Field Study of a Long and Very Narrow Contaminant Plume," *Ground Water*, Vol. 32, No. 6, pp. 1008–1016.

WCH-520, 2013, *Performance Assessment for the Environmental Restoration Disposal Facility, Hanford Site, Washington*, Rev. 1, Washington Closure Hanford, Richland, Washington.

WHC-SD-EN-WP-012, 1996, *Groundwater Screening Evaluation/Monitoring Plan -- 200 Area Treated Effluent Disposal Facility, Project W-049H*, Rev. 1, Westinghouse Hanford Company, Richland, Washington.

Xu, M. and Y. Eckstein, 1995, "Use of Weighted Least-Squares Method in Evaluation of the Relationship Between Dispersivity and Field Scale," *Ground Water*, Vol. 33, No. 6, pp. 905–908.